
Water entry problem in the presence of another floating or submerged body

A thesis submitted to the School of Mathematics at the University of East Anglia in partial fulfilment of the requirements for the degree of Doctor of Philosophy

Amer Al Khulayf

February 2024

© This copy of the thesis has been supplied on condition that anyone who consults it is understood to recognise that its copyright rests with the author and that use of any information derived there from must be in accordance with current UK Copyright Law. In addition, any quotation or extract must include full attribution.

Abstract

Water entry problems are important for those who work in the naval sector. Water impacts of practical rigid bodies in the presence of a submerged circular cylinder or floating flat plates are studied in this thesis. The presence of these bodies nearby the impact place can significantly change the water impact process or cause a crash.

These two problems are two-dimensional. The gravity and surface tension effects are neglected due to the impacting body is large and the acceleration of the fluid particles during the impact are much greater than the gravitational acceleration. The fluids in both problems are incompressible and inviscid. The flows caused by impact are potential with the velocity potentials of the flows being solutions of the Laplace equation. The hydrodynamic pressure in the flow regions are described by the Bernoulli's equation, where the hydrostatic pressure is neglected because the dynamic pressure components much higher than the hydrostatic components in the water impact problems. Water impacts of problems in the presence of a submerged circular cylinder or floating flat plates are studied using Wagner model of water impact.

Both problems are boundary value problems with mixed boundary conditions. Such problems are difficult to solve because of singularity of the solution at the points where the boundary conditions change their type. The problems are solved using conformal mappings of the flow regions onto a ring for the problem of impact in the presence of a submerged body, and onto a circle for the problem with several floating plates.

The mixed boundary value problems are reduced to coupled singular integral equations on the boundaries of the flow regions. The integral equations are formulated in terms of the distributions of the velocity potentials along the solid boundaries. The problems are studied with the submerged or floating bodies being either stationary or free to move.

The solutions of the integral equations are obtained in the form of Fourier series with unknown coefficients, which are solutions of linear algebraic equations. The systems of the algebraic equations are carefully analysed with obtaining asymptotic behaviour of the matrices of the system for limiting cases. The numerical distributions of the velocity potentials were compared with approximate analytical solutions for the cases where floating or submerged bodies are far away of the impact place.

Access Condition and Agreement

Each deposit in UEA Digital Repository is protected by copyright and other intellectual property rights, and duplication or sale of all or part of any of the Data Collections is not permitted, except that material may be duplicated by you for your research use or for educational purposes in electronic or print form. You must obtain permission from the copyright holder, usually the author, for any other use. Exceptions only apply where a deposit may be explicitly provided under a stated licence, such as a Creative Commons licence or Open Government licence.

Electronic or print copies may not be offered, whether for sale or otherwise to anyone, unless explicitly stated under a Creative Commons or Open Government license. Unauthorised reproduction, editing or reformatting for resale purposes is explicitly prohibited (except where approved by the copyright holder themselves) and UEA reserves the right to take immediate 'take down' action on behalf of the copyright and/or rights holder if this Access condition of the UEA Digital Repository is breached. Any material in this database has been supplied on the understanding that it is copyright material and that no quotation from the material may be published without proper acknowledgement.

Contents

Abstract	iii
Dedication	vii
Acknowledgements	viii
Chapter 1: Introduction	1
1.1 Literature review	2
1.2 Motivations	5
Chapter 2: Formulation of the problem of water impact in the presence of a submerged body	7
2.1 Description of the problem	8
2.2 Boundary conditions	11
2.3 Summary of formulation	12
2.4 Non-dimensional variables for blunt body impact	14
2.5 Wagner model of water impact	16

Chapter 3: Formulation of the Wagner problem in the presence of a submerged circular cylinder using conformal mapping of the flow region	18
3.1 Physical formulation	19
3.1.1 The submerged body	19
3.1.2 Summary of the formulation	21
3.2 Wagner model of water impact	21
3.3 Conformal mapping of the flow region	22
3.3.1 Summary of the water impact problem within the Wagner model formulated in the ζ -plane	32
 Chapter 4: Analytical solution of the water impact problem in the presence of a submerged circular cylinder within the Wagner model	 34
4.1 The coefficients $F_{1n}(\lambda)$, $F_{20}(\lambda)$ and $F_{2n}(\lambda)$	36
4.2 Convergence of the series for $F_{1n}(\lambda)$ and $F_{2n}(\lambda)$	40
4.3 Potential of flow caused by the cylinder moving under the free surface	42
4.3.1 Velocity potential $\Phi_i(\rho, \theta, t)$	45
4.3.2 Asymptotic behaviour of the matrices $A_{nm}^{(cc)}$ and $A_{nm}^{(ss)}$ as $A \rightarrow 0$ and $A \rightarrow 1$	60
4.4 Hydrodynamic loads acting on the cylinder	69
4.4.1 Motion of the cylinder during water impact process	74
4.5 Verification of the numerical solution	75
4.6 Verification of the numerical algorithm on the exact solution	78

Chapter 5: Water entry problem in the presence of floating body	90
5.1 Motivations	91
5.2 Formulation of the problem	91
5.2.1 Governing equations	91
5.2.2 Formulation of the problem and flow in the main region	93
5.2.3 Non-dimensional variables for blunt body impact	94
5.2.4 Transformation of the boundary problem to the ζ -plane	98
Chapter 6: Analytical solution of the water impact problem in the presence of a floating plate within the Wagner model	102
6.1 Elements of the matrices	119
6.1.1 Calculating $\vec{Z}_{c1,s1}$ and $\vec{Z}_{c2,s2}$	121
6.2 Motion of the floating plate	132
6.3 Verification of the numerical solution	141
Chapter 7: Conclusion and future work	145
7.1 Summary and conclusion	146
7.2 Future work	147
Bibliography	149
Chapter A: Appendix	153
A.1	153
A.2	161

Dedication

I dedicate this thesis with all its words and meaning
to my first teachers and mentors,
my beloved parents.
May God forgive them and grant them heaven and
the peace of paradise.

Acknowledgements

Firstly and foremost I want to express my deep sense of thanks and gratitude to my primary supervisor Prof. Alexander Korobkin for his guidance, motivation, patience and kindness. He was always available for advice and support, which helped me to a very great extent to accomplish this thesis.

I would like to extend my thanks to Prof. David Stevens and Dr. Tatyana Khabakhpasheva for their academic feedback.

My Ph.D work was funded by Saudi Government Scholarship, I am very thankful for the opportunity provided.

Nathaa, my lovely wife, thank you very much for your support, encourage, sacrifice, and tolerance during the every stage of this Ph.D.

My boys Mahdi, Sultan, and Nawaf, the source of my strength in this journey, there are no words to describe my love and gratitude for having you in my life.

1

Introduction

Water impact of a rigid body in the presence of other bodies and a free water surface is studied. The presence of other bodies nearby the impact place may significantly change the water impact process. Practical problems include water entry of a lifeboat in the presence of floating ice floes or debris near the place of the entry.

The aim of this research is to investigate how the body penetrating into the water is affected by another body inside water or floating on water surface. We shall investigate how strong is this effect in terms of the impact loads. The research will produce useful results for deep understanding of the water impact processes in complex environmental conditions, allowing us to apply these concepts in real life, such as using lifeboats and emergency aircraft landing.

1.1 Literature review

When an object falls into water, it creates an impact force on the body's surface. The body impacts on water surface generate high impulsive pressures which may damage the body. Because of the importance of this phenomenon, the water entry problem has been investigated by numerous researchers.

The water entry problem has been firstly studied by Von Karman and Wagner [32, 33]. They used asymptotic theory to develop theoretically formulas for water entry. These works were for the case of wedge section, where the deadrise angle of the wedge is small.

In 1929, Von Karman investigated the impact loads on seaplane floats during water landings. His work is considered as the first physical model of water entry using conservation of momentum and added mass [32]. He assumed that the velocity of the entering body is reduced because the added mass of the body rapidly increases with the penetration depth. The maximum impact forces are evaluated through the added mass and its time derivative. If the added mass $m(h)$ is known, then the approximate velocity of free-falling body onto water surface is given by

$$MV = (M + m)v, \quad (1.1.1)$$

where M is the body mass and V is the speed of the body just before the impact, $h(t)$ is the penetration depth. Because the approximations are often made regarding the added mass, the solutions obtained are rough. The model by Von Karman is a valuable physical picture of the water entry problem, which was adopted in various later works. For instances of water entry are routinely found in engineering and life science, such as water landings of crew capsules and seaplanes in aerospace engineering [29], plunging and diving of seabirds [7], and basilisk lizards running on water [12].

In 1932, Wagner published his paper on the theoretical analysis of water entry by analysing the vertical water impact of a wedge in two-dimension [33]. His solution accounts for the increase of the wetted part of entering body due to the so-called piled-up effect [32].

The developed water impact theories for seaplane have been reviewed by Monaghan [24]. He calculated the maximum deceleration during the impact by taking into account the momentum shed in the wake. In 1952, Monaghan re-examined the theoretical solution of a two-dimensional wedge entering water vertically and compared the result with those of Wagner [33, 25]. He calculated the wetted area of wedges with larger deadrise angles.

Zhao and Faltinsen presented a numerical method for studying water entry of a two-dimensional body of arbitrary cross-section using a nonlinear boundary element method with a jet flow approximation [34]. They verified the method by comparisons with new similarity solution results for wedges with deadrise angles varying from 4° to 81° . Also, the paper continued a simple asymptotic solution for small α based on Wagner (1932) [33] and it showed to give good predictions of slamming pressures for small deadrise angles α . The researchers found when α larger than approximately 30° , the pressure distribution on the body surface does not show the typical slamming behaviour of high impulse pressures concentrated over small surface areas.

In 2004, Korobkin described different approaches that had been proposed to improve the accuracy of Wagner's theory [16]. He investigated different mathematical models for predicting the hydrodynamic pressure distribution and

the force on a body entering liquid. Also, the analytical models were tested against both numerical and experimental results in [16]. He took higher order terms in the Bernoulli equation into account within the generalized Wagner model and the Logvinovich model. Logvinovich model predicts the hydrodynamic loads on an entering body, which are almost identical to the measured ones even for moderate penetration depth and for bodies with moderate deadrise angles. He found that the Logvinovich model corresponds better to the experimental data than the generalized Wagner model, where a rational derivation of the Logvinovich model is given for the two-dimensional case.

In 2015, Facci and Ubertini investigated the influence of non-dimensional parameters on hull slamming events, with particular attention to the hydrodynamic loading exerted by the water during the impact [9]. Their analysis focused on different flow regimes produced by the variation of inertia and acceleration and was carried out by studying the water entry of a two-dimensional wedge through computational fluid dynamics. This paper is quantitatively assess the interplay between the relevant non-dimensional parameters for the water entry of a two-dimensional body, evidencing the similitude conditions that allow the transition from scaled experiments to real-size applications. They proved when designing physical as well as numerical experiments under laboratory scale dimensions or utilizing different parameters compared to the real object in the study, the experimental parameters must be selected carefully.

Compressibility effects in water entry of wedges and cylinders are studied where the slamming force occurring in the free-fall impact of cylindrical bodies over the water surface analysed in both compressible and incompressible stages [5]. In these two phases, the hydrodynamic force is coupled to the rigid body motion to update the entry velocity of the body. However, the hydrodynamic analysis is carried out by the acoustic approximation and a closed-form expression for the impact force for the compressible phase and for the incompressible stage is approached through an unsteady boundary element method to compute the free surface evolution and the slamming force on the body.

Recently, the water entry of a rigid wedge in the presence of a neutrally buoyant solid cylinder under the water surface was studied [15]. This paper delves into critical interactions during water entry and provides an experimental study of the water entry of a rigid wedge in the presence of a neutrally buoyant cylinder below the water surface. The experimental setup used in the study is similar to the one from [28]. It was found that the presence of the cylinder provides a confined flow between the wedge and the cylinder, resulting in an asymmetric velocity distribution with regard to the wedge keel. Additionally, the presence of the cylinder causes an expected increase in pressure near the keel, but it also causes a pressure reduction near the pileup.

1.2 Motivations

When the hull of a lifeboat impacts the water surface in the presence of another body submerged or floating, the hydrodynamic pressures acting on the hull are expected to be higher than in the case without other bodies nearby. As a result, the deceleration of the lifeboat can exceed a critical value leading to injuries to the people inside the lifeboat. Generally, water entry refers to problems in which a solid body, rigid or compliant enters the surface of a fluid at high speed [1]. During the entry, there is a pileup region and spray jet forms at the periphery of the wetted part of the body surface. Water entry of a rigid wedge in the presence of a submerged cylinder under the water surface caused non-symmetric effect for the pileup and spray jet, where the cylinder is fixed [15]. The velocity potential was obtained through the method of Green's functions [8]. In this research, the velocity potential is obtained as Fourier series for fixed or free-to-move cylinders.

Hull slamming of marine vessels is considered to be the most studied part of water entry, where the repeated entry of the hull of a vessel on the water surface induces frequent and large impulsive loadings on the body structure, which potentially reduce the lifetime of the vessel and hinder its manoeuvrability [10]. In addition to naval engineering, there are applications of water entry in engineering and life science, such as water landings of crew capsules and seaplanes in aerospace engineering [29].

In 2017, the Wagner model of water entry problem has been generalised to account for several ice floes floating near the place of impact in two-dimensions [23]. The obtained solution is for a ice floes of negligible thickness. This solution can not be used for any shape of a floating body [23]. Also, the solution provided for a submerged body [15] can be used for a fixed cylinder only . In the present thesis, the conformal mapping technique is used, which helps to find a solution for any floating or submerged body.

We study the water entry problems in presence of another body which is floating or submerged under the liquids. This problem is with mixed boundary conditions on the upper boundary of the flow region and with several free moving bodies.

This research has various applications, where it will be interesting to investigate such problems deeply. For instance, securing the using of lifeboats, escape crew capsule and aircraft emergency landing.

Formulation of the problem of water
impact in the presence of a
submerged body

where $v(t) = h'(t)$ and $h(t)$ is the vertical displacement of the body downwards. The shape function $f(x, t)$ is assumed given. The shape function is such that $f(0, 0) = 0$ and $|f_x(x, t)| \ll 1$ in the wetted part of the body surface. The body is not symmetric in general, $f(-x, t) \neq f(x, t)$. The body displacement $h(t)$ is either given or should be determined using the equation of the body motion.

If the body penetrates water of a constant speed v , then $h(t) = vt$. The impact stage of the entry process is only considered, when the contact region increases at a speed much higher than the speed of the body entry. The wetted part of the body surface, which is the region of contact between the body surface and the fluid, is denoted by $\Gamma_w(t)$. The contact region grows in time. It is bounded on the left and on the right by the jet-root regions, positions of which are described by x -coordinates, $x_w^{(L)}(t)$ and $x_w^{(R)}(t)$, of the points of the water free surface with vertical tangents at the points, see figures 2.1.1 and 3.3.1. The superscripts (R) and (L) correspond to the right and left parts of the flow region. The subscript w stands for Wagner model, who distinguished the main flow region, jet-root regions and jet regions in the water entry problems [33]. The points of the free surface with x -coordinates $x_w^{(L)}(t)$ and $x_w^{(R)}(t)$ will be called the Wagner contact points, see section 2.4. The Wagner contact points play an important role in the modelling of impact problems. The positions of the points are unknown in advance and should be determined as part of the solution. The positions of these points depend on the motion of the free surface, the body shape and the body motion. The horizontal length of the contact region $\Gamma_w(t)$ is approximately equal to

$$x_w^{(L)}(t) + x_w^{(R)}(t), \tag{2.1.2}$$

The shape of the free surface, which is denoted by $\Gamma_f(t)$, is described by the equation

$$y = \eta(x, t), \tag{2.1.3}$$

where $\eta(-x, t) \neq \eta(x, t)$ if the flow is non symmetric, due to the presence of a submerged body. The flow is assumed potential, where the velocity potential of the flow $\varphi(x, y, t)$ satisfies Laplace equation

$$\nabla^2 \varphi = 0, \tag{2.1.4}$$

the Laplacian ∇^2 is given by

$$\nabla^2 = \frac{\partial^2}{\partial x^2} + \frac{\partial^2}{\partial y^2}, \quad (2.1.5)$$

for two-dimensional flows. The Laplace equation (2.1.4) should be solved in the time-dependent flow region $\Omega(t)$, where the boundary $\partial\Omega(t)$ of the flow region is given by

$$\partial\Omega(t) = \Gamma_w(t) \cup \Gamma_f(t) \cup \Gamma_c(t), \quad (2.1.6)$$

where $\Gamma_w(t)$ is the wetted part of the body surface, $\Gamma_f(t)$ is the free surface including free boundaries of the spray jet, and $\Gamma_c(t)$ is the boundary of the submerged body.

The hydrodynamic pressure in the flow region $\Omega(t)$ is described by the Bernoulli's equation, where the hydrostatic pressure is neglected from the problem because of the penetration depth is small, where

$$p(x, y, t) = -\rho \left(\frac{\partial\varphi}{\partial t} + \frac{1}{2} |\nabla\varphi|^2 \right). \quad (2.1.7)$$

Initially, $t = 0$, there is no flow, which gives

$$\varphi(x, y, 0) = 0, \quad (2.1.8)$$

and

$$\Omega(0) = \{x, y | -\infty < x < \infty, y < 0\} \setminus \Omega_c, \quad (2.1.9)$$

where $\Omega_c(0)$ is the initial area of the submerged cylinder. Equations (2.1.7) and (2.1.8) implying that $p(x, y, t) \equiv 0$ in $\Omega(t)$ when $t < 0$, which means the equation (2.1.7) gives the dynamic components of the pressure but not the total pressure.

The total pressure is given by

$$p_{total} = p + p_{atm}, \quad (2.1.10)$$

where p_{atm} is the atmospheric pressure, which is constant in our model. We assume the atmospheric pressure does not vary in time and in space.

2.2 Boundary conditions

The problem involved mixed boundary conditions to deal with because there are different shapes for this action and different potentials. Therefore, this research will apply the Laplace equation together with different boundary conditions which are known as the mixed boundary value problem of potential.

Two boundary conditions are imposed on the free surface $\Gamma_f(t)$, which are the dynamic and kinematic conditions for the potential φ and for finding the current shape of the free surface. Also, body boundary condition (BBC) and submerged body conditions imposed in the contact region $\Gamma_w(t)$. Boundary conditions on the free surface $\Gamma_f(t)$ are dynamic boundary condition (DBC)

$$p = 0, \quad (2.2.1)$$

which means that the total pressure on the water surface, $p(x, \eta(x, t), t) + p_{atm}$, is equal to the atmospheric pressure p_{atm} , and kinematic boundary condition (KBC):

$$\frac{\partial \varphi}{\partial y} = \frac{\partial \eta}{\partial x} \frac{\partial \varphi}{\partial x} + \frac{\partial \eta}{\partial t}, \quad \text{on } \Gamma_f(t), \quad (2.2.2)$$

where

$$\Gamma_f(t) = \left\{ y = \eta(x, t), \quad x < x_w^{(L)}(t), \quad x_w^{(R)}(t) < x \right\}, \quad (2.2.3)$$

which means that the liquid particles of the free surface cannot leave this surface. The boundary condition on the wetted part $\Gamma_w(t)$ of the entering body surface is given by

$$\frac{\partial \varphi}{\partial y} = \frac{\partial f}{\partial x} \frac{\partial \varphi}{\partial x} + \frac{\partial \eta}{\partial t} - h'(t), \quad \text{on } \Gamma_w(t), \quad (2.2.4)$$

where

$$\Gamma_w(t) = \left\{ y = f(x, t) - h(t), \quad x_w^{(L)}(t) < x < x_w^{(R)}(t) \right\}, \quad (2.2.5)$$

which states that the liquid particles can move along the body surface but cannot penetrate or separate from the surface of the body. For the submerged body we imposed the following condition,

$$\frac{\partial \varphi}{\partial n} = \mathbf{v}_c \cdot \mathbf{n}, \quad \text{on } \Gamma_c(t), \quad (2.2.6)$$

where

$$\Gamma_c(t) = \left\{ \sqrt{[x - x_c(t)]^2 + [y - y_c(t)]^2} = r = R \right\}, \quad (2.2.7)$$

R is the radius of the cylinder, $\mathbf{n} = (\cos \alpha, \sin \alpha)$ is the outward unit normal vector to the cylinder, $\mathbf{v}_c(t) = (\dot{x}_c(t), \dot{y}_c(t))$ is velocity of the cylinder and $(x_c(t), y_c(t))$ is the position of the center of the cylinder, and $x = x_c(t) + r \cos \alpha$, $y = y_c(t) + r \sin \alpha$. The Cartesian coordinate x, y and polar coordinate r, α are given by

$$\frac{\partial \varphi}{\partial n} = \frac{\partial \varphi}{\partial r} = \dot{x}_c(t) \cos \alpha + \dot{y}_c(t) \sin \alpha, \quad (r = R), \quad 0 < \alpha < 2\pi. \quad (2.2.8)$$

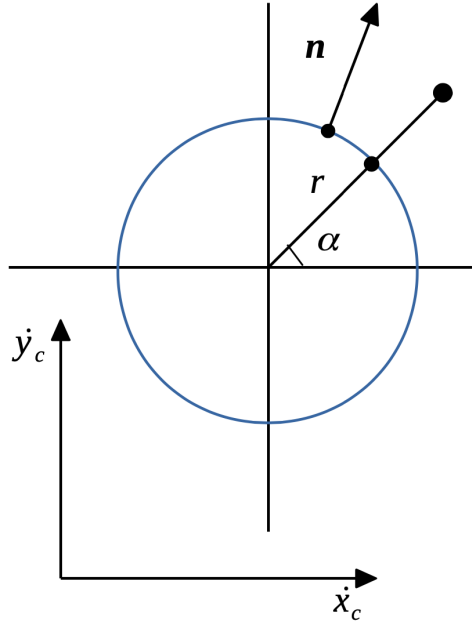


Figure 2.2.1: The polar coordinate r, α with the origin at the moving center of the cylinder.

2.3 Summary of formulation

$$\nabla^2 \varphi = 0 \quad \text{in} \quad \Omega(t), \quad (2.3.1)$$

$$\Omega(t) = \{x, y\} \begin{cases} -\infty < x < x_w^{(L)}, & y \leq \eta(x, t), \\ x_w^{(L)} < x < x_w^{(R)}, & y \leq f(x, t) - h(t), \\ x_w^{(R)} < x < \infty, & y \leq \eta(x, t), \end{cases}$$

$$\Omega(0) = \{x, y \mid -\infty < x < \infty, y \leq 0\} \setminus \Omega_c(0),$$

$$p = -\rho \left(\varphi_t + \frac{1}{2} |\nabla \varphi|^2 \right) \quad \text{in } \Omega(t), \quad (2.3.2)$$

$$p = 0, \quad \varphi_y = \eta_x \varphi_x + \eta_t \quad \text{on } \Gamma_f(t), \quad (2.3.3)$$

$$\varphi_y = f_x \varphi_x + f_t - h'(t) \quad \text{on } \Gamma_w(t), \quad (2.3.4)$$

$$\varphi_n = \mathbf{v}_c \cdot \mathbf{n}, \quad \text{on } \Gamma_c(t), \quad (2.3.5)$$

$$\varphi \rightarrow 0 \quad (\text{as } x^2 + y^2 \rightarrow \infty), \quad (2.3.6)$$

$$\varphi = 0 \quad \varphi_t = 0 \quad (t = 0). \quad (2.3.7)$$

To formulate equations for functions $x_w^{(L)}(t)$ and $x_w^{(R)}(t)$, we need to describe explicit elements of the boundaries $\Gamma_f(t)$ and $\Gamma_w(t)$ by considering the turn-over region in more details. These equations are required to formulate the so-called Wagner conditions for the size of the wetted area of the entering body surface.

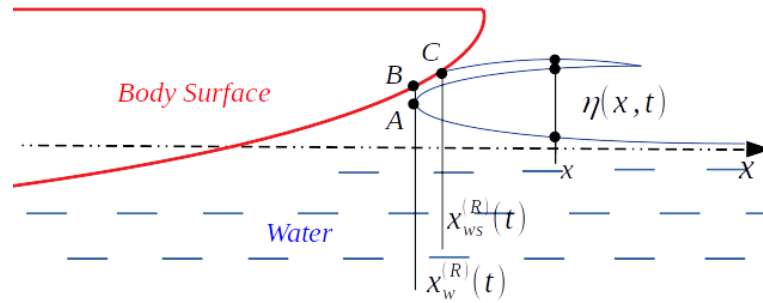


Figure 2.3.1: Scheme of the flow in the turn-over region.

The turn-over regions on the right side and on the left side of the entering body are considered in a similar way. Let $x_w^{(R)}(t)$ be the x -coordinate of the turn-over point A and $x_{ws}^{(R)}(t)$ be the x -coordinate of the separation point C , respectively, see figure 2.3.1. Then the vertical y -coordinate denotes of points B and A are

$$y_B^{(R)} = f \left[x_w^{(R)}(t) \right] - h(t), \quad (2.3.8)$$

$$y_A^{(R)} = \eta \left[x_w^{(R)}(t), t \right], \quad (2.3.9)$$

and from geometrical considerations, we find Wagner conditions:

$$y_B^{(R)} = \eta \left[x_w^{(R)}, t \right] + |AB|(t) = f \left[x_w^{(R)} \right] - h(t), \quad (2.3.10)$$

$$y_B^{(L)} = \eta [x_w^{(L)}, t] + |AB|(t) = f [x_w^{(L)}] - h(t). \quad (2.3.11)$$

Blunt body: Compressibility is important for the impact of a blunt body on the water surface at the very beginning of water entry. At small penetration depths, a blunt body contour approximates a parabola shape with the expansion velocity of the Wagner wetted area, see figure 2.1.1. The blunt body has a small non-dimensional parameter $\varepsilon = H/L$, ($\varepsilon \ll 1$), where $2L$ is the horizontal size of the body and H is the height of the body. The turn-over region is small and the separation point is outside of this region for both blunt body and impact stage, where the size of the turn-over region is of order $O(|AB|)$ and $|AB| \ll y_B(t)$ as $\varepsilon \rightarrow 0$ ($\varepsilon \ll 1$).

2.4 Non-dimensional variables for blunt body impact

Equation (2.1.1) is the equation of the penetrating body in the dimensional variables, where $h(0) = 0$, $h'(0) = v$, $f(x)$ is not necessary even, $f(-x) \neq f(x)$ in general and $f(0) = 0$, $f(x) > 0$ for $x \neq 0$. The width of the body is equal to $2L$ and H is the body height. The shape function $f(x)$ is convenient to be presented by

$$f(x) = H\tilde{f}(x/L), \quad (2.4.1)$$

where tilde denotes dimensionless variables and

$$\tilde{x} = x/L, \quad -1 \leq \tilde{x} \leq 1, \quad 0 \leq \tilde{f}(\tilde{x}) \leq 1, \quad |d\tilde{f}/d\tilde{x}| \ll 1, \quad (2.4.2)$$

for the body surface. By taking L to be the length scale, H the displacement scale, H/v the time scale and the product vL as the scale of the velocity potential, we introduce the dimensionless variables as

$$x = L\tilde{x}, \quad y = L\tilde{y}, \quad h(t) = H\tilde{h}(\tilde{t}), \quad t = \frac{H}{v}\tilde{t}, \quad \varphi = vL\tilde{\varphi}(\tilde{x}, \tilde{y}, \tilde{t}),$$

$$f(x) = H\tilde{f}(\tilde{x}), \quad \eta = H\tilde{\eta}(\tilde{x}, \tilde{t}), \quad p = \frac{1}{\varepsilon}\rho v^2\tilde{p}. \quad (2.4.3)$$

Derivatives in the dimensionless variables are given by

$$\frac{\partial \varphi}{\partial x} = \frac{\partial [vL\tilde{\varphi}]}{\partial (L\tilde{x})} = \frac{vL}{L} \frac{\partial \tilde{\varphi}}{\partial \tilde{x}} = v \frac{\partial \tilde{\varphi}}{\partial \tilde{x}}, \quad (2.4.4)$$

$$\frac{\partial f}{\partial x} = H \frac{\partial \tilde{f}}{\partial \tilde{x}} \frac{1}{L} = \varepsilon \frac{\partial \tilde{f}}{\partial \tilde{x}}, \quad (\varepsilon = H/L), \quad (2.4.5)$$

$$\frac{\partial \varphi}{\partial t} = \frac{vL}{H/v} \frac{\partial \tilde{\varphi}}{\partial \tilde{t}} = \frac{1}{\varepsilon} v^2 \frac{\partial \tilde{\varphi}}{\partial \tilde{t}}. \quad (2.4.6)$$

The body position in the dimensionless variables is described by the equation

$$L\tilde{y} = H\tilde{f}(\tilde{x}) - H\tilde{h}(\tilde{t}), \quad (2.4.7)$$

thus

$$\tilde{y} = \varepsilon \left[\tilde{f}(\tilde{x}) - \tilde{h}(\tilde{t}) \right]. \quad (2.4.8)$$

The free-surface shape, $y = \eta(x, t)$, takes the form in the dimensionless variables,

$$L\tilde{y} = H\tilde{\eta}(\tilde{x}, \tilde{t}), \quad (2.4.9)$$

$$\tilde{y} = \varepsilon \tilde{\eta}(\tilde{x}, \tilde{t}). \quad (2.4.10)$$

The entry speed of the entering body is equal to

$$\frac{dh}{dt} = H\tilde{h}'(\tilde{t}) \frac{v}{H} = v\tilde{h}'(\tilde{t}), \quad (2.4.11)$$

where, $\tilde{h}'(0) = 1$, in the dimensionless variables.

The Wagner conditions (2.3.10) and (2.3.11), where $|AB|(t)$ is negligibly small, imply that the vertical coordinates of the body at the contact points, where $x = x_w^{(L)}(t)$ and $y = x_w^{(R)}(t)$, and the elevations of the free surfaces at these points are equal to each other. These conditions do not account for the jets at the contact points, because the dimensions of the jet-root regions are of order $O(\varepsilon^2)$ in the dimensionless variables.

In the leading order as $\varepsilon \rightarrow 0$, the equations (2.3.1 - 2.3.7) and (2.3.10 -

2.3.11) read in the dimensionless variables,

$$\tilde{\nabla}^2 \tilde{\varphi} = 0 \quad \tilde{\Omega}(\tilde{t}), \quad (2.4.12)$$

$$\tilde{p} = -\frac{\partial \tilde{\varphi}}{\partial \tilde{t}} \quad (\tilde{y} \leq 0), \quad (2.4.13)$$

$$\frac{\partial \tilde{\varphi}}{\partial \tilde{y}} = \frac{\partial \tilde{\eta}}{\partial \tilde{t}}, \quad \tilde{\varphi} = 0, \quad (\tilde{y} = 0, \quad \tilde{x} < \tilde{x}_w^{(L)}(\tilde{t}), \quad \tilde{x} > \tilde{x}_w^{(R)}(\tilde{t})), \quad (2.4.14)$$

$$\frac{\partial \tilde{\varphi}}{\partial \tilde{y}} = -h'(\tilde{t}) \quad (\tilde{y} = \tilde{\eta}(\tilde{x}, \tilde{y}), \quad \tilde{x}_w^{(L)}(\tilde{t}) < \tilde{x} < \tilde{x}_w^{(R)}(\tilde{t})), \quad (2.4.15)$$

$$\frac{\partial \tilde{\varphi}}{\partial \tilde{n}} = [\mathbf{v}_c \cdot \mathbf{n}], \quad \text{on } \Gamma_c(\tilde{t}) = \left\{ \tilde{R} = \sqrt{[\tilde{x} - \tilde{x}_c(\tilde{t})]^2 + [\tilde{y} - \tilde{y}_c(\tilde{t})]^2} \right\}, \quad (2.4.16)$$

$$\tilde{\varphi} \rightarrow 0 \quad (\text{as } \tilde{x}^2 + \tilde{y}^2 \rightarrow \infty), \quad (2.4.17)$$

$$\tilde{\varphi} = 0, \quad \tilde{\varphi}_{\tilde{t}} = 0 \quad (\text{at } \tilde{t} = 0), \quad (2.4.18)$$

$$\tilde{\eta}[\tilde{x}_w^{(L)}(\tilde{t}), \tilde{t}] = \tilde{f}[\tilde{x}_w^{(L)}(\tilde{t})] - h(\tilde{t}), \quad (2.4.19)$$

$$\tilde{\eta}[\tilde{x}_w^{(R)}(\tilde{t}), \tilde{t}] = \tilde{f}[\tilde{x}_w^{(R)}(\tilde{t})] - h(\tilde{t}). \quad (2.4.20)$$

where the unknown functions

$$\tilde{\varphi}(\tilde{x}, \tilde{y}, \tilde{t}), \quad \tilde{p}(\tilde{x}, \tilde{y}, \tilde{t}), \quad \tilde{\eta}(\tilde{x}, \tilde{t}), \quad \tilde{x}_w^{(R)}(\tilde{t}), \quad \tilde{x}_w^{(L)}(\tilde{t}).$$

2.5 Wagner model of water impact

By assuming that the unknown functions $\tilde{\varphi}(\tilde{x}, \tilde{y}, \tilde{t}; \varepsilon)$, $\tilde{p}(\tilde{x}, \tilde{y}, \tilde{t}; \varepsilon)$, $\tilde{\eta}(\tilde{x}, \tilde{t}; \varepsilon)$ and $\tilde{x}_w^{(R)}(\tilde{t}; \varepsilon)$, $\tilde{x}_w^{(L)}(\tilde{t}; \varepsilon)$, where their derivatives as shown in (2.4.12 - 2.4.20) with certain limits $\varepsilon \rightarrow 0$ and $|AB|(\tilde{t}; \varepsilon)/v \rightarrow 0$ as $\varepsilon \rightarrow 0$. Thereafter the equations for limiting values of the unknown functions for the equations (2.4.12 - 2.4.20), where ε is set zero become as

$$\tilde{\nabla}^2 \tilde{\varphi} = 0 \quad \tilde{\Omega}(\tilde{t}), \quad (2.5.1)$$

$$\tilde{p} = -\frac{\partial \tilde{\varphi}}{\partial \tilde{t}} \quad (\tilde{y} \leq 0), \quad (2.5.2)$$

$$\tilde{\varphi} = 0, \quad \frac{\partial \tilde{\varphi}}{\partial \tilde{y}} = \frac{\partial \tilde{\eta}}{\partial \tilde{t}} \quad \text{on} \quad \tilde{\Gamma}_f(\tilde{t}) = \{\tilde{y} = 0, \quad |\tilde{x}| > \tilde{x}_w^{(R)}(\tilde{t})\}, \quad (2.5.3)$$

$$\frac{\partial \tilde{\varphi}}{\partial \tilde{y}} = -h'(\tilde{t}) \quad \text{on} \quad \tilde{\Gamma}_f(\tilde{t}) = \{\tilde{y} = 0, \quad |\tilde{x}| < \tilde{x}_w^{(R)}(\tilde{t})\}, \quad (2.5.4)$$

$$\frac{\partial \tilde{\varphi}}{\partial \tilde{n}} = [\mathbf{v}_c \cdot \mathbf{n}], \quad \text{on} \quad \Gamma_c(t) = \left\{ \tilde{R} = \sqrt{[\tilde{x} - \tilde{x}_c(\tilde{t})]^2 + [\tilde{y} + \tilde{y}_c(\tilde{t})]^2} \right\}, \quad (2.5.5)$$

$$\tilde{\varphi} \rightarrow 0 \quad (\text{as} \quad \tilde{x}^2 + \tilde{y}^2 \rightarrow \infty), \quad (2.5.6)$$

$$\tilde{\varphi} = 0 \quad \tilde{\varphi}_t = 0 \quad (\text{at} \quad \tilde{t} = 0), \quad (2.5.7)$$

$$\frac{\partial \tilde{\eta}}{\partial \tilde{t}} = \frac{\partial \tilde{\varphi}}{\partial \tilde{y}}(\tilde{x}, 0, \tilde{t}; 0) \quad (|\tilde{x}| > \tilde{x}_w^{(R)}(\tilde{t})), \quad (2.5.8)$$

$$\tilde{\eta}[\tilde{x}_w^{(R)}(\tilde{t}, 0), \tilde{t}, 0] = \tilde{f}[\tilde{x}_w^{(R)}(\tilde{t})] - h(\tilde{t}). \quad (2.5.9)$$

$$\tilde{\eta}[\tilde{x}_w^{(L)}(\tilde{t}, 0), \tilde{t}, 0] = \tilde{f}[\tilde{x}_w^{(L)}(\tilde{t})] - h(\tilde{t}). \quad (2.5.10)$$

where the original problem (2.4.12 - 2.4.20) are represented by the boundary value problem (2.5.1 - 2.5.10) with respect to the leading-order approximation of the original solution as $\varepsilon \rightarrow 0$.

The submerged body is a circular cylinder for simplicity.

Formulation of the Wagner problem
in the presence of a submerged
circular cylinder using conformal
mapping of the flow region

In this chapter, we illustrated the formulation of the Wagner problem for a submerged circular cylinder. Firstly, formulating the problem physically. Secondly, determining the Wagner model of water impact from the physical plane to Wagner plane. Thirdly, transform the complex potential region φ into a ring in ζ -plane by using conformal mapping method.

3.1 Physical formulation

3.1.1 The submerged body

The circular cylinder is initially centred at (x_0, y_0) with radius R in the dimensional variables. The cylinder can be displaced from its original position by $x_c(t)$ and $y_c(t)$ in x and y directions respectively. The corresponding dimensionless variables and parameters are

$$\begin{aligned} x_0 &= L\tilde{x}_0, & y_0 &= L\tilde{y}_0, & R &= L\tilde{R}, \\ x_c &= H\tilde{x}_c(\tilde{t}), & y_c &= H\tilde{y}_c(\tilde{t}), \end{aligned} \tag{3.1.1}$$

where the distances and the radius are scaled with the characteristic horizontal dimension of the impacting body, L , but the displacements with the characteristic vertical dimensions of the entering body, H . Within the Wagner model, we neglect the displacements of the cylinder and impose the body boundary condition for the normal velocity of the flow at the original surface of the cylinder. To formulate the boundary condition on the cylinder, we introduce the local polar coordinates

$$x = x_c(t) + r \cos \alpha \quad \text{and} \quad y = y_c(t) + r \sin \alpha, \tag{3.1.2}$$

where $r = R$ is the equation of the cylinder surface, $0 \leq \alpha < 2\pi$. On the cylinder,

$$\frac{\partial \varphi}{\partial r} = \dot{x}_c(t) \cos \alpha + \dot{y}_c(t) \sin \alpha, \tag{3.1.3}$$

and in the dimensionless variables,

$$\frac{vL}{L} \frac{\partial \tilde{\varphi}}{\partial \tilde{r}} = H \cdot \tilde{x}'_c(\tilde{t}) \frac{v}{H} \cos \alpha + H \cdot \tilde{y}'_c(\tilde{t}) \frac{v}{H} \sin \alpha, \quad (\tilde{r} = \tilde{R}), \quad (3.1.4)$$

and

$$\frac{\partial \tilde{\varphi}}{\partial \tilde{r}} = \frac{d\tilde{x}_c}{d\tilde{t}} \cos \alpha + \frac{d\tilde{y}_c}{d\tilde{t}} \sin \alpha, \quad (\tilde{r} = \tilde{R}). \quad (3.1.5)$$

If the cylinder is stationary, then $\dot{x}_c(t) = const$, $\dot{y}_c(t) = const$ and

$$\frac{\partial \tilde{\varphi}}{\partial \tilde{r}} = 0, \quad (\tilde{r} = \tilde{R}). \quad (3.1.6)$$

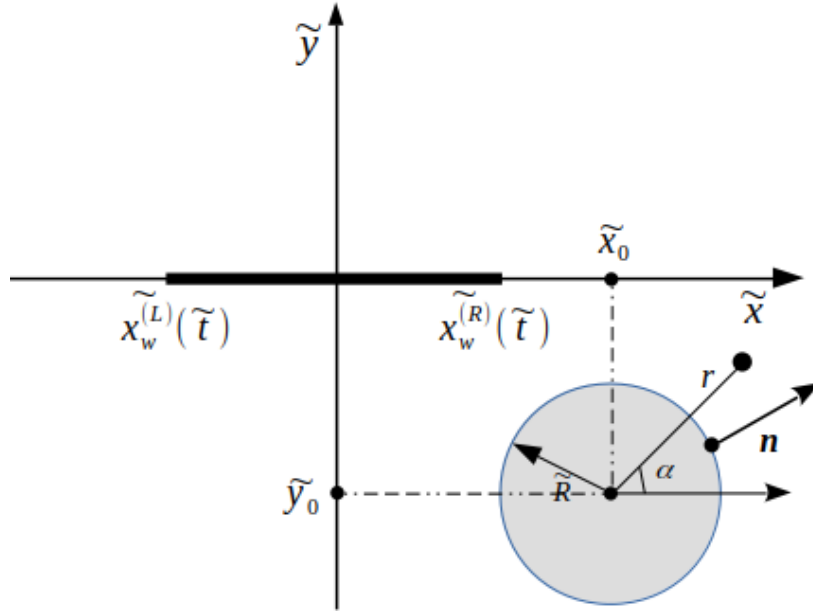


Figure 3.1.1: The sketch shows the boundaries of the flow region.

3.1.2 Summary of the formulation

$$\left\{ \begin{array}{ll}
 \tilde{\nabla}^2 \tilde{\varphi} = 0 & (\tilde{y} < 0), \\
 \tilde{p} = -\tilde{\varphi}_{\tilde{t}} & (\tilde{y} \leq 0), \\
 \tilde{p} = 0, \tilde{\varphi}_{\tilde{y}} = \tilde{\eta}_{\tilde{t}}, \tilde{\varphi} = 0 & \left(\tilde{y} = 0, \tilde{x} < \tilde{x}_w^{(L)}(\tilde{t}), \tilde{x} > \tilde{x}_w^{(R)}(\tilde{t}) \right), \\
 \tilde{\varphi}_{\tilde{y}} = -h'(\tilde{t}) & \left(\tilde{y} = 0, \tilde{x}_w^{(L)}(\tilde{t}) < \tilde{x} < \tilde{x}_w^{(R)}(\tilde{t}) \right), \\
 \tilde{\varphi} \rightarrow 0 & (\text{as } \tilde{x}^2 + \tilde{y}^2 \rightarrow \infty), \\
 \tilde{\varphi} = 0, \quad \tilde{\varphi}_{\tilde{t}} = 0 & (\text{at } \tilde{t} = 0), \\
 \tilde{\varphi}_{\tilde{r}} = \frac{d\tilde{x}_c}{d\tilde{t}} \cos \alpha + \frac{d\tilde{y}_c}{d\tilde{t}} \sin \alpha, & (\tilde{r} = \tilde{R}), \\
 \tilde{\eta}_{\tilde{t}} = \tilde{\varphi}_{\tilde{y}}(\tilde{x}, 0, \tilde{t}; 0) & (|\tilde{x}| > \tilde{x}_w^{(R)}(\tilde{t})), \\
 \tilde{\eta} \left[\tilde{x}_w^{(L)}(\tilde{t}), \tilde{t} \right] = \tilde{f} \left[\tilde{x}_w^{(L)}(\tilde{t}) \right] - h(\tilde{t}), \\
 \tilde{\eta} \left[\tilde{x}_w^{(R)}(\tilde{t}), \tilde{t} \right] = \tilde{f} \left[\tilde{x}_w^{(R)}(\tilde{t}) \right] - h(\tilde{t}).
 \end{array} \right. \quad (3.1.7)$$

3.2 Wagner model of water impact

Wagner problem in the dimensional (original) variables

$$\left\{ \begin{array}{ll}
 \nabla^2 \varphi = 0 & (y < 0), \\
 p = -\varphi_t & (y \leq 0), \\
 p = 0, \varphi_y = \eta_t, \varphi = 0 & \left(y = 0, x < x_w^{(L)}(t), x > x_w^{(R)}(t) \right), \\
 \varphi_y = -h'(t) & \left(y = 0, x_w^{(L)}(t) < x < x_w^{(R)}(t) \right), \\
 \varphi \rightarrow 0 & (\text{as } x^2 + y^2 \rightarrow \infty), \\
 \varphi = 0, \quad \varphi_t = 0 & (\text{at } t = 0), \\
 \varphi_r = \frac{dx_c}{dt} \cos \alpha + \frac{dy_c}{dt} \sin \alpha & (r = R), \\
 \eta_t = \varphi_y(x, 0, t; 0) & (|x| > x_w^{(R)}(t)), \\
 \eta \left[x_w^{(L)}(t), t \right] = f \left[x_w^{(L)}(t) \right] - h(t), \\
 \eta \left[x_w^{(R)}(t), t \right] = f \left[x_w^{(R)}(t) \right] - h(t).
 \end{array} \right. \quad (3.2.1)$$

Figure 2.1.1 shows the Wagner problem and the relation between the flow boundaries in the physical plane and Wagner plane is illustrated in figure 3.2.1.

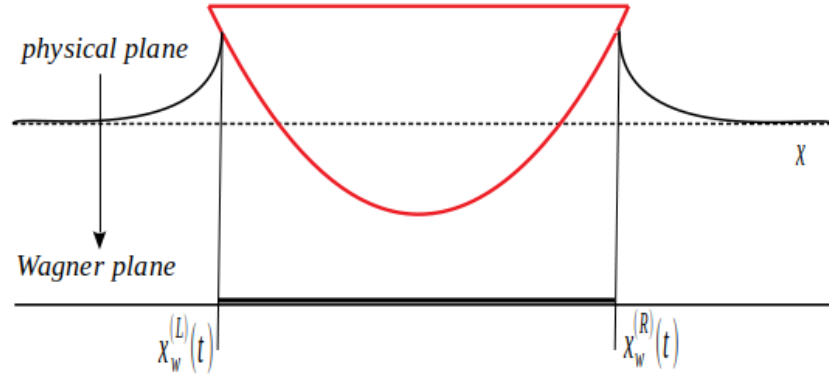


Figure 3.2.1: Graph shows the physical plane and the Wagner plane of the flow.

3.3 Conformal mapping of the flow region

It is convenient to map the flow region onto a ring in the image of the conformal mapping $\zeta = \zeta(z, t)$. The boundary value problem for equation (2.4.12) is transformed to a ζ -plane, where the cylinder surface, $r = R$, corresponds to a circle $|\zeta| = R_1$, and the upper boundary of the flow region, $y = 0$, to the unit circle $|\zeta| = 1$. The conformal mapping of the ring, $R_1 < |\zeta| < 1$, in the ζ -plane onto the Wagner flow region in the physical plane is given by

$$\frac{z - x_c(t)}{\sqrt{y_c^2(t) - R^2}} = i + \frac{2}{\zeta + i}, \quad (z = x + iy, \zeta = \xi + i\eta), \quad (3.3.1)$$

where the outer circle, $|\zeta| = 1$, corresponds to the upper boundary of the flow region, $y = 0$, and (x_c, y_c) are the coordinates of the circular center of the cylinder in the original z -plane. In the polar coordinates (ρ, θ) , see figure 3.3.1, $\zeta = \rho e^{i(\pi/2 - \theta)} = i\rho e^{-i\theta}$, the surface $y = 0$ corresponds to $\rho = 1$ and $-\pi < \theta < \pi$, where

$$\zeta = e^{i(\pi/2 - \theta)} = e^{i\pi/2} e^{-i\theta} = i(\cos \theta - i \sin \theta) = \sin \theta + i \cos \theta, \quad (3.3.2)$$

and the right hand side of (3.3.1) reads

$$\begin{aligned} i + \frac{2}{e^{i(\pi/2-\theta)} + i} &= i + \frac{2}{\sin \theta + i(\cos \theta + 1)} \\ &= i + 2 \frac{\sin \theta - i(\cos \theta + 1)}{\sin^2 \theta + (\cos \theta + 1)^2} = i + 2 \frac{\sin \theta - i(\cos \theta + 1)}{2(1 + \cos \theta)} \\ &= \frac{\sin \theta}{1 + \cos \theta}. \end{aligned} \quad (3.3.3)$$

The left hand side of (3.3.1),

$$\frac{x - x_c(t) + iy}{\sqrt{y_c^2(t) - R^2}}, \quad (3.3.4)$$

and (3.3.3) provide

$$y = 0, \quad \frac{x - x_c(t)}{\sqrt{y_c^2(t) - R^2}} = \frac{\sin \theta}{1 + \cos \theta}. \quad (3.3.5)$$

The point $\zeta = -i$ corresponds to the infinity in the z -plane. At $\zeta = -i$, $|x| \rightarrow \infty$ for $\theta = \pm\pi$, $\sin(\theta) = 0$ and $\cos(\theta) = -1$, see (3.3.5). The contact points, $x = x_w^{(L)}(t)$ and $x = x_w^{(R)}(t)$ on the boundary $y = 0$, see figure 2.1.1, correspond to points $\theta^L(t)$ and $\theta^R(t)$ on the circle $|\zeta| = 1$, see figure 3.3.1.

To determine θ^L and θ^R we use the formulae

$$\tan \frac{x}{2} = \frac{\sin x}{1 + \cos x}, \quad (3.3.6)$$

then equation (3.3.5) at $x = x_w^{(L)}$ gives

$$\tan \left(\frac{\theta^L}{2} \right) = \frac{x_w^{(L)} - x_c(t)}{\sqrt{y_c^2(t) - R^2}}. \quad (3.3.7)$$

Let $x_c > 0$ and $x_w^{(L)} < 0$ as in figure 2.1.1. Then right hand side of (3.3.7) is negative and

$$\frac{\theta^L}{2} = -\arctan \left(\frac{x_c(t) - x_w^{(L)}}{\sqrt{y_c^2(t) - R^2}} \right), \quad (3.3.8)$$

where the value of $\arctan(x)$ are from $-\pi/2$ to $\pi/2$. For positive x , one has

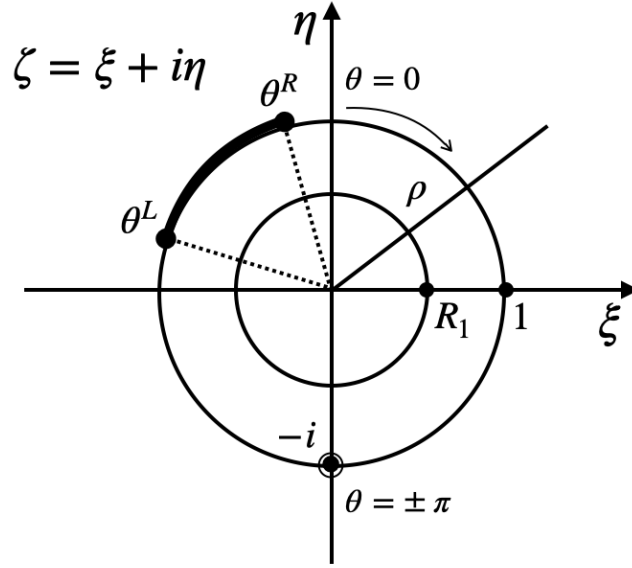


Figure 3.3.1: The complex ζ -plane.

$0 < \arctan x < \pi/2$. Finally

$$\theta^L(t) = -2 \arctan \left(\frac{x_c(t) - x_w^{(L)}(t)}{\sqrt{y_c^2(t) - R^2}} \right), \quad (3.3.9)$$

and $-\pi < \theta^L < \theta^R < 0$ because the cylinder is located in the right of the entering body as in the figure 2.1.1, where the whole contact region will be in the left otherwise if the cylinder is located under the entering body then $-\pi < \theta^L < \theta^R < \pi$ and if the cylinder is located in the left of entering body then $0 < \theta^L < \theta^R < \pi$. Clearly we can obtain θ^R from (3.3.9) by changing $x_w^{(L)}$ to $x_w^{(R)}$:

$$\theta^R(t) = -2 \arctan \left(\frac{x_c(t) - x_w^{(R)}(t)}{\sqrt{y_c^2(t) - R^2}} \right). \quad (3.3.10)$$

Using the mapping (3.3.1), where $\zeta = \rho e^{i(\pi/2 - \theta)}$ and $R_1 \leq \rho \leq 1$, we can define the corresponding velocity potential in the ζ -plane,

$$\varphi(x, y, t) = \varphi [x(\rho, \theta, t), y(\rho, \theta, t)] = \Phi(\rho, \theta, t). \quad (3.3.11)$$

In other words, a conformal mapping transfers a velocity potential in the

original z -plane to the potential in the complex ζ -plane, where $\Phi(\rho, \theta, t)$ satisfies the Laplace equation in the ring $R_1 < \rho < 1$. The dynamic boundary condition in (3.2.1) where the total pressure in the water is equal to the atmospheric pressure, gives

$$\Phi(1, \theta, t) = 0 \quad (\rho = 1, \quad -\pi < \theta < \theta^L, \quad \theta^R < \theta < \pi). \quad (3.3.12)$$

The hydrodynamic dimensionless pressure on the submerged cylinder is given by

$$p = -\frac{\partial \varphi}{\partial t}(x, y, t) \Big|_{x=cons, y=cons} \quad (x = x_c(t) + \cos \alpha, \quad y = y_c(t) + \sin \alpha). \quad (3.3.13)$$

Here

$$\varphi(x, y, t) = \Phi[\rho(x, y, t), \theta(x, y, t), t], \quad (3.3.14)$$

and by using the chain rule we calculate

$$\frac{\partial \varphi}{\partial t} = \frac{\partial \Phi}{\partial \rho} \frac{\partial \rho}{\partial t} + \frac{\partial \Phi}{\partial \theta} \frac{\partial \theta}{\partial t} + \frac{\partial \Phi}{\partial t}. \quad (3.3.15)$$

If the cylinder is stationary, then (3.1.6) gives

$$\frac{\partial \Phi}{\partial \rho}(R_1, \theta, t) = 0 \quad (\rho = R_1, \quad -\pi \leq \theta < \pi). \quad (3.3.16)$$

By differentiated (3.3.11) in ρ and set $\rho = 1$, we get

$$\Phi_\rho(1, \theta, t) = \varphi_x x_\rho + \varphi_y y_\rho. \quad (3.3.17)$$

Equation (3.3.1) defines $z = z(\zeta)$ as analytic function in $R_1 < \rho < 1$. For an analytic function

$$\frac{dz}{d\zeta} = \frac{dz}{d\rho} = \frac{dz}{i\rho d\theta} = x_\rho + iy_\rho = \frac{1}{i\rho} (x_\theta + iy_\theta). \quad (3.3.18)$$

At $\rho = 1 : x_\rho = y_\theta, y_\rho = -x_\theta$. However, $y(1, \theta, t) = 0$, which gives $y_\theta(1, \theta, t) = 0$ and $x_\rho(1, \theta, t) = 0$. Also using (3.3.5) gives

$$y_\rho(1, \theta, t) = -x_\theta(1, \theta, t) = -\sqrt{y_0^2 - R^2} \frac{d}{d\theta} \left(\frac{\sin \theta}{1 + \cos \theta} \right). \quad (3.3.19)$$

Therefore,

$$\begin{aligned} \Phi_\rho(1, \theta, t) &= \varphi_x \cdot 0 + \varphi_y \cdot y_\rho(1, \theta, t) \\ &= -h'(t) \sqrt{y_0^2 - R^2} \left(\frac{\cos \theta (1 + \cos(\theta)) + \sin^2(\theta)}{(1 + \cos(\theta))^2} \right) \\ &= -h'(t) \sqrt{y_0^2 - R^2} \left(\frac{1 + \cos(\theta)}{(1 + \cos \theta)^2} \right) \\ &= \frac{-h'(t) \sqrt{y_c^2(t) - R^2}}{1 + \cos \theta}, \quad (\theta^L < \theta < \theta^R). \end{aligned} \quad (3.3.20)$$

Thus, the water impact problem within the Wagner model formulated in the ζ -plane for a stationary submerged cylinder reads

$$\left\{ \begin{array}{ll} \nabla^2 \Phi = 0 & (R_1 < \rho < 1), \\ \Phi = 0 & (\rho = 1, (-\pi, \pi) \setminus (\theta^L, \theta^R)), \\ \Phi_\rho = \frac{-h'(t) \sqrt{y_c^2(t) - R^2}}{1 + \cos \theta} & (\rho = 1, \theta^L < \theta < \theta^R) \\ \Phi_\rho = 0 & (\rho = R_1, \theta \leq \theta < 2\pi). \end{array} \right. \quad (3.3.21)$$

Now we need to find R_1 for the submerged cylinder, $z = z_c + e^{i\alpha}$, $z_c = x_c(t) + iy_c(t)$, $0 < \alpha < 2\pi$. Equation (3.3.1) with $\zeta = R_1 e^{i(\pi/2 - \theta)}$ gives

$$\frac{z_c + e^{i\alpha} - x_c(t)}{\sqrt{y_c^2(t) - R^2}} = i + \frac{2}{iR_1 e^{-i\theta} + i}, \quad (3.3.22)$$

where the right hand side is

$$\begin{aligned}
 i + \frac{2}{i(\rho e^{-i\theta} + 1)} \frac{i}{i} \\
 &= i - \frac{2i}{\rho \cos(\theta) + 1 - i\rho \sin(\theta)} \frac{(\rho \cos(\theta) + 1 + i\rho \sin(\theta))}{(\rho \cos(\theta) + 1 + i\rho \sin(\theta))} \\
 &= i - \frac{2i(\rho \cos(\theta) + 1 - i\rho \sin(\theta))}{(\rho \cos(\theta) + 1)^2 + \rho \sin(\theta)^2} \\
 &= i \left\{ 1 - 2 \frac{\rho \cos(\theta) + 1 + i\rho \sin(\theta)}{\rho^2 + 2\rho \cos(\theta) + 1} \right\}, \quad (3.3.23)
 \end{aligned}$$

and the left hand side is

$$\begin{aligned}
 \frac{z - x_c(t)}{\sqrt{y_c^2(t) - R^2}} &= \frac{x + iy - x_c(t)}{\sqrt{y_c^2(t) - R^2}} = \frac{z_c + e^{i\alpha} - x_c(t)}{\sqrt{y_c^2(t) - R^2}} \\
 &= \frac{\cos(\alpha) + iy_c(t) + i \sin(\alpha)}{\sqrt{y_c^2(t) - R^2}}, \quad (3.3.24)
 \end{aligned}$$

separating real and imaginary parts using (3.3.23) and (3.3.24) gives

$$\frac{R \cos(\alpha)}{\sqrt{y_c^2(t) - R^2}} = 2 \frac{\rho \sin(\theta)}{\rho^2 + 2\rho \cos(\theta) + 1}, \quad (3.3.25)$$

and

$$\frac{y_c(t) + R \sin(\alpha)}{\sqrt{y_c^2(t) - R^2}} = 1 - 2 \frac{\rho \cos(\theta) + 1}{\rho^2 + 2\rho \cos(\theta) + 1}, \quad (3.3.26)$$

for $\rho = R_1$ we have

$$\frac{R \cos(\alpha)}{\sqrt{y_c^2(t) - R^2}} = 2 \frac{R_1 \sin(\theta)}{R_1^2 + 2R_1 \cos(\theta) + 1}, \quad (3.3.27)$$

and

$$\frac{R \sin(\alpha)}{\sqrt{y_c^2(t) - R^2}} = -\frac{y_c(t)}{\sqrt{y_c^2(t) - R^2}} + 1 - 2 \frac{R_1 \cos(\theta) + 1}{R_1^2 + 2R_1 \cos(\theta) + 1}. \quad (3.3.28)$$

Then we have

$$\frac{R^2}{y_c^2(t) - R^2} = \left(1 - \frac{y_c(t)}{\sqrt{y_c^2(t) - R^2}}\right)^2 + \frac{4}{R_1^2 + 1 + 2R_1 \sin \theta} \underbrace{\left\{1 - \left(1 - \frac{y_c(t)}{\sqrt{y_c^2(t) - R^2}}\right) (1 + R_1 \sin \theta)\right\}}_{\bar{A}}. \quad (3.3.29)$$

and

$$\begin{aligned} \bar{A} &= \frac{y_c(t)}{\sqrt{y_c^2(t) - R^2}} - R_1 \left(1 - \frac{y_c(t)}{\sqrt{y_c^2(t) - R^2}}\right) \sin \theta \\ &= - \left(1 - \frac{y_c(t)}{\sqrt{y_c^2(t) - R^2}}\right) \\ &\quad \cdot \frac{1}{2} \left(2R_1 \sin \theta - \frac{2y_c(t)}{\sqrt{y_c^2(t) - R^2}} \frac{1}{1 - \frac{y_c(t)}{\sqrt{y_c^2(t) - R^2}}}\right). \end{aligned} \quad (3.3.30)$$

Then

$$\frac{2y_c(t)/\sqrt{y_c^2(t) - R^2}}{y_c(t)/\sqrt{y_c^2(t) - R^2} - 1} = R_1^2 + 1. \quad (3.3.31)$$

Using the equation (3.3.29) gives

$$\begin{aligned} \frac{R^2}{y_c^2(t) - R^2} &= 1 - \frac{2y_c(t)}{\sqrt{y_c^2(t) - R^2}} - 2 \left(1 - \frac{y_c(t)}{\sqrt{y_c^2(t) - R^2}}\right) \\ &= -1 + \frac{y_c(t)2}{\sqrt{y_c^2(t) - R^2}} = \frac{R^2}{\sqrt{y_c^2(t) - R^2}}, \end{aligned} \quad (3.3.32)$$

and using (3.3.31) to finding R_1 gives

$$2 \frac{y_c(t)}{\sqrt{y_c^2(t) - R^2}} = R_1^2 \left(\frac{y_c(t)}{\sqrt{y_c^2(t) - R^2}} - 1 \right) + \frac{y_c(t)}{\sqrt{y_c^2(t) - R^2}} - 1,$$

this gives

$$R_1 = \frac{- \left(y_c(t) + \sqrt{y_c^2(t) - R^2} \right)}{R}. \quad (3.3.33)$$

where the minus in (3.3.33) is because of $R_1 > 0$ and $y_c < 0$.

A relation between α and θ at $|\zeta| = R_1$ follows from (3.3.28). By denote $R_1^2 + 1 + 2R_1 \cos(\theta) = D$ in (3.3.27), we find from (3.3.27) and (3.3.28),

$$\frac{R}{\sqrt{y_c^2(t) - R^2}} \cos \alpha = \frac{2}{D} R_1 \sin \theta, \quad (3.3.34)$$

$$\frac{R}{\sqrt{y_c^2(t) - R^2}} \sin \alpha = 1 - \frac{y_c(t)}{\sqrt{y_c^2(t) - R^2}} - \frac{2}{D} (1 + R_1 \cos \theta), \quad (3.3.35)$$

Dividing (3.3.35) by (3.3.34), we obtain

$$\begin{aligned} \tan \alpha &= \frac{\sin \alpha}{\cos \alpha} = \frac{1 - y_c(t)/\sqrt{y_c^2(t) - R^2} - 2(1 + R_1 \cos \theta)/D}{2R_1 \sin \theta/D} \\ &= \frac{\frac{D}{2} \left(1 - y_c(t)/\sqrt{y_c^2(t) - R^2}\right) - 1 - R_1 \cos \theta}{R_1 \sin \theta} = \\ &= \frac{\frac{R_1^2+1}{2} \left(1 - y_c(t)/\sqrt{y_c^2(t) - R^2}\right)}{R_1 \sin \theta} \\ &+ \frac{R_1 \cos \theta \left(1 - y_c(t)/\sqrt{y_c^2(t) - R^2}\right) - 1 - R_1 \cos \theta}{R_1 \sin \theta}, \end{aligned} \quad (3.3.36)$$

where

$$\begin{aligned} &\frac{R_1^2+1}{2} \left(1 - y_c(t)/\sqrt{y_c^2(t) - R^2}\right) = \\ &\frac{1}{2\sqrt{y_c^2(t) - R^2}R^2} \left(y_c(t) + \sqrt{y_c^2(t) - R^2}\right) (y_c^2(t) - R^2 - y_0^2) \\ &\quad + \left(\frac{\sqrt{y_c^2(t) - R^2} - y_c(t)}{2\sqrt{y_c^2(t) - R^2}}\right) \\ &= -\frac{R^2}{2\sqrt{y_c^2(t) - R^2}R^2} \left(y_c(t) + \sqrt{y_c^2(t) - R^2}\right) + \frac{1}{2} - \frac{y_c(t)}{2\sqrt{y_c^2(t) - R^2}} \\ &= -\frac{1}{2\sqrt{y_c^2(t) - R^2}} \left(y_c(t) + \sqrt{y_c^2(t) - R^2}\right) + \frac{1}{2} - \frac{y_c(t)}{2\sqrt{y_c^2(t) - R^2}} \\ &= -\frac{y_c(t)}{\sqrt{y_c^2(t) - R^2}}, \frac{R_1^2+1}{2} \left(1 - y_c(t)/\sqrt{y_c^2(t) - R^2}\right) - 1 \\ &= -\frac{y_c(t)}{\sqrt{y_c^2(t) - R^2}} - 1 = -\frac{y_c(t)}{\sqrt{y_c^2(t) - R^2}} - 1 \\ &= \frac{R_1 \cdot R}{\sqrt{y_c^2(t) - R^2}}, \end{aligned} \quad (3.3.37)$$

then

$$\tan \alpha = \frac{R_1 \cdot R / \sqrt{y_c^2(t) - R^2} - R_1 \cos \theta \left(y_c(t) / \sqrt{y_c^2(t) - R^2} \right)}{R_1 \sin \theta} = \frac{R - \cos \theta y_c(t)}{\sqrt{y_c^2(t) - R^2} \sin \theta}. \quad (3.3.38)$$

Let $y_c = -H$, $H > 0$ is the distance of the center of the cylinder from the Wagner free surface $y = 0$. Then

$$\tan \alpha = \frac{R + H \cos \theta}{\sqrt{H^2 - R^2} \sin \theta} = \frac{\lambda + \cos \theta}{\sqrt{1 - \lambda^2} \sin \theta}, \quad (3.3.39)$$

where $\lambda = R/H$. Here $\lambda = 1$ when the cylinder touches the water surface, which is not allowed in this analysis.

Similar to (3.3.18), where $z = z_* + (\rho - R + iR(\alpha - \alpha_*))e^{-i\alpha_*}$ at a point z_* on the cylinder surface and $\zeta = \zeta_* + (r - R_1 + iR_1(\theta - \theta_*))e^{-i\theta_*}$, see figure 3.3.2.

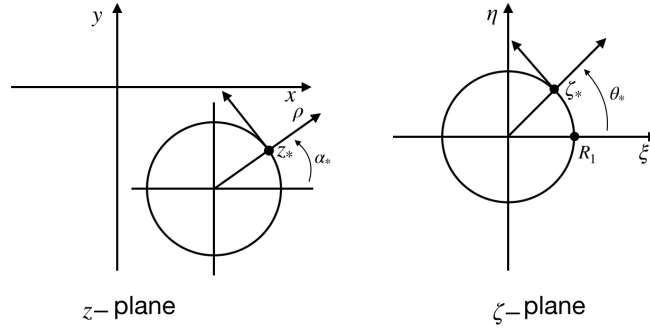


Figure 3.3.2: The original z -plane and the complex ζ -plane.

Then

$$\frac{dz}{d\zeta} = \left(\frac{\partial \rho}{\partial r} + iR \frac{\partial \alpha}{\partial r} \right) e^{-i\alpha_*} = \left(\frac{1}{iR_1} \frac{\partial \rho}{\partial \theta} + \frac{R}{R_1} \frac{\partial \alpha}{\partial \theta} \right) e^{-i\alpha_*}, \quad (3.3.40)$$

and by comparing real and imaginary parts in (3.3.40),

$$\frac{\partial \rho}{\partial r} = \frac{R}{R_1} \frac{\partial \alpha}{\partial \theta} \quad \text{and} \quad \frac{\partial \alpha}{\partial r} = \frac{1}{RR_1} \frac{\partial \rho}{\partial \theta}, \quad (3.3.41)$$

at $r = R_1$ where $\rho = R$, therefore $\partial\rho/\partial\theta = 0$ and $\partial\alpha/\partial r = 0$. To find the derivative $\partial\alpha/\partial\theta(R_1, \theta)$ we differentiate (3.3.39) with respect to θ ,

$$\begin{aligned} \frac{1}{\cos^2 \alpha} \frac{\partial \alpha}{\partial \theta} &= \frac{-\sin \theta}{\sqrt{1-\lambda^2} \sin \theta} - \frac{\lambda + \cos \theta}{\sqrt{1-\lambda^2} \sin^2 \theta} (\cos \theta) \\ &= \frac{1}{\sqrt{1-\lambda^2}} \left(-1 - \frac{\lambda \cos \theta + \cos^2 \theta}{\sin^2 \theta} \right) \\ &= \frac{-1}{\sqrt{1-\lambda^2}} \frac{1 + \lambda \cos \theta}{\sin^2 \theta}, \end{aligned} \quad (3.3.42)$$

and $\cos^2 \alpha$ is also calculated by using (3.3.39)

$$\begin{aligned} \frac{1}{\cos^2 \alpha} &= 1 + \tan^2 \alpha = 1 + \frac{(\lambda + \cos \theta)^2}{(1-\lambda^2) \sin^2 \theta} \\ &= \frac{\sin^2 \theta - \lambda^2 \sin^2 \theta + \lambda^2 + 2\lambda \cos \theta + \cos^2 \theta}{(1-\lambda^2) \sin^2 \theta} \\ &= \frac{1 + 2\lambda \cos \theta + \lambda^2 \cos^2 \theta}{(1-\lambda^2) \sin^2 \theta} = \frac{(1 + \lambda \cos \theta)^2}{(1-\lambda^2) \sin^2 \theta}. \end{aligned} \quad (3.3.43)$$

Substituting (3.3.43) in (3.3.42), we obtain

$$\frac{\partial \alpha}{\partial \theta}(R_1, \theta) = \frac{-1}{\sqrt{1-\lambda^2}} \frac{1 + \lambda \cos \theta}{\sin^2 \theta} \frac{(1-\lambda^2) \sin^2 \theta}{(1 + \lambda \cos \theta)^2} = -\sqrt{1-\lambda^2} \frac{1}{1 + \lambda \cos \theta}. \quad (3.3.44)$$

Equation (3.3.43) also gives

$$\cos \alpha = \frac{\sqrt{1-\lambda^2} \sin \theta}{(1 + \lambda \cos \theta)}, \quad (3.3.45)$$

and

$$\begin{aligned} \sin \alpha &= \tan \alpha \cdot \cos \alpha = \frac{\lambda + \cos \theta}{\sqrt{1-\lambda^2} \sin \theta} \cdot \sqrt{1-\lambda^2} \frac{\sin \theta}{1 + \lambda \cos \theta} \\ &= \frac{\lambda + \cos \theta}{1 + \lambda \cos \theta}. \end{aligned} \quad (3.3.46)$$

Similarly to (3.3.20) we calculate $\partial\Phi/\partial\rho(R_1, \theta, t)$ as

$$\begin{aligned} \frac{\partial\Phi}{\partial\rho}(R_1, \theta, t) &= \frac{\partial\varphi}{\partial r} \frac{\partial\rho}{\partial r} + \frac{\partial\varphi}{\partial\alpha} \frac{\partial\alpha}{\partial r} = \frac{\partial\varphi}{\partial r} \frac{R}{R_1} \frac{\partial\alpha}{\partial\theta}(R_1, \theta) + \frac{\partial\varphi}{\partial\alpha} \cdot 0 \\ &= -\frac{R}{R_1} \sqrt{1-\lambda^2} \frac{1}{1+\lambda\cos\theta} \left(\frac{dx_c}{dt} \cos\alpha + \frac{dy_c}{dt} \sin\alpha \right). \end{aligned} \quad (3.3.47)$$

Substituting (3.3.45) and (3.3.46) into (3.3.47) gives

$$\frac{\partial\Phi}{\partial\rho}(R_1, \theta, t) = -\frac{R}{R_1} \sqrt{1-\lambda^2} \frac{\dot{x}_c \sqrt{1-\lambda^2} \sin\theta + \dot{y}_c (\lambda + \cos\theta)}{(1+\lambda\cos\theta)^2}. \quad (3.3.48)$$

For a stationary cylinder, when $\dot{x}_c = 0$ and $\dot{y}_c = 0$, then (3.3.48) provides

$$\frac{\partial\Phi}{\partial\rho} = 0, \quad (3.3.49)$$

as in (3.3.21).

3.3.1 Summary of the water impact problem within the Wagner model formulated in the ζ -plane

Our formulated impact problem within the Wagner model is written as

$$\left\{ \begin{array}{ll} \nabla^2\Phi = 0 & (R_1 < \rho < 1), \\ \Phi = 0 & (\rho = 1, (-\pi, \pi) \setminus (\theta^L, \theta^R)), \\ \Phi_\rho = \frac{-h'(t)\sqrt{y_c^2(t) - R^2}}{1 + \cos\theta} & (\rho = 1, \theta^L < \theta < \theta^R), \\ \Phi = 0 & (\rho = 1, \theta = \pm\pi), \\ \Phi_\rho = -\frac{R}{R_1} \sqrt{1-\lambda^2} \frac{\dot{x}_c \sqrt{1-\lambda^2} \sin\theta + \dot{y}_c (\lambda + \cos\theta)}{(1+\lambda\cos\theta)^2} & (\rho = R_1, -\pi < \theta < \pi). \end{array} \right. \quad (3.3.50)$$

The first equation in (3.3.50) implies that the velocity potential of the flow $\Phi(\rho, \theta, t)$ satisfies the Laplace equation in the ring $R_1 < \rho < 1$. The second line is the dynamic boundary condition of the free-surface image in the ζ -plane which is given by (3.3.12). The third line is the boundary condition on the image of the contact region in ζ -plane. The fourth line is the far-field

condition corresponding to infinity in the z -plane, where the fluid is at rest at any time. The fifth line is the boundary condition on the surface of the stationary circular cylinder. For a stationary cylinder where $(\dot{x}_c = \dot{y}_c = 0)$ the boundary condition on $\rho = R_1$ reads $\Phi_\rho = 0$.

Analytical solution of the water
impact problem in the presence of a
submerged circular cylinder within
the Wagner model

In this chapter, the solution of the water impact problem (3.3.50) formulated within the Wagner model in the ζ -plane is derived.

From (3.3.50) and (3.3.20) let the function $f(\theta)$ as

$$f(\theta) = \frac{-h'(t)\sqrt{y_c^2(t) - R^2}}{1 + \cos \theta}, \quad (4.0.1)$$

The boundary condition at ($\rho = R_1$) can be written as

$$\Phi_\rho = -\frac{R}{R_1}(1 - \lambda^2)\dot{x}_c F_1(\theta) + \frac{R}{R_1}\sqrt{1 - \lambda^2}\dot{y}_c F_2(\theta), \quad (\rho = R_1, -\pi < \theta < \pi), \quad (4.0.2)$$

where

$$F_1(\theta) = \frac{\sin \theta}{(1 + \lambda \cos \theta)^2} \quad \text{and} \quad F_2(\theta) = \frac{\lambda + \cos \theta}{(1 + \lambda \cos \theta)^2}. \quad (4.0.3)$$

Note that $F_1(\theta)$ is an odd function and $F_2(\theta)$ is an even function. Their Fourier series are

$$F_1(\theta) = \sum_{n=1}^{\infty} F_{1n}(\lambda) \sin(n\theta), \quad (4.0.4)$$

$$F_2(\theta) = F_{20}(\lambda) + \sum_{n=1}^{\infty} F_{2n}(\lambda) \cos(n\theta), \quad (4.0.5)$$

where

$$F_{1n}(\lambda) = \frac{1}{\pi} \int_{-\pi}^{\pi} F_1(\theta) \sin(n\theta) d\theta = \frac{1}{\pi} \int_{-\pi}^{\pi} \frac{\sin \theta \sin(n\theta)}{(1 + \lambda \cos \theta)^2} d\theta, \quad (4.0.6)$$

$$F_{20}(\lambda) = \frac{1}{2\pi} \int_{-\pi}^{\pi} F_2(\theta) \cos(n\theta) d\theta = \frac{1}{2\pi} \int_{-\pi}^{\pi} \frac{\lambda + \cos \theta}{(1 + \lambda \cos \theta)^2} d\theta, \quad (4.0.7)$$

$$F_{2n}(\lambda) = \frac{1}{\pi} \int_{-\pi}^{\pi} F_2(\theta) \cos(n\theta) d\theta = \frac{1}{\pi} \int_{-\pi}^{\pi} \frac{(\lambda + \cos \theta) \cos(n\theta)}{(1 + \lambda \cos \theta)^2} d\theta. \quad (4.0.8)$$

Thus

$$\begin{aligned} \Phi_\rho(R_1, \theta, t) = & -\frac{R}{R_1}(1 - \lambda^2)\dot{x}_c \sum_{n=1}^{\infty} F_{1n}(\lambda) \sin(n\theta) \\ & + \frac{R}{R_1}\sqrt{1 - \lambda^2}\dot{y}_c \left(F_{20}(\lambda) + \sum_{n=1}^{\infty} F_{2n}(\lambda) \cos(n\theta) \right), \end{aligned}$$

(4.0.9) $(R_1, -\pi < \theta < \pi)$.

By using the separation of variable method for Laplace's equation in polar coordinates, we find a general solution for the velocity potential,

$$\begin{aligned} \Phi(\rho, \theta, t) = & (a_0 + b_0 \log \rho) + \sum_{n=1}^{\infty} (\rho^n + d_n \rho^{-n}) (a_n \cos(n\theta) + b_n \sin(n\theta)), \\ & (R_1 < \rho < 1), \quad (-\pi < \theta < \pi), \end{aligned}$$

(4.0.10)

where the coefficients $a_0(t)$, $b_0(t)$, $d_n(t)$, $a_n(t)$ and $b_n(t)$ are to be determined using the boundary conditions and the far-field condition,

$$\Phi(1, \pm\pi) = 0. \tag{4.0.11}$$

and

$$\begin{aligned} \Phi_\rho(\rho, \theta, t) = & b_0 \frac{1}{\rho} + \sum_{n=1}^{\infty} (n\rho^{n-1} + d_n(-n)\rho^{-n-1}) (a_n \cos(n\theta) + b_n \sin(n\theta)), \\ & (R_1 < \rho < 1), \quad (-\pi < \theta < \pi). \end{aligned}$$

(4.0.12)

4.1 The coefficients $F_{1n}(\lambda)$, $F_{20}(\lambda)$ and $F_{2n}(\lambda)$

To evaluate $F_{1n}(\lambda)$, we use the following equality,

$$\frac{d}{d\theta}(1 + \lambda \cos \theta)^{-1} = -(1 + \lambda \cos \theta)^{-2}(-\lambda \sin \theta) = \lambda \frac{\sin \theta}{(1 + \lambda \cos \theta)^2}.$$

Then integrating by parts,

$$\begin{aligned}
 F_{1n}(\lambda) &= \frac{1}{\pi\lambda} \int_{-\pi}^{\pi} \sin(n\theta) \left(\frac{1}{1 + \lambda \cos \theta} \right)' d\theta \\
 &= -\frac{1}{\pi\lambda} \int_{-\pi}^{\pi} n \cos(n\theta) \left(\frac{1}{1 + \lambda \cos \theta} \right) d\theta \\
 &= -\frac{n}{\pi\lambda} \int_{-\pi}^{\pi} \frac{\cos(n\theta)}{1 + \lambda \cos \theta} d\theta, \quad (4.1.1)
 \end{aligned}$$

where Tables of Integrals [13] provide

$$\int_0^{\pi} \frac{\cos(n\theta)}{1 + \lambda \cos \theta} d\theta = \frac{\pi}{\sqrt{1 - \lambda^2}} \left(\frac{\sqrt{1 - \lambda^2} - 1}{\lambda} \right)^n, \quad 0 < \lambda < 1. \quad (4.1.2)$$

Therefore,

$$\begin{aligned}
 F_{1n}(\lambda) &= -\frac{n}{\pi\lambda} \int_{-\pi}^{\pi} \frac{\cos(n\theta)}{1 + \lambda \cos \theta} d\theta = -\frac{2n}{\lambda\sqrt{1 - \lambda^2}} \left(\frac{\sqrt{1 - \lambda^2} - 1}{\lambda} \right)^n, \\
 &\quad (0 < \lambda < 1). \quad (4.1.3)
 \end{aligned}$$

Using the definitions,

$$R_1 = \frac{-\left(y_c(t) + \sqrt{y_c^2(t) - R^2}\right)}{R}, \quad \lambda = \frac{R}{H}, \quad y_c(t) = -H, \quad (4.1.4)$$

we find

$$R_1 = -\frac{1}{R} \left(-H + \sqrt{H^2 - R^2} \right) = \frac{H}{R} \left(1 - \sqrt{1 - \frac{R^2}{H^2}} \right) = \frac{1 - \sqrt{1 - \lambda^2}}{\lambda}. \quad (4.1.5)$$

And finally

$$F_{1n}(\lambda) = \frac{2nR_1^n (-1)^{n+1}}{\lambda\sqrt{1 - \lambda^2}} \quad (0 < \lambda < 1). \quad (4.1.6)$$

Then by using Matlab for checking and confirming the formulae (4.1.6) we find that the formulae has good evaluation for the F_{1n} (4.0.6) as shown in Table 4.1.

$F_{1n}(\lambda)$			
λ	Integral (4.0.6)	Formulae (4.1.6)	Differences
0.01	0.0049507	0.0049507	$1.1227E-14$
0.15	0.0043976	0.0043976	$2.2898E-16$
0.29	0.0040551	0.0040552	$-4.1633E-17$
0.43	0.0038728	0.0038728	$6.9389E-18$
0.57	0.0038761	0.0038763	$-2.7756E-17$
0.71	0.0041522	0.0041522	$-2.7756E-17$
0.85	0.0051292	0.0051292	$-2.7756E-17$
0.99	0.0022088	0.0022088	$-2.3037E-15$

Table 4.1: Table to show the differences between (4.0.6) and (4.1.6) with different λ where $n = 20$.

To evaluate $F_{2n}(\lambda)$ we use Tables of Integrals [13],

$$\begin{aligned} \int_0^\pi \frac{\cos(n\theta)}{(1 - 2a \cos \theta + a^2)^2} d\theta &= \int_0^\pi \frac{\cos(n\theta)}{(1 + a^2)^2 \left(1 - \frac{2a}{1+a^2} \cos \theta\right)^2} d\theta \\ &= \frac{\pi a^{4+n-2}}{(1 - a^2)^3} \left[\binom{n+1}{0} \binom{2}{1} + \binom{1+n}{1} \binom{1}{1} \left(\frac{1-a^2}{a^2}\right) \right], \\ &\hspace{15em} (a^2 < 1). \end{aligned} \quad (4.1.7)$$

This table integral is related to the integral (4.0.8) if λ and a are related by

$$\lambda = \frac{-2a}{1 + a^2}, \quad (4.1.8)$$

which gives

$$a = \frac{-1 + \sqrt{1 - \lambda^2}}{\lambda} = -R_1. \quad (4.1.9)$$

Then

$$\begin{aligned} \int_{-\pi}^\pi \frac{\cos(n\theta)}{(1 + \lambda \cos \theta)^2} d\theta &= 2\pi \frac{(1 + R_1^2)^2 (-R_1)^{n+2}}{(1 - R_1^2)^3} \left[2 + (n+1) \frac{1 - R_1^2}{R_1^2} \right] \\ &= \frac{2\pi}{1 - \lambda^2} (-R_1)^n \left(\frac{1}{\sqrt{1 - \lambda^2}} + n \right). \end{aligned} \quad (4.1.10)$$

The integral (4.0.8) can be decomposed as

$$\begin{aligned}
 F_{2n}(\lambda) &= \frac{1}{\pi} \int_{-\pi}^{\pi} \frac{(\lambda + \cos \theta) \cos(n\theta)}{(1 + \lambda \cos \theta)^2} d\theta \\
 &= \frac{1}{\pi} \int_{-\pi}^{\pi} \frac{\lambda \cos(n\theta) + \cos \theta \cos n\theta}{(1 + \lambda \cos \theta)^2} d\theta = \frac{1}{\pi} \int_{-\pi}^{\pi} \frac{\lambda \cos(n\theta)}{(1 + \lambda \cos \theta)^2} d\theta \\
 &\quad + \frac{1}{2\pi} \int_{-\pi}^{\pi} \frac{\cos((n+1)\theta)}{(1 + \lambda \cos \theta)^2} d\theta + \frac{1}{2\pi} \int_{-\pi}^{\pi} \frac{\cos((n-1)\theta)}{(1 + \lambda \cos \theta)^2} d\theta. \quad (4.1.11)
 \end{aligned}$$

Applying (4.1.10) to these three integrals, we obtain

$$\begin{aligned}
 F_{2n}(\lambda) &= \frac{1}{\pi} \int_{-\pi}^{\pi} \frac{(\lambda + \cos \theta) \cos(n\theta)}{(1 + \lambda \cos \theta)^2} d\theta \\
 &= \frac{2(1+a^2)^2 a^{2+n} \lambda}{(1-a^2)^3} \left[2 + (1+n) \left(\frac{1-a^2}{a^2} \right) \right] \\
 &\quad + \frac{(1+a^2)^2 a^{3+n}}{(1-a^2)^3} \left[2 + (2+n) \left(\frac{1-a^2}{a^2} \right) \right] \\
 &\quad + \frac{(1+a^2)^2 a^{n+1}}{(1-a^2)^3} \left[2 + n \left(\frac{1-a^2}{a^2} \right) \right]. \quad (4.1.12)
 \end{aligned}$$

By algebra,

$$\begin{aligned}
 F_{2n}(\lambda) &= \frac{(1+a^2)^2}{(1-a^2)^3} a^{n+1} \left[2\lambda a \left(\frac{2a^2 + 1 - a^2 + n(1-a^2)}{a^2} \right) \right. \\
 &\quad \left. + a^2 \frac{2a^2 + 2 - 2a^2 + n(1-a^2)}{a^2} + \frac{2a^2 + n(1-a^2)}{a^2} \right] \\
 &= \frac{(1+a^2)^2}{(1-a^2)^3} a^{n+1} \left[\frac{n(1-a^2)}{a^2} (2\lambda a + a^2 + 1) + 2\lambda a \frac{a^2 + 1}{a^2} + 2 + 2 \right], \quad (4.1.13)
 \end{aligned}$$

where $a^2 + 1 = -2a/\lambda$, see (4.1.8). Then

$$F_{2n}(\lambda) = \frac{(1+a^2)^2 a^{n-1} n}{(1-a^2)^2} \left(2\lambda a - \frac{2a}{\lambda} \right) = (-1)^{n+1} R_1^n \frac{2n}{\lambda}. \quad (4.1.14)$$

The differences of (4.0.8) and (4.1.14) has been illustrated in Table 4.2.

$F_{2n}(\lambda)$					
λ	Integral (4.0.8)	Formulae (4.1.12)	Formulae (4.1.14)	(4.0.8) and (4.1.12) Differences	(4.0.8) and (4.1.14) Differences
0.01	0.049505	0.049505	0.049505	$-1.1102E-16$	$1.1227E-14$
0.15	0.043478	0.043478	0.043478	$-2.7756E-17$	$2.2204E-16$
0.29	0.038763	0.038763	0.038763	$-2.7756E-17$	$-6.9389E-17$
0.43	0.034965	0.034965	0.034965	$-1.3878E-17$	0
0.57	0.031847	0.031847	0.031847	$6.9389E-18$	$-1.3878E-17$
0.71	0.029241	0.029241	0.029241	$-2.0817E-17$	$1.0408E-17$
0.85	0.027022	0.027022	0.027022	$-4.1633E-17$	0
0.99	0.031158	0.031158	0.031158	$8.9512E-15$	$-3.747E-16$

Table 4.2: Table to show the differences between (4.0.8) and (4.1.12) with different λ where $n = 20$.

Finally, to evaluate $F_{20}(\lambda)$ (4.0.7), we use (4.1.7)

$$\begin{aligned}
 F_{20}(\lambda) &= \frac{1}{2\pi} \int_{-\pi}^{\pi} \frac{\lambda + \cos \theta}{(1 + \lambda \cos \theta)^2} d\theta = \frac{1}{2\pi} \int_{-\pi}^{\pi} \frac{\lambda}{(1 + \lambda \cos \theta)^2} d\theta \\
 &+ \frac{1}{2\pi} \int_{-\pi}^{\pi} \frac{\cos \theta}{(1 + \lambda \cos \theta)^2} d\theta = \frac{1}{(1 - \lambda^2)^{\frac{3}{2}}} \left(\lambda - R_1 \left(1 + \sqrt{1 - \lambda^2} \right) \right) = 0,
 \end{aligned}
 \tag{4.1.15}$$

because,

$$R_1 = \frac{1 - \sqrt{1 - \lambda^2}}{\lambda} = \frac{\lambda}{1 + \sqrt{1 - \lambda^2}}.
 \tag{4.1.16}$$

4.2 Convergence of the series for $F_{1n}(\lambda)$ and $F_{2n}(\lambda)$

The series

$$F_1(\theta) = \sum_{n=1}^{\infty} F_{1n}(\lambda) \sin(n\theta),
 \tag{4.2.1}$$

calculated with only three terms in shown in figure 4.2.1 for $\lambda = 1/2$ as function of θ . We introduce the difference as

$$D_N(\theta) = \frac{\sin \theta}{(1 + \lambda \cos \theta)^2} - \sum_{n=1}^N F_{1n}(\lambda) \sin(n\theta). \quad (4.2.2)$$

The difference $D_N(\theta)$ where N terms are retained in the series is shown in figure 4.2.2 for $\lambda = 0.5$. We obtain

$$|D_{10}(\theta)| < 4 \times 10^{-5},$$

$$|D_{20}(\theta)| < 1.5 \times 10^{-11},$$

$$|D_{40}(\theta)| < 1.5 \times 10^{-15}.$$

It is seen that the series for $F_1(\theta)$ converges quickly with the number of the retained terms, see (4.1.6).

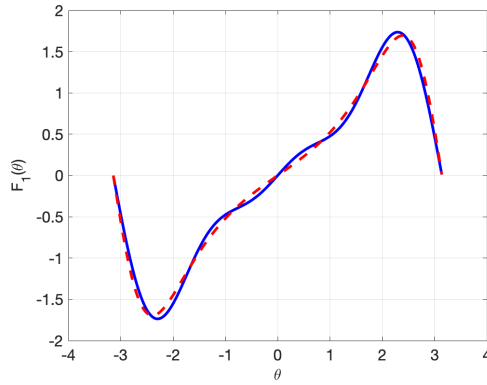


Figure 4.2.1: The series for $F_1(\theta)$ with three retained terms (blue line) and the function $F_1(\theta)$ (red line) for $\lambda = 0.5$.

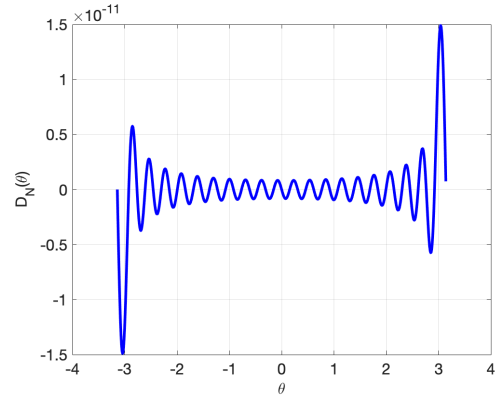


Figure 4.2.2: The differences $D(\theta)$ where the series for $F_1(\theta)$ with 20 terms and the function $F_1(\theta)$ for $\lambda = 0.5$.

Convergence of the series for shown in the same way as $F_1(\theta)$. $F_2(\theta)$ is

$$F_2(\theta) = \sum_{n=1}^{\infty} F_{2n}(\lambda) \cos(n\theta). \quad (4.2.3)$$

We introduce the difference

$$D_N^{(2)}(\theta) = \frac{\lambda + \cos \theta}{(1 + \lambda \cos \theta)^2} - \left(\sum_{n=1}^N F_{2n}(\lambda) \cos(n\theta) \right), \quad (4.2.4)$$

and calculate

$$\left| D_{10}^{(2)}(\theta) \right| < 3.8 \times 10^{-10}, \quad (4.2.5)$$

$$\left| D_{20}^{(2)}(\theta) \right| < 3 \times 10^{-14}, \quad (4.2.6)$$

$$\left| D_{40}^{(2)}(\theta) \right| < 2.4 \times 10^{-17}, \quad (4.2.7)$$

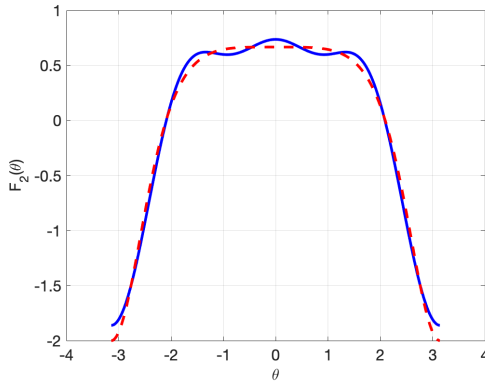


Figure 4.2.3: The series for $F_2(\theta)$ with three retained terms (blue line) and the function $F_2(\theta)$ (red line) for $\lambda = 0.5$.

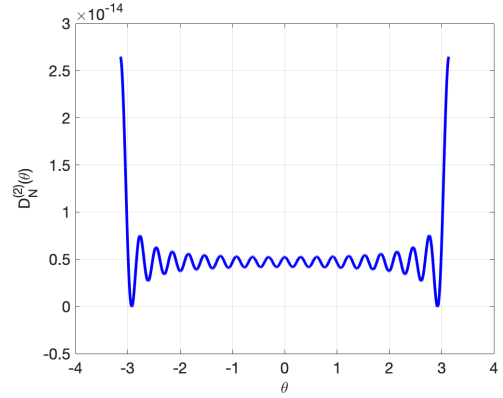


Figure 4.2.4: The differences $D_N^{(2)}(\theta)$ where the series for $F_2(\theta)$ with 20 terms and the function $F_2(\theta)$ for $\lambda = 0.5$.

4.3 Potential of flow caused by the cylinder moving under the free surface

It is convenient to present the potential in (3.3.50) as

$$\Phi(\rho, \theta, t) = \Phi_c(\rho, \theta, t) + \Phi_i(\rho, \theta, t), \quad (4.3.1)$$

where $\Phi_c(\rho, \theta, t)$ is the solution of the flow caused by motion of the cylinder without the impact on the water surface. The boundary value problem for

$\Phi_c(\rho, \theta, t)$ reads

$$\left\{ \begin{array}{ll} \nabla^2 \Phi_c = 0 & (R_1 < \rho < 1), \\ \Phi_c = 0 & (\rho = 1, \quad -\pi < \theta < \pi), \\ \frac{\partial \Phi_c}{\partial \rho} = \frac{R}{R_1} \sqrt{1 - \lambda^2} \left(\frac{\dot{x}_c \sqrt{1 - \lambda^2} \sin \theta + \dot{y}_c (\lambda + \cos \theta)}{(1 + \lambda \cos \theta)^2} \right) & (\rho = R_1, \quad -\pi \leq \theta < \pi). \end{array} \right. \quad (4.3.2)$$

The potential $\Phi_i(\rho, \theta, t)$ accounts for the flow caused by the impact.

In this section, the potential Φ_c is determined. Substituting (4.0.10) in the boundary condition $\Phi_c = 0$ at $\rho = 1$, we find

$$\Phi_c(1, \theta, t) = a_0^c + \sum_{n=0}^{\infty} (1 + d_n^c) (a_n^c \cos n\theta + b_n^c \sin n\theta) = 0, \quad (-\pi < \theta < \pi). \quad (4.3.3)$$

which gives $d_n^c = -1$ and $a_0^c = 0$. Substituting (4.3.3) in the boundary condition at $\rho = R_1$ and using the series for $F_{1n}(\theta)$ and $F_{2n}(\theta)$, we obtain

$$\begin{aligned} \frac{\partial \Phi_c}{\partial \rho}(R_1, \theta, t) &= b_0^c \frac{1}{R_1} + \sum_{n=1}^{\infty} (nR_1^{n-1} + d_n^c (-n)R_1^{-n-1}) (a_n^c \cos n\theta + b_n^c \sin n\theta) \\ &= -\frac{R}{R_1} (1 - \lambda^2) \dot{x}_c \sum_{n=1}^{\infty} F_{1n}(\theta) \sin n\theta \\ &\quad + \frac{R}{R_1} \sqrt{1 - \lambda^2} \dot{y}_c \left(+ \sum_{n=1}^{\infty} F_{2n}(\theta) \cos n\theta \right). \end{aligned} \quad (4.3.4)$$

Comparing the Fourier coefficients in (4.3.4) and using $d_n^c = -1$, we find

$$\frac{b_0^c}{R_1} = 0, \quad (4.3.5)$$

$$n (R_1^{n-1} + R_1^{-n-1}) a_n^c = \frac{R}{R_1} \sqrt{1 - \lambda^2} \dot{y}_c F_{2n}(\lambda), \quad (4.3.6)$$

$$n (R_1^{n-1} + R_1^{-n-1}) b_n^c = -\frac{R}{R_1} (1 - \lambda^2) \dot{x}_c F_{1n}(\lambda), \quad (4.3.7)$$

Thus

$$b_0^c = 0, \quad a_n^c = R \dot{y}_c \tilde{a}_n(\lambda) \quad \text{and} \quad b_n^c = -R \dot{x}_c \tilde{b}_n(\lambda), \quad (4.3.8)$$

where

$$\tilde{a}_n^c = (-1)^{n+1} 2 \frac{\sqrt{1-\lambda^2}}{\lambda} \frac{R_1^{2n}}{R_1^{2n}+1}, \quad (4.3.9)$$

and

$$\tilde{b}_n^c = -2 \frac{\sqrt{1-\lambda^2}}{\lambda} \frac{R_1^{2n}}{R_1^{2n}+1}. \quad (4.3.10)$$

Therefore

$$\Phi_c(\rho, \theta, t) = 2 \frac{R\sqrt{1-\lambda^2}}{\lambda} \sum_{n=1}^{\infty} \frac{(\rho^n - \rho^{-n}) R_1^{2n}}{R_1^{2n}+1} ((-1)^{n+1} \dot{y}_c \cos n\theta + \dot{x}_c \sin n\theta),$$

$$(R_1 < \rho < 1), \quad (-\pi < \theta < \pi). \quad (4.3.11)$$

where R_1 given by the equation (4.1.5). After, we found $\Phi_c(\rho, \theta, t)$ in (4.3.1), in following section the $\Phi_i(\rho, \theta, t)$ will be evaluated.

4.3.1 Velocity potential $\Phi_i(\rho, \theta, t)$

The potential $\Phi_i(\rho, \theta, t)$ in (4.3.1) describes the flow caused by impact on water surface in the presence of a stationary circular cylinder. The motion of the cylinder is taken into account through the modified boundary condition in the contact region, which corresponds to the interval $\theta^R(t) < \theta < \theta^L(t)$ of the circle $\rho = 1$ in the ζ -plane, see figure 3.3.1. The functions of time $\theta^R(t)$ and $\theta^L(t)$ are assumed given. The boundary condition for $\partial\Phi_i/\partial\rho(1, \theta, t)$ in the image of the contact region on the ζ -plane is obtained by using (4.3.1) gives

$$\frac{\partial\Phi_i}{\partial\rho}(1, \theta, t) = f(\theta, t) - \frac{\partial\Phi_c}{\partial\rho}(1, \theta, t) \quad (\rho = 1, \theta^L < \theta < \theta^R). \quad (4.3.12)$$

Therefore, the boundary value problem for Φ_i reads

$$\left\{ \begin{array}{ll} \nabla^2\Phi_i = 0 & (R_1 < \rho < 1), \\ \Phi_i = 0 & (\rho = 1, (-\pi, \pi) \setminus (\theta^L, \theta^R)), \\ \frac{\partial\Phi_i}{\partial\rho} = f(\theta) - \frac{\partial\Phi_c}{\partial\rho} & (\rho = 1, \theta^L < \theta < \theta^R), \\ \frac{\partial\Phi_i}{\partial\rho} = 0 & (\rho = R_1, -\pi \leq \theta < \pi). \end{array} \right. \quad (4.3.13)$$

To solve this mixed boundary value problem, we assume that Φ_i is given in the interval $\theta^L < \theta < \theta^R$. Let

$$\Phi_i(1, \theta, t) = F(\theta, t) \quad (\theta^L < \theta < \theta^R), \quad (4.3.14)$$

where the function $F(\theta, t)$ is zero at the ends of the interval because the potential should be continuous up to the boundary to avoid high singularity of the velocity potential there. This function should be determined to satisfy the condition in the contact region,

$$\frac{\partial\Phi_i}{\partial\rho}(1, \theta, t)\langle F \rangle = f(\theta, t) - \frac{\partial\Phi_c}{\partial\rho}, \quad (\theta^L < \theta < \theta^R), \quad (4.3.15)$$

where $\partial\Phi_i/\partial\rho(1, \theta, t)\langle F \rangle$ is a linear operator acting on the unknown function

$F(\theta, t)$. It is convenient to introduce the Fourier series of $\Phi_i(1, \theta, t)$

$$\Phi_i(1, \theta, t) = \begin{cases} F(\theta, t) & (\theta^L < \theta < \theta^R) \\ 0 & \text{otherwise} \end{cases} = a_0 + \sum_{n=1}^{\infty} \{a_n \cos(n\theta) + b_n \sin(n\theta)\}, \quad (4.3.16)$$

where

$$\begin{aligned} a_0(t) &= \frac{1}{2\pi} \int_{\theta^L}^{\theta^R} F(\theta, t) d\theta, \\ a_n(t) &= \frac{1}{\pi} \int_{\theta^L}^{\theta^R} F(\theta, t) \cos(n\theta) d\theta, \\ b_n(t) &= \frac{1}{\pi} \int_{\theta^L}^{\theta^R} F(\theta, t) \sin(n\theta) d\theta, \end{aligned} \quad (4.3.17)$$

are unknown coefficients. The solution of problem (4.3.13) with the condition (4.3.16) at $\rho = 1$ is

$$\Phi_i(\rho, \theta, t) = a_0(t)\Phi_{i0}(\rho, \theta) + \sum_{n=1}^{\infty} \{a_n(t)\Phi_{in}^{(c)}(\rho, \theta) + b_n(t)\Phi_{in}^{(s)}(\rho, \theta)\}, \quad (4.3.18)$$

where

$$\begin{cases} \nabla^2 \Phi_{in}^{(c)} = 0 & (R_1 < \rho < 1), \\ \Phi_{in}^{(c)}(1, \theta) = \cos(n\theta), & \frac{\partial \Phi_{in}^{(c)}}{\partial \rho}(R_1, \theta) = 0, \end{cases} \quad (4.3.19)$$

and

$$\begin{cases} \nabla^2 \Phi_{in}^{(s)} = 0 & (R_1 < \rho < 1), \\ \Phi_{in}^{(s)}(1, \theta) = \sin(n\theta), & \frac{\partial \Phi_{in}^{(s)}}{\partial \rho}(R_1, \theta) = 0. \end{cases} \quad (4.3.20)$$

The solutions of (4.3.19) and (4.3.20) are

$$\Phi_{in}^{(c)}(\rho, \theta) = \frac{(\rho^n + R_1^{2n} \rho^{-n}) \cos(n\theta)}{1 + R_1^{2n}}, \quad \Phi_{i0}^{(c)}(\rho, \theta) = 1, \quad (4.3.21)$$

$$\Phi_{in}^{(s)}(\rho, \theta) = \frac{(\rho^n + R_1^{2n} \rho^{-n}) \sin(n\theta)}{1 + R_1^{2n}}, \quad (4.3.22)$$

where $n \gg 1$, which can be confirmed by substitution. By using the

obtained solutions, we find,

$$\frac{\partial \Phi_i}{\partial \rho}(1, \theta, t) \langle F \rangle = \sum_{n=1}^{\infty} n \frac{1 - R_1^{2n}}{1 + R_1^{2n}} (a_n(t) \cos(n\theta) + b_n(t) \sin(n\theta)), \quad (-\pi < \theta < \pi). \quad (4.3.23)$$

The Fourier coefficients (4.3.17) cannot be used in (4.3.23) to reduce the problem to an integral equation for the function $F(\theta, t)$ as

$$\begin{aligned} \frac{\partial \Phi_i}{\partial \rho}(1, \theta) &= \frac{1}{\pi} \int_{\theta^L}^{\theta^R} F(\theta_0, t) \sum_{n=1}^{\infty} n \frac{1 - R_1^{2n}}{1 + R_1^{2n}} \\ &\quad \cdot \{ \cos(n\theta_0) \cos(n\theta) + \sin(n\theta_0) \sin(n\theta) \} d\theta_0 \\ &= \int_{\theta^L}^{\theta^R} F(\theta_0, t) \mathcal{K}(\theta - \theta_0) d\theta_0, \end{aligned} \quad (4.3.24)$$

because the series for $\mathcal{K}(\alpha)$ does not converge. This implies that the operator $(\partial \Phi_i / \partial \rho)(1, \theta) \langle F \rangle$ is not a standard integral operator. Note that, to satisfy the functional equation (4.3.15), we required $F(\theta^L, t) = F(\theta^R, t) = 0$, because the velocity potential should be at least continuous everywhere including the boundary of the flow region, to describe a flow with finite kinetic energy. The theory of mixed boundary value problems [11] provides that in this case the derivative $dF/d\theta$ is square-root singular at the ends of the contact region, $\theta = \theta^L$ and $\theta = \theta^R$.

The equation (4.3.15) will be understood as the limit

$$\lim_{\rho \rightarrow 1-0} \left\{ \frac{\partial \Phi_i}{\partial \rho}(\rho, \theta, t) \langle F \rangle \right\} = \tilde{f}(\theta, t), \quad (\theta^L(t) < \theta < \theta^R(t)), \quad (4.3.25)$$

where

$$\tilde{f}(\theta, t) = f(\theta, t) - \partial \Phi_c / \partial \rho(1, \theta, t), \quad (4.3.26)$$

is a known smooth function of θ . The time t is a parameter in the problem (4.3.13), which does not contain time derivatives. This parameter is dragged below. In the equation (4.3.25), we have

$$\frac{\partial \Phi_i}{\partial \rho}(\rho, \theta) = \int_{\theta^L}^{\theta^R} F(\theta_0, t) \mathcal{K}(\rho, \theta - \theta_0) d\theta_0, \quad (4.3.27)$$

where

$$\mathcal{K}(\rho, \theta) = \frac{1}{\pi\rho} \sum_{n=1}^{\infty} \frac{1 - (R_1/\rho)^{2n}}{1 + R_1^{2n}} n\rho^n \cos(n\theta), \quad (4.3.28)$$

and $R_1 < \rho < 1$, see equations (4.3.21)-(4.3.24). The series (4.3.28) does not converge at $\rho = 1$. To regularise equation (4.3.25), we notice that

$$\mathcal{K}(\rho, \theta - \theta_0) = \frac{\partial^2}{\partial\theta\partial\theta_0} S(\rho, \theta - \theta_0), \quad (4.3.29)$$

$$S(\rho, \theta) = \frac{1}{\pi\rho} \sum_{n=1}^{\infty} \frac{1 - (R_1/\rho)^{2n}}{1 + R_1^{2n}} \rho^n \frac{\cos(n\theta)}{n}. \quad (4.3.30)$$

The series (4.3.30) converges at $\rho = 1$ but it is log-singular at $\theta = 0$. Substituting (4.3.27) and (4.3.29) in (4.3.25) and integrating in (4.3.27) by part using equalities $F(\theta^L, t) = F(\theta^R, t) = 0$, we obtain

$$\begin{aligned} \lim_{\rho \rightarrow 1-0} \left\{ \frac{\partial\Phi_i}{\partial\rho}(\rho, \theta) \langle F \rangle \right\} &= \lim_{\rho \rightarrow 1-0} \frac{\partial}{\partial\theta} \left[\int_{\theta^L}^{\theta^R} F(\theta_0, t) d\{S(\rho, \theta - \theta_0)\} \right] \\ &= - \lim_{\rho \rightarrow 1} \frac{\partial}{\partial\theta} \int_{\theta^L}^{\theta^R} F'(\theta_0) S(\rho, \theta - \theta_0) d\theta_0 = \tilde{f}(\theta), \quad (\theta^L < \theta < \theta^R). \end{aligned} \quad (4.3.31)$$

It is convenient to introduce a new unknown function,

$$-U(\theta) = F'(\theta), \quad (4.3.32)$$

integrate both sides of (4.3.31) from θ^L to θ and take the limit as $\rho \rightarrow 1$. This gives the following equation for the function $U(\theta)$,

$$\int_{\theta^L}^{\theta^R} U(\theta_0) \{S(1, \theta - \theta_0) - S(1, \theta^L - \theta_0)\} d\theta_0 = \bar{f}(\theta), \quad (\theta^L < \theta < \theta^R), \quad (4.3.33)$$

where $\bar{f}(\theta)$ is a known function given by

$$\bar{f}(\theta) = \int_{\theta^L}^{\theta} \tilde{f}(\theta_0) d\theta_0. \quad (4.3.34)$$

From (4.3.33) and (4.3.30), we have

$$S(1, \theta - \theta_0) - S(1, \theta^L - \theta_0) = \frac{1}{\pi} \sum_{n=1}^{\infty} \frac{1 - R_1^{2n}}{1 + R_1^{2n}} \frac{1}{n} \cdot \{ \cos[n(\theta - \theta_0)] - \cos[n(\theta^L - \theta_0)] \}. \quad (4.3.35)$$

The interval (θ^L, θ^R) in (4.3.33) is mapped onto $(-\pi, \pi)$, in order to apply the classical theory of Fourier series, by introducing new variable ξ such that $-\pi < \xi < \pi$ and

$$\theta = A\xi + B, \quad (4.3.36)$$

maps $(-\pi, \pi)$ onto (θ^L, θ^R) . The coefficients A and B are obtained from the equations:

$$\theta^L = A(-\pi) + B \quad \text{and} \quad \theta^R = A\pi + B, \quad (4.3.37)$$

which gives

$$A = \frac{\theta^R - \theta^L}{2\pi} \quad \text{and} \quad B = \frac{\theta^L + \theta^R}{2}. \quad (4.3.38)$$

Introducing $U(\theta) = U(A\xi + B) = \tilde{U}(\xi)$ and $\theta_0 = A\xi_0 + B$, we transform (4.3.33) to the following equation

$$\int_{-\pi}^{\pi} \tilde{U}(\xi_0) \{ S(1, A(\xi - \xi_0)) - S(1, A(-\pi - \xi_0)) \} d\xi_0 = \frac{1}{A} G(\xi), \quad (-\pi < \xi < \pi), \quad (4.3.39)$$

where $G(\xi) = \bar{f}(A\xi + B)$. The function $\tilde{U}(\xi)$ is sought as the Fourier series

$$\tilde{U}(\xi) = \frac{1}{2} \bar{a}_0 + \sum_{n=1}^{\infty} (\bar{a}_n \cos(n\xi) + \bar{b}_n \sin(n\xi)), \quad (4.3.40)$$

where the coefficients \bar{a}_n and \bar{b}_n are to be determined. Equation (4.3.32) and the conditions $F(\theta^R) = F(\theta^L) = 0$ gives

$$-\int_{-\pi}^{\pi} \tilde{U}(\xi) d\xi = -\int_{\theta^L}^{\theta^R} U(\theta) d\theta = \int_{\theta^L}^{\theta^R} F'(\theta) d\theta = F(\theta^L) - F(\theta^R) = 0, \quad (4.3.41)$$

this provides $\bar{a}_0 = 0$ in (4.3.40). We substitute the series (4.3.40) in (4.3.39) multiply both sides of (4.3.39) by $\sin(m\xi)$ and $\cos(m\xi)$, $m \geq 1$, and integrate the result in ξ from $-\pi$ to π :

$$\begin{aligned} \sum_{n=1}^{\infty} \left\{ \bar{a}_n \int_{-\pi}^{\pi} \left(\int_{-\pi}^{\pi} \cos(n\xi_0) T(\xi, \xi_0) d\xi_0 \right) \cos(m\xi) d\xi \right. \\ \left. + \bar{b}_n \int_{-\pi}^{\pi} \left(\int_{-\pi}^{\pi} \sin(n\xi_0) T(\xi, \xi_0) d\xi_0 \right) \cos(m\xi) d\xi \right\} \\ = \frac{1}{A} \int_{-\pi}^{\pi} G(\xi) \cos(m\xi) d\xi, \quad (4.3.42) \end{aligned}$$

$$\begin{aligned} \sum_{n=1}^{\infty} \left\{ \bar{a}_n \int_{-\pi}^{\pi} \left(\int_{-\pi}^{\pi} \cos(n\xi_0) T(\xi, \xi_0) d\xi_0 \right) \sin(m\xi) d\xi \right. \\ \left. + \bar{b}_n \int_{-\pi}^{\pi} \left(\int_{-\pi}^{\pi} \sin(n\xi_0) T(\xi, \xi_0) d\xi_0 \right) \sin(m\xi) d\xi \right\} \\ = \frac{1}{A} \int_{-\pi}^{\pi} G(\xi) \sin(m\xi) d\xi, \quad (4.3.43) \end{aligned}$$

where

$$T(\xi, \xi_0) = S(1, A(\xi - \xi_0)) - S(1, -A(\pi + \xi_0)). \quad (4.3.44)$$

The system (4.3.42) and (4.3.43) can be written in the form

$$\begin{cases} A^{(cc)} \vec{a} + A^{(sc)} \vec{b} = \vec{G}_c, \\ A^{(cs)} \vec{a} + A^{(ss)} \vec{b} = \vec{G}_s, \end{cases} \quad (4.3.45)$$

where $\vec{a} = (\bar{a}_1, \bar{a}_2, \bar{a}_3, \dots)^T$, $\vec{b} = (\bar{b}_1, \bar{b}_2, \bar{b}_3, \dots)^T$ and $A^{(cc)}$, $A^{(sc)}$, $A^{(cs)}$ and $A^{(ss)}$ are matrices with the elements defined by the integrals in (4.3.42) and (4.3.43). By substituting (4.3.30) into (4.6.38), we find that

$$T(\xi, \xi_0) = \frac{1}{\pi} \sum_{k=1}^{\infty} W_k \frac{1}{k} \{ \cos(kA(\xi - \xi_0)) - \cos(kA(\pi + \xi_0)) \}, \quad (4.3.46)$$

where

$$W_k = \frac{1 - R_1^{2k}}{1 + R_1^{2k}}. \quad (4.3.47)$$

We calculate

$$\begin{aligned}
 A_{nm}^{(cc)} &= \int_{-\pi}^{\pi} \left(\int_{-\pi}^{\pi} \cos(n\xi_0) T(\xi, \xi_0) d\xi_0 \right) \cos(m\xi) d\xi \\
 &= \frac{1}{\pi} \sum_{k=1}^{\infty} W_k \frac{1}{k} \int_{-\pi}^{\pi} \left(\int_{-\pi}^{\pi} \{ \cos(kA(\xi - \xi_0)) - \cos(kA(\pi + \xi_0)) \} \right. \\
 &\quad \left. \cos(n\xi_0) d\xi_0 \right) \cos(m\xi) d\xi \\
 &= \frac{1}{\pi} \sum_{k=1}^{\infty} \frac{1}{k} W_k \left\{ \int_{-\pi}^{\pi} \cos(kA\xi_0) \cos(n\xi_0) d\xi_0 \int_{-\pi}^{\pi} \cos(kA\xi) \cos(m\xi) d\xi \right. \\
 &\quad \left. - \cos(kA\pi) \int_{-\pi}^{\pi} \cos(kA\xi_0) \cos(n\xi_0) d\xi_0 \int_{-\pi}^{\pi} \cos(m\xi) d\xi \right\}, \quad (4.3.48)
 \end{aligned}$$

where it was used that

$$\cos[kA(\xi - \xi_0)] = \cos(kA\xi) \cos(kA\xi_0) + \sin(kA\xi) \sin(kA\xi_0). \quad (4.3.49)$$

Let us denote the integrals in (4.3.48), by

$$\int_{-\pi}^{\pi} \cos(kA\xi) \cos(m\xi) d\xi = Q_{km}(A), \quad (4.3.50)$$

which makes it possible to present (4.3.48) in a compact form,

$$A_{nm}^{(cc)} = \frac{1}{\pi} \sum_{k=1}^{\infty} \frac{1}{k} W_k Q_{kn}(A) Q_{km}(A). \quad (4.3.51)$$

The integrals $Q_{km}(A)$ are evaluated as

$$Q_{km}(A) = \frac{2kA}{(kA)^2 - m^2} \sin(kA\pi) \cos(m\pi). \quad (4.3.52)$$

Substituting (4.3.52) into (4.3.51), we find

$$A_{nm}^{(cc)} = \frac{1}{\pi} (2A)^2 (-1)^{n+m} \sum_{k=1}^{\infty} \frac{1}{k} \frac{k^2}{(kA)^2 - m^2} \frac{1}{(kA)^2 - n^2} \sin^2(kA\pi) W_k, \quad (4.3.53)$$

where $0 < R_1 < 1$ and $0 < A < 1$.

Let A be not rational number. Then $A \neq m/k$ for any integer m and k . By introducing $m/A = a$, $n/A = b$, and $\pi A = x$, we can write

$$A_{nm}^{(cc)} = \frac{4}{\pi A^2} (-1)^{n+m} \sum_{k=1}^{\infty} \frac{k \sin^2(kx) W_k}{(k^2 - a^2)(k^2 - b^2)}, \quad (4.3.54)$$

If A is a rational number and $k = a$, then $kx = (m/A)\pi A = \pi m$ and $\sin(kx) = 0$. Therefore, we can apply L'Hopital's rule to the corresponding term,

$$\begin{aligned} \lim_{A \rightarrow m/k} \frac{\sin(kx)}{k^2 - a^2} &= \lim_{A \rightarrow m/k} \frac{\sin(k\pi A)}{k^2 - (m/A)^2} = \frac{\cos(k\pi(m/k))k\pi}{-2(m/A)(-m/A^2)} \\ &= \frac{\cos(\pi m)k\pi}{2m^2} \left(\frac{m}{k}\right)^3 = \frac{\pi}{2} (-1)^m \frac{m}{k^2}. \end{aligned} \quad (4.3.55)$$

If a and b are not integer, then we just calculate the series (4.3.54). Second case, If a is integer, $a = M$, but b is not, then the series (4.3.54) is evaluated as

$$\begin{aligned} A_{nm}^{(cc)} &= \frac{4}{\pi A^2} \cos(m\pi) \cos(n\pi) \sum_{k=1, k \neq M}^{\infty} \left\{ \frac{k \sin^2(kx) W_k}{(k^2 - a^2)(k^2 - b^2)} \right. \\ &\quad \left. + \frac{\pi}{2} \cos(\pi m) \frac{m}{M^2} \frac{M \sin(Mx) W_M}{M^2 - b^2} \right\}, \end{aligned} \quad (4.3.56)$$

If a is not integer, but b is integer, $b = N$, then

$$\begin{aligned} A_{nm}^{(cc)} &= \frac{4}{\pi A^2} (-1)^{n+m} \left\{ \sum_{k=1, k \neq N}^{\infty} \frac{k \sin^2(kx) W_k}{(k^2 - a^2)(k^2 - b^2)} \right. \\ &\quad \left. + \frac{\pi}{2} (-1)^m \frac{n}{N^2} \frac{N \sin(Nx) W_N}{N^2 - a^2} \right\}, \end{aligned} \quad (4.3.57)$$

If a and b are integer but not equal to each other, $a = M$, $b = N$, $M \neq N$,

then

$$A_{nm}^{(cc)} = \frac{4}{\pi A^2} (-1)^{n+m} \left\{ \sum_{k=1, k \neq M, N}^{\infty} \frac{k \sin^2(kx) W_k}{(k^2 - a^2)(k^2 - b^2)} + \frac{\pi}{2} \cos(\pi m) \frac{m}{M^2} \frac{M \sin(Mx) W_M}{M^2 - N^2} + \frac{\pi}{2} \cos(\pi n) \frac{n}{N^2} \frac{N \sin(Nx) W_N}{N^2 - M^2} \right\}, \quad (4.3.58)$$

Last case if a and b are integer and equal to each other, $a = b = N$, which is possible only for $n = m$, then

$$A_{nm}^{(cc)} = \frac{4}{\pi A^2} \left\{ \sum_{k=1, k \neq N}^{\infty} \frac{k \sin^2(kx) W_k}{(k^2 - a^2)^2} + \frac{\pi^2 n^2}{4 N^3} W_N \right\}. \quad (4.3.59)$$

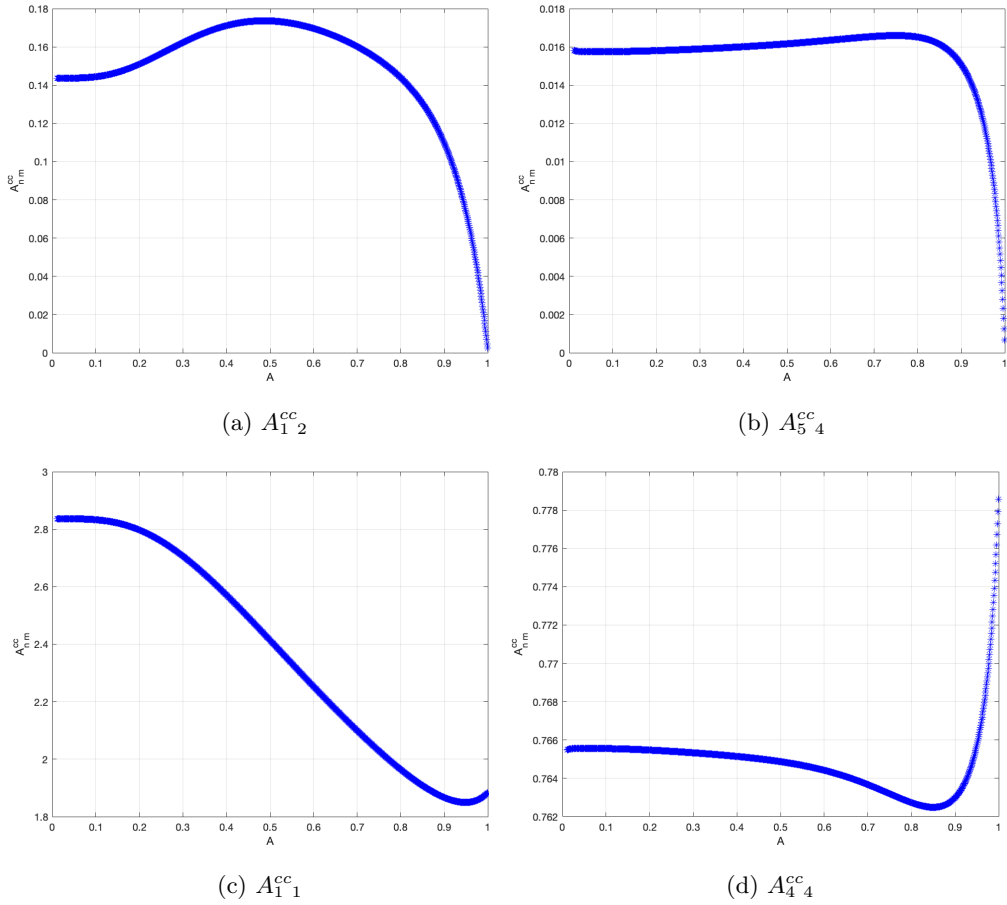


Figure 4.3.1: Elements of the matrix A_{nm}^{cc} as a function of A .

For illustrating the elements of the matrix A_{nm}^{cc} , we selected vary values for

n and m as shown in Figure 4.3.1. For more investigation we have

$$\frac{k^2}{(k^2 - a^2)(k^2 - b^2)} = \frac{a^2}{(k^2 - a^2)(a^2 - b^2)} - \frac{b^2}{(k^2 - b^2)(a^2 - b^2)}, \quad (4.3.60)$$

and introduce a new $S(x, a)$ by

$$\sum_{k=1}^{\infty} \frac{1}{k} \frac{\sin^2(kx)}{k^2 - a^2} W_k = S(x, a), \quad (4.3.61)$$

and for $x = \pi A$ and $a = m/A$ we got

$$\sum_{k=1}^{\infty} \frac{1}{k} \frac{\sin^2(k\pi A)}{k^2 - (m/A)^2} W_k = S\left(\pi A, \frac{m}{A}\right), \quad (4.3.62)$$

Then equation (4.3.61) takes the form,

$$A_{nm}^{(cc)} = \frac{4}{\pi A^2} \frac{(-1)^{n+m}}{m^2 - n^2} \left\{ m^2 S\left(\pi A, \frac{m}{A}\right) - n^2 S\left(\pi A, \frac{n}{A}\right) \right\}, \quad (4.3.63)$$

for $n \neq m$ and

$$A_{nn}^{(cc)} = \frac{4}{\pi A^2} \sum_{k=1}^{\infty} \frac{1}{k} \frac{k^2 \sin^2(\pi k A)}{(k^2 - \frac{n^2}{A^2})^2} W_k. \quad (4.3.64)$$

In (4.3.64),

$$\frac{k^2}{(k^2 - b^2)^2} = \frac{k^2 - b^2 + b^2}{(k^2 - b^2)^2} = \frac{1}{k^2 - b^2} + \frac{b^2}{(k^2 - b^2)^2}, \quad (4.3.65)$$

$$A_{nn}^{(cc)} = \frac{4}{\pi A^2} \left\{ S\left(x, \frac{n}{A}\right) + \frac{n^2}{A^2} \sum_{k=1}^{\infty} \frac{1}{k} \frac{\sin^2(\pi k A)}{(k^2 - \frac{n^2}{A^2})^2} W_k \right\}, \quad (4.3.66)$$

We introduce a new function $S_2(x, a)$ by

$$S_2(x, a) = \sum_{k=1}^{\infty} \frac{1}{k} \frac{\sin^2(kx)}{(k^2 - a^2)^2} W_k. \quad (4.3.67)$$

Then

$$A_{nn}^{(cc)} = \frac{4}{\pi A^2} \left\{ S\left(x, \frac{n}{A}\right) + \frac{n^2}{A^2} S_2\left(x, \frac{n}{A}\right) \right\}. \quad (4.3.68)$$

The terms in $S_2(x, a)$ decay as k^{-5} for $k \rightarrow \infty$. Calculations of $S(x, a)$ and $S_2(x, a)$ require the same as calculations of the matrix elements for the special case, where a is integer.

Next we calculate

$$\begin{aligned} A_{nm}^{(sc)} &= \int_{-\pi}^{\pi} \left(\int_{-\pi}^{\pi} \sin(n\xi_0) T(\xi, \xi_0) d\xi_0 \right) \cos(m\xi) d\xi \\ &= \frac{1}{\pi} \sum_{k=1}^{\infty} \frac{1}{k} W_k \left\{ \int_{-\pi}^{\pi} \cos(kA\xi_0) \sin(n\xi_0) d\xi_0 \int_{-\pi}^{\pi} \cos(kA\xi) \cos(m\xi) d\xi \right. \\ &\quad \left. - \cos(kA\pi) \int_{-\pi}^{\pi} \cos(kA\xi_0) \sin(n\xi_0) d\xi_0 \int_{-\pi}^{\pi} \cos(m\xi) d\xi \right\}, \quad (4.3.69) \end{aligned}$$

where $n \gg 1$, $m \gg 1$ and

$$\int_{-\pi}^{\pi} \cos(kA\xi) \sin(n\xi) d\xi = 0, \quad (4.3.70)$$

Because the product $\cos(kA\xi) \sin(n\xi)$ is odd and continuous function of ξ in the symmetric interval $-\pi < \xi < \pi$. This gives

$$A_{nm}^{(sc)} = 0. \quad (4.3.71)$$

Similar,

$$\begin{aligned} A_{nm}^{(cs)} &= \int_{-\pi}^{\pi} \left(\int_{-\pi}^{\pi} \cos(n\xi_0) T(\xi, \xi_0) d\xi_0 \right) \sin(m\xi) d\xi \\ &= \frac{1}{\pi} \sum_{k=1}^{\infty} \frac{1}{k} W_k \left\{ \int_{-\pi}^{\pi} \cos(kA\xi_0) \cos(n\xi_0) d\xi_0 \int_{-\pi}^{\pi} \cos(kA\xi) \sin(m\xi) d\xi \right. \\ &\quad \left. - \cos(kA\pi) \int_{-\pi}^{\pi} \cos(kA\xi_0) \cos(n\xi_0) d\xi_0 \int_{-\pi}^{\pi} \sin(m\xi) d\xi \right\}, \quad (4.3.72) \end{aligned}$$

giving

$$A_{nm}^{(cs)} = 0. \quad (4.3.73)$$

Finally,

$$\begin{aligned}
 A_{nm}^{(ss)} &= \int_{-\pi}^{\pi} \left(\int_{-\pi}^{\pi} \sin(n\xi_0) T(\xi, \xi_0) d\xi_0 \right) \sin(m\xi) d\xi \\
 &= \frac{1}{\pi} \sum_{k=1}^{\infty} \frac{1}{k} W_k \left\{ \int_{-\pi}^{\pi} \sin(kA\xi_0) \sin(n\xi_0) d\xi_0 \int_{-\pi}^{\pi} \sin(kA\xi) \sin(m\xi) d\xi \right. \\
 &\quad \left. - \cos(kA\pi) \int_{-\pi}^{\pi} \cos(kA\xi_0) \sin(n\xi_0) d\xi_0 \int_{-\pi}^{\pi} \sin(m\xi) d\xi \right\}, \quad (4.3.74)
 \end{aligned}$$

Introducing

$$\int_{-\pi}^{\pi} \sin(kA\xi) \sin(m\xi) d\xi = J_{km}(A), \quad (4.3.75)$$

we can write (4.3.74) as

$$A_{nm}^{(ss)} = \frac{1}{\pi} \sum_{k=1}^{\infty} \frac{1}{k} W_k J_{kn}(A) J_{km}(A). \quad (4.3.76)$$

The integrals $J_{km}(A)$ are evaluated analytically

$$J_{km}(A) = \int_{-\pi}^{\pi} \sin(kA\xi) \sin(m\xi) d\xi = \frac{2m}{(kA)^2 - m^2} \sin(kA\pi) \cos(m\pi), \quad (4.3.77)$$

correspondingly for $J_{kn}(A)$, we have

$$J_{kn}(A) = \frac{2n}{(kA)^2 - n^2} \sin(kA\pi) \cos(n\pi), \quad (4.3.78)$$

Substituting (4.3.77) and (4.3.78) into (4.3.76) gives

$$A_{nm}^{(ss)} = \frac{4mn}{\pi} (-1)^{n+m} \sum_{k=1}^{\infty} \frac{1}{k} \frac{1}{(kA)^2 - m^2} \frac{1}{(kA)^2 - n^2} \sin^2(kA\pi) W_k. \quad (4.3.79)$$

Introducing $m/A = a$, $n/A = b$, and $\pi A = x$, see equation (4.3.54), we find

$$A_{nm}^{(ss)} = \frac{4mn}{\pi A^4} (-1)^{n+m} \sum_{k=1}^{\infty} \frac{\sin^2(kx) W_k}{k(k^2 - a^2)(k^2 - b^2)}. \quad (4.3.80)$$

Using the similar analysis for $A_{nm}^{(cc)}$ (4.3.56-4.3.59), we obtain

$$A_{nm}^{(ss)} = \frac{4mn}{\pi A^4} (-1)^{n+m} \sum_{k=1, k \neq M}^{\infty} \left\{ \frac{\sin^2(kx)W_k}{k(k^2 - a^2)(k^2 - b^2)} \right\} + \frac{\pi}{2} \cos(\pi m) \frac{m}{M^2} \frac{\sin(Mx)W_M}{M(M^2 - a^2)}, \quad (4.3.81)$$

for $a = M$ and b is not integer,

$$A_{nm}^{(ss)} = \frac{4mn}{\pi A^4} \cos(m\pi) \cos(n\pi) \sum_{k=1, k \neq N}^{\infty} \left\{ \frac{\sin^2(kx)W_k}{k(k^2 - a^2)(k^2 - b^2)} \right\} + \frac{\pi}{2} \cos(\pi n) \frac{n}{N^2} \frac{\sin(Nx)W_N}{N(N^2 - b^2)}, \quad (4.3.82)$$

for $a = M$ and $b = N$ both integer and $N \neq M$,

$$A_{nm}^{(ss)} = \frac{4mn}{\pi A^4} (-1)^{n+m} \sum_{k=1, k \neq M, N}^{\infty} \left\{ \frac{\sin^2(kx)W_k}{k(k^2 - a^2)(k^2 - b^2)} \right\} + \frac{\pi}{2} \cos(\pi m) \frac{m}{M^2} \frac{\sin(Mx)W_M}{M(M^2 - a^2)} + \frac{\pi}{2} \cos(\pi n) \frac{n}{N^2} \frac{\sin(Nx)W_N}{N(N^2 - b^2)}, \quad (4.3.83)$$

$$A_{nn}^{(ss)} = \frac{4n^2}{\pi A^4} (-1)^{n+m} \sum_{k=1, k \neq N}^{\infty} \left\{ \frac{\sin^2(kx)W_k}{k(k^2 - b^2)^2} \right\} + \frac{\pi^2}{4} \frac{n^2}{N^5} W_N. \quad (4.3.84)$$

for $a = b = N$.

Figure 4.3.2 shows the elements of the matrix A_{nm}^{ss} , were we selected different values for n and m .

If we restrict ourselves to only five terms in the Fourier series (4.3.40) and calculate matrix $A^{(cc)}$ for $A = 0.5$ with 6000 terms in the series, then we

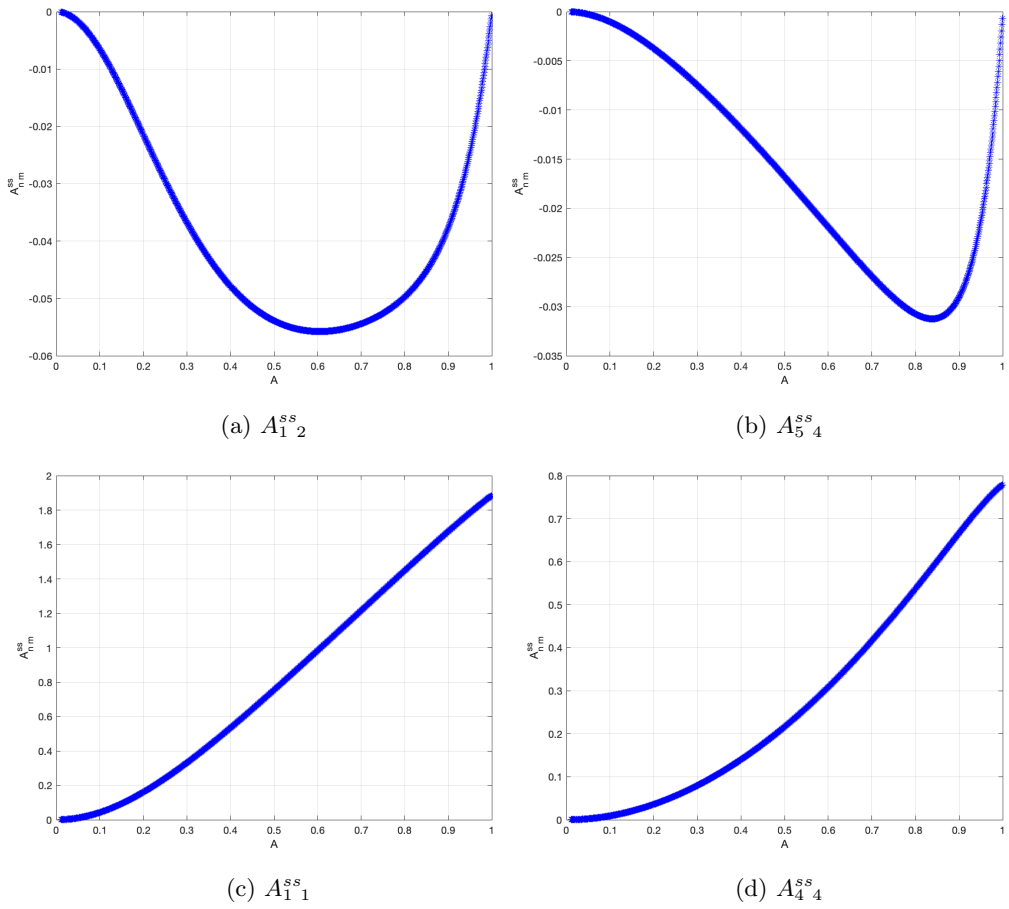


Figure 4.3.2: Elements of the matrix A_{nm}^{ss} as a function of A .

find

$$A_{5 \times 5}^{(cc)} = \begin{pmatrix} 1.02797 & -0.71251 & 0.66074 & -0.63837 & 0.62701 \\ -0.71251 & 0.68809 & -0.38117 & 0.3418 & -0.32165 \\ 0.66074 & -0.38117 & 0.4858 & -0.22933 & 0.20541 \\ -0.63837 & 0.3418 & -0.22933 & 0.37218 & -0.15373 \\ 0.62701 & -0.32165 & 0.20541 & -0.15373 & 0.30119 \end{pmatrix}, \quad (4.3.85)$$

and the inverse matrix of $A_{5 \times 5}^{(cc)}$ as

$$\left[A_{5 \times 5}^{(cc)} \right]^{-1} = \begin{pmatrix} -1.2407 & 1.04716 & 0.72512 & -1.67065 & 2.3539 \\ 1.04716 & 3.84168 & 0.78353 & -0.85627 & 0.95129 \\ 0.72512 & 0.78353 & 3.40193 & 1.75392 & -2.09765 \\ -1.67065 & -0.85627 & 1.75392 & 2.85514 & 2.82455 \\ 2.3539 & 0.95129 & -2.09765 & 2.82455 & 2.30805 \end{pmatrix}, \quad (4.3.86)$$

where

$$A_{5 \times 5}^{(cc)} \times \left[A_{5 \times 5}^{(cc)} \right]^{-1} = \begin{pmatrix} 1 & 0 & 0 & 0 & 0 \\ 0 & 1 & 0 & 0 & 0 \\ 0 & 0 & 1 & 0 & 0 \\ 0 & 0 & 0 & 1 & 0 \\ 0 & 0 & 0 & 0 & 1 \end{pmatrix} = I, \quad (4.3.87)$$

with accuracy better than 10^{-16} .

$$\left(3.33E - 16 \quad 2.22E - 16 \quad 4.44E - 16 \quad 4.44E - 16 \quad 2.22E - 16 \right). \quad (4.3.88)$$

which is the accuracy of Matlab calculation. Similarly, we have also

$$A_{5 \times 5}^{(ss)} = \begin{pmatrix} 0.40817 & -0.21557 & 0.16804 & -0.13458 & 0.11143 \\ -0.21557 & 0.24236 & -0.1497 & 0.12088 & -0.10072 \\ 0.16804 & -0.1497 & 0.1606 & -0.09697 & 0.08134 \\ -0.13458 & 0.12088 & -0.09697 & 0.11806 & -0.06711 \\ 0.11143 & -0.10072 & 0.08134 & -0.06711 & 0.09276 \end{pmatrix}, \quad (4.3.89)$$

and the inverse matrix of $A_{5 \times 5}^{(ss)}$ as

$$\left[A_{5 \times 5}^{(ss)} \right]^{-1} = \begin{pmatrix} 5.2099 & 2.31774 & -1.91562 & 1.3933 & -1.05422 \\ 2.31774 & 13.24663 & 5.41033 & -4.38305 & 3.68424 \\ -1.915629 & 5.41033 & 18.54151 & 4.94485 & -4.50546 \\ 1.3933 & -4.38305 & 4.94485 & 21.20780 & 4.57357 \\ -1.05422 & 3.68424 & -4.50546 & 4.57357 & 23.30695 \end{pmatrix}, \quad (4.3.90)$$

where

$$A_{5 \times 5}^{(ss)} \times [A_{5 \times 5}^{(ss)}]^{-1} = \begin{pmatrix} 1 & 0 & 0 & 0 & 0 \\ 0 & 1 & 0 & 0 & 0 \\ 0 & 0 & 1 & 0 & 0 \\ 0 & 0 & 0 & 1 & 0 \\ 0 & 0 & 0 & 0 & 1 \end{pmatrix} = I, \quad (4.3.91)$$

with accuracy better than 10^{-15} .

4.3.2 Asymptotic behaviour of the matrices $A_{nm}^{(cc)}$ and $A_{nm}^{(ss)}$ as $A \rightarrow 0$ and $A \rightarrow 1$

The matrices $A_{nm}^{(cc)}$ and $A_{nm}^{(ss)}$ are computed by the series (4.3.56 - 4.3.59) and (4.3.59 - 4.3.84) corresponding. The terms of the series decay as $O(k^{-3})$ as $k \rightarrow \infty$. Accurate calculations of the matrix requires many terms. In addition, the number of terms retained in the series should be bigger than a and b . However, for example $a = m/A$ is large for small A and large m . Therefore, calculations of elements $A_{nm}^{(cc)}$ and $A_{nm}^{(ss)}$ by series (4.3.56 - 4.3.59) and (4.3.59 - 4.3.84) are not practical for small A , which is for small dimensions of the impact region. To find asymptotic behavior of $A_{nm}^{(cc)}$ and $A_{nm}^{(ss)}$ for small A and $A \rightarrow 1$, it is suggested to use another formulae for the matrix elements. We derived another formulae for $A_{nm}^{(cc)}$ and $A_{nm}^{(ss)}$ which are suitable for calculations when $A \rightarrow 0$ or $A \rightarrow 1$, see Appendix A.1, for more details.

Figure 4.3.3 shows $S(\pi A, \frac{m}{A})$ for some small values of A , where $m = 10$ and figure 4.3.4 shows the differences between S and asymptotic S for small A , where $m = 10$. In figure 4.3.5 (a) we illustrated S and asymptotic S where we added five terms in the series and figure 4.3.5 (b) when added ten terms. In figure 4.3.6 we plotted A_{nm}^{cc} directly and comparing by using asymptotic S , where $k = 55000$ for selected n and m and similarly for A_{nm}^{ss} in figure 4.3.7.

Now we shall be dealing with the vectors on right hand side in (4.3.45).

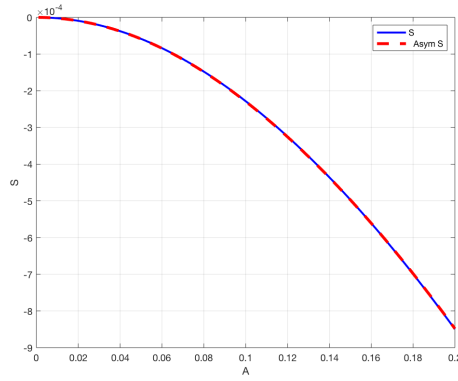


Figure 4.3.3: Illustration of $S(\pi A, \frac{m}{A})$ for some small values of A , where $m = 10$.

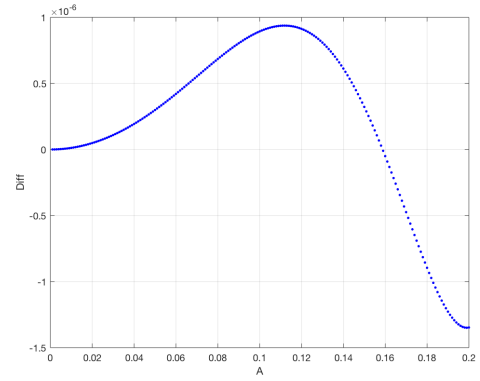
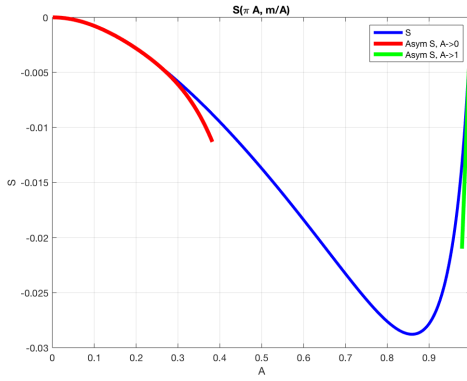
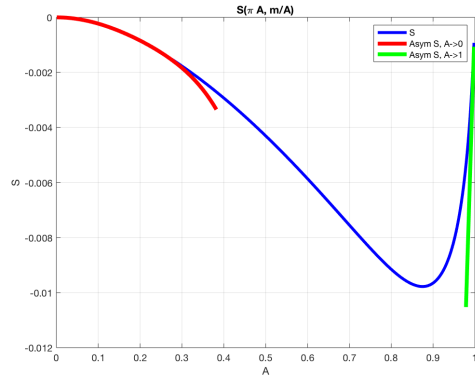


Figure 4.3.4: The differences between S and asymptotic S for small A , where $m = 10$.



(a) $m = 5$



(b) $m = 10$

Figure 4.3.5: Plot of S and asymptotic S where $m = 5, 10$.

Then we can find \vec{a} and \vec{b} , which are given by

$$\vec{a} = [A^{(cc)}]^{-1} \vec{G}_c \quad \text{and} \quad \vec{b} = [A^{(ss)}]^{-1} \vec{G}_s, \quad (4.3.92)$$

where the \vec{G}_c and \vec{G}_s of the system (4.3.45) are calculated using their definitions in (4.3.42) and (4.3.43). Equation (4.3.42) provides

$$G_{c,m} = \frac{1}{A} \int_{-\pi}^{\pi} G(\xi) \cos(m\xi) d\xi, \quad (4.3.93)$$

where

$$G(\xi) = \bar{f}(A\xi + B), \quad (4.3.94)$$

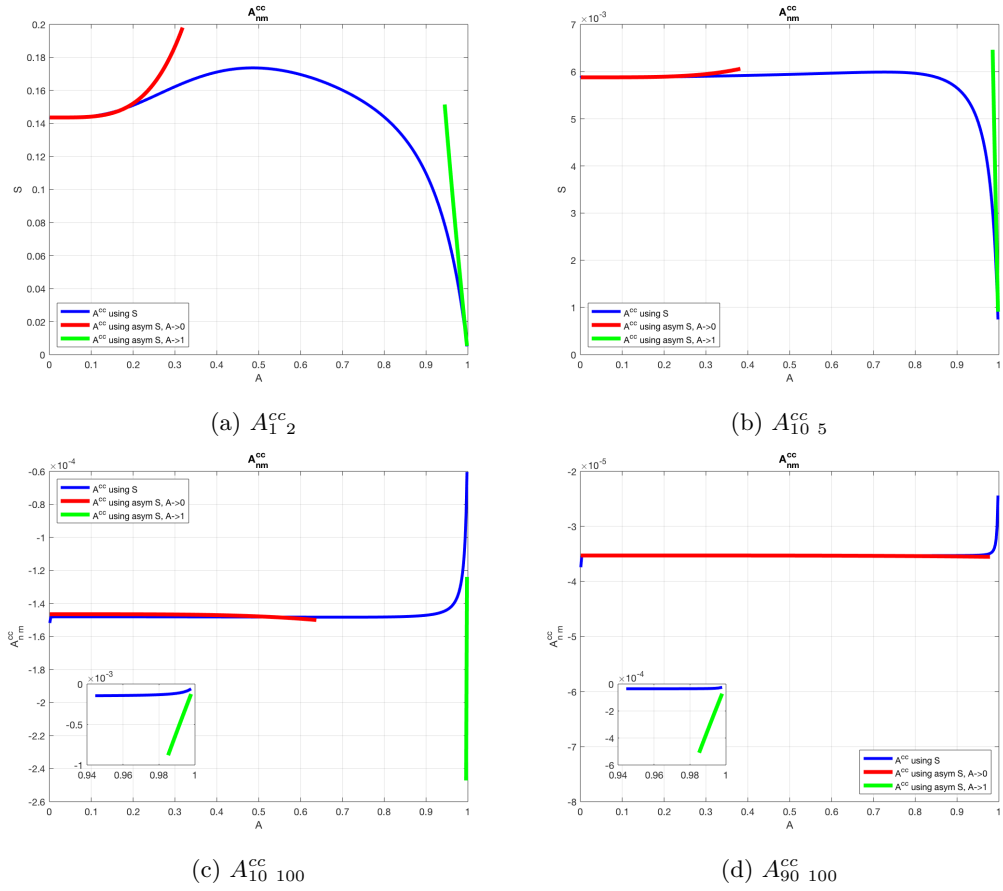


Figure 4.3.6: Plot of A_{nm}^{cc} where $k = 55000$ comparing by using asymptotic S .

and $\bar{f}(\theta)$ is defined by (4.3.34)

$$\bar{f}(\theta) = \int_{\theta^L}^{\theta} \tilde{f}(\theta_0) d\theta_0, \quad (4.3.95)$$

Here $\theta = A\xi + B$,

$$A = \frac{\theta^R - \theta^L}{2\pi} \quad \text{and} \quad B = \frac{\theta^L + \theta^R}{2}. \quad (4.3.96)$$

The function $\tilde{f}(\theta)$ in (4.3.95) is given by (4.3.26) as

$$\tilde{f}(\theta) = f(\theta, t) - \partial\Phi_c/\partial\rho(1, \theta), \quad (4.3.97)$$

where

$$f(\theta, t) = \frac{-h'(t)\sqrt{y_c^2(t) - R^2}}{1 + \cos(\theta)}, \quad (4.3.98)$$

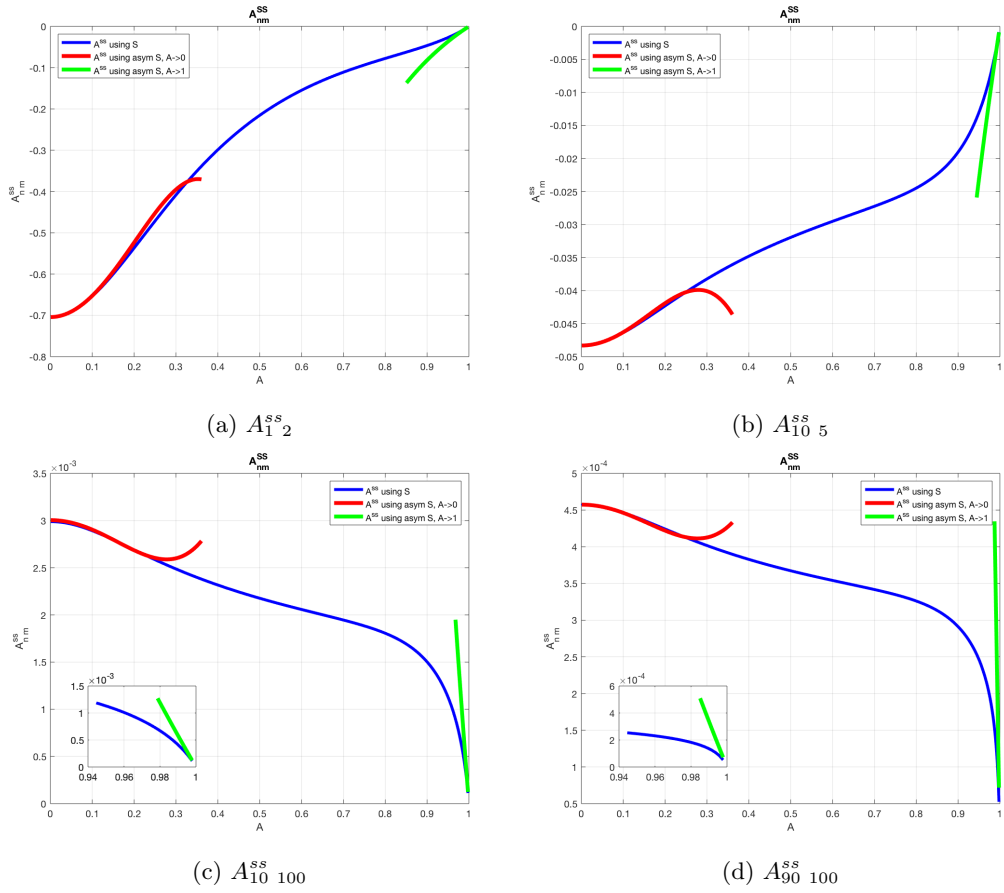


Figure 4.3.7: Plot of A_{nm}^{ss} where $k = 200000$ comparing by using asymptotic S .

$h(t)$ is the vertical displacement of the body at speed $h'(t)$, R is the ratio of the cylinder radius to the horizontal dimension of the entering body, and $y_c(t) = -H(t)$, $H(t) > 0$ is the distance of the center of the cylinder at time t . Equation (4.3.11) yields

$$\frac{\partial \Phi_c}{\partial \rho}(1, \theta, t) = 2 \frac{R\sqrt{1-\lambda^2}}{\lambda} \sum_{k=1}^{\infty} 2k \frac{R_1^{2k}}{R_1^{2k} + 1} \cdot ((-1)^{k+1} \dot{y}_c \cos(k\theta) + \dot{x}_c \sin(k\theta)). \quad (4.3.99)$$

Then

$$\bar{f}(\theta) = \int_{\theta_L}^{\theta} \tilde{f}(\theta_0) d\theta_0 = \int_{\theta_L}^{\theta} (f(\theta_0, t) - \partial \Phi_c / \partial \rho(1, \theta_0)) d\theta_0. \quad (4.3.100)$$

Integrating (4.3.93) by parts, we find

$$\begin{aligned} G_{c,m} &= \frac{1}{Am} \sin(m\xi)G(\xi) \Big|_{-\pi}^{\pi} - \frac{1}{A} \int_{-\pi}^{\pi} G'(\xi) \frac{1}{m} \sin(m\xi) d\xi \\ &= -\frac{1}{A} \int_{-\pi}^{\pi} \frac{A}{m} \left(f(A\xi + B, t) - \frac{\partial \Phi_c}{\partial \rho}(1, A\xi + B) \right) \sin(m\xi) d\xi, \end{aligned} \quad (4.3.101)$$

where we used,

$$G'(\xi) = \bar{f}'(A\xi + B)A. \quad (4.3.102)$$

Changing the variable of integration in (4.3.101) from ξ to $\theta = A\xi + B$, gives

$$\begin{aligned} G_{c,m} &= -\frac{1}{Am} \int_{\theta_L}^{\theta_R} \left(f(\theta, t) - \frac{\partial \Phi_c}{\partial \rho}(1, \theta) \right) \sin\left(m \frac{\theta - B}{A}\right) d\theta \\ &= -\frac{1}{Am} \int_{\theta_L}^{\theta_R} f(\theta, t) \sin\left(m \frac{\theta - B}{A}\right) d\theta \\ &\quad + \frac{1}{Am} \int_{\theta_L}^{\theta_R} \frac{\partial \Phi_c}{\partial \rho}(1, \theta) \sin\left(m \frac{\theta - B}{A}\right) d\theta. \end{aligned} \quad (4.3.103)$$

Thus

$$\begin{aligned} G_{c,m} &= -\frac{1}{Am} \int_{\theta_L}^{\theta_R} f(\theta, t) \sin\left(m \frac{\theta - B}{A}\right) d\theta + \frac{2R}{Am} \frac{\sqrt{1-\lambda^2}}{\lambda} \sum_{k=1}^{\infty} 2k \frac{R_1^{2k}}{R_1^{2k} + 1} \\ &\cdot \left(\int_{\theta_L}^{\theta_R} \left[(-1)^{k+1} \dot{y}_c \cos(k\theta) \sin\left(m \frac{\theta - B}{A}\right) + \dot{x}_c \sin(k\theta) \left(m \frac{\theta - B}{A}\right) \right] d\theta \right), \end{aligned} \quad (4.3.104)$$

where

$$\begin{aligned} &\int_{\theta_L}^{\theta_R} \cos(k\theta) \sin\left(m \frac{\theta - B}{A}\right) d\theta \\ &= \frac{1}{2} \int_{\theta_L}^{\theta_R} \left\{ \sin\left[\left(k + \frac{m}{A}\right)\theta - \frac{mB}{A}\right] + \sin\left[\left(\frac{m}{A} - k\right)\theta - \frac{mB}{A}\right] \right\} d\theta \\ &= -\frac{4mA(-1)^m}{(kA)^2 - m^2} \sin(kB) \sin(\pi kA). \end{aligned} \quad (4.3.105)$$

similar

$$\int_{\theta^L}^{\theta^R} \sin(k\theta) \sin\left(m\frac{\theta-B}{A}\right) d\theta = \frac{4mA^2(-1)^m}{(kA)^2 - m^2} \sin(kB) \sin(\pi kA). \quad (4.3.106)$$

Then

$$\int_{\theta^L}^{\theta^R} f(\theta, t) \sin\left(m\frac{\theta-B}{A}\right) d\theta = -h'(t) \sqrt{y_c^2(t) - R^2} \int_{\theta^L}^{\theta^R} \frac{\sin\left(m\frac{\theta-B}{A}\right)}{1 + \cos(\theta)} d\theta, \quad (4.3.107)$$

$$I_m^s = \int_{\theta^L}^{\theta^R} \frac{\sin\left(m\frac{\theta-B}{A}\right)}{1 + \cos(\theta)} d\theta. \quad (4.3.108)$$

Substitution (4.3.107), (4.3.106) and (4.3.105) into (4.3.104) gives

$$\begin{aligned} G_{c,m} = & -\frac{1}{Am} \left(-h'(t) \sqrt{y_c^2(t) - R^2} I_m^s \right) \\ & + \frac{2R}{Am} \frac{\sqrt{1-\lambda^2}}{\lambda} \sum_{k=1}^{\infty} 2k \frac{R_1^{2k}}{R_1^{2k} + 1} \\ & \cdot \left((-1)^{k+1} \dot{y}_c \frac{4mA(-1)^m}{(kA)^2 - m^2} \sin(kB) \sin(\pi kA) \right. \\ & \left. - \dot{x}_c \frac{4mA^2(-1)^m}{(kA)^2 - m^2} \sin(kB) \sin(\pi kA) \right), \quad (4.3.109) \end{aligned}$$

were I_m^s in (4.3.108) evaluated numerically.

Similarly for G_s we have

$$\begin{aligned} G_{s,m} = & -\frac{1}{Am} \int_{\theta^L}^{\theta^R} f(\theta, t) \cos\left(m\frac{\theta-B}{A}\right) d\theta + \frac{2R}{Am} \frac{\sqrt{1-\lambda^2}}{\lambda} \sum_{k=1}^{\infty} 2k \frac{R_1^{2k}}{R_1^{2k} + 1} \\ & \cdot \left(\int_{\theta^L}^{\theta^R} \left[(-1)^{k+1} \dot{y}_c \cos(k\theta) \cos\left(m\frac{\theta-B}{A}\right) + \dot{x}_c \sin(k\theta) \cos\left(m\frac{\theta-B}{A}\right) \right] d\theta \right), \quad (4.3.110) \end{aligned}$$

where

$$\int_{\theta^L}^{\theta^R} \sin(k\theta) \cos\left(m\frac{\theta-B}{A}\right) d\theta = -\frac{4mA(-1)^m}{(kA)^2 - m^2} \sin(kB) \sin(\pi kA). \quad (4.3.111)$$

and

$$\int_{\theta^L}^{\theta^R} \cos(k\theta) \cos\left(m\frac{\theta-B}{A}\right) d\theta = \frac{4mA^2(-1)^m}{(kA)^2 - m^2} \sin(kB) \sin(\pi kA). \quad (4.3.112)$$

Then

$$\int_{\theta^L}^{\theta^R} f(\theta, t) \cos\left(m\frac{\theta-B}{A}\right) d\theta = -h'(t) \sqrt{y_0^2 - R^2} \int_{\theta^L}^{\theta^R} \frac{\cos\left(m\frac{\theta-B}{A}\right)}{1 + \cos(\theta)} d\theta, \quad (4.3.113)$$

$$I_m^c = \int_{\theta^L}^{\theta^R} \frac{\cos\left(m\frac{\theta-B}{A}\right)}{1 + \cos(\theta)} d\theta, \quad (4.3.114)$$

where (4.3.114) calculated numerically.

Substitution (4.3.111) (4.3.112) and (4.3.113) into (4.3.110) gives

$$\begin{aligned} G_{s,m} = & -\frac{1}{Am} \left(-h'(t) \sqrt{y_c^2(t) - R^2} I_m^c \right) \\ & + \frac{2R}{Am} \frac{\sqrt{1-\lambda^2}}{\lambda} \sum_{k=1}^{\infty} 2k \frac{R_1^{2k}}{R_1^{2k} + 1} \\ & \cdot \left(\dot{y}_c (-1)^{k+1} \frac{4mA^2(-1)^m}{(kA)^2 - m^2} \sin(kB) \sin(\pi kA) \right. \\ & \left. - \dot{x}_c \frac{4mA(-1)^m}{(kA)^2 - m^2} \sin(kB) \sin(\pi kA) \right), \quad (4.3.115) \end{aligned}$$

where I_m^c is given by (4.3.114).

By substituting (4.3.109) and (4.3.115) into the formulae (4.3.92) then we find unknown vector \vec{a} and \vec{b} and evaluate the function (4.3.40) as

$$\tilde{U}(\xi) = \sum_{m=1}^{\infty} (\bar{a}_m \cos(m\xi) + \bar{b}_m \sin(m\xi)), \quad (4.3.116)$$

then we find the $F(\theta)$ using the function

$$-U(\theta) = F'(\theta), \quad (4.3.117)$$

integrating (4.3.117) gives

$$-\int_{\theta^L}^{\theta} U(\theta_0) d\theta_0 = \int_{\theta^L}^{\theta} F'(\theta_0) d\theta_0 = F(\theta) - F(\theta^L) = F(\theta), \quad (4.3.118)$$

since $F(\theta^L) = 0$. Here

$$U(\theta) = U(A\xi + B) = \tilde{U}(\xi). \quad (4.3.119)$$

Changing the variable of integration in (4.3.118) to ξ , $\theta_0 = A\xi_0 + B$, where A and B are given by (4.3.38), we obtain

$$\begin{aligned} F(\theta) &= -\int_{\theta^L}^{\theta} U(\theta_0) d\theta_0 = -A \int_{\frac{\theta^L - B}{A}}^{\frac{\theta - B}{A}} U(A\xi_0 + B) d\xi_0 \\ &= -A \int_{-\pi}^{\frac{\theta - B}{A}} U(A\xi_0 + B) d\xi_0 = -A \int_{-\pi}^{\frac{\theta - B}{A}} \tilde{U}(\xi_0) d\xi_0. \end{aligned} \quad (4.3.120)$$

The integral in (4.3.120) is evaluated using the series (4.3.116), From (4.3.116) we have

$$\begin{aligned} F(\theta) &= -A \int_{-\pi}^{\frac{\theta - B}{A}} \tilde{U}(\xi) d\xi = -A \int_{-\pi}^{\frac{\theta - B}{A}} \sum_{m=1}^{\infty} (\bar{a}_m \cos(m\xi) + \bar{b}_m \sin(m\xi)) d\xi \\ &= -A \sum_{m=1}^{\infty} \left[\frac{\bar{a}_m}{m} \sin(m\xi) - \frac{\bar{b}_m}{m} \cos(m\xi) \right]_{-\pi}^{\frac{\theta - B}{A}} \\ &= -A \sum_{m=1}^{\infty} \left[\frac{\bar{a}_m}{m} \sin\left(m \frac{\theta - B}{A}\right) - \frac{\bar{b}_m}{m} \cos\left(m \frac{\theta - B}{A}\right) \right. \\ &\quad \left. - \frac{\bar{a}_m}{m} \sin(-m\pi) + \frac{\bar{b}_m}{m} \cos(-m\pi) \right], \end{aligned} \quad (4.3.121)$$

then

$$\begin{aligned} F(\theta) &= -A \sum_{m=1}^{\infty} \left[\frac{\bar{a}_m}{m} \sin\left(m \frac{\theta - B}{A}\right) - \frac{\bar{b}_m}{m} \cos\left(m \frac{\theta - B}{A}\right) \right. \\ &\quad \left. + \frac{\bar{b}_m}{m} \cos(-m\pi) \right], \quad (\theta^L < \theta < \theta^R). \end{aligned} \quad (4.3.122)$$

Substituting the results into (4.3.14) to get

$$\Phi_i(1, \theta) = F(\theta, t) \quad (\theta^L < \theta < \theta^R), \quad (4.3.123)$$

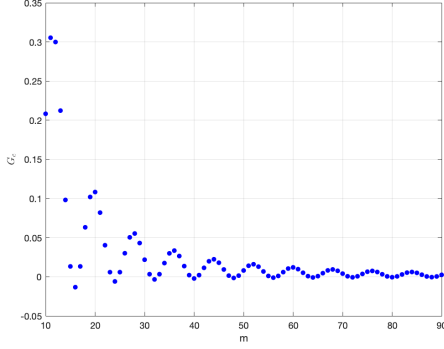


Figure 4.3.8: G_c

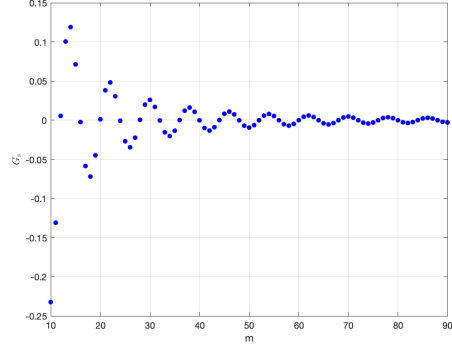


Figure 4.3.9: G_s

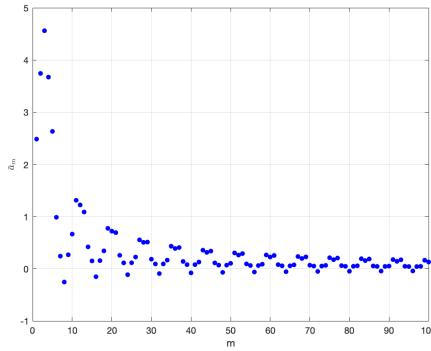


Figure 4.3.10: \bar{a}_m

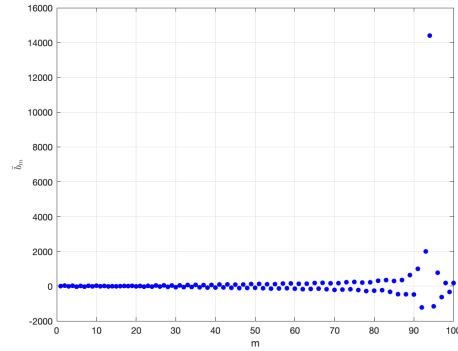


Figure 4.3.11: \bar{b}_m

The total velocity potential,

$$\Phi(\rho, \theta, t) = \Phi_c(\rho, \theta, t) + \Phi_i(\rho, \theta, t), \quad (4.3.124)$$

in the contact region, $(\theta^L < \theta < \theta^R)$ and $\rho = 1$, is equal to $F(\theta)$ because $\Phi_c(\rho, \theta, t) = 0$. We obtained

$$\Phi(1, \theta, t) = -A \sum_{m=1}^{\infty} \left[\frac{\bar{a}_m}{m} \sin\left(m \frac{\theta - B}{A}\right) - \frac{\bar{b}_m}{m} \cos\left(m \frac{\theta - B}{A}\right) + \frac{\bar{b}_m}{m} (-1)^m \right], \quad (\theta^L < \theta < \theta^R), \quad (4.3.125)$$

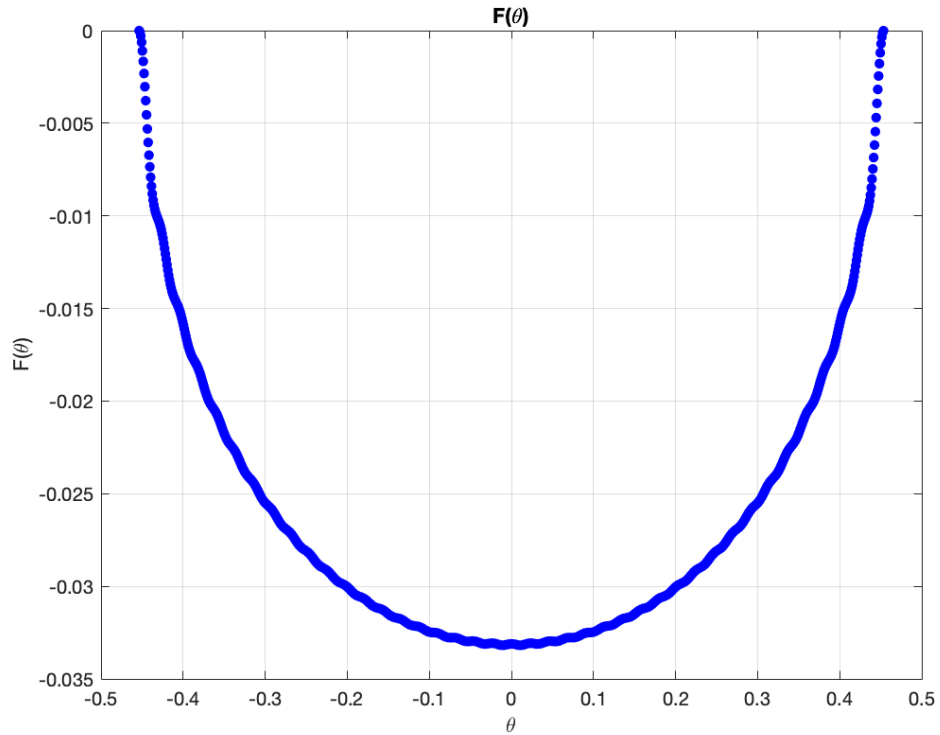


Figure 4.3.12: Plot of $F(\theta)$ in (4.3.122) for $m = 40$, where $h' = 1$, $R = 1/4$ and $(x_c, y_c) = (0, -650)$.

The G_c (4.3.109) and G_s (4.3.115) plotted and shown in figure 4.3.8 and 4.3.9 respectively. Figure 4.3.11 shows \bar{a}_m and \bar{b}_m where they are defined in (4.3.92). Finally, after \bar{a}_m and \bar{b}_m founded we substituted in the series (4.3.122), plotted the $F(\theta)$, see figure 4.3.12. The velocity potential $\Phi(\theta)$ (4.3.125) is plotted for $m = 40$, where $h' = 1$, $R = 1/4$, $x_c = 0$ with different interacted values of y_c , see 4.3.13.

4.4 Hydrodynamic loads acting on the cylinder

In this section, we shall derive equations of motion of the cylinder including the hydrodynamic pressure and the force acting on the cylinder in dimensionless variables

The hydrodynamic pressure along the cylinder within the Wagner model is

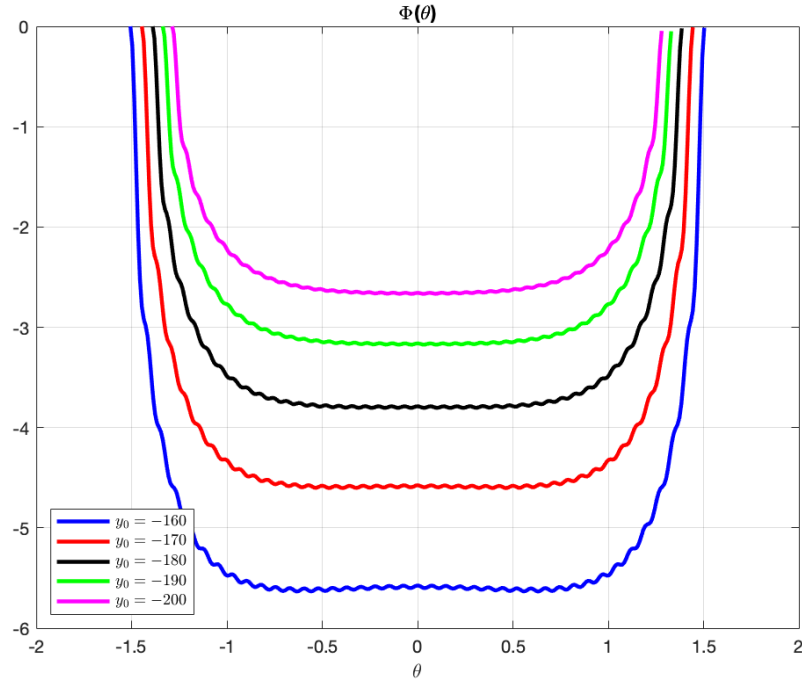


Figure 4.3.13: Plot of $\Phi(\theta)$ in (4.3.125) for $m = 40$, where $h' = 1$, $R = 1/4$, $x_c = 0$ with different interacted values of y_c .

given by

$$p = -\frac{\partial}{\partial t}\varphi(x, y, t), \quad \text{where} \quad (x - x_c(t))^2 + (y - y_c(t))^2 = R^2. \quad (4.4.1)$$

In the previous section, the velocity potential was determined in the ζ -plane where

$$\varphi(x, y, t) = \varphi[x(\rho, \theta, t), y(\rho, \theta, t)] = \Phi(\rho, \theta, t), \quad (4.4.2)$$

or

$$\varphi(x, y, t) = \Phi[\rho(x, y, t), \theta(x, y, t), t]. \quad (4.4.3)$$

By using the chain rule, we calculate

$$\frac{\partial \varphi}{\partial t} = \frac{\partial \Phi}{\partial \rho} \frac{\partial \rho}{\partial t} + \frac{\partial \Phi}{\partial \theta} \frac{\partial \theta}{\partial t} + \frac{\partial \Phi}{\partial t}. \quad (4.4.4)$$

To determine the derivatives ρ_t and θ_t , we differentiate the conformal

mapping (3.3.1), where $\zeta = \rho(x, y, t)ie^{-i\theta(x, y, t)}$. We obtain

$$\frac{-x'_c(t)}{\sqrt{y_c^2(t) - R^2}} - \frac{1}{2} \frac{z - x_c(t)}{(y_c^2(t) - R^2)^{3/2}} 2y_c(t)y'_c(t) = -\frac{2}{(\zeta + i)^2} \frac{\partial \zeta}{\partial t}, \quad (4.4.5)$$

$$\frac{-x'_c(t)}{\sqrt{y_c^2(t) - R^2}} - y_c(t)y'_c(t) \left(i + \frac{2}{\zeta + i} \right) \frac{1}{y_c^2(t) - R^2} = -\frac{2}{(\zeta + i)^2} \frac{\partial \zeta}{\partial t}, \quad (4.4.6)$$

then

$$\frac{\partial \zeta}{\partial t} = \frac{1}{2} \frac{x'_c(t)}{\sqrt{y_c^2(t) - R^2}} (\zeta + i)^2 + \frac{y_c(t)y'_c(t)}{2(y_c^2(t) - R^2)} (i(\zeta + i)^2 + 2(\zeta + i)), \quad (4.4.7)$$

where

$$\begin{aligned} i(\zeta + i)^2 + 2(\zeta + i) &= i(\zeta^2 + 2i\zeta - 1) + 2(\zeta + i) = i\zeta^2 - 2\zeta - i + 2\zeta + 2i \\ &= i\zeta^2 + i = i(1 + \zeta^2), \end{aligned} \quad (4.4.8)$$

and

$$\frac{\partial \zeta}{\partial t} = \frac{\partial \rho}{\partial t} ie^{-i\theta} + \rho ie^{-i\theta} \left(-i \frac{\partial \theta}{\partial t} \right). \quad (4.4.9)$$

Multiplying (4.4.7) by $-ie^{i\theta}$, we find

$$\frac{\partial \rho}{\partial t} - \rho i \frac{\partial \theta}{\partial t} = \frac{1}{2} \frac{x'_c(t)}{\sqrt{y_c^2(t) - R^2}} (-i)e^{i\theta} (\zeta + i)^2 + \frac{y_c(t)y'_c(t)}{2(y_c^2(t) - R^2)} (1 + \zeta^2)e^{i\theta}, \quad (4.4.10)$$

where

$$-ie^{i\theta} (\zeta + i)^2 = -ie^{i\theta} (-\rho^2 e^{-2i\theta} + 2i\rho e^{-i\theta} - 1) = i\rho^2 e^{-i\theta} + i\rho + ie^{i\theta}, \quad (4.4.11)$$

then

$$\begin{aligned} \frac{\partial \rho}{\partial t} - \rho i \frac{\partial \theta}{\partial t} &= \frac{1}{2} \frac{x'_c(t)}{\sqrt{y_c^2(t) - R^2}} \cdot \{ \rho^2 (i \cos(\theta) + \sin(\theta)) + i\rho + i \cos(\theta) - \sin(\theta) \} \\ &\quad + \frac{y_c(t)y'_c(t)}{2(y_c^2(t) - R^2)} (\cos(\theta)(1 - \rho^2) + i \sin(\theta)(1 + \rho^2)). \end{aligned} \quad (4.4.12)$$

Separating the real and imaginary parts, we obtain

$$\frac{\partial \rho}{\partial t} = \frac{1}{2} \frac{x'_c(t)}{\sqrt{y_c^2(t) - R^2}} \{ \rho^2 \sin(\theta) - \sin(\theta) \} + \frac{y_c(t)y'_c(t)}{2(y_c^2(t) - R^2)} (1 - \rho^2) \cos(\theta), \quad (4.4.13)$$

and

$$\begin{aligned} \frac{\partial \theta}{\partial t} = & -\frac{1}{2} \frac{x'_c(t)}{\sqrt{y_c^2(t) - R^2}} \left\{ \rho \cos(\theta) + 1 + \frac{1}{\rho} \cos(\theta) \right\} \\ & - \frac{y_c(t)y'_c(t)}{2(y_c^2(t) - R^2)} ((1 + \rho^2) \sin(\theta)). \end{aligned} \quad (4.4.14)$$

At the image of the liquid surface, $y = 0$, where $\rho = 1$, we obtain

$$\frac{\partial \rho}{\partial t} = 0, \quad (4.4.15)$$

and

$$\frac{\partial \theta}{\partial t} = -\frac{x'_c(t)(1 + 2 \cos(\theta))}{2\sqrt{y_c^2(t) - R^2}} - \frac{y_c(t)y'_c(t) \sin(\theta)}{(y_c^2(t) - R^2)}, \quad (4.4.16)$$

and on the surface of the cylinder, $\rho = R_1$, we have

$$\frac{\partial \rho}{\partial t} = \frac{1}{2} \frac{x'_c(t)}{\sqrt{y_c^2(t) - R^2}} (R_1^2 - 1) \sin(\theta) + \frac{y_c(t)y'_c(t)}{2(y_c^2(t) - R^2)} (1 - R_1^2) \cos(\theta), \quad (4.4.17)$$

$$\begin{aligned} \frac{\partial \theta}{\partial t} = & -\frac{1}{2} \frac{x'_c(t)}{\sqrt{y_c^2(t) - R^2}} \left\{ R_1 \cos(\theta) + \frac{1}{R_1} \cos(\theta) + 1 \right\} \\ & - \frac{y_c(t)y'_c(t)}{2(y_c^2(t) - R^2)} ((1 + R_1^2) \sin(\theta)). \end{aligned} \quad (4.4.18)$$

Stationary cylinder

If the cylinder is fixed, $x_c = \text{const}$ and $y_c = \text{const}$, then $x'_c = 0$ and $y'_c = 0$ and equations (4.4.17) and (4.4.18) gives

$$\frac{\partial \rho}{\partial t} = 0 \quad \text{and} \quad \frac{\partial \theta}{\partial t} = 0. \quad (4.4.19)$$

Therefore, on the surface of the cylinder,

$$\frac{\partial \varphi}{\partial t} = \frac{\partial \Phi}{\partial t}(R_1, \theta, t), \quad (4.4.20)$$

where the potential $\Phi(\rho, \theta, t)$ consists of two parts Φ_c and Φ_i , see (4.3.1). The component $\Phi_c(\rho, \theta, t) \equiv 0$ for a stationary cylinder. The component $\Phi_c(\rho, \theta, t)$ was determined in section 4.3.1. The dependence of this component on time is complicated because $\theta^L(t)$ and $\theta^R(t)$ in (4.3.13) are function of time, as well as $f(\theta, t)$. $\Phi_i(\rho, \theta, t)$ on the image of the liquid surface and $\Phi_c(\rho, \theta, t)$ on the image of the surface of the cylinder are obtained by (4.3.18), where R_1 , $\Phi_{in}^{(c)}(\rho, \theta)$ and $\Phi_{in}^{(s)}(\rho, \theta)$ are independent of time.

Therefore, the pressure on the cylinder is given by

$$p = -\frac{\partial \varphi}{\partial t} = -\frac{\partial \Phi}{\partial t}(R_1, \theta, t) = -\dot{a}_0(t) + \sum_{n=1}^{\infty} \left\{ \dot{a}_n(t) \frac{2R_1^2}{1+R_1^{2n}} \cos(n\theta) + \dot{b}_n(t) \frac{2R_1^2}{1+R_1^{2n}} \sin(n\theta) \right\}, \quad (4.4.21)$$

where the coefficients $a_n(t)$ and $b_n(t)$ are calculated using (4.3.17) with \bar{a}_n and \bar{b}_n being solution of (4.3.92).

Free to move cylinder

In this case, the cylinder moves due to the pressure generated in the liquid by the entering body. The pressure on the surface of the cylinder is calculated using (4.4.4), where the derivative $\partial \rho / \partial t$ and $\partial \theta / \partial t$ the potential $\Phi(\rho, \theta, t)$ is given by (4.3.1).

We calculate

$$\frac{\partial \Phi_c}{\partial \theta}(R_1, \theta, t) = 2 \frac{R\sqrt{1-\lambda^2}}{\lambda} \sum_{n=1}^{\infty} n^2 \frac{R_1^{3n} - R_1^n}{R_1^{2n} + 1} \left(-(-1)^{n+1} \dot{y}_c \sin n\theta + \dot{x}_c \cos n\theta \right), \quad (-\pi < \theta < \pi), \quad (4.4.22)$$

and

$$\frac{\partial \Phi_c}{\partial \rho}(R_1, \theta, t) = 2 \frac{R\sqrt{1-\lambda^2}}{\lambda} \sum_{n=1}^{\infty} n \frac{R_1^{3n-1} + R_1^{n-1}}{R_1^{2n} + 1} \cdot ((-1)^{n+1} \dot{y}_c \cos n\theta + \dot{x}_c \sin n\theta), \quad (-\pi < \theta < \pi). \quad (4.4.23)$$

The derivatives of $\Phi_i(\rho, \theta, t)$ with respect to ρ and θ at $(\rho = R_1)$ are calculated using (4.3.18). The derivatives of Φ_c and Φ_i in time are more complicated to determine because R_1 is also a function of time for this case.

4.4.1 Motion of the cylinder during water impact process

The 2nd Newton's law provides equations of the cylinder motion

$$m_c \ddot{x}_c = F_h(t) \quad \text{and} \quad m_c \ddot{h}_c = F_v(t), \quad (4.4.24)$$

where $m_c = M_c/(\rho R H)$, M_c is the mass of the cylinder per unit width, F_h and F_v are the dimensionless horizontal and vertical components of the dynamic force acting on the cylinder,

$$\vec{F}(t) = (F_h, F_v) = - \int_S p \vec{n} ds, \quad (4.4.25)$$

where $\vec{n} = (\cos \alpha, \sin \alpha)$ is the outer unit normal and ds is the dimensionless element of the surface $ds = d\alpha$

$$F_h = \frac{\partial}{\partial t} \int_{-\pi}^{\pi} \varphi(R, \alpha, t) \cos(\alpha) d\alpha, \quad (4.4.26)$$

$$F_v = \frac{\partial}{\partial t} \int_{-\pi}^{\pi} \varphi(R, \alpha, t) \sin(\alpha) d\alpha, \quad (4.4.27)$$

The motion equation (4.4.24) can be integrated using (4.4.26 - 4.4.27) and

the initial conditions $x_c(0) = x_{c0}$, $\dot{x}_c(0) = 0$, $y_c(0) = y_{c0}$, $\dot{y}_c(0) = 0$,

$$m_c \dot{x}_c(t) = \int_{-\pi}^{\pi} \varphi(R, \alpha, t) \cos(\alpha) d\alpha, \quad (4.4.28)$$

$$m_c \dot{y}_c(t) = \int_{-\pi}^{\pi} \varphi(R, \alpha, t) \sin(\alpha) d\alpha, \quad (4.4.29)$$

where the potential on the surface of the cylinder $\varphi(R, \alpha, t)$ depends on \dot{x}_c , \dot{y}_c , x_c and y_c . Equation (4.4.28 - 4.4.29) leads to two first order differential equations of the form

$$\dot{x}_c = K_h(x_c, y_c) \quad \text{and} \quad \dot{y}_c = K_v(x_c, y_c), \quad (4.4.30)$$

because the potential $\varphi(R, \alpha, t)$ depends on \dot{x}_c and \dot{y}_c linearly. The system (4.4.30) is integrated numerically. Note that the time derivative φ_t is not required in calculations of the cylinder motion.

4.5 Verification of the numerical solution

To validate the numerical solution described above, a parabolic contour entering water with a given speed $h(t)$ in the dimensionless variables.

$$f(x) = H \tilde{f}(x/L), \quad \tilde{f}(\tilde{x}) = \frac{\tilde{x}^2}{2\gamma}, \quad (4.5.1)$$

where $2L$ is the horizontal size of the entering body and H is the height of the body [17]. From (2.4.12-2.4.20) we have

$$\tilde{\nabla}^2 \tilde{\varphi} = 0 \quad (\tilde{y} < 0), \quad (4.5.2)$$

$$\tilde{p} = -\frac{\partial \tilde{\varphi}}{\partial \tilde{t}} \quad (\tilde{y} \leq 0), \quad (4.5.3)$$

$$\tilde{p} = 0, \quad \frac{\partial \tilde{\varphi}}{\partial \tilde{y}} = \frac{\partial \tilde{\eta}}{\partial \tilde{t}}, \quad \tilde{\varphi} = 0, \quad (\tilde{y} = \tilde{\eta}(\tilde{x}, \tilde{y}), \quad \tilde{x} < \tilde{x}_w^{(L)}(\tilde{t}), \quad \tilde{x} > \tilde{x}_w^{(R)}(\tilde{t})), \quad (4.5.4)$$

$$\frac{\partial \tilde{\varphi}}{\partial \tilde{y}} = -h'(\tilde{t}) \quad (\tilde{y} = \tilde{\eta}(\tilde{x}, \tilde{y}), \quad \tilde{x}_w^{(L)}(\tilde{t}) < \tilde{x} < \tilde{x}_w^{(R)}(\tilde{t})), \quad (4.5.5)$$

$$\frac{\partial \tilde{\varphi}}{\partial \tilde{n}} = L[\mathbf{v}_c \cdot \mathbf{n}], \text{ on } \Gamma_c(t) = \left\{ \tilde{R} = \sqrt{[\tilde{x} - \tilde{x}_c(\tilde{t})]^2 + [\tilde{y} + \tilde{y}_c(\tilde{t})]^2} \right\}, \quad (4.5.6)$$

$$\tilde{\varphi} \rightarrow 0 \quad (\text{as } \tilde{x}^2 + \tilde{y}^2 \rightarrow \infty), \quad (4.5.7)$$

$$\tilde{\varphi} = 0, \quad \tilde{\varphi}_{\tilde{t}} = 0 \quad (\text{at } \tilde{t} = 0), \quad (4.5.8)$$

$$\tilde{\eta} [\tilde{x}_w^{(L)}(\tilde{t}), \tilde{t}] = \tilde{f} [\tilde{x}_w^{(L)}(\tilde{t})] - h(\tilde{t}), \quad (4.5.9)$$

$$\tilde{\eta} [\tilde{x}_w^{(R)}(\tilde{t}), \tilde{t}] = \tilde{f} [\tilde{x}_w^{(R)}(\tilde{t})] - h(\tilde{t}). \quad (4.5.10)$$

without a submerged cylinder, the solution of the problem (2.4.12 - 2.4.20) for the parabolic contour within the Wagner model Φ reads

$$\tilde{\varphi}(\tilde{x}, 0, \tilde{t}) = -\tilde{h}'(\tilde{t}) \sqrt{\tilde{a}^2(\tilde{t}) - \tilde{x}^2} \quad (-\tilde{a}(\tilde{t}) < \tilde{x} < \tilde{a}(\tilde{t})), \quad (4.5.11)$$

where $\tilde{a}(\tilde{t}) = 2\sqrt{\gamma\tilde{t}}$, $\tilde{x}_w^{(L)}(\tilde{t}) = -\tilde{a}(\tilde{t})$ and $\tilde{x}_w^{(R)}(\tilde{t}) = \tilde{a}(\tilde{t})$. The numerical solution of this problem with a submerged circular cylinder is expected to approach the velocity potential (4.5.11), where the cylinder is placed far from the impact region.

The numerical solution to be compared with (4.5.11) is

$$\Phi(1, \theta, t) = -A \sum_{m=1}^{\infty} \left[\frac{\bar{a}_m}{m} \sin\left(m \frac{\theta - B}{A}\right) - \frac{\bar{b}_m}{m} \cos\left(m \frac{\theta - B}{A}\right) + \frac{b_m}{m} (-1)^m \right], \quad (\theta^L < \theta < \theta^R), \quad (4.5.12)$$

where

$$\varphi(x, 0, t) = \Phi(1, \theta, t), \quad (4.5.13)$$

and

$$\frac{x - x_{c0} + iy}{\sqrt{y_{c0}^2 - R^2}} = \frac{\cos \theta}{1 + \sin \theta}, \quad (4.5.14)$$

which gives

$$\theta^L = -2 \arctan \left(\frac{x_{c0} - x_w^{(L)}(t)}{\sqrt{y_{c0}^2 - R^2}} \right) \quad \text{and} \quad \theta^R = -2 \arctan \left(\frac{x_{c0} - x_w^{(R)}(t)}{\sqrt{y_{c0}^2 - R^2}} \right). \quad (4.5.15)$$

We take that $-\tilde{x}_w^{(L)} = \tilde{x}_w^{(R)} = a(\tilde{t}) = 150$ and $h'(\tilde{t}) = 1$.

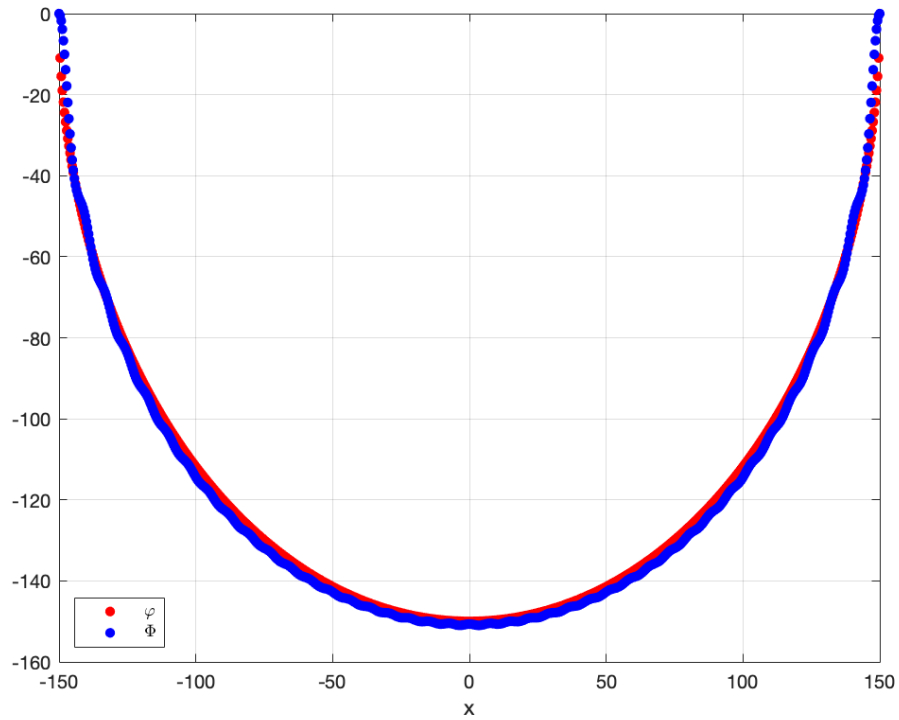


Figure 4.5.1: Plot of the analytical solution $\varphi(x, 0, t)$ in (4.5.11) and the numerical solution given by $\Phi(1, \theta, t)$ in (4.5.12), where $h' = 1$ and $(x_{c0}, y_{c0}) = (0, -650)$.

The numerical solutions (4.5.12) and analytical approximate solution (4.5.11) are compared in figure 4.5.1. We can get a good approximation when we add 40 retained terms in the series (4.5.12). Figure 4.5.2 shows the improvement of the numerical solution when increasing the add retained terms n . In Figure 4.5.3 we can see the effect of the submerged cylinder vanishes when the distances of the body from the impact place exceed two diameters of the impacting surface.

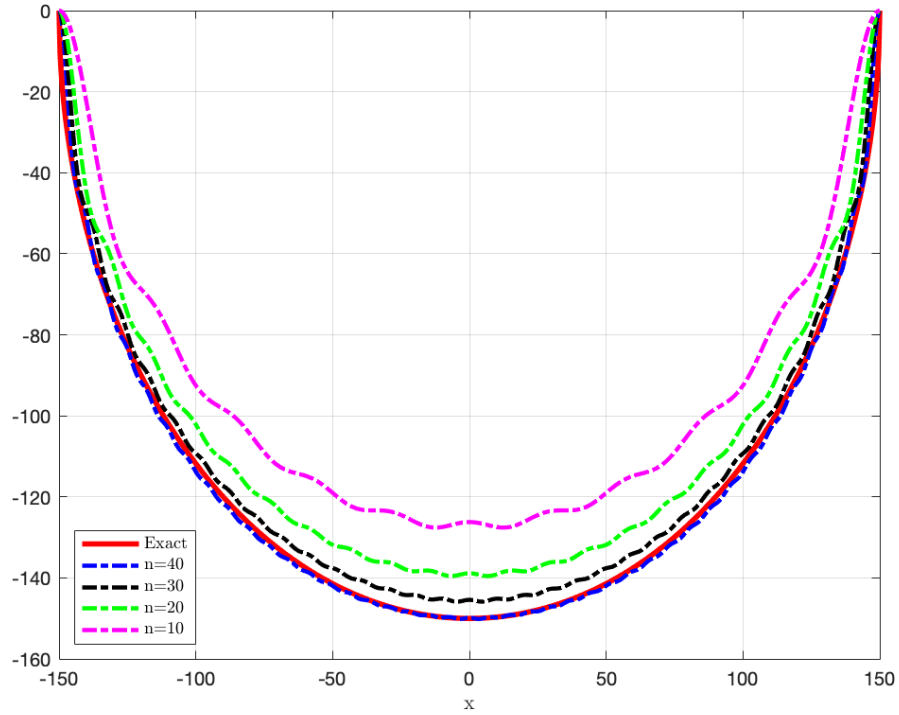


Figure 4.5.2: Plot of the analytical solution $\varphi(x, 0, t)$ in (4.5.11) and the numerical solution given by $\Phi(1, \theta, t)$ in (4.5.12), were $h' = 1$ and $(x_{c0}, y_{c0}) = (0, -650)$ with different number of terms n .

4.6 Verification of the numerical algorithm on the exact solution

Consider the following problem

$$\left\{ \begin{array}{ll} \nabla^2 \phi_i = 0 & (R_1 < \rho < 1), \\ \phi_i = 0 & (\rho = 1, \theta^R < \theta < \theta^L), \\ \frac{\partial \phi_i}{\partial \rho} = g(\theta) & (\rho = 1, \theta^L < \theta < \theta^R), \\ \frac{\partial \phi_i}{\partial \rho} = 0 & (\rho = R_1, 0 \leq \theta < 2\pi). \end{array} \right. \quad (4.6.1)$$

Let

$$\phi_i(1, \theta) = \begin{cases} \sqrt{(\theta^R - \theta)(\theta - \theta^L)} & (\theta^L < \theta < \theta^R), \\ 0 & (\theta^R < \theta < \theta^L), \end{cases} \quad (4.6.2)$$

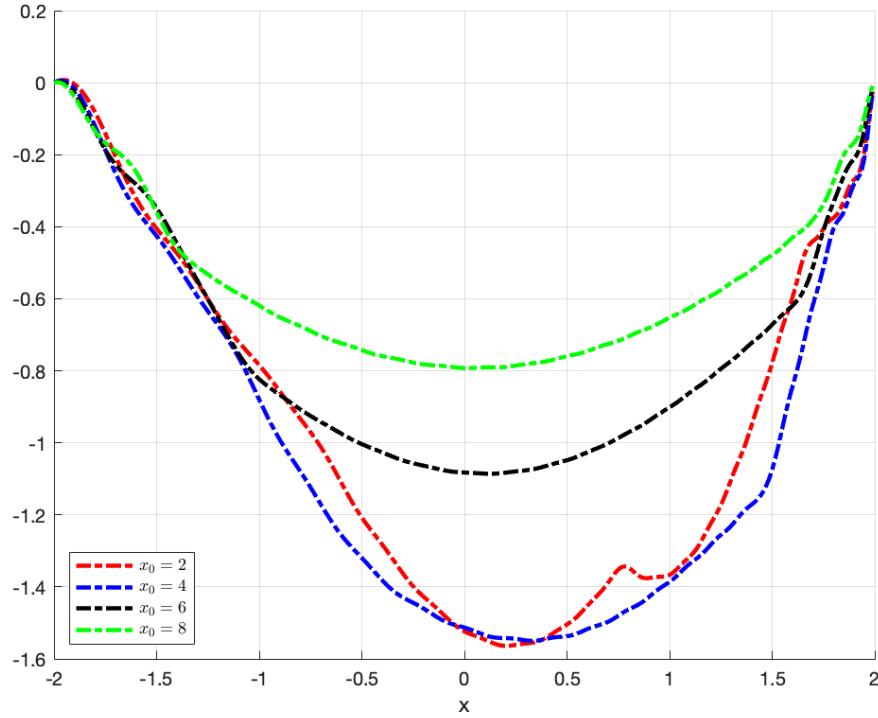


Figure 4.5.3: Velocity potential $\Phi(1, \theta, t)$ in (4.5.12), where $h' = 1$ and $y_0 = 2.5$ with different values of x_0 .

where

$$\phi_i(1, \theta) = G(\theta, t) \quad (\theta^L < \theta < \theta^R), \quad (4.6.3)$$

introduce the Fourier series of $\phi_i(1, \theta)$ as

$$\left\{ \begin{array}{l} G(\theta, t) \quad (\theta^L < \theta < \theta^R) \\ 0 \quad (\theta^R < \theta < \theta^L) \end{array} \right\} = a_0 + \sum_{n=1}^{\infty} \{a_n \cos(n\theta) + b_n \sin(n\theta)\}, \quad (4.6.4)$$

where

$$\begin{aligned} a_0 &= \frac{1}{2\pi} \int_{\theta^L}^{\theta^R} G(\theta, t) d\theta, \\ a_n &= \frac{1}{\pi} \int_{\theta^L}^{\theta^R} G(\theta, t) \cos(n\theta) d\theta, \\ b_n &= \frac{1}{\pi} \int_{\theta^L}^{\theta^R} G(\theta, t) \sin(n\theta) d\theta, \end{aligned} \quad (4.6.5)$$

are unknown coefficients. Thus

$$a_0 = \frac{1}{2\pi} \int_{\theta^L}^{\theta^R} \sqrt{(\theta^R - \theta)(\theta - \theta^L)} d\theta. \quad (4.6.6)$$

It is convenient to map the interval $(-\pi, \pi)$ onto the integration (4.6.6), $\theta = A\xi + B$, where $\theta^L = -A\pi + B$ and $\theta^R = A\pi + B$, which gives,

$$A = \frac{\theta^R - \theta^L}{2\pi} \quad \text{and} \quad B = \frac{\theta^L + \theta^R}{2}, \quad (4.6.7)$$

then $\theta^R - \theta = \theta^R - B - A\xi = A(\pi - \xi)$ and $\theta - \theta^L = B - \theta^L + A\xi = A(\pi + \xi)$, this gives $\sqrt{(\theta^R - \theta)(\theta - \theta^L)} = A\sqrt{(\pi^2 - \xi^2)}$, Thus

$$a_0 = \frac{1}{2\pi} \int_{-\pi}^{\pi} A\sqrt{(\pi^2 - \xi^2)} A d\xi = \frac{A^2\pi}{2} \int_0^{\pi/2} (\cos(2u) + 1) du = \frac{A^2\pi^2}{4}. \quad (4.6.8)$$

For the coefficients a_n we have

$$a_n = \frac{1}{\pi} \int_{\theta^L}^{\theta^R} \sqrt{(\theta^R - \theta)(\theta - \theta^L)} \cos(n\theta) d\theta, \quad (4.6.9)$$

then

$$a_n = \frac{2A^2 \cos(nB)}{\pi} \int_0^{\pi} \sqrt{\pi^2 - \xi^2} \cos(nA\xi) d\xi = \frac{A\pi}{n} \cos(nB) J_1(nA\pi), \quad (4.6.10)$$

where $J_1(x)$ is Bessel function [13]. The coefficients b_n in (4.6.5) are calculated similarly as

$$b_n = \frac{A\pi}{n} \sin(nB) J_1(nA\pi), \quad (4.6.11)$$

The Fourier series of the function $\phi_i(1, \theta)$ from (4.6.2) has the form

$$\phi_i(1, \theta) = \frac{A^2\pi^2}{4} + A\pi \sum_{n=1}^{\infty} \frac{1}{n} J_1(nA\pi) \cos[n(\theta - B)]. \quad (4.6.12)$$

Correspondingly the solution of problem (4.6.1) with the condition (4.6.12)

at $\rho = 1$ reads

$$\phi_i(\rho, \theta) = \frac{A^2\pi^2}{4} + A\pi \sum_{n=1}^{\infty} \frac{1}{n} \rho^n J_1(nA\pi) \cos[n(\theta - B)], \quad (4.6.13)$$

where figures 4.6.2 and 4.6.1 show the Fourier series (4.6.12) we obtain can give a approximation of $G(\theta, t)$, and figure 4.6.5 shows the differences between the exact solution and the the solution obtain by the series.

Now we have

$$\frac{\partial \phi_i}{\partial \rho}(1, \theta) = A\pi \sum_{n=1}^{\infty} J_1(nA\pi) \cos[n(\theta - B)] = g(\theta). \quad (4.6.14)$$

which is taken as the function $g(\theta)$ in (4.6.1). For illustrating we assumed that $x_w^L = -150$ and $x_w^R = 150$.

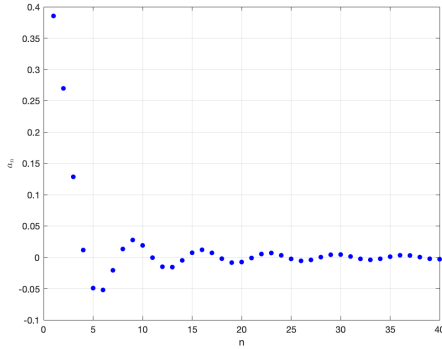


Figure 4.6.1: a_n

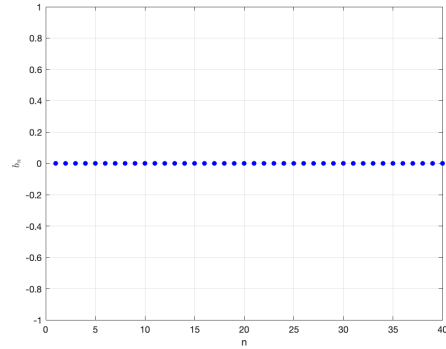


Figure 4.6.2: b_n

Figure 4.6.3: Plot of a_n and b_n , where $\theta^L = -\pi/2$ and $\theta^R = \pi/2$.

Solving (4.6.1) with $g(\theta)$ given by (4.6.14) we should obtain (4.6.2) on $\rho = 1$. Using similar steps as we did for solving the problem in (4.3.13). From (4.3.26) let

$$\tilde{f}(\theta) = g(\theta), \quad (4.6.15)$$

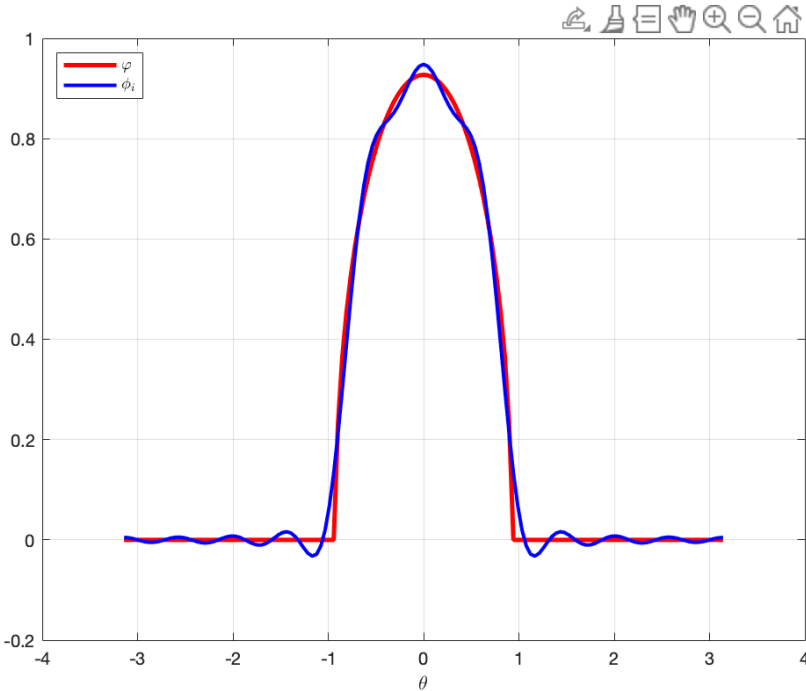


Figure 4.6.4: Plot of $\phi_i(1, \theta)$ in (4.6.12) for $n = 10$.

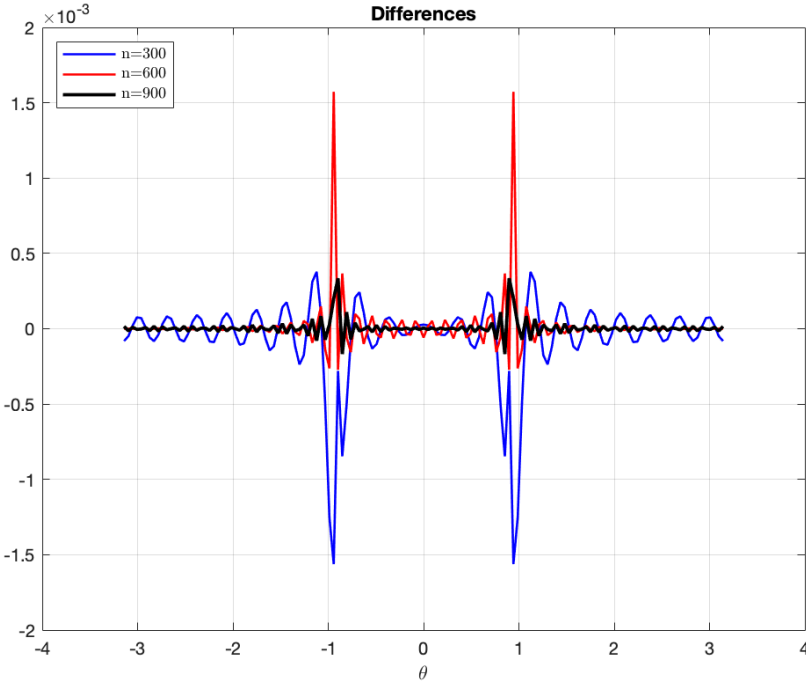


Figure 4.6.5: Plot of the differences between φ and $\phi_i(1, \theta)$ when $n = 300$, $n = 600$ and $n = 900$.

and using (4.3.31) gives

$$\begin{aligned} \lim_{\rho \rightarrow 1-0} \left\{ \frac{\partial \phi_i}{\partial \rho}(\rho, \theta) \langle G \rangle \right\} &= \lim_{\rho \rightarrow 1-0} \frac{\partial}{\partial \theta} \left[\int_{\theta^L}^{\theta^R} G(\theta_0, t) d\{S(\rho, \theta - \theta_0)\} \right] \\ &= - \lim_{\rho \rightarrow 1} \frac{\partial}{\partial \theta} \int_{\theta^L}^{\theta^R} G'(\theta_0) S(\rho, \theta - \theta_0) d\theta_0 = g(\theta) \quad (\theta^L < \theta < \theta^R). \end{aligned} \quad (4.6.16)$$

where $S(\rho, \theta)$ as from (4.3.30) as

$$S(\rho, \theta) = \frac{1}{\pi \rho} \sum_{n=1}^{\infty} \rho^n \frac{\cos(n\theta)}{n}, \quad (4.6.17)$$

let

$$-U(\theta) = G'(\theta), \quad (4.6.18)$$

where

$$\frac{dG}{d\theta} = \frac{-2\theta + \theta^L + \theta^R}{2\sqrt{(\theta^R - \theta)(\theta - \theta^L)}}, \quad (4.6.19)$$

integrate both sides of (4.6.18) from θ^L to θ as did in (4.3.33) gives

$$\begin{aligned} \int_{\theta^L}^{\theta^R} \frac{-2\theta_0 + \theta^L + \theta^R}{2\sqrt{(\theta^R - \theta_0)(\theta_0 - \theta^L)}} \{S(1, \theta - \theta_0) - S(1, \theta^L - \theta_0)\} d\theta_0 &= \bar{g}(\theta), \\ &(\theta^L < \theta < \theta^R), \end{aligned} \quad (4.6.20)$$

where $\bar{g}(\theta)$ is given by

$$\bar{g}(\theta) = \int_{\theta^L}^{\theta} g(\theta_0) d\theta_0. \quad (4.6.21)$$

From (4.6.17) and (4.6.20), we have

$$S(1, \theta - \theta_0) - S(1, \theta^L - \theta_0) = \frac{1}{\pi} \sum_{n=1}^{\infty} \frac{1}{n} \{ \cos[n(\theta - \theta_0)] - \cos[n(\theta^L - \theta_0)] \}, \quad (4.6.22)$$

apply the mapped interval $(-\pi, \pi)$ as in (4.6.7), gives

$$\int_{-\pi}^{\pi} \tilde{U}(\xi_0) \{S(1, A(\xi - \xi_0)) - S(1, A(-\pi - \xi_0))\} A d\xi_0 = D(\xi),$$

$$(-\pi < \xi < \pi), \quad (4.6.23)$$

and

$$\tilde{U}(\xi_0) = \frac{\xi_0}{\sqrt{\pi^2 - \xi_0^2}}, \quad (4.6.24)$$

where $U(\theta) = U(A\xi + B) = \tilde{U}(\xi)$, $\theta_0 = A\xi_0 + B$ and $D(\xi) = \bar{g}(A\xi + B)$. By substituting (4.6.17) into (4.6.23), then the right hand side gives

$$\begin{aligned} & \frac{A}{\pi} \sum_{k=1}^{\infty} \frac{1}{k} \int_{-\pi}^{\pi} \frac{\xi_0}{\sqrt{\pi^2 - \xi_0^2}} \{ \cos(kA(\xi - \xi_0)) - \cos(kA(\pi + \xi_0)) \} d\xi_0 \\ &= \frac{A}{\pi} \sum_{k=1}^{\infty} \left\{ \frac{\sin(kA\xi)}{k} \int_{-\pi}^{\pi} \frac{\xi_0 \sin(kA\xi_0)}{\sqrt{\pi^2 - \xi_0^2}} - \frac{\sin(kA\pi)}{k} \int_{-\pi}^{\pi} \frac{\xi_0 \sin(kA\xi_0)}{\sqrt{\pi^2 - \xi_0^2}} \right\} d\xi_0 \\ &= A\pi \sum_{k=1}^{\infty} \left\{ \frac{\sin(kA\xi)}{k} J_1(kA\pi) - \frac{\sin(kA\pi)}{k} J_1(kA\pi) \right\}, \quad (4.6.25) \end{aligned}$$

where we used Tables of Integrals [13] to find the integrals and the following identity

$$\cos[kA(\xi - \xi_0)] = \cos(kA\xi) \cos(kA\xi_0) + \sin(kA\xi) \sin(kA\xi_0). \quad (4.6.26)$$

Then we have

$$\int_{-\pi}^{\pi} \frac{\xi_0 \sin(kA\xi_0)}{\sqrt{\pi^2 - \xi_0^2}} d\xi_0 = 2\pi \int_0^1 \frac{u \sin(kA\pi u)}{\sqrt{1 - u^2}} du = \pi^2 J_1(kA\pi), \quad (4.6.27)$$

from (4.6.23) and (4.6.21) we have

$$\bar{g}(\theta) = \int_{\theta^L}^{\theta} g(\theta_0) d\theta_0, \quad (4.6.28)$$

then from (4.6.14) we have

$$\begin{aligned} D(\xi) &= \int_{-\pi}^{\xi} g(A\xi_0 + B)d\xi_0 = A\pi \sum_{k=1}^{\infty} J_1(kA\pi) \int_{-\pi}^{\xi} \cos(kA\xi_0)Ad\xi_0 \\ &= A\pi \sum_{k=1}^{\infty} \left\{ \frac{\sin(kA\xi)}{k} J_1(kA\pi) + \frac{\sin(kA\pi)}{k} J_1(kA\pi) \right\}. \end{aligned} \quad (4.6.29)$$

substituting $\theta = A\xi + B$ gives

$$D(\theta) = A\pi \sum_{k=1}^{\infty} \left\{ \frac{\sin[k(\theta - B)]}{k} J_1(kA\pi) + \frac{\sin(kA\pi)}{k} J_1(kA\pi) \right\}, \quad (\theta^L < \theta < \theta^R), \quad (4.6.30)$$

Substituting the results into (4.6.3) to get

$$\phi_i(1, \theta) = G(\theta, t), \quad (\theta^R < \theta < \theta^L). \quad (4.6.31)$$

This means that the integral equation for $U(\theta)$ in (4.6.23) is correct, there is no mistake in this equation. It seems the potential $G(\theta)$ is a linear function, but we can not prove this, see figure 4.6.6.

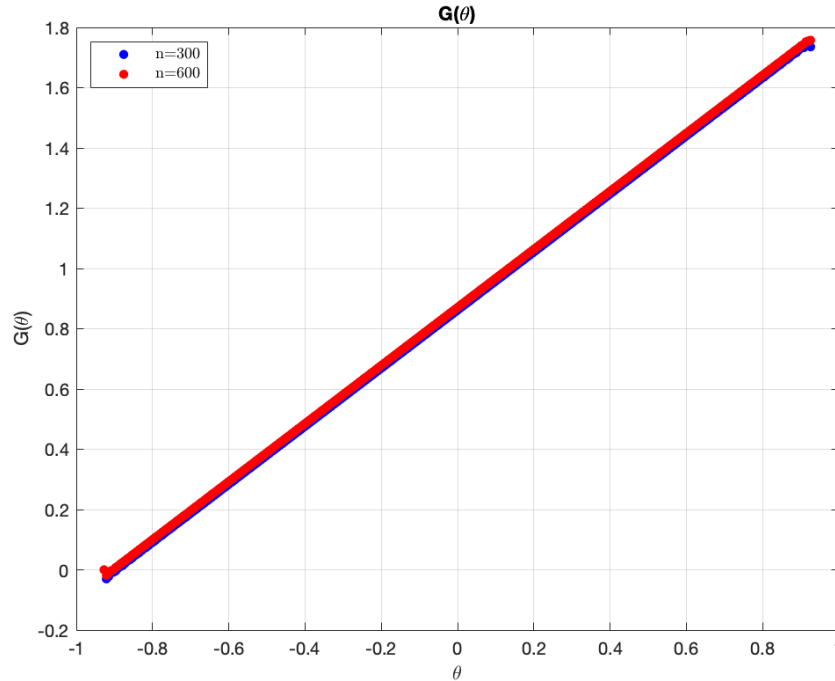


Figure 4.6.6: Plot of $G(\theta)$ in (4.6.30).

From (4.3.40) we have the function $\tilde{U}(\xi)$ is sought as the Fourier series

$$\tilde{U}(\xi) = \frac{1}{2}\bar{a}_0 + \sum_{n=1}^{\infty} (\bar{a}_n \cos(n\xi) + \bar{b}_n \sin(n\xi)), \quad (4.6.32)$$

where $\tilde{U}(\xi)$ shown in (4.6.24). From (4.6.5) we can calculate \bar{a}_n and \bar{b}_n as

$$\bar{a}_0 = \frac{1}{2\pi} \int_{-\pi}^{\pi} \tilde{U}(\xi) d\xi = \frac{1}{2\pi} \int_{-\pi}^{\pi} \frac{\xi}{\sqrt{\pi^2 - \xi^2}} d\xi = 0, \quad (4.6.33)$$

and

$$\bar{a}_n = \frac{1}{\pi} \int_{-\pi}^{\pi} \tilde{U}(\xi) \cos(n\xi) d\xi = \frac{1}{\pi} \int_{-\pi}^{\pi} \frac{\xi}{\sqrt{\pi^2 - \xi^2}} \cos(n\xi) d\xi = 0, \quad (4.6.34)$$

and

$$\bar{b}_n = \frac{1}{\pi} \int_{-\pi}^{\pi} \tilde{U}(\xi) \sin(n\xi) d\xi = \frac{1}{\pi} \int_{-\pi}^{\pi} \frac{\xi}{\sqrt{\pi^2 - \xi^2}} \sin(n\xi) d\xi = \pi J_1(n\pi), \quad (4.6.35)$$

where we used the formulae in (4.6.27). The figure 4.6.7 shows the Fourier series (4.6.32) we obtain can give a good approximation for \tilde{U} in (4.6.24).

Substituting the series (4.6.32) in (4.6.23) gives

$$\begin{aligned} \sum_{n=1}^{\infty} \left\{ \bar{a}_n \int_{-\pi}^{\pi} \left(\int_{-\pi}^{\pi} \cos(n\xi_0) T(\xi, \xi_0) d\xi_0 \right) \cos(m\xi) d\xi \right. \\ \left. + \bar{b}_n \int_{-\pi}^{\pi} \left(\int_{-\pi}^{\pi} \sin(n\xi_0) T(\xi, \xi_0) d\xi_0 \right) \cos(m\xi) d\xi \right\} \\ = \frac{1}{A} \int_{-\pi}^{\pi} D(\xi) \cos(m\xi) d\xi, \quad (4.6.36) \end{aligned}$$

$$\begin{aligned} \sum_{n=1}^{\infty} \left\{ \bar{a}_n \int_{-\pi}^{\pi} \left(\int_{-\pi}^{\pi} \cos(n\xi_0) T(\xi, \xi_0) d\xi_0 \right) \sin(m\xi) d\xi \right. \\ \left. + \bar{b}_n \int_{-\pi}^{\pi} \left(\int_{-\pi}^{\pi} \sin(n\xi_0) T(\xi, \xi_0) d\xi_0 \right) \sin(m\xi) d\xi \right\} \\ = \frac{1}{A} \int_{-\pi}^{\pi} D(\xi) \sin(m\xi) d\xi, \quad (4.6.37) \end{aligned}$$

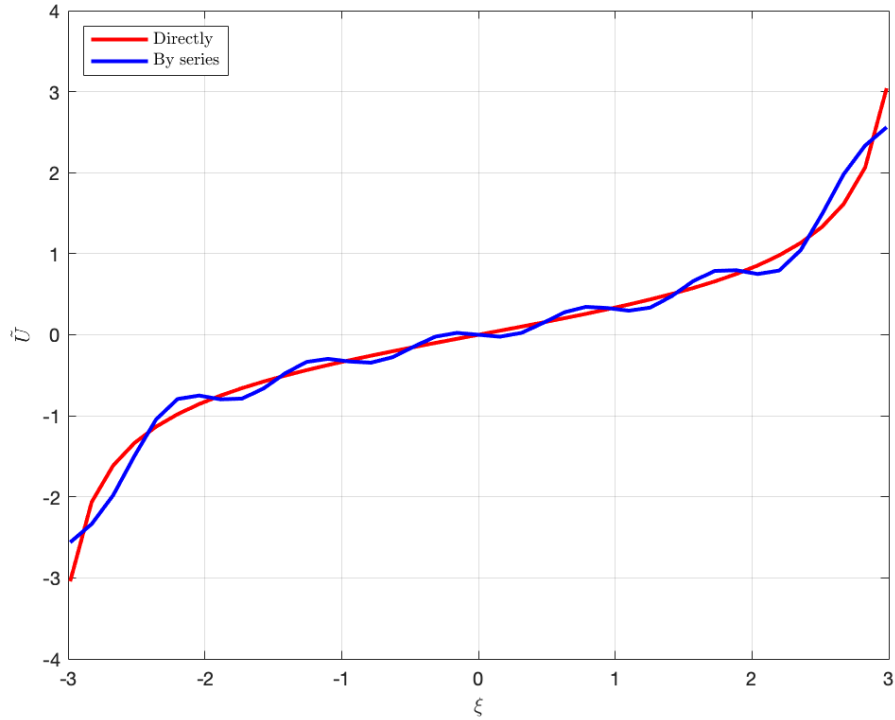


Figure 4.6.7: Plot of \tilde{U} in (4.6.24) and (4.6.32) where $n = 20$.

where

$$T(\xi, \xi_0) = S(1, A(\xi - \xi_0)) - S(1, -A(\pi + \xi_0)). \quad (4.6.38)$$

Recall the system in (4.3.45) where \vec{G} substituting by D in (4.6.29) as

$$\begin{cases} A^{(cc)}\vec{a} = \vec{D}_c, \\ A^{(ss)}\vec{b} = \vec{D}_s, \end{cases} \quad (4.6.39)$$

where $A^{(cc)}$ and $A^{(ss)}$ are evaluated by (4.3.54) and (4.3.80) respectively.

$D_{c,m}$ is given by

$$D_{c,m} = \frac{1}{A} \int_{-\pi}^{\pi} D(\xi) \cos(m\xi) d\xi, \quad (4.6.40)$$

where $D(\xi) = \bar{g}(A\xi + B)$. Substituting (4.6.29) into (4.6.40) gives

$$D_{c,m} = \pi \sum_{k=1}^{\infty} \int_{-\pi}^{\pi} \left\{ \frac{\sin(kA\xi)}{k} J_1(kA\pi) + \frac{\sin(kA\pi)}{k} J_1(kA\pi) \right\} \cos(m\xi) d\xi, \quad (4.6.41)$$

then

$$D_{c,m} = \pi \sum_{k=1}^{\infty} \frac{\sin(kA\pi)}{k} J_1(kA\pi) \delta_m, \quad (4.6.42)$$

where

$$\delta_m = \int_{-\pi}^{\pi} \cos(m\xi) d\xi = \begin{cases} 2\pi & \text{for } m = 0, \\ 0 & \text{for } m \neq 0, \end{cases} \quad (4.6.43)$$

Similarly for $D_{s,m}$

$$D_{s,m} = \pi \sum_{k=1}^{\infty} \int_{-\pi}^{\pi} \left\{ \frac{\sin(kA\xi)}{k} J_1(kA\pi) + \frac{\sin(kA\pi)}{k} J_1(kA\pi) \right\} \sin(m\xi) d\xi, \quad (4.6.44)$$

gives

$$D_{s,m} = \pi \sum_{k=1}^{\infty} \frac{J_1(kA\pi)}{k} \frac{2m}{(kA)^2 - m^2} \sin(kA\pi) \cos(m\pi), \quad (4.6.45)$$

From (4.3.92) and (4.6.39) we have

$$\vec{a} = [A^{(cc)}]^{-1} \vec{D}_c \quad \text{and} \quad \vec{b} = [A^{(ss)}]^{-1} \vec{D}_s, \quad (4.6.46)$$

From (4.3.122) we have

$$G(\theta) = -A \sum_{m=1}^{\infty} \left[\frac{\bar{a}_m}{m} \sin\left(m \frac{\theta - B}{A}\right) - \frac{\bar{b}_m}{m} \cos\left(m \frac{\theta - B}{A}\right) + \frac{\bar{b}_m}{m} \cos(-m\pi) \right], \quad (\theta^L < \theta < \theta^R). \quad (4.6.47)$$

where

$$\phi_i(1, \theta) = G(\theta, t) \quad (\theta^R < \theta < \theta^L), \quad (4.6.48)$$

where figure 4.6.8 shows $G(\theta, t)$ in (4.6.47) where $m = 20$.

Finally, figure 4.6.9 shows the the exact solution of (4.6.1) compared with the solution that obtained by Fourier series $G(\theta)$, where figure 4.6.9(a) shows

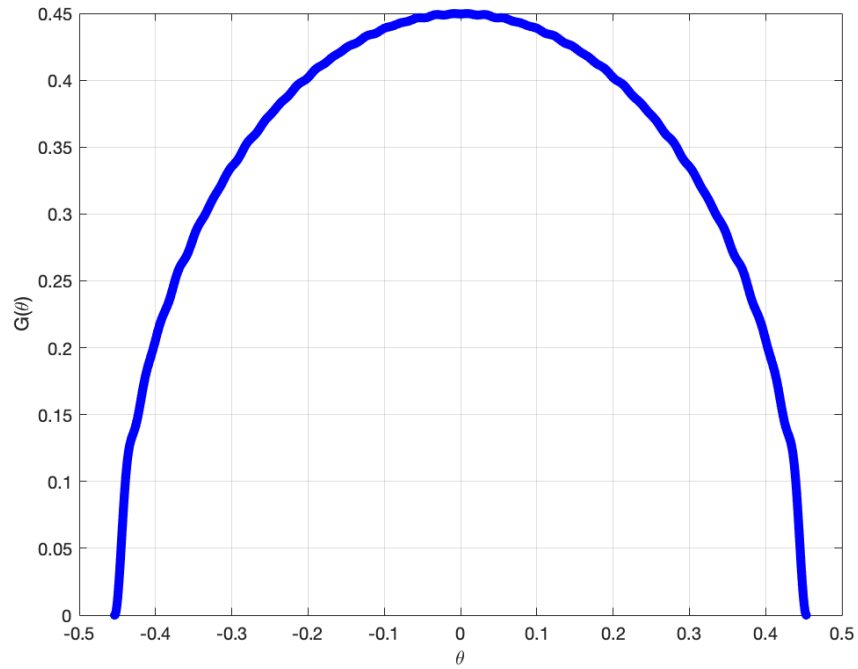


Figure 4.6.8: Plot of $G(\theta)$ in (4.6.47) for $m = 20$.

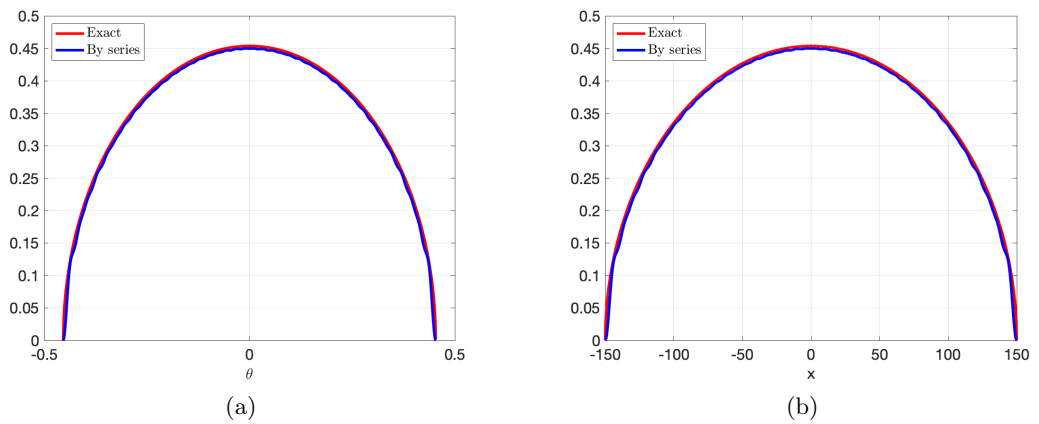


Figure 4.6.9: Plot of $\phi_i(1, \theta)$ in (4.6.48) for $m = 40$.

the solutions in terms of conformal mapping ζ -plane and figure 4.6.9(b) shows the solutions after returning back to the original z -plane. This confirmed that the approach used are correct and the transformation of the problem from original z -plane to ζ -plane and returning back is also correct.

**Water entry problem in the presence
of floating body**

In this chapter, we study the water entry problem in the presence of another floating body. The floating body is a rigid flat plate of small draft in our study. This problem is asymmetric, even for symmetric entering body, and with mixed boundary conditions.

5.1 Motivations

The water impact of a rigid body in the presence of a floating flat plate will be studied. The presence of a floating flat plate nearby the impacted place can significantly change the water impact process or cause a crash. When the hull of a lifeboat impacts the water surface in the presence of floating flat plate, the hydrodynamic pressures acting on the hull is expected to be higher than in the case without other bodies nearby. As a result, the deceleration of the lifeboat can exceed a critical value leading to injuries to the people inside the lifeboat.

5.2 Formulation of the problem

5.2.1 Governing equations

The fluid is assumed in a two-dimensional coordinate system. We neglected the gravity and surface tension effects because the body is large where the shape of the body is larger than the capillary length of water which is around 2.7mm and the acceleration of the fluid particles are much greater than the gravitational acceleration. Figure 5.2.3 illustrates the geometry of the problem and the coordinate system.

Initially ($t = 0$) the water free surface is flat, $y = 0$. A body touches the free surface at a single point taken as the origin of the Cartesian coordinate system xy , see figure 5.2.3. Then, the body suddenly starts to penetrate water at speed $h(t)$.

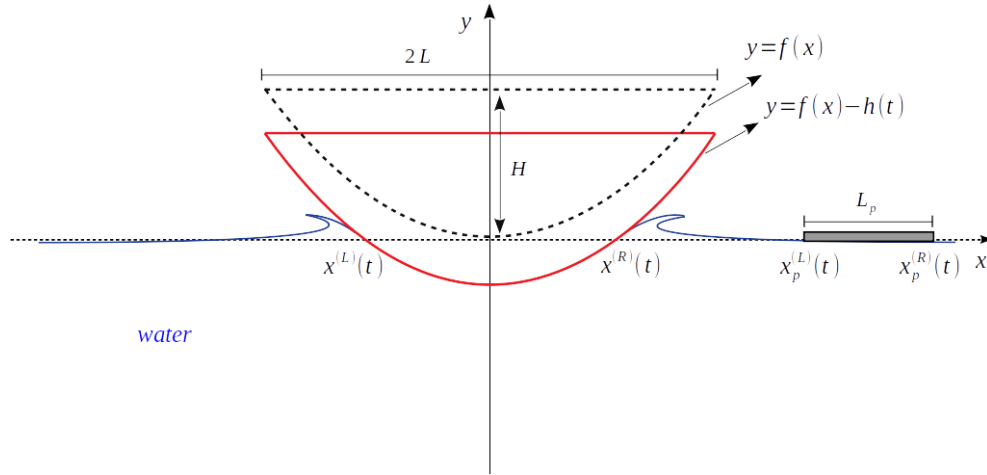


Figure 5.2.1: Sketch of a rigid body entering water in the presence of a floating plate nearby.

The resulting flow is assumed irrotational. The flow is described by the velocity potential $\varphi(x, y, t)$ which satisfies Laplace's equation

$$\nabla^2 \varphi = 0, \quad (5.2.1)$$

in the flow region. The boundary conditions for the equation (5.2.1) include the condition on the wetted surface of the entering body, the condition on the lower surface of the free floating plate, and the dynamic and kinematic conditions on the intervals of the free surface of the fluid. The condition on the floating plate reads

$$y_t = \varphi_y(x, y_p(x, t), t) = \dot{Y}_p(t) + \dot{\Omega}_p(t)[x - X_p(t)] + \Omega_p(t)[\varphi_x(x, y_p(x, t), t) - \dot{X}_p(t)], \quad (5.2.2)$$

where

$$y(x, t) = Y_p(t) + \Omega_p(t)[x - X_p(t)], \quad (5.2.3)$$

$\dot{X}_p(t)$ and $\dot{Y}_p(t)$ are the horizontal and vertical velocity components of the flat plate and $(X_p(t), Y_p(t))$ is the position vector of the center of the flat plate. The floating flat plate can move vertically and rotate only in the present study $X_p(t) \equiv X_p(0)$.

5.2.2 Formulation of the problem and flow in the main region

$$\nabla^2 \varphi = 0 \quad \text{in } \Omega(t), \quad \text{where} \quad (5.2.4)$$

$$\Omega(t) = \{x, y\} \left\{ \begin{array}{ll} -\infty < x < x^{(L)}(t), & y \leq \eta(x, t), \\ x^{(R)}(t) < x < x_p^{(L)}(t), \quad x > x_p^{(R)}(t), & \\ x^{(L)}(t) < x < x^{(R)}(t), & y \leq f(x) - h(t), \\ x_p^{(L)} < x < x_p^{(R)}, & y \leq Y_p(t) + \Omega_p(t)(x - X_p(t)), \end{array} \right.$$

$$\Omega(0) = \{x, y \mid -\infty < x < \infty, y \leq 0\}.$$

$$p = -\rho \left(\varphi_t + \frac{1}{2} |\nabla \varphi|^2 \right) \quad \text{in } \Omega(t), \quad (5.2.5)$$

$$p = 0, \quad \varphi_y = \eta_x \varphi_x + \eta_t \quad \text{on } \Gamma_f(t), \quad (5.2.6)$$

$$\varphi_y = f_x \varphi_x - h'(t) \quad \text{on } \Gamma_w(t), \quad (5.2.7)$$

$$\varphi_y = \dot{Y}_p(t) + \dot{\Omega}_p(t)[x - X_p(0)] + \Omega_p(t)\varphi_x, \quad y = Y_p(t) + \Omega_p(t)[x - X_p(0)], \quad (5.2.8)$$

$$\varphi \rightarrow 0 \quad (\text{as } x^2 + y^2 \rightarrow \infty), \quad (5.2.9)$$

$$\varphi = 0, \quad \varphi_t = 0, \quad (t = 0), \quad (5.2.10)$$

where $X_p(0)$ is the center of rigid floating plate. $f(x)$ and $h(t)$ will be given where the motion of the rigid plate, pressure and force change due to impact plate. The velocity displacement of the plate $Y_p(t)$ and the angle of its rotation $\alpha(t)$, where $\Omega_p(t) = \tan[\alpha(t)]$, are governed by the equations

$$m_p \frac{d^2 Y_p}{dt^2} = \int_{x_p^{(L)}}^{x_p^{(R)}} p(x, [Y_p + \Omega_p(x - X_p(0)), t] \cos[\alpha(t)] dx, \quad (5.2.11)$$

$$m_p \frac{d^2 X_p}{dt^2} = \int_{x_p^{(L)}}^{x_p^{(R)}} p(x, [Y_p + \Omega_p(x - X_p(0)), t] \sin[\alpha(t)] dx, \quad (5.2.12)$$

and

$$J_p \frac{d^2 \alpha}{dt^2} = \int_{x_p^{(L)}(t)}^{x_p^{(R)}(t)} p(x, [X_p + \Omega_p(x - X_p(0)), t] (x - X_p(0)) dx, \quad (5.2.13)$$

where J_p is the moment of inertia.

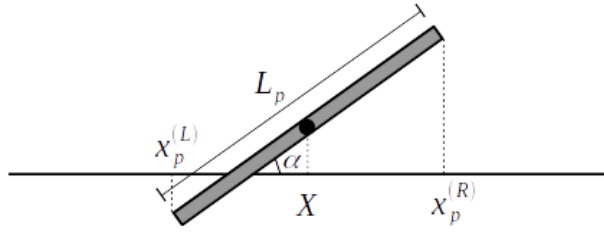


Figure 5.2.2: Sketch of the angle of inclination.

The impact of short duration, the angle of inclination of the floating plate the vertical displacement are small, because of that the horizontal force of the plate is negligible only if the plate is inclined. The force on the sidewall of the plate is small because the draft of the plate is negligible. This means that the force on the sidewall is neglected due to the thickness of the plate being small.

5.2.3 Non-dimensional variables for blunt body impact

Horizontal motion is neglected which leads to the plate can move vertically only. Dimensions of the blunt body are given by $2L$ for the x -axis and H for the y -axis. Now represent the shape function $f(t)$ by

$$f(x) = H\tilde{f}(x/L), \quad (5.2.14)$$

where tilde denotes the non-dimensional variables and

$$\tilde{x} = x/L, \quad -1 \leq \tilde{x} \leq 1, \quad 0 \leq \tilde{f}(\tilde{x}) \leq 1, \quad |d\tilde{f}/d\tilde{x}| \leq 1. \quad (5.2.15)$$

Now by taking L to be the length scale, H the displacement scale, H/v the time scale and the product vL the scale of the velocity potential:

$$x = L\tilde{x}, \quad y = L\tilde{y}, \quad h(t) = H\tilde{h}(\tilde{t}), \quad t = \frac{H}{v}\tilde{t}, \quad \varphi = vL\tilde{\varphi}(\tilde{x}, \tilde{y}, \tilde{t}),$$

$$f(x) = H\tilde{f}(\tilde{x}), \quad \eta = H\tilde{\eta}(\tilde{x}, \tilde{t}), \quad p = \frac{1}{\epsilon}\rho v^2\tilde{p}(\tilde{x}, \tilde{y}, \tilde{t}), \quad (5.2.16)$$

where $\varepsilon = H/L$ is small parameter of the problem. Derivatives in the dimensionless variables are given by

$$\frac{\partial \varphi}{\partial x} = \frac{\partial [vL\tilde{\varphi}]}{\partial (L\tilde{x})} = \frac{vL}{L} \frac{\partial \tilde{\varphi}}{\partial \tilde{x}} = v \frac{\partial \tilde{\varphi}}{\partial \tilde{x}}, \quad (5.2.17)$$

$$\frac{\partial f}{\partial x} = H \frac{\partial \tilde{f}}{\partial \tilde{x}} \frac{1}{L} = \varepsilon \frac{\partial \tilde{f}}{\partial \tilde{x}}, \quad (5.2.18)$$

$$\frac{\partial \varphi}{\partial t} = \frac{vL}{H/v} \frac{\partial \tilde{\varphi}}{\partial \tilde{t}} = \frac{1}{\varepsilon} v^2 \frac{\partial \tilde{\varphi}}{\partial \tilde{t}}, \quad (5.2.19)$$

where the body position in the non-dimensional variables is described by the equation

$$\tilde{y} = \varepsilon \left[\tilde{f}(\tilde{x}) - \tilde{h}(\tilde{t}) \right]. \quad (5.2.20)$$

The free-surface shape, $y = \eta(x, t)$, takes the form in the dimensionless variables,

$$\tilde{y} = \varepsilon \tilde{\eta}(\tilde{x}, \tilde{t}). \quad (5.2.21)$$

The speed of the entering body is

$$\frac{dh}{dt} = H \tilde{h}'(\tilde{t}) \frac{v}{H} = v \tilde{h}'(\tilde{t}), \quad (5.2.22)$$

where, $\tilde{h}'(0) = 1$, in the dimensionless variables. By taking that

$$X_p(t) = H \tilde{X}_p \tilde{t}, \quad Y_p(t) = H \tilde{Y}_p \tilde{t}, \quad \alpha(t) = \frac{H}{L_p} \tilde{\alpha} \tilde{t}, \quad t = \frac{H}{v} \tilde{t}, \quad (5.2.23)$$

and using (5.2.12) gives

$$m_p \frac{H}{(H/v)^2} \frac{d^2 \tilde{X}_p}{dt^2} = \int_{\tilde{x}_p^{(L)}(t)}^{\tilde{x}_p^{(R)}(t)} \frac{1}{\varepsilon} \rho v^2 \tilde{p}(\tilde{x}, \varepsilon [\tilde{X}_p + \tilde{\Omega}(\tilde{x} - \tilde{X}_p(0))]) \sin \left[\frac{H}{L_p} \tilde{\alpha} \right] L d\tilde{x}, \quad (5.2.24)$$

where m_p denotes the mass of the plate. Then

$$\frac{d^2 \tilde{X}_p}{dt^2} = \delta \int_{\tilde{x}_p^{(L)}(t)}^{\tilde{x}_p^{(R)}(t)} \tilde{p}(\tilde{x}, \varepsilon [\tilde{X}_p + \tilde{\Omega}(\tilde{x} - \tilde{X}_p(0))]) \sin \left[\frac{H}{L_p} \tilde{\alpha} \right] \frac{L_p}{H} d\tilde{x}, \quad (5.2.25)$$

where

$$\delta = \frac{(L/H)\rho v^2(H/L_p)L}{m_p H(v^2/H^2)} = \frac{\rho L^2/L_p}{m_p/H} = \frac{\rho L^2}{m_p} \frac{H}{L_p}. \quad (5.2.26)$$

We assume that

$$\frac{\rho L^2}{m_p} \frac{H}{L_p} = \beta \frac{H}{L_p} \ll 1, \quad \left(\frac{\rho L^2}{m_p} \right) \quad (5.2.27)$$

which gives

$$m_p \gg \rho H \frac{L^2}{L_p}, \quad (5.2.28)$$

where

$$m_p = L_p h_p \rho_p \quad \text{and} \quad \rho_p < \rho_w, \quad (5.2.29)$$

Then (5.2.28 - 5.2.29) provide

$$\frac{h_p}{H} \gg \frac{\rho}{\rho_p} \left(\frac{L}{L_p} \right)^2, \quad (5.2.30)$$

and, therefore, the assumption $X_p(t) \approx X_p(0)$ is justified for long floating plates with $L_p \gg L$.

Correspondingly, in the leading order as $\varepsilon \rightarrow 0$,

$$\begin{aligned} \frac{d^2 \tilde{Y}_p}{dt^2} &= \delta \frac{L_p}{H} \int_{\tilde{x}_p^{(L)}(t)}^{\tilde{x}_p^{(R)}(t)} \tilde{p}(\tilde{x}, \varepsilon[\tilde{Y}_p + \tilde{\Omega}_p(\tilde{x} - \tilde{X}_p(0)), t]) \cos \left[\frac{H}{L_p} \tilde{\alpha} \right] d\tilde{x} \\ &\approx \beta \int_{\tilde{x}_p^{(L)}(t)}^{\tilde{x}_p^{(R)}(t)} \tilde{p}(\tilde{x}, 0, \tilde{t}) d\tilde{x}, \end{aligned} \quad (5.2.31)$$

where $\tilde{x}_p^{(R)} = (X_p(0) + L_p/2)/L$, $\tilde{x}_p^{(L)} = (X_p(0) - L_p/2)/L$.

Similar, we find the equation for $\tilde{\alpha}(\tilde{t})$ in the dimensionless variables,

$$\frac{d^2 \tilde{\alpha}}{d\tilde{t}^2} = 48\delta \frac{H}{L} \int_{\tilde{x}_p^{(L)}}^{\tilde{x}_p^{(R)}} \tilde{p}(\tilde{x}, 0, \tilde{t})(\tilde{x} - \tilde{X}_p(0)) d\tilde{x}. \quad (5.2.32)$$

Here we assumed $\delta \ll 1$, see (5.2.26). Therefore, the plate rotation can be neglected together with the horizontal displacement of the plate. However, we will assume below that $48\delta H/L = O(1)$.

5.2.4 Transformation of the boundary problem to the ζ -plane

The flow region xy -plane is conformally mapped onto a circle in the ζ -plane. The boundary value problem for equation (5.2.33) is transformed to a ζ -plane, where the boundary of the flow region, $y = 0$, corresponds to the unit circle $|\zeta| = 1$. The appropriate conformal mapping from the circle, $|\zeta| < 1$, in the ζ -plane to the flow region, $y < 0$, in the physical plane is given by

$$z = i + \frac{2}{\zeta + i}, \quad (z = x + iy, \zeta = \xi + i\eta), \quad (5.2.36)$$

where $|\zeta| = 1$ corresponds to $y = 0$ in the original z -plane, see figure 5.2.4. In the polar coordinates $\zeta = \rho e^{i(\pi/2-\theta)} = i\rho e^{-i\theta}$, where $\rho \leq 1$ and $-\pi < \theta < \pi$, we have for $\rho = 1$,

$$\zeta = e^{i(\pi/2-\theta)} = e^{i\pi/2} e^{-i\theta} = i(\cos \theta - i \sin \theta) = \sin \theta + i \cos \theta, \quad (5.2.37)$$

then (5.2.36) reads

$$\begin{aligned} x + iy &= i + \frac{2}{e^{i(\pi/2-\theta)} + i} = i + \frac{2}{\sin \theta + i(\cos \theta + 1)} \\ &= i + 2 \frac{\sin \theta - i(\cos \theta + 1)}{\sin^2 \theta + (\cos \theta + 1)^2} = i + 2 \frac{\sin \theta - i(\cos \theta + 1)}{2(1 + \cos \theta)} \\ &= \frac{\sin \theta}{1 + \cos \theta}. \end{aligned} \quad (5.2.38)$$

Thus

$$y = 0, \quad x = \frac{\sin \theta}{1 + \cos \theta}, \quad (5.2.39)$$

on the boundary $y = 0$, we have $x = x^{(L)}$ and $x = x^{(R)}$ for the entering body, $x = x_p^{(L)}$ and $x = x_p^{(R)}$ for the rigid floating plate, correspond to points θ^L , θ^R , θ_p^L and θ_p^R on the circle $|\zeta| = 1$, see figure 5.2.4, where $\zeta = -i$ corresponds to the infinity in the z -plane. At $\zeta = -i$, we have $\theta = \pm\pi$, $\cos \theta = -1$ and $|x| = \infty$. To determine θ^L , θ^R , θ_p^L and θ_p^R we have the

formulae

$$\tan \frac{x}{2} = \frac{\sin x}{1 + \cos x}, \quad (5.2.40)$$

from equation (5.2.39) at $x = x_w^{(L)}$ we have

$$\tan \left(\frac{\theta^L}{2} \right) = x^{(L)}, \quad (5.2.41)$$

then

$$\theta^L = -2 \arctan (-x^{(L)}), \quad (5.2.42)$$

and

$$\theta^R = -2 \arctan (-x^{(R)}), \quad (5.2.43)$$

where the value of $\arctan(x)$ are from $-\pi/2$ to $\pi/2$. For positive x , $0 < \arctan x < \pi/2$. Clearly we can obtained θ_p^L and θ_p^R from (5.2.42) as

$$\theta_p^L = -2 \arctan (-x_p^{(L)}), \quad (5.2.44)$$

$$\theta_p^R = -2 \arctan (-x_p^{(R)}), \quad (5.2.45)$$

where $0 < \theta_p^L < \theta_p^R < \pi$ and $\theta^R(t) < \theta_p^L$ because the floating plate is located on the right of the entering body.

From (5.2.36), where $\zeta = \rho e^{i(\pi/2 - \theta)}$ and $0 \leq \rho \leq 1$, we can define the corresponding velocity potential $\Phi(\rho, \theta, t)$ in the ζ -plane,

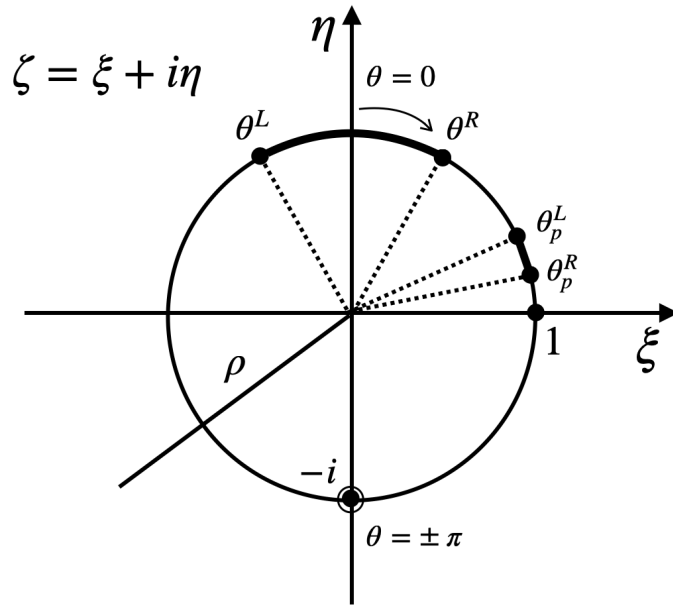
$$\varphi(x, y, t) = \varphi[x(\rho, \theta, t), y(\rho, \theta, t)] = \Phi(\rho, \theta, t). \quad (5.2.46)$$

The $\Phi(\rho, \theta, t)$ satisfies the Laplace equation in the ring $0 < \rho < 1$. By using the chain rule, the derivative φ_t is obtained as

$$\frac{\partial \varphi}{\partial t} = \frac{\partial \Phi}{\partial \rho} \frac{\partial \rho}{\partial t} + \frac{\partial \Phi}{\partial \theta} \frac{\partial \theta}{\partial t} + \frac{\partial \Phi}{\partial t}. \quad (5.2.47)$$

By differentiating (5.2.46) in ρ and setting $\rho = 1$, we find

$$\Phi_\rho(1, \theta, t) = \varphi_x x_\rho + \varphi_y y_\rho. \quad (5.2.48)$$

Figure 5.2.4: The complex ζ -plane.

Equation (5.2.36) defines $z = z(\zeta)$ as an analytic function in $\rho < 1$. For an analytic function

$$\frac{dz}{d\zeta} = \frac{dz}{d\rho} = \frac{dz}{i\rho d\theta} = x_\rho + iy_\rho = \frac{1}{i\rho} (x_\theta + iy_\theta). \quad (5.2.49)$$

At $\rho = 1$: $x_\rho = y_\theta$ and $y_\rho = -x_\theta$. However, $y(1, \theta, t) = 0$, which gives $y_\theta(1, \theta, t) = 0$ and $x_\rho(1, \theta, t) = 0$ in (5.2.47) and (5.2.48). Also using (5.2.39), we obtain

$$y_\rho(1, \theta, t) = -x_\theta(1, \theta, t) = -\frac{d}{d\theta} \left(\frac{\sin \theta}{1 + \cos \theta} \right) = \frac{-1}{1 + \cos \theta}. \quad (5.2.50)$$

Therefore,

$$\Phi_\rho(1, \theta, t) = \varphi_x \cdot 0 + \varphi_y \cdot y_\rho(1, \theta, t) = \frac{-\dot{Y}(t)}{1 + \cos \theta}, \quad (\theta^L < \theta < \theta^R). \quad (5.2.51)$$

on the impact of the wetted surface of the entering body, and

$$\Phi_\rho(1, \theta, t) = \varphi_x \cdot 0 + \varphi_y \cdot y_\rho(1, \theta, t) = \frac{-\dot{Y}_p(t) - \dot{\Omega}_p(t) \left(\frac{\sin(\theta)}{1 + \cos(\theta)} - X_p(0) \right)}{1 + \cos(\theta)},$$

$$(\theta_p^L < \theta < \theta_p^R), \quad (5.2.52)$$

on the image of the floating plate.

Thus, the water impact problem within the Wagner model formulated in the ζ -plane with respect to $\Phi(\rho, \theta, t)$ for a floating plate reads

$$\left\{ \begin{array}{ll} \nabla^2 \Phi = 0 & (0 < \rho < 1), \\ \Phi = 0 & (\rho = 1, ((-\pi, \pi) \setminus (\theta^L, \theta^R) \& (\theta_p^L, \theta_p^R))), \\ \Phi_\rho = \frac{-\dot{Y}(t)}{1 + \cos \theta} & (\rho = 1, \theta^L < \theta < \theta^R), \\ \Phi_\rho = \frac{-\dot{Y}_p(t) - \dot{\Omega}_p(t) \left(\frac{\sin(\theta)}{1 + \cos(\theta)} - X_p(0) \right)}{1 + \cos(\theta)} & (\rho = 1, \theta_p^L < \theta < \theta_p^R). \end{array} \right. \quad (5.2.53)$$

Analytical solution of the water
impact problem in the presence of a
floating plate within the Wagner
model

In this chapter, we will find the solution of Wagner's model of water impact in the ζ -plane (5.2.53) which can be written in a more general form as

$$\left\{ \begin{array}{ll} \nabla^2 \Phi = 0 & (0 < \rho < 1), \\ \Phi = 0 & (\rho = 1, ((-\pi, \pi) \setminus (\theta^L, \theta^R) \& (\theta_p^L, \theta_p^R))), \\ \Phi_\rho = f(\theta) & (\rho = 1, \theta^L < \theta < \theta^R), \\ \Phi_\rho = g(\theta) & (\rho = 1, \theta_p^L < \theta < \theta_p^R), \end{array} \right. \quad (6.0.1)$$

where $f(\theta)$ and $g(\theta)$ follow from (5.2.53).

For solving this mixed boundary value problem, we assume that $\Phi(1, \theta, t)$ is given in the intervals $\theta^L < \theta < \theta^R$ and $\theta_p^L < \theta < \theta_p^R$. Let

$$\Phi(1, \theta, t) = \left\{ \begin{array}{ll} F(\theta, t) & (\theta^L < \theta < \theta^R), \\ G(\theta, t) & (\theta_p^L < \theta < \theta_p^R), \\ 0 & \text{otherwise,} \end{array} \right. \quad (6.0.2)$$

where the functions $F(\theta, t)$ and $G(\theta, t)$ are zero at the ends of the corresponding intervals because the potential should be continuous for flows with finite kinetic energy. These functions should be determined to satisfy the conditions in the contact regions,

$$\frac{\partial \Phi}{\partial \rho}(1, \theta) \langle F, G \rangle = f(\theta) \quad (\theta^L < \theta < \theta^R), \quad (6.0.3)$$

and

$$\frac{\partial \Phi}{\partial \rho}(1, \theta) \langle F, G \rangle = g(\theta) \quad (\theta_p^L < \theta < \theta_p^R). \quad (6.0.4)$$

It is convenient to introduce the Fourier series of $\Phi(1, \theta, t)$,

$$\Phi(1, \theta, t) = \left\{ \begin{array}{ll} F(\theta) & (\theta^L < \theta < \theta^R) \\ G(\theta) & (\theta_p^L < \theta < \theta_p^R) \\ 0 & \text{otherwise} \end{array} \right\} = a_0 + \sum_{n=1}^{\infty} \{a_n \cos(n\theta) + b_n \sin(n\theta)\}, \quad (6.0.5)$$

where

$$\begin{aligned} a_0 &= \frac{1}{2\pi} \int_{\theta^L}^{\theta^R} F(\theta) d\theta + \frac{1}{2\pi} \int_{\theta_p^L}^{\theta_p^R} G(\theta) d\theta, \\ a_n &= \frac{1}{\pi} \int_{\theta^L}^{\theta^R} F(\theta) \cos(n\theta) d\theta + \frac{1}{\pi} \int_{\theta_p^L}^{\theta_p^R} G(\theta) \cos(n\theta) d\theta, \\ b_n &= \frac{1}{\pi} \int_{\theta^L}^{\theta^R} F(\theta) \sin(n\theta) d\theta + \frac{1}{\pi} \int_{\theta_p^L}^{\theta_p^R} G(\theta) \sin(n\theta) d\theta, \end{aligned} \quad (6.0.6)$$

are unknown coefficients. It follows from (6.0.2) that

$$\Phi(\rho, \theta, t) = \Phi(\rho, \theta) \Big|_{F \neq 0, G = 0} + \Phi(\rho, \theta) \Big|_{F = 0, G \neq 0} = \Phi_F(\rho, \theta) + \Phi_G(\rho, \theta), \quad (6.0.7)$$

substituting (6.0.7) into (6.0.3) and (6.0.4) gives

$$\frac{\partial \Phi}{\partial \rho}(1, \theta) = \frac{\partial \Phi_F}{\partial \rho} + \frac{\partial \Phi_G}{\partial \rho} = f(\theta), \quad (\rho = 1, \theta^L < \theta < \theta^R), \quad (6.0.8)$$

and

$$\frac{\partial \Phi}{\partial \rho}(1, \theta) = \frac{\partial \Phi_F}{\partial \rho} + \frac{\partial \Phi_G}{\partial \rho} = g(\theta), \quad (\rho = 1, \theta_p^L < \theta < \theta_p^R). \quad (6.0.9)$$

The potentials Φ_F and Φ_G were calculated in chapter 4 (4.3.1). The solution of problem (6.0.1) with the condition (6.0.5) at $\rho = 1$ is

$$\Phi(\rho, \theta) = a_0 \Phi_0(\rho, \theta) + \sum_{n=1}^{\infty} \{a_n \Phi_n^{(c)}(\rho, \theta) + b_n \Phi_n^{(s)}(\rho, \theta)\}, \quad (6.0.10)$$

where

$$\begin{cases} \nabla^2 \Phi_n^{(c)} = 0 & (0 < \rho < 1), \\ \Phi_n^{(c)}(1, \theta) = \cos(n\theta), \end{cases} \quad (6.0.11)$$

and

$$\begin{cases} \nabla^2 \Phi_n^{(s)} = 0 & (0 < \rho < 1), \\ \Phi_n^{(s)}(1, \theta) = \sin(n\theta). \end{cases} \quad (6.0.12)$$

The solutions of (6.0.11) and (6.0.12) are

$$\Phi_n^{(c)}(\rho, \theta) = \rho^n \cos(n\theta), \quad \Phi_n^{(s)}(\rho, \theta) = \rho^n \sin(n\theta) \quad \text{and} \quad \Phi_0^{(c)}(\rho, \theta) = 1. \quad (6.0.13)$$

The formula (6.0.10) gives

$$\frac{\partial \Phi}{\partial \rho}(1, \theta) \langle F, G \rangle = \sum_{n=1}^{\infty} n (a_n \cos(n\theta) + b_n \sin(n\theta)) \quad (-\pi < \theta < \pi). \quad (6.0.14)$$

The Fourier coefficients (6.0.6) cannot be used in (6.0.14) to reduce the problem to an integral equation for the functions $F(\theta, t)$ and $G(\theta, t)$ as

$$\begin{aligned} \frac{\partial \Phi}{\partial \rho}(1, \theta) &= \frac{1}{\pi} \int_{\theta^L}^{\theta^R} F(\theta_0) \sum_{n=1}^{\infty} n \{ \cos(n\theta_0) \cos(n\theta) + \sin(n\theta_0) \sin(n\theta) \} d\theta_0 \\ &+ \frac{1}{\pi} \int_{\theta_p^L}^{\theta_p^R} G(\theta_0) \sum_{n=1}^{\infty} n \{ \cos(n\theta_0) \cos(n\theta) + \sin(n\theta_0) \sin(n\theta) \} d\theta_0 \\ &= \int_{\theta^L}^{\theta^R} F(\theta_0) \mathcal{K}(\theta - \theta_0) d\theta_0 + \int_{\theta_p^L}^{\theta_p^R} G(\theta_0) \mathcal{K}(\theta - \theta_0) d\theta_0, \end{aligned} \quad (6.0.15)$$

because the series for $\mathcal{K}(\alpha)$ does not converge. This implies that the operator $(\partial \Phi / \partial \rho)(1, \theta) \langle F \rangle$ is not a standard integral operator. Note that, to satisfy the functional equation (6.0.8), we required $F(\theta^L) = F(\theta^R) = 0$ and $G(\theta_p^L) = G(\theta_p^R) = 0$, because the velocity potential should be at least continuous everywhere including the boundary of the flow region, to describe a flow with finite kinetic energy.

The equation (6.0.8) will be understood as the limit, see section 4.3.1 for more details,

$$\lim_{\rho \rightarrow 1-0} \left\{ \frac{\partial \Phi}{\partial \rho}(\rho, \theta) \langle F, G \rangle \right\} = \begin{cases} f(\theta) & (\theta^L < \theta < \theta^R), \\ g(\theta) & (\theta_p^L < \theta < \theta_p^R), \end{cases} \quad (6.0.16)$$

where $f(\theta)$ and $g(\theta)$ are known smooth functions of θ . The time t is a parameter in the present analysis, which does not contain time derivatives.

In the equation (6.0.16), we have

$$\frac{\partial \Phi}{\partial \rho}(\rho, \theta) = \int_{\theta^L}^{\theta^R} F(\theta_0) \mathcal{K}(\rho, \theta - \theta_0) d\theta_0 + \int_{\theta_p^L}^{\theta_p^R} G(\theta_0) \mathcal{K}(\rho, \theta - \theta_0) d\theta_0, \quad (6.0.17)$$

where

$$\mathcal{K}(\rho, \theta) = \frac{1}{\pi \rho} \sum_{n=1}^{\infty} n \rho^n \cos(n\theta), \quad (6.0.18)$$

and $0 < \rho < 1$. The series (6.0.18) does not converge at $\rho = 1$. To regularise equation (6.0.16), we notice that

$$\mathcal{K}(\rho, \theta - \theta_0) = \frac{\partial^2}{\partial \theta \partial \theta_0} S(\rho, \theta - \theta_0), \quad (6.0.19)$$

$$S(\rho, \theta) = \frac{1}{\pi \rho} \sum_{n=1}^{\infty} \rho^n \frac{\cos(n\theta)}{n}. \quad (6.0.20)$$

The series (6.0.20) converges at $\rho = 1$ but it is log-singular at $\theta = 0$. Substituting (6.0.17) and (6.0.19) in (6.0.16) and integrating in (6.0.17) by part using equalities $F(\theta^L) = F(\theta^R) = 0$ and $G(\theta_p^L) = G(\theta_p^R) = 0$, we obtain

$$\begin{aligned} \lim_{\rho \rightarrow 1-0} \left\{ \frac{\partial \Phi}{\partial \rho}(\rho, \theta) \langle F \rangle \right\} &= \lim_{\rho \rightarrow 1-0} \frac{\partial}{\partial \theta} \left(\int_{\theta^L}^{\theta^R} F(\theta_0) d\{S(\rho, \theta - \theta_0)\} \right. \\ &\quad \left. + \int_{\theta_p^L}^{\theta_p^R} G(\theta_0) d\{S(\rho, \theta - \theta_0)\} \right) \\ &= - \lim_{\rho \rightarrow 1} \frac{\partial}{\partial \theta} \left(\int_{\theta^L}^{\theta^R} F'(\theta_0) S(\rho, \theta - \theta_0) d\theta_0 + \int_{\theta_p^L}^{\theta_p^R} G'(\theta_0) S(\rho, \theta - \theta_0) d\theta_0 \right) \\ &= \frac{\partial}{\partial \theta} \left(\int_{\theta^L}^{\theta^R} U(\theta_0) S(1, \theta - \theta_0) d\theta_0 + \int_{\theta_p^L}^{\theta_p^R} V(\theta_0) S(1, \theta - \theta_0) d\theta_0 \right) \quad (\theta^L < \theta < \theta^R), \end{aligned} \quad (6.0.21)$$

where

$$-U(\theta_0) = F'(\theta_0) \quad \text{and} \quad -V(\theta_0) = G'(\theta_0), \quad (6.0.22)$$

Then equation (6.0.16) and (6.0.21) provides after integration in θ from θ^L

$$\begin{aligned} & \int_{\theta^L}^{\theta^R} U(\theta_0) \{S(1, \theta - \theta_0) - S(1, \theta^L - \theta_0)\} d\theta_0 \\ & + \int_{\theta_p^L}^{\theta_p^R} V(\theta_0) \{S(1, \theta - \theta_0) - S(1, \theta^L - \theta_0)\} d\theta_0 = \bar{f}(\theta), \end{aligned} \quad (\theta^L < \theta < \theta^R), \quad (6.0.23)$$

where $\bar{f}(\theta)$ is a known function given by

$$\bar{f}(\theta) = \int_{\theta^L}^{\theta} f(\theta_0) d\theta_0, \quad (6.0.24)$$

and after integration in θ from θ_p^L

$$\begin{aligned} & \int_{\theta^L}^{\theta^R} U(\theta_0) \{S(1, \theta - \theta_0) - S(1, \theta_p^L - \theta_0)\} d\theta_0 \\ & + \int_{\theta_p^L}^{\theta_p^R} V(\theta_0) \{S(1, \theta - \theta_0) - S(1, \theta_p^L - \theta_0)\} d\theta_0 = \bar{g}(\theta), \end{aligned} \quad (\theta_p^L < \theta < \theta_p^R), \quad (6.0.25)$$

where $\bar{g}(\theta)$ is a known function given by

$$\bar{g}(\theta) = \int_{\theta_p^L}^{\theta} g(\theta_0) d\theta_0. \quad (6.0.26)$$

From (6.0.23), (6.0.25) and (6.0.20), we have

$$S(1, \theta - \theta_0) - S(1, \theta^L - \theta_0) = \frac{1}{\pi} \sum_{n=1}^{\infty} \frac{1}{n} \{ \cos[n(\theta - \theta_0)] - \cos[n(\theta^L - \theta_0)] \}, \quad (6.0.27)$$

and

$$S(1, \theta - \theta_0) - S(1, \theta_p^L - \theta_0) = \frac{1}{\pi} \sum_{n=1}^{\infty} \frac{1}{n} \{ \cos[n(\theta - \theta_0)] - \cos[n(\theta_p^L - \theta_0)] \}, \quad (6.0.28)$$

The intervals (θ^L, θ^R) and (θ_p^L, θ_p^R) in (6.0.23) and (6.0.25) correspondingly

are mapped onto $(-\pi, \pi)$, in order to apply the classical theory of Fourier series, by introducing new variable ξ and η such that $-\pi < (\xi, \eta) < \pi$, where

$$\theta = A\xi + B \quad \text{For the interval } (\theta^L, \theta^R), \quad (6.0.29)$$

$$\theta = A_p\eta + B_p \quad \text{For the interval } (\theta_p^L, \theta_p^R), \quad (6.0.30)$$

the coefficients A , B , A_p and B_p are obtained from the equations:

$$\theta^L = A(-\pi) + B \quad \text{and} \quad \theta^R = A\pi + B, \quad (6.0.31)$$

$$\theta_p^L = A_p(-\pi) + B_p \quad \text{and} \quad \theta_p^R = A_p\pi + B_p, \quad (6.0.32)$$

then

$$A(t) = \frac{\theta^R - \theta^L}{2\pi} \quad \text{and} \quad B(t) = \frac{\theta^L + \theta^R}{2}, \quad (6.0.33)$$

$$A_p = \frac{\theta_p^R - \theta_p^L}{2\pi} \quad \text{and} \quad B_p = \frac{\theta_p^L + \theta_p^R}{2}. \quad (6.0.34)$$

where A_p and B_p are constants and $(0 \leq A(t) \leq 1)$ which means that the whole water surface is covered by the entering body when A close to 1. For A small, the contact region is small. Introducing $U(\theta) = U(A\xi + B) = \tilde{U}(\xi)$, $V(\eta) = V(A_p\eta + B_p) = \tilde{V}(\eta)$ with $\theta_0 = A\xi_0 + B$, and $\theta_0 = A_p\eta_0 + B_p$ in the corresponding intervals, we transform (6.0.23) and (6.0.25) to the following equations

$$\begin{aligned} & \int_{-\pi}^{\pi} \tilde{U}(\xi_0) \{S(1, A(\xi - \xi_0)) - S(1, A(-\pi - \xi_0))\} A d\xi_0 \\ & + \int_{-\pi}^{\pi} \tilde{V}(\eta_0) \{S(1, A\xi + B - A_p\eta_0 - B_p) - S(1, -A\pi + B - A_p\eta_0 - B_p)\} A d\eta_0 \\ & = G_1(\xi), \quad (-\pi < \xi < \pi), \quad (6.0.35) \end{aligned}$$

$$\begin{aligned} & \int_{-\pi}^{\pi} \tilde{U}(\xi_0) \{S(1, A_p\eta + B_p - A\xi_0 - B) - S(1, -A_p\pi + B_p - A\xi_0 - B)\} A d\xi_0 \\ & + \int_{-\pi}^{\pi} \tilde{V}(\eta_0) \{S(1, A_p(\eta - \eta_0)) - S(1, A_p(-\pi - \eta_0))\} A d\eta_0 \\ & = G_2(\eta), \quad (-\pi < \eta < \pi), \quad (6.0.36) \end{aligned}$$

where $G_1(\xi) = \bar{f}(A\xi + B)$ and $G_2(\eta) = \bar{g}(A_p\eta + B_p)$. The functions $\tilde{U}(\xi)$ and $\tilde{V}(\eta)$ are sought as the Fourier series

$$\tilde{U}(\xi) = \frac{1}{2}\bar{a}_0 + \sum_{n=1}^{\infty} (\bar{a}_n \cos(n\xi) + \bar{b}_n \sin(n\xi)), \quad (6.0.37)$$

and

$$\tilde{V}(\eta) = \frac{1}{2}\hat{a}_0 + \sum_{n=1}^{\infty} (\hat{a}_n \cos(n\eta) + \hat{b}_n \sin(n\eta)), \quad (6.0.38)$$

where the coefficients \bar{a}_n , \bar{b}_n , \hat{a}_n and \hat{b}_n are to be determined. Equations (6.0.22) and the conditions $F(\theta^R) = F(\theta^L) = G(\theta_p^R) = G(\theta_p^L) = 0$ gives

$$-\int_{-\pi}^{\pi} \tilde{U}(\xi) d\xi = -\int_{\theta^L}^{\theta^R} U(\theta) d\theta \int_{\theta^L}^{\theta^R} F'(\theta) d\theta = F(\theta^L) - F(\theta^R) = 0, \quad (6.0.39)$$

this provides $\bar{a}_0 = 0$ in (6.0.37) and similarly $\hat{a}_0 = 0$ in (6.0.38). Substituting the series (6.0.37) and (6.0.38) into (6.0.35) and (6.0.36) and multiplying both sides of (6.0.35) by $\sin(m\xi)$ and $\cos(m\xi)$, $m \geq 1$, and integrating the result in ξ from $-\pi$ to π , then multiplying both sides of (6.0.36) by $\sin(m\eta)$ and $\cos(m\eta)$, $m \geq 1$, and integrating the result in η from $-\pi$ to π , we obtain

$$\begin{aligned} & \sum_{n=1}^{\infty} \left\{ \bar{a}_n \int_{-\pi}^{\pi} \left(\int_{-\pi}^{\pi} \cos(n\xi_0) \bar{T}(\xi, \xi_0) d\xi_0 \right) \cos(m\xi) d\xi \right. \\ & \quad \left. + \bar{b}_n \int_{-\pi}^{\pi} \left(\int_{-\pi}^{\pi} \sin(n\xi_0) \bar{T}(\xi, \xi_0) d\xi_0 \right) \cos(m\xi) d\xi \right\} \\ & + \sum_{n=1}^{\infty} \left\{ \hat{a}_n \int_{-\pi}^{\pi} \left(\int_{-\pi}^{\pi} \cos(n\eta_0) \hat{T}(\xi, \eta_0) d\eta_0 \right) \cos(m\xi) d\xi \right. \\ & \quad \left. + \hat{b}_n \int_{-\pi}^{\pi} \left(\int_{-\pi}^{\pi} \sin(n\eta_0) \hat{T}(\xi, \eta_0) d\eta_0 \right) \cos(m\xi) d\xi \right\} \\ & = \frac{1}{A} \int_{-\pi}^{\pi} G_1(\xi) \cos(m\xi) d\xi, \quad (6.0.40) \end{aligned}$$

$$\begin{aligned}
 & \sum_{n=1}^{\infty} \left\{ \bar{a}_n \int_{-\pi}^{\pi} \left(\int_{-\pi}^{\pi} \cos(n\xi_0) \bar{T}(\xi, \xi_0) d\xi_0 \right) \sin(m\xi) d\xi \right. \\
 & \quad \left. + \bar{b}_n \int_{-\pi}^{\pi} \left(\int_{-\pi}^{\pi} \sin(n\xi_0) \bar{T}(\xi, \xi_0) d\xi_0 \right) \sin(m\xi) d\xi \right\} \\
 & + \sum_{n=1}^{\infty} \left\{ \hat{a}_n \int_{-\pi}^{\pi} \left(\int_{-\pi}^{\pi} \cos(n\eta_0) \hat{T}(\xi, \eta_0) d\eta_0 \right) \sin(m\xi) d\xi \right. \\
 & \quad \left. + \hat{b}_n \int_{-\pi}^{\pi} \left(\int_{-\pi}^{\pi} \sin(n\eta_0) \hat{T}(\xi, \eta_0) d\eta_0 \right) \sin(m\xi) d\xi \right\} \\
 & = \frac{1}{A} \int_{-\pi}^{\pi} G_1(\xi) \sin(m\xi) d\xi, \quad (6.0.41)
 \end{aligned}$$

and

$$\begin{aligned}
 & \sum_{n=1}^{\infty} \left\{ \bar{a}_n \int_{-\pi}^{\pi} \left(\int_{-\pi}^{\pi} \cos(n\xi_0) \hat{T}(\eta, \xi_0) d\xi_0 \right) \cos(m\eta) d\eta \right. \\
 & \quad \left. + \bar{b}_n \int_{-\pi}^{\pi} \left(\int_{-\pi}^{\pi} \sin(n\xi_0) \hat{T}(\eta, \xi_0) d\xi_0 \right) \cos(m\eta) d\eta \right\} \\
 & + \sum_{n=1}^{\infty} \left\{ \hat{a}_n \int_{-\pi}^{\pi} \left(\int_{-\pi}^{\pi} \cos(n\eta_0) \bar{T}(\eta, \eta_0) d\eta_0 \right) \cos(m\eta) d\eta \right. \\
 & \quad \left. + \hat{b}_n \int_{-\pi}^{\pi} \left(\int_{-\pi}^{\pi} \sin(n\eta_0) \bar{T}(\eta, \eta_0) d\eta_0 \right) \cos(m\eta) d\eta \right\} \\
 & = \frac{1}{A} \int_{-\pi}^{\pi} G_2(\eta) \cos(m\eta) d\eta, \quad (6.0.42)
 \end{aligned}$$

$$\begin{aligned}
 & \sum_{n=1}^{\infty} \left\{ \bar{a}_n \int_{-\pi}^{\pi} \left(\int_{-\pi}^{\pi} \cos(n\xi_0) \hat{T}(\eta, \xi_0) d\xi_0 \right) \sin(m\eta) d\eta \right. \\
 & \quad \left. + \bar{b}_n \int_{-\pi}^{\pi} \left(\int_{-\pi}^{\pi} \sin(n\xi_0) \hat{T}(\eta, \xi_0) d\xi_0 \right) \sin(m\eta) d\eta \right\} \\
 & + \sum_{n=1}^{\infty} \left\{ \hat{a}_n \int_{-\pi}^{\pi} \left(\int_{-\pi}^{\pi} \cos(n\eta_0) \bar{T}(\eta, \eta_0) d\eta_0 \right) \sin(m\eta) d\eta \right. \\
 & \quad \left. + \hat{b}_n \int_{-\pi}^{\pi} \left(\int_{-\pi}^{\pi} \sin(n\eta_0) \bar{T}(\eta, \eta_0) d\eta_0 \right) \sin(m\eta) d\eta \right\} \\
 & = \frac{1}{A} \int_{-\pi}^{\pi} G_2(\eta) \sin(m\eta) d\eta, \quad (6.0.43)
 \end{aligned}$$

where

$$\bar{T}(\xi, \xi_0) = S(1, A(\xi - \xi_0)) - S(1, -A(\pi + \xi_0)), \quad (6.0.44)$$

$$\bar{T}(\eta, \eta_0) = S(1, A_p(\eta - \eta_0)) - S(1, A_p(-\pi - \eta_0)), \quad (6.0.45)$$

$$\hat{T}(\xi, \eta_0) = S(1, A\xi + B - A_p\eta_0 - B_p) - S(1, -A\pi + B - A_p\eta_0 - B_p), \quad (6.0.46)$$

$$\hat{T}(\eta, \xi_0) = S(1, A_p\eta + B_p - A\xi_0 - B) - S(1, -A_p\pi + B_p - A\xi_0 - B). \quad (6.0.47)$$

The system (6.0.40) and (6.0.42) can be written in the matrix form:

$$\begin{cases} A^{(cc)}\vec{a} + A^{(sc)}\vec{b} + A_p^{(cc)}\vec{\hat{a}} + A_p^{(sc)}\vec{\hat{b}} = \vec{Z}_{c1}, \\ A^{(cs)}\vec{a} + A^{(ss)}\vec{b} + A_p^{(cs)}\vec{\hat{a}} + A_p^{(ss)}\vec{\hat{b}} = \vec{Z}_{s1}, \\ B^{(cc)}\vec{a} + B^{(sc)}\vec{b} + B_p^{(cc)}\vec{\hat{a}} + B_p^{(sc)}\vec{\hat{b}} = \vec{Z}_{c2}, \\ B^{(cs)}\vec{a} + B^{(ss)}\vec{b} + B_p^{(cs)}\vec{\hat{a}} + B_p^{(ss)}\vec{\hat{b}} = \vec{Z}_{s2}, \end{cases} \quad (6.0.48)$$

where

$$\begin{aligned} \vec{a} &= (\bar{a}_1, \bar{a}_2, \bar{a}_3, \dots)^T & \text{and} & \quad \vec{b} = (\bar{b}_1, \bar{b}_2, \bar{b}_3, \dots)^T, \\ \vec{\hat{a}} &= (\hat{a}_1, \hat{a}_2, \hat{a}_3, \dots)^T & \text{and} & \quad \vec{\hat{b}} = (\hat{b}_1, \hat{b}_2, \hat{b}_3, \dots)^T, \end{aligned}$$

and $A^{(cc)}$ to $B_p^{(ss)}$ are matrices with the elements, where $A^{(cc)}$, $A^{(sc)}$, $A^{(cs)}$, $A^{(ss)}$, $B_p^{(cc)}$, $B_p^{(sc)}$, $B_p^{(cs)}$ and $B_p^{(ss)}$ can be evaluated using similar calculation in Chapter 4, see (4.3.1).

By substituting (6.0.20) into (6.0.44 - 6.0.47), we find that

$$\bar{T}(\xi, \xi_0) = \frac{1}{\pi} \sum_{k=1}^{\infty} \frac{1}{k} \{ \cos(kA(\xi - \xi_0)) - \cos(kA(\pi + \xi_0)) \}, \quad (6.0.49)$$

$$\bar{T}(\eta, \eta_0) = \frac{1}{\pi} \sum_{k=1}^{\infty} \frac{1}{k} \{ \cos(kA_p(\eta - \eta_0)) - \cos(kA_p(\pi + \eta_0)) \}, \quad (6.0.50)$$

and

$$\begin{aligned} \hat{T}(\xi, \eta_0) &= \frac{1}{\pi} \sum_{k=1}^{\infty} \frac{1}{k} \{ \cos(k(A\xi + B - A_p\eta_0 - B_p)) \\ &\quad - \cos(k(-A\pi + B - A_p\eta_0 - B_p)) \}, \quad (6.0.51) \end{aligned}$$

$$\hat{T}(\eta, \xi_0) = \frac{1}{\pi} \sum_{k=1}^{\infty} \frac{1}{k} \{ \cos(k(A_p \eta + B_p - A\xi_0 - B)) - \cos(k(-A_p \pi + B_p - A\xi_0 - B)) \}, \quad (6.0.52)$$

Similar as in Chapter 4, it can be shown that

$$A_{nm}^{(sc)} = A_{nm}^{(cs)} = B_{p,nm}^{(sc)} = B_{p,nm}^{(cs)} = 0. \quad (6.0.53)$$

Then the system (6.0.48) takes the form,

$$\begin{cases} A^{(cc)} \vec{a} + A_p^{(cc)} \vec{\tilde{a}} + A_p^{(sc)} \vec{\tilde{b}} = \vec{Z}_{c1}, \\ A^{(ss)} \vec{b} + A_p^{(cs)} \vec{\tilde{a}} + A_p^{(ss)} \vec{\tilde{b}} = \vec{Z}_{s1}, \\ B^{(cc)} \vec{a} + B^{(sc)} \vec{\tilde{b}} + B_p^{(cc)} \vec{\tilde{a}} = \vec{Z}_{c2}, \\ B^{(cs)} \vec{a} + B^{(ss)} \vec{\tilde{b}} + B_p^{(ss)} \vec{\tilde{b}} = \vec{Z}_{s2}. \end{cases} \quad (6.0.54)$$

The elements of the matrices in (6.0.54) are calculated as shown below.

We have

$$A_{nm}^{(cc)} = \int_{-\pi}^{\pi} \left(\int_{-\pi}^{\pi} \cos(n\xi_0) \bar{T}(\xi, \xi_0) d\xi_0 \right) \cos(m\xi) d\xi, \quad (6.0.55)$$

and from (4.3.54) we find

$$A_{nm}^{(cc)} = \frac{4}{\pi A^2} (-1)^{(n+m)} \sum_{k=1}^{\infty} \frac{k \sin^2(kx)}{(k^2 - a^2)(k^2 - b^2)}, \quad (6.0.56)$$

where $m/A = a$, $n/A = b$, and $\pi A = x$. Similar,

$$A_{nm}^{(ss)} = \int_{-\pi}^{\pi} \left(\int_{-\pi}^{\pi} \sin(n\xi_0) \bar{T}(\xi, \xi_0) d\xi_0 \right) \sin(m\xi) d\xi, \quad (6.0.57)$$

and from (4.3.80) we have

$$A_{nm}^{(ss)} = \frac{4mn}{\pi A^4} (-1)^{(n+m)} \sum_{k=1}^{\infty} \frac{\sin^2(kx)}{k(k^2 - a^2)(k^2 - b^2)}. \quad (6.0.58)$$

These series are similar to the series in chapter 4, see (4.3.53) and (4.3.79).

However, there is no W_k in the present series, because of another configuration of the flow region.

Similarly, we find

$$B_{p,nm}^{(cc)} = \frac{4}{\pi A_p^2} (-1)^{(n+m)} \sum_{k=1}^{\infty} \frac{k \sin^2(kx_p)}{(k^2 - c^2)(k^2 - d^2)}, \quad (6.0.59)$$

and

$$B_{p,nm}^{(ss)} = \frac{4mn}{\pi A_p^4} (-1)^{(n+m)} \sum_{k=1}^{\infty} \frac{\sin^2(kx_p)}{k(k^2 - c^2)(k^2 - d^2)}, \quad (6.0.60)$$

where $m/A_p = c$, $n/A_p = d$ and $\pi A_p = x_p$.

Next, we calculate

$$\begin{aligned} A_{p,nm}^{(cc)} &= \int_{-\pi}^{\pi} \left(\int_{-\pi}^{\pi} \cos(n\eta_0) \hat{T}(\xi, \eta_0) d\eta_0 \right) \cos(m\xi) d\xi \\ &= \frac{1}{\pi} \sum_{k=1}^{\infty} \frac{1}{k} \int_{-\pi}^{\pi} \left(\int_{-\pi}^{\pi} \{ \cos(k(A\xi + B - A_p\eta_0 - B_p)) \right. \\ &\quad \left. - \cos(k(-A\pi + B - A_p\eta_0 - B_p)) \} \right. \\ &\quad \left. \cos(n\eta_0) d\eta_0 \right) \cos(m\xi) d\xi \\ &= \frac{1}{\pi} \sum_{k=1}^{\infty} \frac{1}{k} \left\{ \int_{-\pi}^{\pi} \cos(kA_p\eta_0) \cos(n\eta_0) d\eta_0 \int_{-\pi}^{\pi} \cos(kA\xi + kB - kB_p) \cos(m\xi) d\xi \right. \\ &\quad \left. - \cos(kA\pi + kB_p - kB) \int_{-\pi}^{\pi} \cos(kA_p\eta_0) \cos(n\eta_0) d\eta_0 \int_{-\pi}^{\pi} \cos(m\xi) d\xi \right\}, \end{aligned} \quad (6.0.61)$$

evaluate the integrals in (6.0.61) analytically as

$$\int_{-\pi}^{\pi} \cos(kA\xi + kB - kB_p) \cos(m\xi) d\xi = \cos[k(B - B_p)] \frac{2kA(-1)^m \sin(kA\pi)}{(kA)^2 - m^2}. \quad (6.0.62)$$

The integral (6.0.62) is equal to $\pi \cos[k(B - B_p)]$ for $kA = m$.

Similarly

$$\int_{-\pi}^{\pi} \cos(kA_p\eta_0) \cos(n\eta_0) d\eta_0 = \begin{cases} \frac{2kA_p \sin(kA_p\pi)}{(kA_p)^2 - n^2} (-1)^n & \text{for } kA_p \neq n, \\ \pi & \text{for } kA_p = n, \end{cases} \quad (6.0.63)$$

then from (6.0.61) and (6.0.62 - 6.0.63) we have

$$A_{p,nm}^{(cc)} = \frac{1}{\pi} \sum_{k=1}^{\infty} \frac{1}{k} \left\{ \frac{2kA_p}{(kA_p)^2 - n^2} \sin(kA_p\pi) \cos(n\pi) \cdot \cos[k(B - B_p)] \frac{2kA(-1)^m \sin(kA\pi)}{(kA)^2 - m^2} \right\}, \quad (6.0.64)$$

Let A_p and A be not rational numbers. Then $A_p \neq n/k$ for any integer n and k , $A \neq m/k$ for any integer m and k . By introduce $m/A = a$, $n/A = b$, $m/A_p = c$, $n/A_p = d$, $\pi A = x$ and $\pi A_p = x_p$. Then we have

$$A_{p,nm}^{(cc)} = \frac{2AA_p^{-1}(-1)^{(n+m)}}{\pi} \sum_{k=1}^{\infty} \left\{ \frac{1}{k^2 - d^2} \sin(kx_p) \cos[k(B - B_p)] \frac{k \sin(kA\pi)}{a^2 - m^2} \right\}. \quad (6.0.65)$$

using the flowing trigonometric identity

$$\sin[kx \pm m\pi] = \sin(kx) \cos(\pi m) \pm \cos(kx) \sin(\pi m), \quad (6.0.66)$$

gives

$$A_{p,nm}^{(cc)} = \frac{4A}{\pi A_p} (-1)^{(n+m)} \sum_{k=1}^{\infty} \left\{ k \frac{\sin(kx_p) \sin(kx)}{k^2 - d^2} \frac{\sin(kx)}{k^2 - a^2} \cos[k(B - B_p)] \right\}, \quad (6.0.67)$$

Similar we find $B_{nm}^{(cc)}$ as

$$B_{nm}^{(cc)} = \frac{4A_p}{\pi A} (-1)^{(n+m)} \sum_{k=1}^{\infty} \left\{ k \frac{\sin(kx) \sin(kx_p)}{k^2 - a^2} \frac{\sin(kx)}{k^2 - d^2} \cos[k(B_p - B)] \right\} = \frac{A_p^2}{A^2} A_{p,nm}^{(cc)}. \quad (6.0.68)$$

Next, we calculate

$$\begin{aligned}
 A_{p,nm}^{(sc)} &= \int_{-\pi}^{\pi} \left(\int_{-\pi}^{\pi} \sin(n\eta_0) \hat{T}(\xi, \eta_0) d\eta_0 \right) \cos(m\xi) d\xi \\
 &= \frac{1}{\pi} \sum_{k=1}^{\infty} \frac{1}{k} \int_{-\pi}^{\pi} \left(\int_{-\pi}^{\pi} \{ \cos[kA_p\eta_0 - (kA\xi + kB - kB_p)] \right. \\
 &\quad \left. - \cos[kA_p\eta_0 - (-kA\pi + kB - kB_p)] \} \sin(n\eta_0) d\eta_0 \right) \cos(m\xi) d\xi \\
 &= \frac{1}{\pi} \sum_{k=1}^{\infty} \frac{1}{k} \left\{ \int_{-\pi}^{\pi} \sin(kA_p\eta_0) \sin(n\eta_0) d\eta_0 \cdot \int_{-\pi}^{\pi} \cos[kA\xi + k(B - B_p)] \cos(m\xi) d\xi \right. \\
 &\quad \left. - \cos[-kA\pi + k(B - B_p)] \cdot \int_{-\pi}^{\pi} \sin(kA_p\eta_0) \sin(n\eta_0) d\eta_0 \cdot \int_{-\pi}^{\pi} \cos(m\xi) d\xi \right\}, \tag{6.0.69}
 \end{aligned}$$

where

$$\int_{-\pi}^{\pi} \cos(m\xi) d\xi = 0 \quad \text{for } m \geq 1.$$

Substituting (6.0.62), (4.6.43) and (6.0.74) into (6.0.69) gives then

$$A_{p,nm}^{(sc)} = \frac{4nA}{\pi A_p} (-1)^{(n+m)} \sum_{k=1}^{\infty} \left\{ \frac{\sin(kx_p)}{k^2 - d^2} \frac{\sin(kx)}{k^2 - a^2} \cos[k(B - B_p)] \right\}, \tag{6.0.70}$$

and similarly

$$B_{nm}^{(sc)} = \frac{4nA_p}{\pi A} (-1)^{(n+m)} \sum_{k=1}^{\infty} \left\{ \frac{\sin(kx_p)}{k^2 - d^2} \frac{\sin(kx)}{k^2 - a^2} \cos[k(B_p - B)] \right\} = \frac{A_p^2}{A^2} A_{p,nm}^{(sc)}. \tag{6.0.71}$$

Also, we have

$$\begin{aligned}
 A_{p,nm}^{(ss)} &= \int_{-\pi}^{\pi} \left(\int_{-\pi}^{\pi} \sin(n\eta_0) \hat{T}(\xi, \eta_0) d\eta_0 \right) \sin(m\xi) d\xi \\
 &= \frac{1}{\pi} \sum_{k=1}^{\infty} \frac{1}{k} \int_{-\pi}^{\pi} \left(\int_{-\pi}^{\pi} \{ \cos(k(A\xi + B - A_p\eta_0 - B_p)) \right. \\
 &\quad \left. - \cos(k(-A\pi + B - A_p\eta_0 - B_p)) \right\} \\
 &\quad \left. \sin(n\eta_0) d\eta_0 \right) \sin(m\xi) d\xi \\
 &= \frac{1}{\pi} \sum_{k=1}^{\infty} \frac{1}{k} \left\{ \int_{-\pi}^{\pi} \sin(kA_p\eta_0) \sin(n\eta_0) d\eta_0 \int_{-\pi}^{\pi} \sin(kA\xi + kB - kB_p) \sin(m\xi) d\xi \right. \\
 &\quad \left. - \cos(kA\pi + kB_p - kB) \int_{-\pi}^{\pi} \cos(kA_p\eta_0) \sin(n\eta_0) d\eta_0 \int_{-\pi}^{\pi} \sin(m\xi) d\xi \right\}, \tag{6.0.72}
 \end{aligned}$$

The integrals in (6.0.72) are evaluated analytically as

$$\begin{aligned}
 \int_{-\pi}^{\pi} \sin(kA\xi + kB - kB_p) \sin(m\xi) d\xi &= \int_{-\pi}^{\pi} \{ \sin(kA\xi) \cos(kB - kB_p) \\
 &\quad + \cos(kA\xi) \sin(kB - kB_p) \} \sin(m\xi) d\xi \\
 &= \cos(kB - kB_p) \int_{-\pi}^{\pi} \sin(kA\xi) \sin(m\xi) d\xi, \tag{6.0.73}
 \end{aligned}$$

similarly

$$\int_{-\pi}^{\pi} \sin(kA_p\eta_0) \sin(n\eta_0) d\eta_0 = \begin{cases} \frac{2n \sin(kA_p\pi)}{(kA_p)^2 - n^2} \cos(n\pi) & \text{for } kA_p \neq n, \\ \pi & \text{for } kA_p = n. \end{cases} \tag{6.0.74}$$

substituting and (6.0.73-6.0.74) into (6.0.72) gives

$$A_{p,nm}^{(ss)} = \frac{4nm}{\pi A_p A} (-1)^{(n+m)} \sum_{k=1}^{\infty} \frac{1}{k} \left\{ \frac{\sin(kx_p) \sin(kx)}{k^2 - d^2} \frac{\sin(kx)}{k^2 - a^2} \cos(kB - kB_p) \right\}, \tag{6.0.75}$$

and from (6.0.75), we can find $B_{nm}^{(ss)}$ as

$$B_{nm}^{(ss)} = \frac{4nm}{\pi A_p A} (-1)^{(n+m)} \sum_{k=1}^{\infty} \frac{1}{k} \left\{ \frac{\sin(kx_p)}{k^2 - d^2} \frac{\sin(kx)}{k^2 - a^2} \cos(kB - kB_p) \right\} = A_{p,nm}^{(ss)}. \quad (6.0.76)$$

Finally,

$$\begin{aligned} A_{p,nm}^{(cs)} &= \int_{-\pi}^{\pi} \left(\int_{-\pi}^{\pi} \cos(n\eta_0) \hat{T}(\xi, \eta_0) d\eta_0 \right) \sin(m\xi) d\xi \\ &= \frac{1}{\pi} \sum_{k=1}^{\infty} \frac{1}{k} \int_{-\pi}^{\pi} \left(\int_{-\pi}^{\pi} \{ \cos(k(A\xi + B - A_p\eta_0 - B_p)) \right. \\ &\quad \left. - \cos(k(-A\pi + B - A_p\eta_0 - B_p)) \right\} \\ &\quad \left. \cos(n\eta_0) d\eta_0 \right) \sin(m\xi) d\xi \\ &= \frac{1}{\pi} \sum_{k=1}^{\infty} \frac{1}{k} \left\{ \int_{-\pi}^{\pi} \cos(kA_p\eta_0) \cos(n\eta_0) d\eta_0 \int_{-\pi}^{\pi} \cos(kA\xi + kB - kB_p) \sin(m\xi) d\xi \right. \\ &\quad \left. - \cos(kA\pi + kB_p - kB) \int_{-\pi}^{\pi} \cos(kA_p\eta_0) \cos(n\eta_0) d\eta_0 \int_{-\pi}^{\pi} \sin(m\xi) d\xi \right\}, \end{aligned} \quad (6.0.77)$$

then

$$A_{p,nm}^{(cs)} = \frac{4m}{\pi A_p A} (-1)^{(n+m)} \sum_{k=1}^{\infty} \left\{ \frac{\sin(kx_p)}{k^2 - d^2} \frac{\sin(kx)}{k^2 - a^2} \sin(kB - kB_p) \right\}, \quad (6.0.78)$$

From (6.0.78): If $k = d$, then $kx_p = (n/A_p)\pi A_p = \pi n$ and $\sin(kx_p) = 0$.

Applying L'Hopital's rule gives

$$\begin{aligned} \lim_{A_p \rightarrow n/k} \frac{\sin(kx_p)}{k^2 - d^2} &= \lim_{A_p \rightarrow n/k} \frac{\sin(k\pi A_p)}{k^2 - (n/A_p)^2} = \frac{\cos(k\pi(n/k))k\pi}{-2(n/A_p)(-n/A_p^2)} \\ &= \frac{\cos(\pi n)k\pi}{2n^2} \left(\frac{n}{k}\right)^3 = \frac{\pi}{2} \cos(\pi n) \frac{n}{k^2}. \end{aligned} \quad (6.0.79)$$

Similar, if $k = b$, then $kx = (n/A)\pi A = \pi n$, $\sin(kx) = 0$ and

$$\lim_{A \rightarrow n/k} \frac{\sin(kx)}{k^2 - b^2} = \frac{\pi}{2} \cos(\pi n) \frac{n}{k^2}. \quad (6.0.80)$$

If at least one of A and A_p is a rational number, then one or two terms in the series are calculated by L'Hopital's rule. From (6.0.78) there are different cases. In the first case, If d and a are not integers, then we calculate the series in (6.0.78). Second case, If d is integer, $d = N$, but a is not, then the series in (6.0.78) is evaluated as

$$A_{p, nm}^{(cs)} = \frac{4m}{\pi A_p A} \cos(m\pi) \cos(n\pi) \left[\sum_{k=1, k \neq N}^{\infty} \left\{ \frac{\sin(kx_p)}{k^2 - d^2} \frac{\sin(kx)}{k^2 - a^2} \sin[k(B - B_p)] \right\} + \frac{\pi}{2} \cos(\pi n) \frac{n}{N^2} \frac{\sin(Nx)}{N^2 - a^2} \sin[N(B - B_p)] \right]. \quad (6.0.81)$$

If d is not integer, but a is integer, $a = M$, then

$$A_{p, nm}^{(cs)} = \frac{4m}{\pi A_p A} \cos(m\pi) \cos(n\pi) \left[\sum_{k=1, k \neq M}^{\infty} \left\{ \frac{\sin(kx_p)}{k^2 - d^2} \frac{\sin(kx)}{k^2 - a^2} \sin[k(B - B_p)] \right\} + \frac{\sin(Mx_p)}{M^2 - d^2} \frac{\pi}{2} \cos(\pi n) \frac{n}{M^2} \sin[M(B - B_p)] \right]. \quad (6.0.82)$$

If d and a are integer but not equal to each other, $d = N$, $a = M$, $N \neq M$, then

$$A_{p, nm}^{(cs)} = \frac{4m}{\pi A_p A} \cos(m\pi) \cos(n\pi) \left[\sum_{k=1, k \neq M, N}^{\infty} \left\{ \frac{\sin(kx_p)}{k^2 - d^2} \frac{\sin(kx)}{k^2 - a^2} \sin[k(B - B_p)] \right\} + \frac{\sin(Mx_p)}{M^2 - N^2} \frac{\pi}{2} \cos(\pi n) \frac{n}{M^2} \sin[M(B - B_p)] + \frac{\pi}{2} \cos(\pi n) \frac{n}{N^2} \frac{\sin(Nx)}{N^2 - M^2} \sin[N(B - B_p)] \right]. \quad (6.0.83)$$

Last case, if d and a are integer and equal to each other, $d = a = N$, then

$$A_{p, nm}^{(cs)} = \frac{4m}{\pi A_p A} \cos(m\pi) \cos(n\pi) \left[\sum_{k=1, k \neq N}^{\infty} \left\{ \frac{\sin(kx_p)}{k^2 - d^2} \frac{\sin(kx)}{k^2 - a^2} \sin[k(B - B_p)] \right\} + \frac{\pi^2}{4} \frac{n^2}{N^4} \sin[N(B - B_p)] \right]. \quad (6.0.84)$$

For the rest elements we used similar evaluation, see Appendix A.2 for more

details.

6.1 Elements of the matrices

To illustrate the matrices as function of A and A_p for different parameters of the problem, we select the following parameters in dimensionless variables:

$$x^{(L)} = -0.5, \quad x^{(R)} = 0.5, \quad x_p^{(L)} = 1.2, \quad x_p^{(R)} = 3, \quad (6.1.1)$$

where $-1 < x^L < 0 < x^R \leq 1 \leq x_p^L < x_p^R$. Therefore, in the dimensionless variables, the contact region length is $L = 1$, the floating plate length is $L_p = 1.8$ and the center of the floating plate is at $X_p = 2.1$,

$$X_p = x_p^{(R)} - \frac{x_p^{(R)} - x_p^{(L)}}{2}. \quad (6.1.2)$$

The selected values provide in the ζ -plane,

$$\begin{aligned} \theta^L &= -2 \arctan(-x^{(L)}) \approx -0.9272, \\ \theta^R &= -2 \arctan(-x^{(R)}) \approx 0.9272, \\ \theta_p^L &= -2 \arctan(-x_p^{(L)}) \approx 1.7521, \\ \theta_p^R &= -2 \arctan(-x_p^{(R)}) \approx 2.4980, \end{aligned} \quad (6.1.3)$$

where $-\pi/2 < \theta^L < \theta^R < \pi/2$ and $\pi/2 < \theta_p^L < \theta_p^R < \pi$ because the floating plate is located in the right of the of entering body. Also we have

$$A = \frac{\theta^R - \theta^L}{2\pi} = 0.2951, \quad B = \frac{\theta^L + \theta^R}{2} = 0, \quad (6.1.4)$$

$$A_p = \frac{\theta_p^R - \theta_p^L}{2\pi} = 0.1187, \quad B_p = \frac{\theta_p^L + \theta_p^R}{2} = 2.1250, \quad (6.1.5)$$

where $0 < A < 1/2$ and $A_p < 1/4$, $B_p < 3\pi/4$.

In the figures 6.1.1–6.1.2, we illustrated the matrices elements as a function of A for $A_{10\ 20}^{cc}$ and $A_{10\ 20}^{ss}$, where $A_p = 1/4$. Also, figures 6.1.3–6.1.4 shows

the elements as a function of A_p for B_p^{cc} and B_p^{ss} , where $A_p = 1/4$.

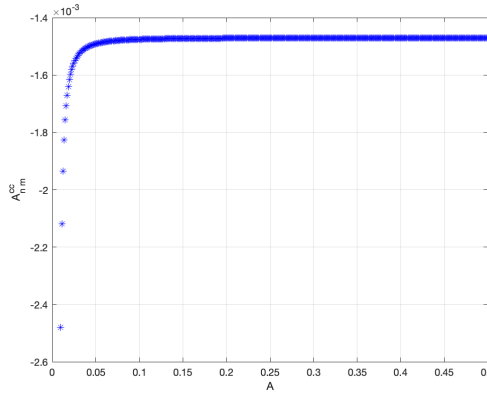


Figure 6.1.1: $A_{10\ 20}^{cc}$

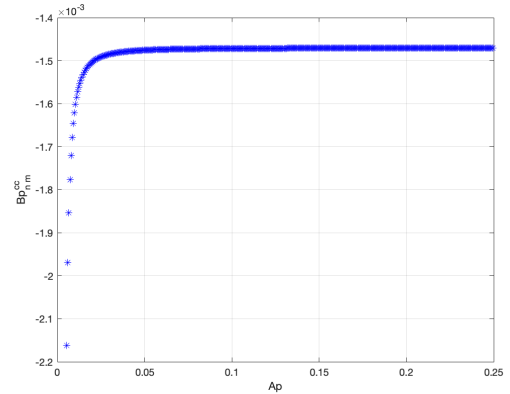


Figure 6.1.2: B_p^{cc}

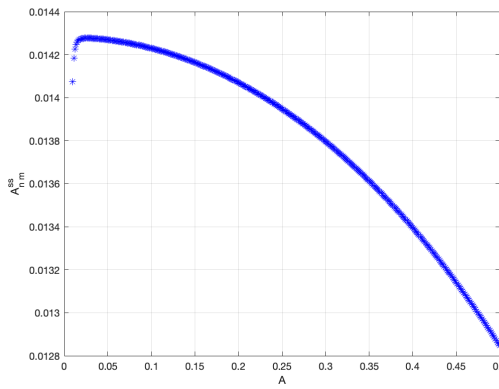


Figure 6.1.3: $A_{10\ 20}^{ss}$

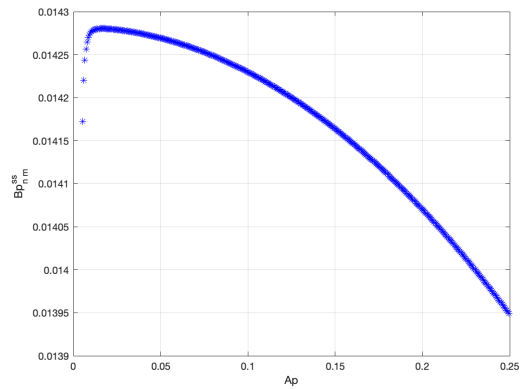


Figure 6.1.4: B_p^{ss}

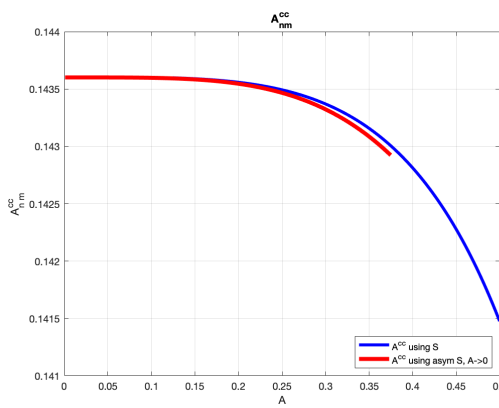


Figure 6.1.5: $A_{1\ 2}^{cc}$

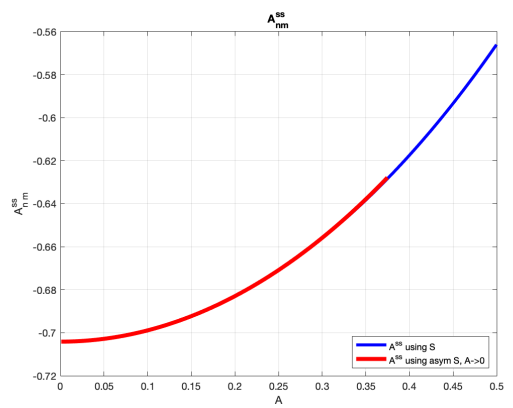


Figure 6.1.6: $A_{1\ 2}^{ss}$

Figure 6.1.7: The elements of A_{nm}^{cc} and A_{nm}^{ss} (Blue lines) calculated with 2500 terms retained in series (6.0.55 - 6.0.58) as function of A and $A_p = 1/4$ compared with its asymptotic using S (Red lines).

6.1.1 Calculating $\vec{Z}_{c1,s1}$ and $\vec{Z}_{c2,s2}$

The right hand side $\vec{Z}_{c1,s1}$ and $\vec{Z}_{c2,s2}$ in the system (6.0.54) are given by

$$Z_{c1,m} = \frac{1}{A} \int_{-\pi}^{\pi} G_1(\xi) \cos(m\xi) d\xi, \quad (6.1.6)$$

$$Z_{s1,m} = \frac{1}{A} \int_{-\pi}^{\pi} G_1(\xi) \sin(m\xi) d\xi, \quad (6.1.7)$$

$$Z_{c2,m} = \frac{1}{A} \int_{-\pi}^{\pi} G_2(\eta) \cos(m\eta) d\eta, \quad (6.1.8)$$

$$Z_{s2,m} = \frac{1}{A} \int_{-\pi}^{\pi} G_2(\eta) \sin(m\eta) d\eta, \quad (6.1.9)$$

where from (6.0.35) (6.0.36),

$$G_1(\xi) = \bar{f}(A\xi + B), \quad (6.1.10)$$

and

$$G_2(\eta) = \bar{f}(A_p\eta + B_p), \quad (6.1.11)$$

and $\bar{f}(\theta)$ is defined in (4.3.34) as

$$\bar{f}(\theta) = \int_{\theta^L}^{\theta} f(\theta_0) d\theta_0, \quad (6.1.12)$$

and $\bar{g}(\theta)$ is defined in (6.0.26) as

$$\bar{g}(\theta) = \int_{\theta_p^L}^{\theta} g(\theta_0) d\theta_0, \quad (6.1.13)$$

where

$$\theta = A\xi + B \quad \text{and} \quad \theta = A_p\eta + B_p, \quad (6.1.14)$$

the coefficients A , B , A_p and B_p are obtained from the equations:

$$\theta^L = A(-\pi) + B \quad \text{and} \quad \theta^R = A\pi + B, \quad (6.1.15)$$

$$\theta_p^L = A_p(-\pi) + B_p \quad \text{and} \quad \theta_p^R = A_p\pi + B_p, \quad (6.1.16)$$

which is gives

$$A = \frac{\theta^R - \theta^L}{2\pi} \quad \text{and} \quad B = \frac{\theta^L + \theta^R}{2}, \quad (6.1.17)$$

$$A_p = \frac{\theta_p^R - \theta_p^L}{2\pi} \quad \text{and} \quad B_p = \frac{\theta_p^L + \theta_p^R}{2}. \quad (6.1.18)$$

Integrating (6.1.6) by parts gives

$$\begin{aligned} Z_{c1,m} &= \left. \frac{1}{A} \frac{1}{m} \sin(m\xi) G_1(\xi) \right]_{-\pi}^{\pi} - \frac{1}{A} \int_{-\pi}^{\pi} G_1'(\xi) \frac{1}{m} \sin(m\xi) d\xi \\ &= -\frac{1}{A} \int_{-\pi}^{\pi} \frac{A}{m} f(A\xi + B, t) \sin(m\xi) d\xi, \end{aligned} \quad (6.1.19)$$

where

$$G'(\xi) = (\bar{f}(A\xi + B))' A, \quad (6.1.20)$$

and

$$G'(\eta) = (\bar{f}(A\eta + B_p))' A_p, \quad (6.1.21)$$

integrating (6.1.19) by substituting $\theta = A\xi + B$ gives

$$Z_{c1,m} = -\frac{1}{Am} \int_{\theta^L}^{\theta^R} f(\theta, t) \sin\left(m \frac{\theta - B}{A}\right) d\theta \quad (6.1.22)$$

where

$$f(\theta, t) = \frac{-\dot{Y}(t)}{1 + \cos(\theta)}, \quad (6.1.23)$$

this gives

$$Z_{c1,m} = -\frac{\dot{Y}(t)}{Am} \int_{\theta^L}^{\theta^R} \frac{\sin\left(m \frac{\theta - B}{A}\right)}{1 + \cos(\theta)} d\theta = -\dot{Y}(t) \tilde{Z}_{c1,m}(\theta^R, \theta^L), \quad (6.1.24)$$

where

$$\tilde{Z}_{c1,m}(\theta^R, \theta^L) = -\frac{1}{Am} \int_{\theta^L}^{\theta^R} \frac{\sin\left(m \frac{\theta - B}{A}\right)}{1 + \cos(\theta)} d\theta \quad (6.1.25)$$

and for $Z_{s1,m}$ we have

$$Z_{s1,m} = -\frac{\dot{Y}(t)}{Am} \int_{\theta^L}^{\theta^R} \frac{\cos\left(m \frac{\theta - B}{A}\right)}{1 + \cos(\theta)} d\theta = -\dot{Y}(t) \tilde{Z}_{s1,m}(\theta^R, \theta^L), \quad (6.1.26)$$

where

$$\tilde{Z}_{s1,m}(\theta^R, \theta^L) = -\frac{1}{Am} \int_{\theta^L}^{\theta^R} \frac{\cos\left(m\frac{\theta-B}{A}\right)}{1+\cos(\theta)} d\theta \quad (6.1.27)$$

Similarly for $Z_{s2,m}$ and $Z_{c2,m}$ we have

$$Z_{c2,m} = -\frac{1}{Am} \int_{\theta_p^L}^{\theta_p^R} g(\theta, t) \sin\left(m\frac{\theta-B_p}{A_p}\right) d\theta, \quad (6.1.28)$$

where

$$g(\theta, t) = \frac{-\dot{Y}_p(t) - \dot{\Omega}_p(t) \left(\frac{\sin(\theta)}{1+\cos(\theta)} - X_p(0) \right)}{1+\cos(\theta)}, \quad (6.1.29)$$

this gives

$$\begin{aligned} Z_{c2,m} &= \frac{\dot{Y}_p(t) - \dot{\Omega}_p(t) X_p(0)}{Am} \int_{\theta_p^L}^{\theta_p^R} \frac{\sin\left(m\frac{\theta-B_p}{A_p}\right)}{1+\cos(\theta)} d\theta \\ &\quad + \frac{\dot{\Omega}_p(t)}{Am} \int_{\theta_p^L}^{\theta_p^R} \frac{\sin(\theta) \sin\left(m\frac{\theta-B_p}{A_p}\right)}{(1+\cos(\theta))^2} d\theta \\ &= -\left(\dot{Y}_p(t) - \dot{\Omega}_p(t) X_p(0)\right) \tilde{Z}_{c2,m}(\theta_p^R, \theta_p^L) - \dot{\Omega}_p(t) \bar{Z}_{c2,m}(\theta_p^R, \theta_p^L), \end{aligned} \quad (6.1.30)$$

where

$$\tilde{Z}_{c2,m}(\theta_p^R, \theta_p^L) = -\frac{1}{Am} \int_{\theta_p^L}^{\theta_p^R} \frac{\sin\left(m\frac{\theta-B_p}{A_p}\right)}{1+\cos(\theta)} d\theta. \quad (6.1.31)$$

and

$$\bar{Z}_{c2,m}(\theta_p^R, \theta_p^L) = -\frac{1}{Am} \int_{\theta_p^L}^{\theta_p^R} \frac{\sin(\theta) \sin\left(m\frac{\theta-B_p}{A_p}\right)}{(1+\cos(\theta))^2} d\theta, \quad (6.1.32)$$

For \vec{Z}_{s2} we have

$$\begin{aligned} Z_{s2,m} &= \frac{\dot{Y}_p(t) - \dot{\Omega}_p(t)X_p(0)}{Am} \int_{\theta_p^L}^{\theta_p^R} \frac{\cos\left(m\frac{\theta-B_p}{A_p}\right)}{1+\cos(\theta)} d\theta \\ &\quad + \frac{\dot{\Omega}_p(t)}{Am} \int_{\theta_p^L}^{\theta_p^R} \frac{\sin(\theta)\cos\left(m\frac{\theta-B_p}{A_p}\right)}{(1+\cos(\theta))^2} d\theta \\ &= -\left(\dot{Y}_p(t) - \dot{\Omega}_p(t)X_p(0)\right) \tilde{Z}_{s2,m}(\theta_p^R, \theta_p^L) - \dot{\Omega}_p(t) \bar{Z}_{s2,m}(\theta_p^R, \theta_p^L), \end{aligned} \quad (6.1.33)$$

where

$$\tilde{Z}_{s2,m}(\theta_p^R, \theta_p^L) = -\frac{1}{Am} \int_{\theta_p^L}^{\theta_p^R} \frac{\cos\left(m\frac{\theta-B_p}{A_p}\right)}{1+\cos(\theta)} d\theta, \quad (6.1.34)$$

and

$$\bar{Z}_{s2,m}(\theta_p^R, \theta_p^L) = -\frac{1}{Am} \int_{\theta_p^L}^{\theta_p^R} \frac{\sin(\theta)\cos\left(m\frac{\theta-B_p}{A_p}\right)}{(1+\cos(\theta))^2} d\theta. \quad (6.1.35)$$

The integrals in (6.1.25), (6.1.27), (6.1.31), (6.1.34), (6.1.32) and (6.1.35) are evaluated numerically.

Then the system (6.0.54) can be written as

$$\begin{cases} A^{(cc)}\vec{a} + A_p^{(cc)}\vec{a} + A_p^{(sc)}\vec{b} = \dot{Y}(t)\vec{Z}_{c1,m}, \\ A^{(ss)}\vec{b} + A_p^{(cs)}\vec{a} + A_p^{(ss)}\vec{b} = \dot{Y}(t)\vec{Z}_{s1,m}, \\ B^{(cc)}\vec{a} + B^{(sc)}\vec{b} + B_p^{(cc)}\vec{a} = \left(\dot{Y}_p(t) - \dot{\Omega}_p(t)X_p(0)\right)\vec{Z}_{c2,m} + \dot{\Omega}_p(t)\vec{Z}_{c2,m}, \\ B^{(cs)}\vec{a} + B^{(ss)}\vec{b} + B_p^{(ss)}\vec{b} = \left(\dot{Y}_p(t) - \dot{\Omega}_p(t)X_p(0)\right)\vec{Z}_{s2,m} + \dot{\Omega}_p(t)\vec{Z}_{s2,m}, \end{cases} \quad (6.1.36)$$

Truncating each matrix in (6.0.54) to m terms, the system (6.0.54) can be written as

$$M\vec{a} = \vec{Z}, \quad (6.1.37)$$

where the matrix M is made of the matrices in (6.0.54),

$$\vec{a} = \left[\bar{a}_1, \bar{a}_2, \dots, \bar{a}_m, \bar{b}_1, \bar{b}_2, \dots, \bar{b}_m, \hat{a}_1, \hat{a}_2, \dots, \hat{a}_m, \hat{b}_1, \hat{b}_2, \dots, \hat{b}_m \right]^T, \quad (6.1.38)$$

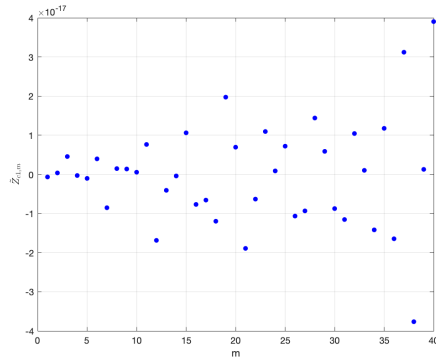


Figure 6.1.8: $\tilde{Z}_{c1,m}$

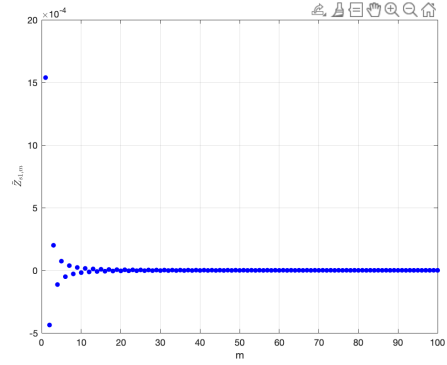


Figure 6.1.9: $\tilde{Z}_{s1,m}$

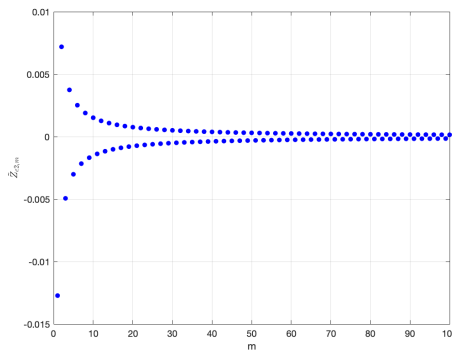


Figure 6.1.10: $\tilde{Z}_{c2,m}$

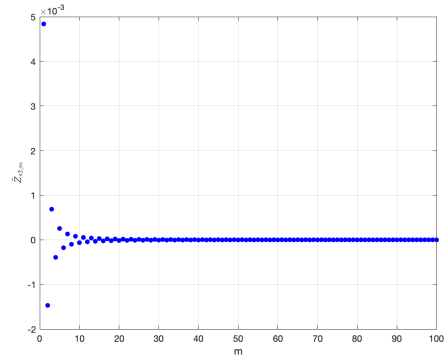


Figure 6.1.11: $\tilde{Z}_{s2,m}$

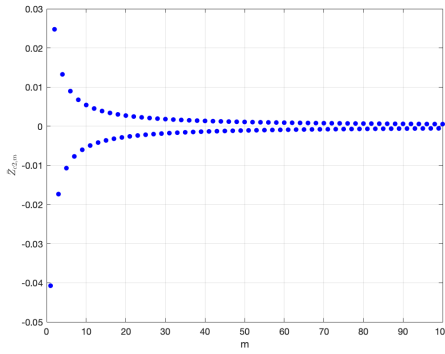


Figure 6.1.12: $\tilde{Z}_{c2,m}$

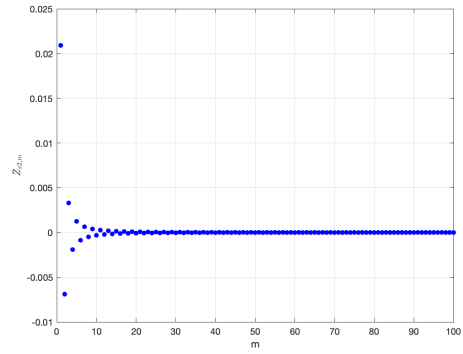


Figure 6.1.13: $\tilde{Z}_{s2,m}$

Figure 6.1.14: Plot of (6.1.25), (6.1.27), (6.1.31), (6.1.34), (6.1.32) and (6.1.35).

and

$$\vec{Z} = \left[Z_{c1}^{(1)}, Z_{c1}^{(2)}, \dots, Z_{c1}^{(m)}, Z_{s1}^{(1)}, Z_{s1}^{(2)}, \dots, Z_{s1}^{(m)}, Z_{c2}^{(1)}, Z_{c2}^{(2)}, \dots, Z_{c2}^{(m)}, Z_{s2}^{(1)}, Z_{s2}^{(2)}, \dots, Z_{s2}^{(m)} \right]^T, \quad (6.1.39)$$

where $Z_{c1}^{(1)}$ is evaluated by (6.1.24) at $m = 1$, $Z_{s1}^{(1)}$ is evaluated by (6.1.26) at

$m = 1$, $Z_{c2}^{(1)}$ is evaluated by (6.1.30) at $m = 1$, $Z_{s2}^{(1)}$ is evaluated by (6.1.33) at $m = 1$, $Z_{c1}^{(2)}$ is evaluated by (6.1.24) at $m = 2$, etc.

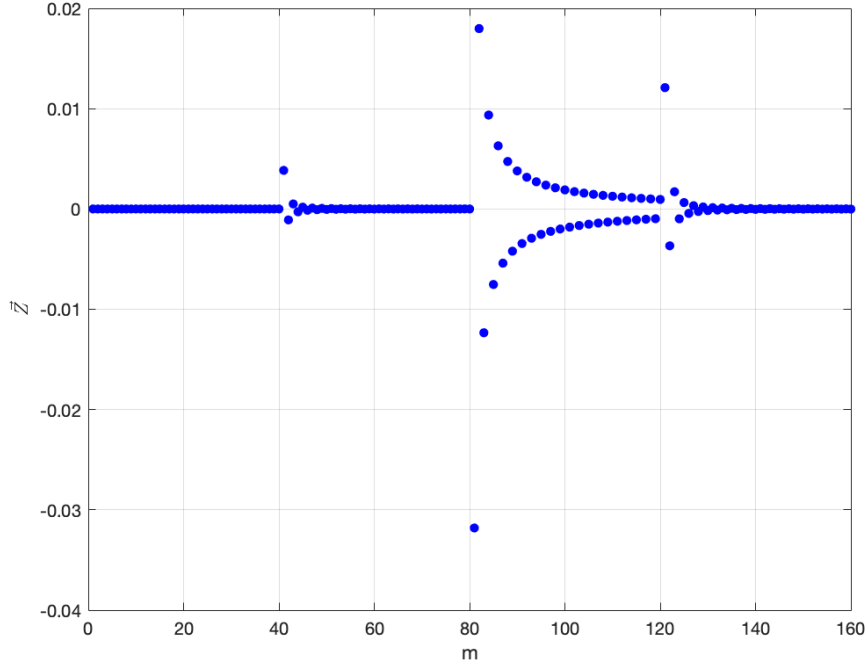


Figure 6.1.15: Plot of \vec{Z} in (6.1.39).

We have, see (6.0.54),

$$\vec{Z} = \dot{Y}_p(t)\vec{Z}_1 + \dot{\Omega}_p(t)X_p(0)\vec{Z}_2 + \dot{Y}(t)\vec{Z}_3, \quad (6.1.40)$$

and

$$\vec{a} = \dot{Y}_p(t)\vec{a}_1 + \dot{\Omega}_p(t)X_p(0)\vec{a}_2 + \dot{Y}(t)\vec{a}_3, \quad (6.1.41)$$

where \vec{a}_3 is the solution of (6.0.54), where $\dot{Y} = 1$, $\dot{Y}_p = 0$ and $\dot{\Omega}_p = 0$. \vec{a}_2 is the solution of (6.0.54), where $\dot{\Omega}_p = 1$, $\dot{Y}_p = 0$ and $\dot{Y} = 0$. \vec{a}_1 is the solution of (6.0.54), where $\dot{Y}_p = 1$, $\dot{\Omega}_p = 0$ and $\dot{Y} = 0$. Using (6.1.38) gives

$$\vec{a}_j = \left[\bar{a}_{j,1}, \bar{a}_{j,2}, \dots, \bar{a}_{j,m}, \bar{b}_{j,1}, \bar{b}_{j,2}, \dots, \bar{b}_{j,m}, \hat{a}_{j,1}, \hat{a}_{j,2}, \dots, \hat{a}_{j,m}, \hat{b}_{j,1}, \hat{b}_{j,2}, \dots, \hat{b}_{j,m} \right]^T, \quad j = 1, 2, 3. \quad (6.1.42)$$

Then the three systems can be written as

$$\begin{cases} M\vec{a}_1 = \vec{Z}_1, \\ M\vec{a}_2 = \vec{Z}_2, \\ M\vec{a}_3 = \vec{Z}_3, \end{cases} \quad (6.1.43)$$

where

$$\vec{Z}_3 = \left[\tilde{Z}_{c1}^{(1)}, \tilde{Z}_{c1}^{(2)}, \dots, \tilde{Z}_{c1}^{(m)}, \tilde{Z}_{s1}^{(1)}, \tilde{Z}_{s1}^{(2)}, \dots, \tilde{Z}_{s1}^{(m)}, 0, 0 \right]^T, \quad (6.1.44)$$

$$\vec{Z}_2 = \left[0, \tilde{Z}_{s1}^{(1)}, \tilde{Z}_{s1}^{(2)}, \dots, \tilde{Z}_{s1}^{(m)}, \tilde{Z}_{c2}^{(1)}, \tilde{Z}_{c2}^{(2)}, \dots, \tilde{Z}_{c2}^{(m)}, 0 \right]^T, \quad (6.1.45)$$

$$\vec{Z}_1 = \left[0, 0, \tilde{Z}_{c2}^{(1)}, \tilde{Z}_{c2}^{(2)}, \dots, \tilde{Z}_{c2}^{(m)}, \tilde{Z}_{s2}^{(1)}, \tilde{Z}_{s2}^{(2)}, \dots, \tilde{Z}_{s2}^{(m)} \right]^T. \quad (6.1.46)$$

Then

$$\vec{a}_3 = [M]^{-1}\vec{Z}_3, \quad (6.1.47)$$

$$\vec{a}_2 = [M]^{-1}\vec{Z}_2, \quad (6.1.48)$$

$$\vec{a}_1 = [M]^{-1}\vec{Z}_1. \quad (6.1.49)$$

where

$$M = \begin{bmatrix} A^{(cc)} & 0 & A_p^{(cc)} & A_p^{(sc)} \\ 0 & A^{(ss)} & A_p^{(cs)} & A_p^{(ss)} \\ B^{(cc)} & B^{(sc)} & B_p^{(cc)} & 0 \\ B^{(cs)} & B^{(ss)} & 0 & B_p^{(ss)} \end{bmatrix}. \quad (6.1.50)$$

In the following figures [6.1.16](#), [6.1.17](#) and [6.1.18](#), we can see the values of Z_3 , Z_2 and Z_1 correspondingly, where $m = 40$ for each.

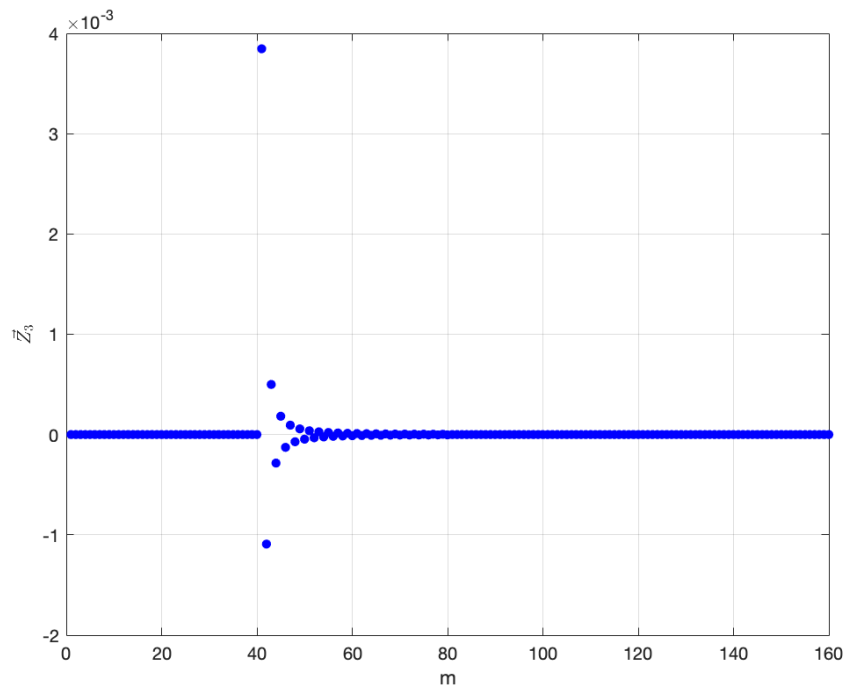


Figure 6.1.16: Plot of \vec{Z}_3 in (6.1.44).

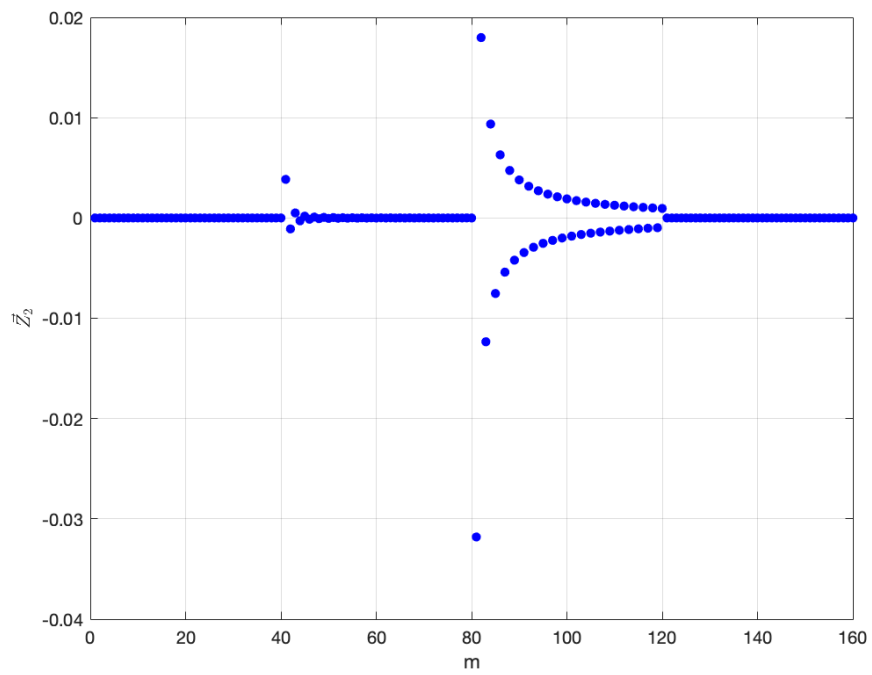


Figure 6.1.17: Plot of \vec{Z}_2 in (6.1.45).

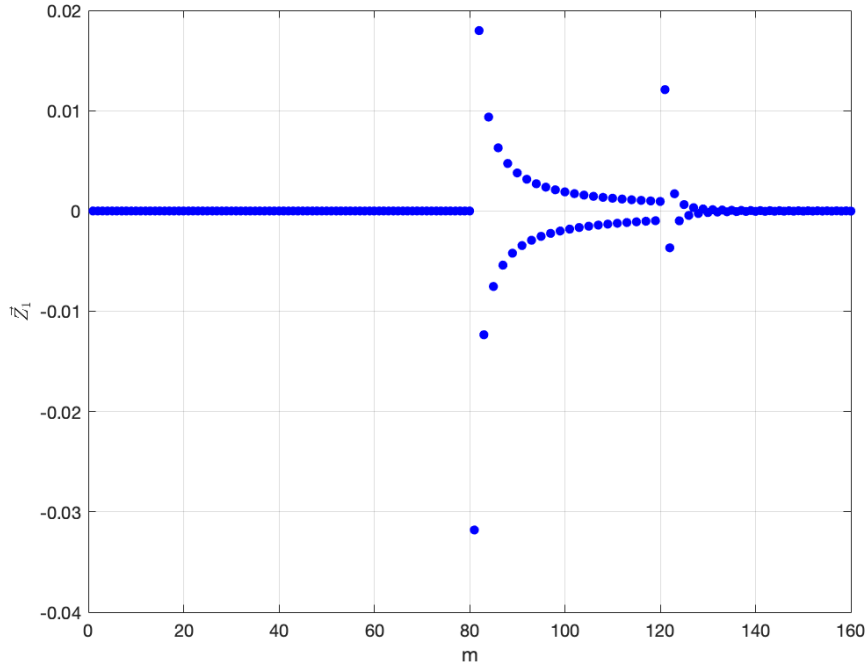


Figure 6.1.18: Plot of \vec{Z}_1 in (6.1.46).

From (6.0.5) and (4.3.1) we have for $\theta_p^L < \theta < \theta_p^R$,

$$\Phi(1, \theta, t) = G(\theta) = \dot{Y}_p(t)Q_1 + \dot{\Omega}_p(t)X_p(0)Q_2 + \dot{Y}(t)Q_3. \quad (6.1.51)$$

From (4.3.123) and (4.3.125) and using (6.1.51) gives

$$\Phi_F(1, \theta, t) = \dot{Y}_p(t)\bar{Q}_1 + \dot{\Omega}_p(t)X_p(0)\bar{Q}_2 + \dot{Y}(t)\bar{Q}_3, \quad (\theta^L < \theta < \theta^R), \quad (6.1.52)$$

where $\dot{Y}_p(t)$, $\dot{\Omega}_p(t)$ to be determined and $\dot{Y}(t)$ is given. The \bar{Q}_1 , \bar{Q}_2 and \bar{Q}_3 are given by

$$\bar{Q}_1 = -A \sum_{m=1}^{\infty} \left[\frac{\bar{a}_{1,m}}{m} \sin\left(m \frac{\theta - B}{A}\right) - \frac{\bar{b}_{1,m}}{m} \cos\left(m \frac{\theta - B}{A}\right) + \frac{\bar{b}_{1,m}}{m} (-1)^m \right], \quad (6.1.53)$$

$$\bar{Q}_2 = -A \sum_{m=1}^{\infty} \left[\frac{\bar{a}_{2,m}}{m} \sin\left(m \frac{\theta - B}{A}\right) - \frac{\bar{b}_{2,m}}{m} \cos\left(m \frac{\theta - B}{A}\right) + \frac{\bar{b}_{2,m}}{m} (-1)^m \right], \quad (6.1.54)$$

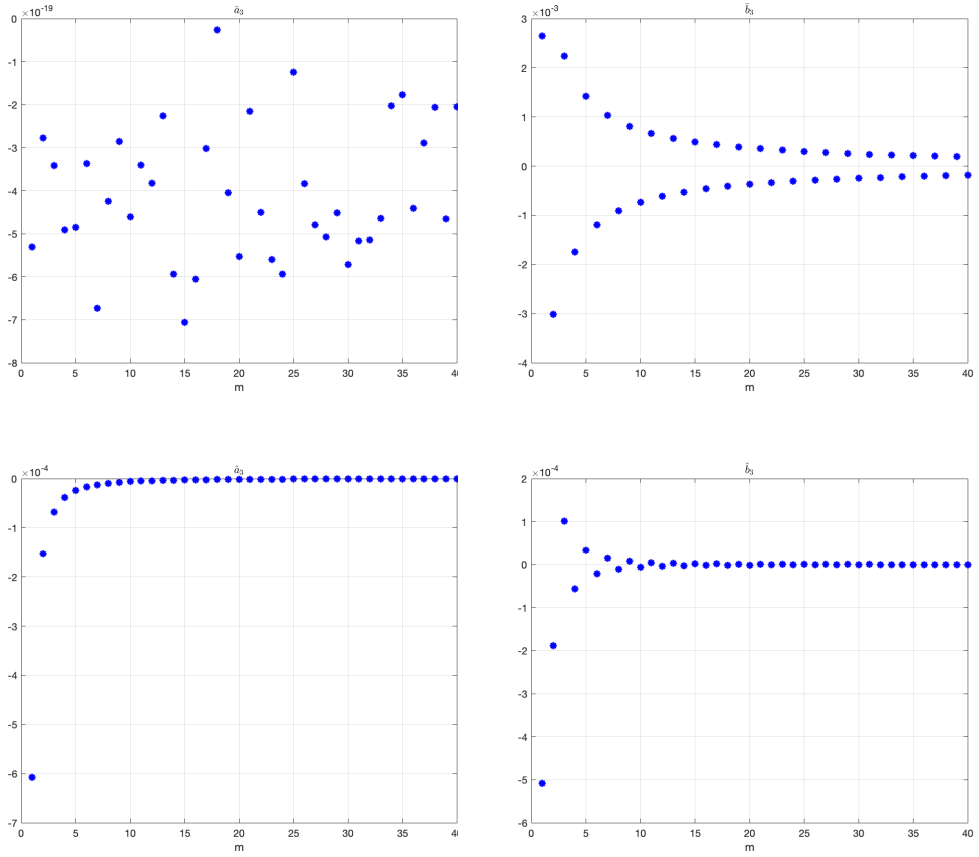


Figure 6.1.19: Plot of a_3 .

$$\bar{Q}_3 = -A \sum_{m=1}^{\infty} \left[\frac{\bar{a}_{3,m}}{m} \sin\left(m \frac{\theta - B}{A}\right) - \frac{\bar{b}_{3,m}}{m} \cos\left(m \frac{\theta - B}{A}\right) + \frac{\bar{b}_{3,m}}{m} (-1)^m \right], \quad (6.1.55)$$

where

$$A = \frac{\theta^R - \theta^L}{2\pi} \quad \text{and} \quad B = \frac{\theta^L + \theta^R}{2}. \quad (6.1.56)$$

Similarly for the floating plate Φ_G we have

$$\Phi_G(1, \theta, t) = \dot{Y}_p(t) \hat{Q}_1 + \dot{\Omega}_p(t) X_p(0) \hat{Q}_2 + \dot{Y}(t) \hat{Q}_3, \quad (\theta_p^L < \theta < \theta_p^R), \quad (6.1.57)$$

The \hat{Q}_1 , \hat{Q}_2 and \hat{Q}_3 are given by

$$\hat{Q}_1 = -A_p \sum_{m=1}^{\infty} \left[\frac{\hat{a}_{1,m}}{m} \sin\left(m \frac{\theta - B_p}{A_p}\right) - \frac{\hat{b}_{1,m}}{m} \cos\left(m \frac{\theta - B_p}{A_p}\right) + \frac{\hat{b}_{1,m}}{m} (-1)^m \right], \quad (6.1.58)$$

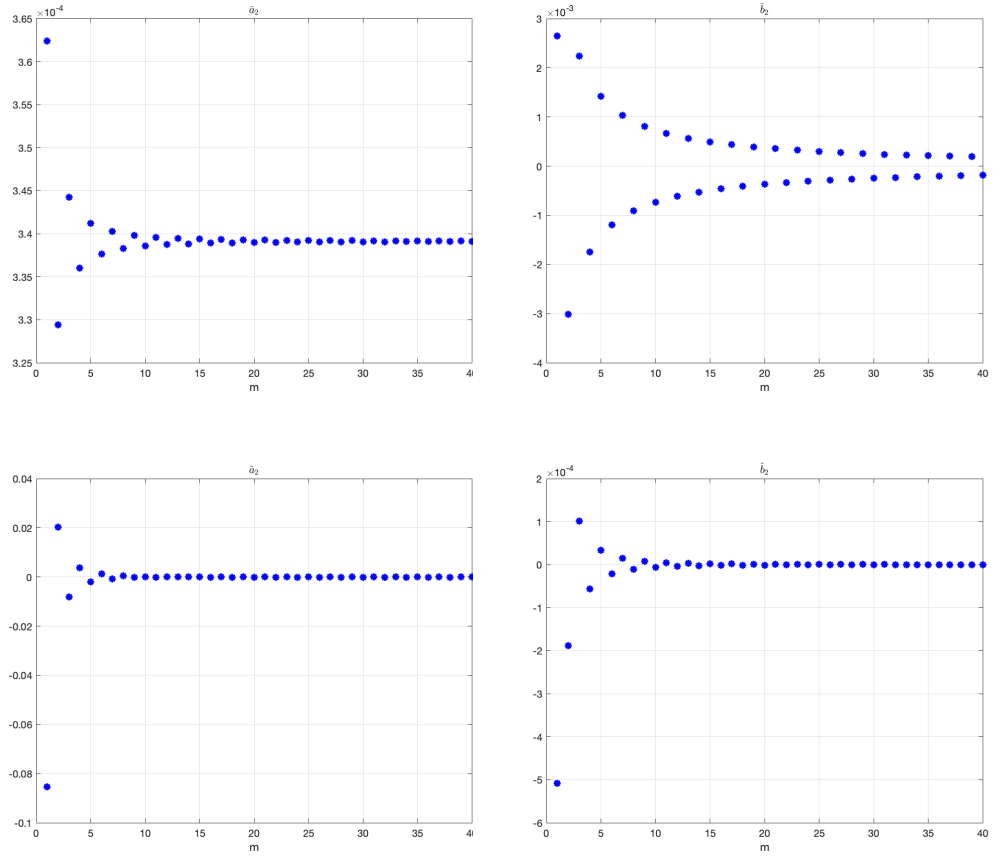


Figure 6.1.20: Plot of a_2 .

$$\hat{Q}_2 = -A_p \sum_{m=1}^{\infty} \left[\frac{\hat{a}_{2,m}}{m} \sin\left(m \frac{\theta - B_p}{A_p}\right) - \frac{\hat{b}_{2,m}}{m} \cos\left(m \frac{\theta - B_p}{A_p}\right) + \frac{\hat{b}_{2,m}}{m} (-1)^m \right], \quad (6.1.59)$$

$$\hat{Q}_3 = -A_p \sum_{m=1}^{\infty} \left[\frac{\hat{a}_{3,m}}{m} \sin\left(m \frac{\theta - B_p}{A_p}\right) - \frac{\hat{b}_{3,m}}{m} \cos\left(m \frac{\theta - B_p}{A_p}\right) + \frac{\hat{b}_{3,m}}{m} (-1)^m \right], \quad (6.1.60)$$

where

$$A_p = \frac{\theta_p^R - \theta_p^L}{2\pi} \quad \text{and} \quad B_p = \frac{\theta_p^L + \theta_p^R}{2}. \quad (6.1.61)$$

The \bar{Q}_1 (6.1.53), \bar{Q}_2 (6.1.54) and \bar{Q}_3 (6.1.55) are illustrated in figures 6.1.22, 6.1.23 and 6.1.24. Also, the \hat{Q}_1 (6.1.58), \hat{Q}_2 (6.1.59) and \hat{Q}_3 (6.1.60) are illustrated in figures 6.1.25, 6.1.26 and 6.1.27.

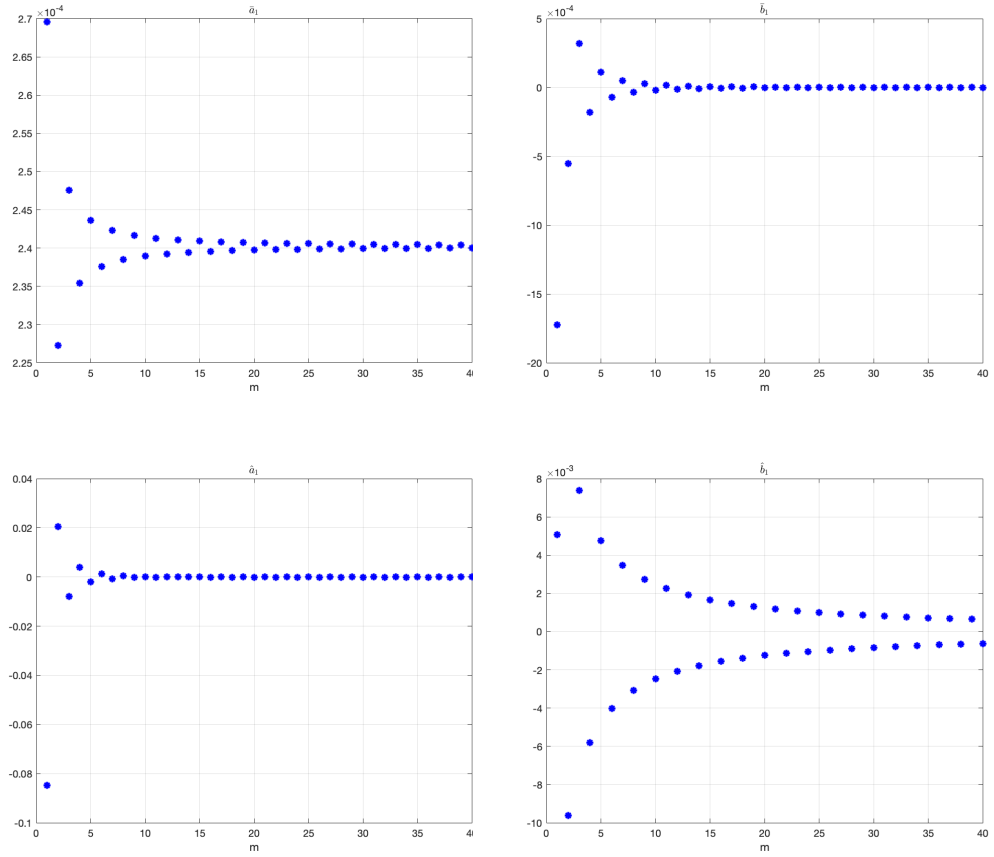


Figure 6.1.21: Plot of a_1 .

6.2 Motion of the floating plate

By recalling (5.2.11) and using (6.1.51) we have

$$m_p \ddot{Y}_p = F_v^p = \int_{x_p^{(L)}}^{x_p^{(R)}} p \cos(\alpha) dx = -\rho \frac{d}{dt} \int_{x_p^{(L)}}^{x_p^{(R)}} \Phi_G dx, \quad (6.2.1)$$

and

$$\int_{x_p^{(L)}}^{x_p^{(R)}} \Phi_G dx = \int_{\theta_p^{(L)}}^{\theta_p^{(R)}} G(\theta) x_\theta d\theta = \int_{\theta_p^{(L)}}^{\theta_p^{(R)}} G(\theta) \frac{-d\theta}{1 + \cos \theta}. \quad (6.2.2)$$

We have

$$\frac{d}{dt} \left(m_p \dot{Y}_p + \rho \int_{\theta_p^{(L)}}^{\theta_p^{(R)}} G(\theta) \frac{-d\theta}{1 + \cos \theta} \right) = 0, \quad (6.2.3)$$

substituting (6.1.51) into (6.2.3) and using the initial conditions $\dot{Y}_p(0) = 0$,

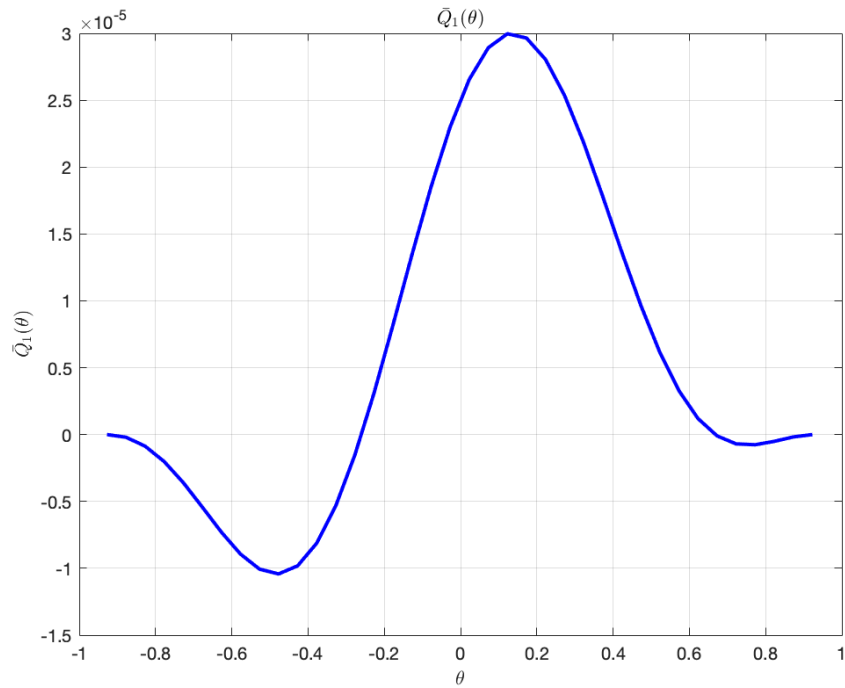


Figure 6.1.22: Plot of \bar{Q}_1 .

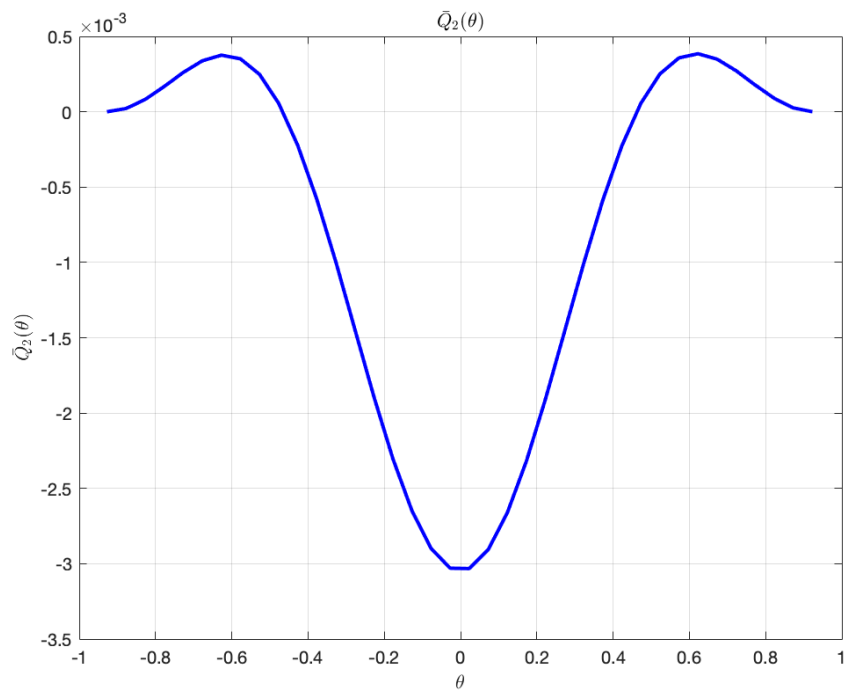


Figure 6.1.23: Plot of \bar{Q}_2 .

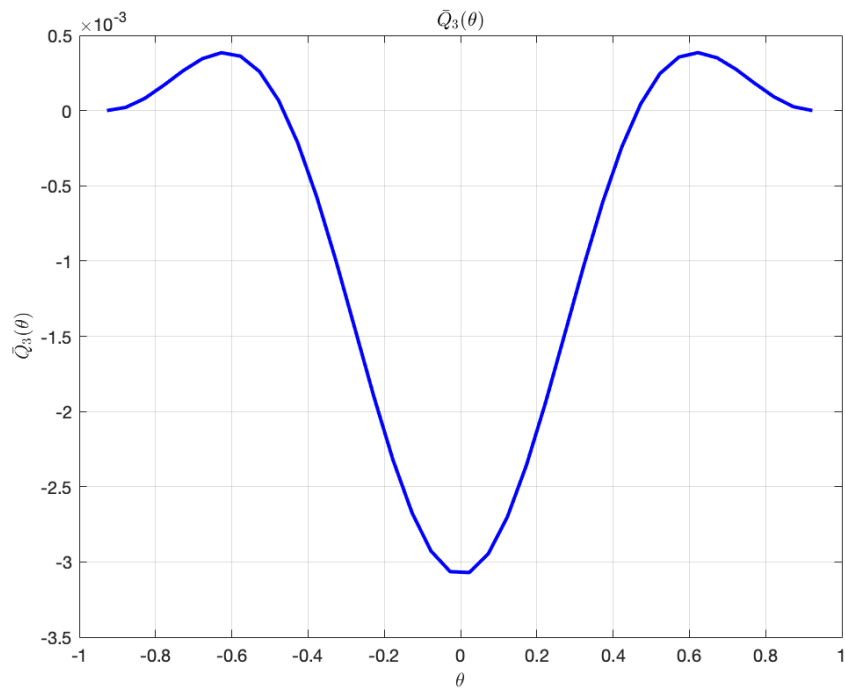


Figure 6.1.24: Plot of \bar{Q}_3 .

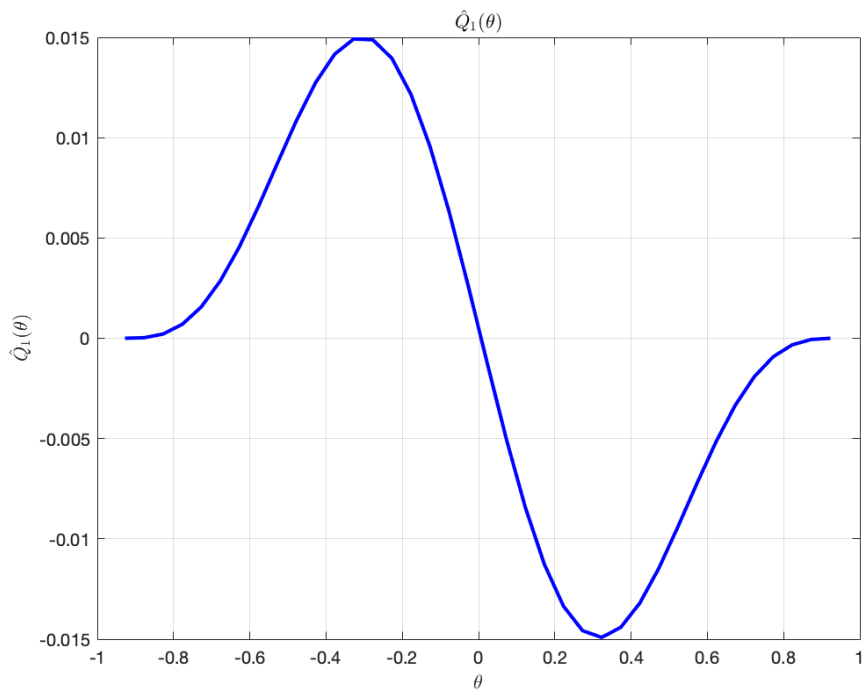


Figure 6.1.25: Plot of \hat{Q}_1 .

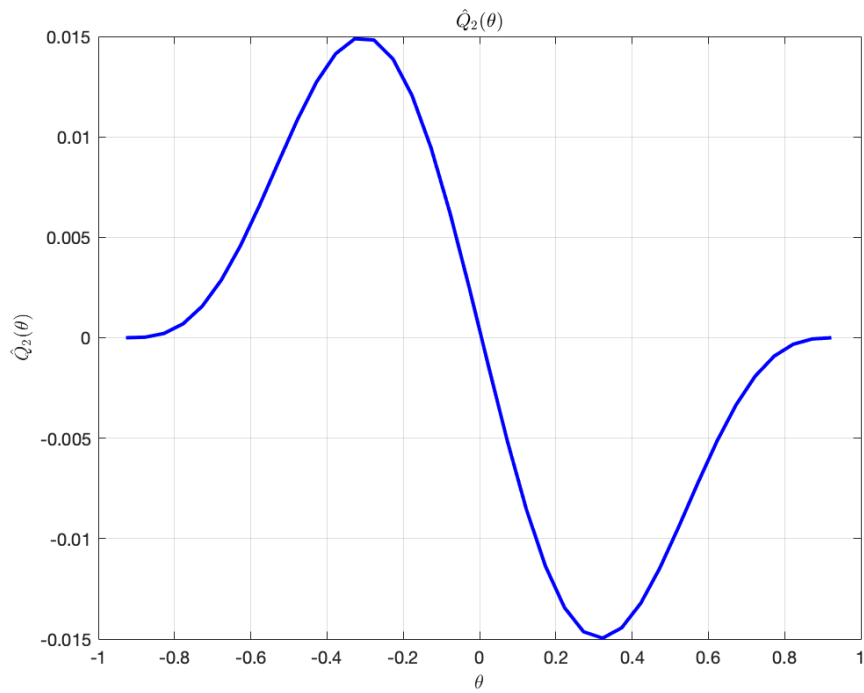


Figure 6.1.26: Plot of \hat{Q}_2 .

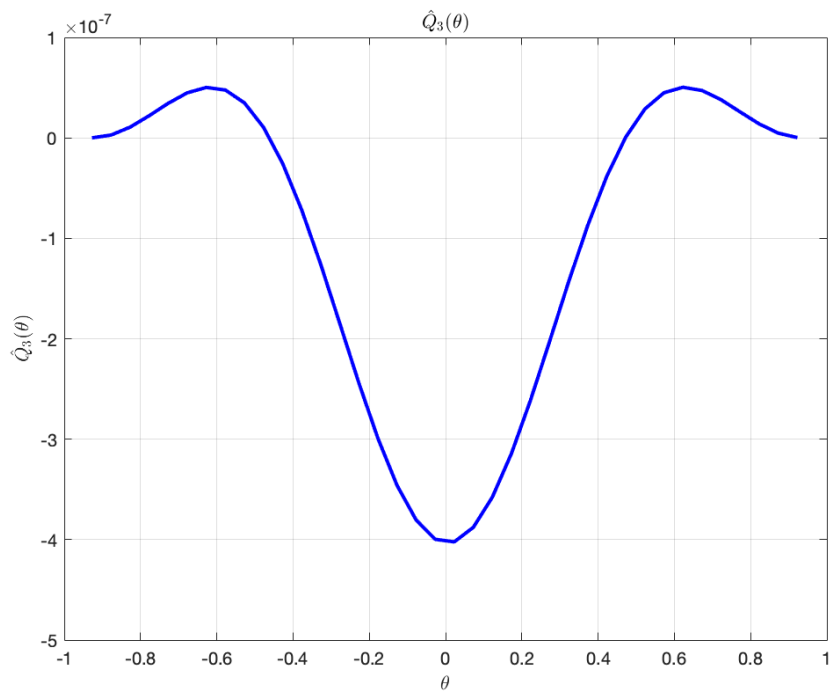


Figure 6.1.27: Plot of \hat{Q}_3 .

$G = 0$, we can integrate (6.2.3) with the result,

$$m_p \dot{Y}_p + \rho \dot{Y}_p \int_{\theta_p^{(L)}}^{\theta_p^{(R)}} Q_1(\theta) \frac{-d\theta}{1 + \cos \theta} + \rho \dot{\Omega}_p \int_{\theta_p^{(L)}}^{\theta_p^{(R)}} Q_2(\theta) \frac{-d\theta}{1 + \cos \theta} + \rho \dot{Y}_p \int_{\theta_p^{(L)}}^{\theta_p^{(R)}} Q_3(\theta) \frac{-d\theta}{1 + \cos \theta} = 0. \quad (6.2.4)$$

now denote (6.2.4) as

$$E_{1,1} \dot{Y}_p + E_{1,2} \dot{\Omega}_p + E_{1,3} \dot{Y}_p = 0. \quad (6.2.5)$$

where

$$\begin{aligned} E_{1,1} &= m_p + \rho \int_{\theta_p^{(L)}}^{\theta_p^{(R)}} Q_1(\theta) \frac{-d\theta}{1 + \cos \theta} \\ &= m_p - \rho A_p \sum_{m=1}^{\infty} \left[-\frac{\hat{a}_{1,m}}{m} \int_{\theta_p^{(L)}}^{\theta_p^{(R)}} \frac{\sin(m \frac{\theta - B_p}{A_p})}{1 + \cos \theta} d\theta \right. \\ &\quad + \frac{\hat{b}_{1,m}}{m} \int_{\theta_p^{(L)}}^{\theta_p^{(R)}} \frac{\cos(m \frac{\theta - B_p}{A_p})}{1 + \cos \theta} d\theta \\ &\quad \left. - \frac{\hat{b}_{1,m}}{m} (-1)^m \int_{\theta_p^{(L)}}^{\theta_p^{(R)}} \frac{1}{1 + \cos \theta} d\theta \right] \\ &= m_p - \rho A_p \sum_{m=1}^{\infty} \left[\hat{a}_{1,m} A \tilde{Z}_{c2,m}(\theta_p^R, \theta_p^L) \right. \\ &\quad - \hat{b}_{1,m} A \tilde{Z}_{s2,m}(\theta_p^R, \theta_p^L) \\ &\quad \left. - \hat{b}_{1,m} (-1)^m (\tan(\theta_p^R/2) - \tan(\theta_p^L/2)) \right], \quad (6.2.6) \end{aligned}$$

$$\begin{aligned} E_{1,2} &= \rho \int_{\theta_p^{(L)}}^{\theta_p^{(R)}} Q_2(\theta) \frac{-d\theta}{1 + \cos \theta} = -\rho A_p \sum_{m=1}^{\infty} \left[\hat{a}_{2,m} A \tilde{Z}_{c2,m}(\theta_p^R, \theta_p^L) \right. \\ &\quad - \hat{b}_{2,m} A \tilde{Z}_{s2,m}(\theta_p^R, \theta_p^L) \\ &\quad \left. - \frac{\hat{b}_{2,m}}{m} (-1)^m (\tan(\theta_p^R/2) - \tan(\theta_p^L/2)) \right], \quad (6.2.7) \end{aligned}$$

and

$$E_{1,3} = \rho \int_{\theta_p^{(L)}}^{\theta_p^{(R)}} Q_3(\theta) \frac{-d\theta}{1 + \cos \theta} = -\rho A_p \sum_{m=1}^{\infty} \left[\hat{a}_{3,m} A \tilde{Z}_{c2,m}(\theta_p^R, \theta_p^L) - \hat{b}_{3,m} A \tilde{Z}_{s2,m}(\theta_p^R, \theta_p^L) - \frac{\hat{b}_{3,m}}{m} (-1)^m (\tan(\theta_p^R/2) - \tan(\theta_p^L/2)) \right]. \quad (6.2.8)$$

Similarly, recalling (5.2.13) gives

$$J_p \ddot{\Omega}_p = \int_{x_p^{(L)}}^{x_p^{(R)}} (x - X_p) p dx = -\rho \frac{d}{dt} \int_{x_p^{(L)}}^{x_p^{(R)}} (x - X_p) \Phi_G dx, \quad (6.2.9)$$

where

$$\begin{aligned} \int_{x_p^{(L)}}^{x_p^{(R)}} (x - X_p) \Phi_G dx &= \int_{\theta_p^{(L)}}^{\theta_p^{(R)}} \left(\frac{\sin \theta}{1 + \cos \theta} - X_p \right) G(\theta) x_\theta d\theta \\ &= \int_{\theta_p^{(L)}}^{\theta_p^{(R)}} - \left(\frac{\sin \theta}{(1 + \cos \theta)^2} - \frac{X_p}{1 + \cos \theta} \right) G(\theta) d\theta, \end{aligned} \quad (6.2.10)$$

and

$$\frac{d}{dt} \left(J_p \dot{\Omega}_p + \rho \int_{\theta_p^{(L)}}^{\theta_p^{(R)}} \left(\frac{-\sin \theta}{(1 + \cos \theta)^2} + \frac{X_p}{1 + \cos \theta} \right) G(\theta) d\theta \right) = 0, \quad (6.2.11)$$

substituting (6.1.51) into (6.2.11) gives

$$\begin{aligned} J_p \dot{\Omega}_p + \rho \dot{Y}_p \int_{\theta_p^{(L)}}^{\theta_p^{(R)}} \left(\frac{-\sin \theta}{(1 + \cos \theta)^2} + \frac{X_p}{1 + \cos \theta} \right) Q_1(\theta) d\theta \\ + \rho \dot{\Omega}_p \int_{\theta_p^{(L)}}^{\theta_p^{(R)}} \left(\frac{-\sin \theta}{(1 + \cos \theta)^2} + \frac{X_p}{1 + \cos \theta} \right) Q_2(\theta) d\theta \\ + \rho \dot{Y} \int_{\theta_p^{(L)}}^{\theta_p^{(R)}} \left(\frac{-\sin \theta}{(1 + \cos \theta)^2} + \frac{X_p}{1 + \cos \theta} \right) Q_3(\theta) d\theta = 0. \end{aligned} \quad (6.2.12)$$

now denote (6.2.12) as

$$E_{2,1} \dot{Y}_p(t) + E_{2,2} \dot{\Omega}_p(t) + E_{2,3} \dot{Y}(t) = 0, \quad (6.2.13)$$

where

$$\begin{aligned}
 E_{2,1} &= \rho \int_{\theta_p^{(L)}}^{\theta_p^{(R)}} \left(\frac{-\sin \theta}{(1 + \cos \theta)^2} + \frac{X_p}{1 + \cos \theta} \right) Q_1(\theta) d\theta \\
 &= -\rho A_p \sum_{m=1}^{\infty} \left[-\frac{\hat{a}_{1,m}}{m} \int_{\theta_p^{(L)}}^{\theta_p^{(R)}} \frac{\sin(\theta) \sin(m \frac{\theta - B_p}{A_p})}{(1 + \cos \theta)^2} d\theta \right. \\
 &\quad + \frac{\hat{b}_{1,m}}{m} \int_{\theta_p^{(L)}}^{\theta_p^{(R)}} \frac{\sin(\theta) \cos(m \frac{\theta - B_p}{A_p})}{(1 + \cos \theta)^2} d\theta \\
 &\quad \left. - \frac{\hat{b}_{1,m}}{m} (-1)^m \int_{\theta_p^{(L)}}^{\theta_p^{(R)}} \frac{\sin(\theta)}{(1 + \cos \theta)^2} d\theta \right] \\
 &\quad - \rho A_p \sum_{m=1}^{\infty} \left[\frac{\hat{a}_{1,m}}{m} \int_{\theta_p^{(L)}}^{\theta_p^{(R)}} \frac{X_p \sin(m \frac{\theta - B_p}{A_p})}{1 + \cos \theta} d\theta \right. \\
 &\quad - \frac{\hat{b}_{1,m}}{m} \int_{\theta_p^{(L)}}^{\theta_p^{(R)}} \frac{X_p \cos(m \frac{\theta - B_p}{A_p})}{1 + \cos \theta} d\theta \\
 &\quad \left. + \frac{\hat{b}_{1,m}}{m} (-1)^m \int_{\theta_p^{(L)}}^{\theta_p^{(R)}} \frac{X_p}{1 + \cos \theta} d\theta \right] \\
 &= -\rho A_p \sum_{m=1}^{\infty} \left[-\hat{a}_{1,m} A \bar{Z}_{c2,m}(\theta_p^R, \theta_p^L) \right. \\
 &\quad + \hat{b}_{1,m} A \bar{Z}_{s2,m}(\theta_p^R, \theta_p^L) \\
 &\quad \left. - \frac{\hat{b}_{1,m}}{m} (-1)^m \left(\frac{1}{2} \tan^2(\theta_p^R/2) - \frac{1}{2} \tan^2(\theta_p^L/2) \right) \right] \\
 &\quad - \rho A_p \sum_{m=1}^{\infty} \left[-\hat{a}_{1,m} A X_p \tilde{Z}_{c2,m}(\theta_p^R, \theta_p^L) \right. \\
 &\quad + \hat{b}_{1,m} A X_p \tilde{Z}_{s2,m}(\theta_p^R, \theta_p^L) \\
 &\quad \left. - \frac{\hat{b}_{1,m}}{m} (-1)^m X_p (\tan(\theta_p^R/2) - \tan(\theta_p^L/2)) \right], \quad (6.2.14)
 \end{aligned}$$

and

$$\begin{aligned}
 E_{2,2} &= J_p + \rho \int_{\theta_p^{(L)}}^{\theta_p^{(R)}} \left(\frac{-\sin \theta}{(1 + \cos \theta)^2} + \frac{X_p}{1 + \cos \theta} \right) Q_2(\theta) d\theta \\
 &= J_p - \rho A_p \sum_{m=1}^{\infty} \left[-\frac{\hat{a}_{2,m}}{m} \int_{\theta_p^{(L)}}^{\theta_p^{(R)}} \frac{\sin(\theta) \sin(m \frac{\theta - B_p}{A_p})}{(1 + \cos \theta)^2} d\theta \right. \\
 &\quad + \frac{\hat{b}_{2,m}}{m} \int_{\theta_p^{(L)}}^{\theta_p^{(R)}} \frac{\sin(\theta) \cos(m \frac{\theta - B_p}{A_p})}{(1 + \cos \theta)^2} d\theta \\
 &\quad \left. - \frac{\hat{b}_{2,m}}{m} (-1)^m \int_{\theta_p^{(L)}}^{\theta_p^{(R)}} \frac{\sin(\theta)}{(1 + \cos \theta)^2} d\theta \right] \\
 &= J_p - \rho A_p \sum_{m=1}^{\infty} \left[\frac{\hat{a}_{2,m}}{m} \int_{\theta_p^{(L)}}^{\theta_p^{(R)}} \frac{X_p \sin(m \frac{\theta - B_p}{A_p})}{1 + \cos \theta} d\theta \right. \\
 &\quad - \frac{\hat{b}_{2,m}}{m} \int_{\theta_p^{(L)}}^{\theta_p^{(R)}} \frac{X_p \cos(m \frac{\theta - B_p}{A_p})}{1 + \cos \theta} d\theta \\
 &\quad \left. + \frac{\hat{b}_{2,m}}{m} (-1)^m \int_{\theta_p^{(L)}}^{\theta_p^{(R)}} \frac{X_p}{1 + \cos \theta} d\theta \right] \\
 &= J_p - \rho A_p \sum_{m=1}^{\infty} \left[-\hat{a}_{2,m} A \bar{Z}_{c2,m}(\theta_p^R, \theta_p^L) \right. \\
 &\quad + \hat{b}_{2,m} A \bar{Z}_{s2,m}(\theta_p^R, \theta_p^L) \\
 &\quad \left. - \frac{\hat{b}_{2,m}}{m} (-1)^m \left(\frac{1}{2} \tan^2(\theta_p^R/2) - \frac{1}{2} \tan^2(\theta_p^L/2) \right) \right] \\
 &= J_p - \rho A_p \sum_{m=1}^{\infty} \left[-\hat{a}_{2,m} A X_p \tilde{Z}_{c2,m}(\theta_p^R, \theta_p^L) \right. \\
 &\quad + \hat{b}_{2,m} A X_p \tilde{Z}_{s2,m}(\theta_p^R, \theta_p^L) \\
 &\quad \left. - \frac{\hat{b}_{2,m}}{m} (-1)^m X_p (\tan(\theta_p^R/2) - \tan(\theta_p^L/2)) \right], \quad (6.2.15)
 \end{aligned}$$

and

$$\begin{aligned}
 E_{2,3} &= \rho \int_{\theta_p^{(L)}}^{\theta_p^{(R)}} \left(\frac{-\sin \theta}{(1 + \cos \theta)^2} + \frac{X_p}{1 + \cos \theta} \right) Q_3(\theta) d\theta \\
 &= -\rho A_p \sum_{m=1}^{\infty} \left[-\frac{\hat{a}_{3,m}}{m} \int_{\theta_p^{(L)}}^{\theta_p^{(R)}} \frac{\sin(\theta) \sin(m \frac{\theta - B_p}{A_p})}{(1 + \cos \theta)^2} d\theta \right. \\
 &\quad + \frac{\hat{b}_{3,m}}{m} \int_{\theta_p^{(L)}}^{\theta_p^{(R)}} \frac{\sin(\theta) \cos(m \frac{\theta - B_p}{A_p})}{(1 + \cos \theta)^2} d\theta \\
 &\quad \left. - \frac{\hat{b}_{3,m}}{m} (-1)^m \int_{\theta_p^{(L)}}^{\theta_p^{(R)}} \frac{\sin(\theta)}{(1 + \cos \theta)^2} d\theta \right] \\
 &= -\rho A_p \sum_{m=1}^{\infty} \left[\frac{\hat{a}_{3,m}}{m} \int_{\theta_p^{(L)}}^{\theta_p^{(R)}} \frac{X_p \sin(m \frac{\theta - B_p}{A_p})}{1 + \cos \theta} d\theta \right. \\
 &\quad - \frac{\hat{b}_{3,m}}{m} \int_{\theta_p^{(L)}}^{\theta_p^{(R)}} \frac{X_p \cos(m \frac{\theta - B_p}{A_p})}{1 + \cos \theta} d\theta \\
 &\quad \left. + \frac{\hat{b}_{3,m}}{m} (-1)^m \int_{\theta_p^{(L)}}^{\theta_p^{(R)}} \frac{X_p}{1 + \cos \theta} d\theta \right] \\
 &= -\rho A_p \sum_{m=1}^{\infty} \left[-\hat{a}_{3,m} A \bar{Z}_{c2,m}(\theta_p^R, \theta_p^L) \right. \\
 &\quad + \hat{b}_{3,m} A \bar{Z}_{s2,m}(\theta_p^R, \theta_p^L) \\
 &\quad \left. - \frac{\hat{b}_{3,m}}{m} (-1)^m \left(\frac{1}{2} \tan^2(\theta_p^R/2) - \frac{1}{2} \tan^2(\theta_p^L/2) \right) \right] \\
 &= -\rho A_p \sum_{m=1}^{\infty} \left[-\hat{a}_{3,m} A X_p \tilde{Z}_{c2,m}(\theta_p^R, \theta_p^L) \right. \\
 &\quad + \hat{b}_{3,m} A X_p \tilde{Z}_{s2,m}(\theta_p^R, \theta_p^L) \\
 &\quad \left. - \frac{\hat{b}_{3,m}}{m} (-1)^m X_p (\tan(\theta_p^R/2) - \tan(\theta_p^L/2)) \right], \quad (6.2.16)
 \end{aligned}$$

where (6.2.4) and (6.2.12) are equal to zero at ($t = 0$).

From (6.2.13) and (6.2.5) we have the following system

$$\begin{cases} E_{1,1} \dot{Y}_p + E_{1,2} \dot{\Omega}_p + E_{1,3} \dot{Y} = 0, \\ E_{2,1} \dot{Y}_p + E_{2,2} \dot{\Omega}_p + E_{2,3} \dot{Y} = 0. \end{cases} \quad (6.2.17)$$

where $\dot{Y} = v$ which is given. Solving the system gives

$$\dot{\Omega}_p(t) = \frac{E_{1,3}v + E_{1,1}E_{2,3}v}{E_{1,1}E_{2,2} - E_{2,1}E_{1,2}}, \quad (6.2.18)$$

and

$$\dot{Y}_p(t) = -\frac{E_{1,2}E_{1,3}v + E_{1,2}E_{1,1}E_{2,3}v}{E_{1,1}^2E_{2,2} - E_{1,1}E_{2,1}E_{1,2}} - \frac{E_{1,3}v}{E_{1,1}}. \quad (6.2.19)$$

where

$$\dot{Y}_p(0) = 0 \quad \text{and} \quad \dot{\Omega}_p(0) = 0. \quad (6.2.20)$$

The systems (6.2.18) and (6.2.19) provides $\dot{Y}_p(t)$ and $\dot{\Omega}_p(t)$ for a given speed $v(t)$ of the entering body

6.3 Verification of the numerical solution

By choosing parabolic body as a particular case for entering a body without floating plate as

$$f(x) = H\tilde{f}(x/L) \quad \longrightarrow \quad f(x) = \frac{x^2}{2R} - vt, \quad (6.3.1)$$

where $2L$ is the horizontal size of the entering body, H is the height of the body and $Y(t) = vt$. From (5.2.33) we have

$$\left\{ \begin{array}{ll}
 \nabla^2 \varphi = 0 & (y < 0), \\
 p = -\varphi_t & (y \leq 0), \\
 p = 0, \varphi_y = \eta_t, \varphi = 0 & \left(y = 0, -\infty < x < x^{(L)} < x_p^{(L)} < x_p^{(R)} \right) \\
 & \left(y = 0, x^{(R)} < x_p^{(L)} < x_p^{(R)} < x < \infty \right), \\
 \varphi_y = -h'(t) & (y = 0, x^{(L)} < x < x^{(R)}) \\
 \varphi_y = \dot{Y}_p(t) + \dot{\Omega}_p(t)(x - X_p(0)), & \left(x_p^{(L)} < x < x_p^{(R)} \right), \\
 m_p \dot{Y}_p = -\rho \int_{x_p^{(L)}}^{x_p^{(R)}} \varphi(x, 0, t) dx, & \left(x_p^{(L)} < x < x_p^{(R)} \right), \\
 J_p \dot{\Omega}_p = -\rho \int_{x_p^{(L)}}^{x_p^{(R)}} (x - X_p(0)) \varphi dx, & \left(x_p^{(L)} < x < x_p^{(R)} \right), \\
 \varphi \rightarrow 0 & (\text{as } x^2 + y^2 \rightarrow \infty), \\
 \varphi = 0, \quad \varphi_t = 0 & (\text{at } t = 0),
 \end{array} \right. \quad (6.3.2)$$

Set

$$x^{(L)} = a(t), \quad x^{(R)} = b(t) \quad \text{and} \quad x_p^{(L)} = a_p(t), \quad x_p^{(R)} = b_p(t), \quad (6.3.3)$$

where the problem is non-symmetric, due to the presence of floating plate nearby. Therefore, the analytical solution for the velocity potential in the contact region, $a(t) < x < b(t)$ can be approximated by

$$\varphi(x, 0, t) = -h'(t) \sqrt{[a(t) - x][x - b(t)]} \quad (a(t) < x < b(t)). \quad (6.3.4)$$

where the floating plate is far enough from the impact region [17]. We have the numerical solution for the problem (5.2.33) by using our numerical solution of the potential Φ_F in (6.1.52) and Φ_G in (6.1.57) which describes the flow caused by impact on water surface with a floating plate nearby. For comparing the analytical solution in (6.3.4) with numerical solution in (6.1.52) and (6.1.57) we need to return (6.1.52) to the original variables z -plane, where

$$\varphi(x, y, t) = \varphi[x(\rho, \theta, t), y(\rho, \theta, t), t] = \Phi(\rho, \theta, t). \quad (6.3.5)$$

For returning to the original variables z -plane we recall (5.2.39)

$$y = 0, \quad x = \frac{\sin \theta}{1 + \cos \theta}, \quad (6.3.6)$$

and from (5.2.41)

$$x^{(L)} = \tan \left(\frac{\theta^L}{2} \right), \quad (6.3.7)$$

which gives

$$\theta^L = -2 \arctan \left(-x^{(L)} \right), \quad (6.3.8)$$

and

$$\theta^R = -2 \arctan \left(-x^{(R)} \right), \quad (6.3.9)$$

For comparing we assume that $a(t) = -0.5$, $b(t) = 0.5$ and from (6.3.8) we have

$$\theta^L = -2 \arctan (0.5), \quad (6.3.10)$$

$$\theta^R = -2 \arctan (-0.5), \quad (6.3.11)$$

and

$$\theta = -2 \arctan (-x), \quad (6.3.12)$$

letting $\dot{Y}_p(t) = 0$, $\dot{\Omega}_p(t) = 0$ and $\dot{Y}(t) = 1/2$ in (6.1.52), gives

$$\Phi_F(x, 0, t) = \frac{1}{2} \bar{Q}_3, \quad (\theta^L < \theta < \theta^R), \quad (6.3.13)$$

where θ^L , θ^R and θ calculated by (6.3.10), (6.3.11) and (6.3.12).

The numerical solutions (6.3.13) and analytical approximate solution (6.3.4) are compared in figure 6.3.1. We can get a good approximation when we add 40 retained terms in the series (6.3.13). Figure 6.3.2 shows the improvement of the numerical solution when increasing the added retained terms n .

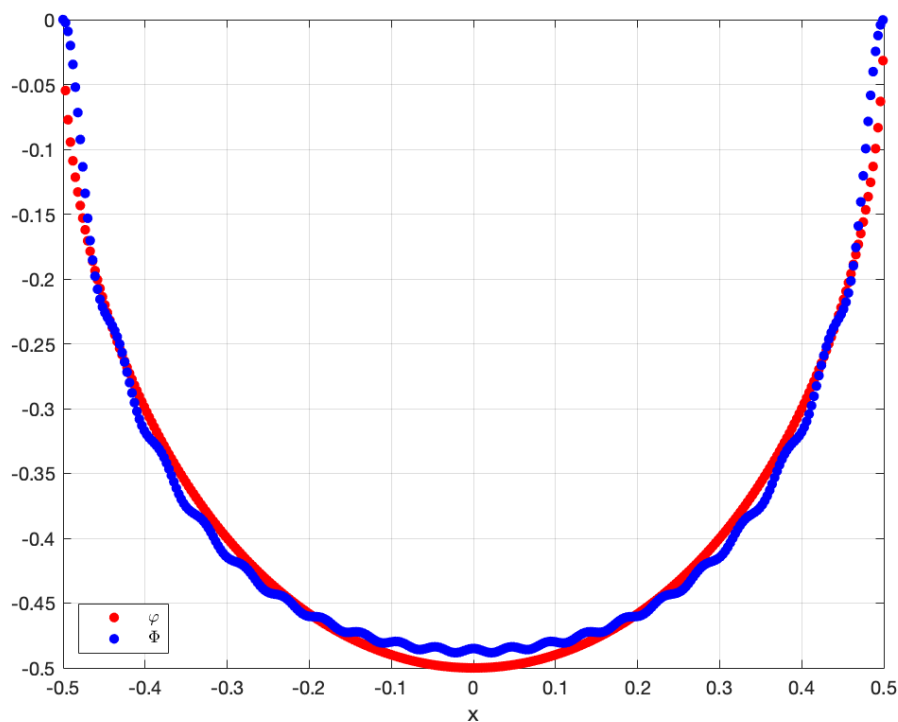


Figure 6.3.1: Plot of φ in (6.3.4) and Φ_F in (6.3.13), were $h' = 1$ and $\dot{Y}(t) = 1$.

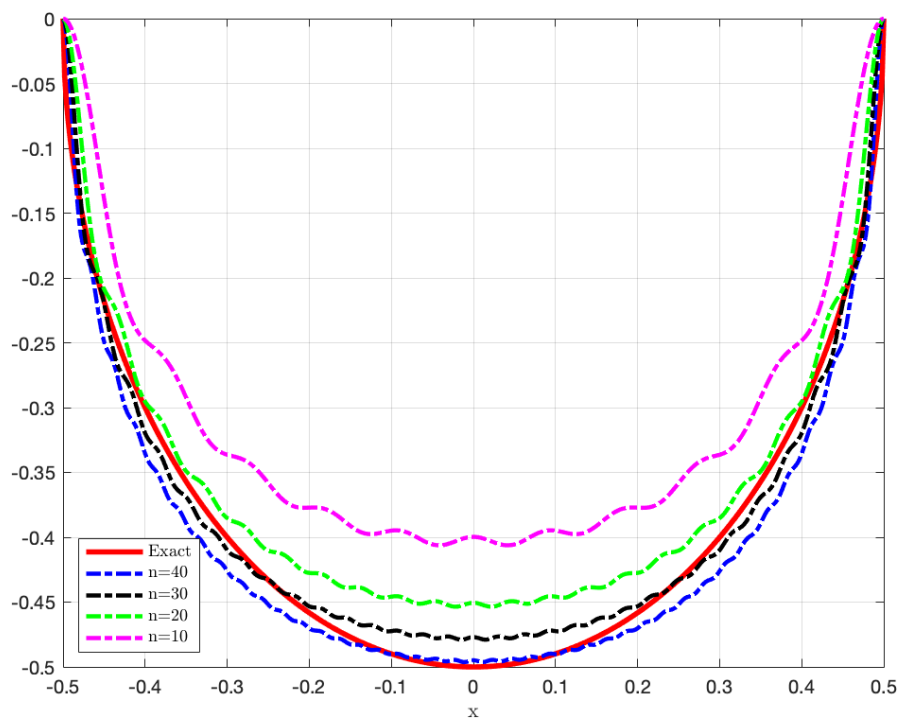


Figure 6.3.2: Plot of φ in (6.3.4) and Φ_F with different numbers of terms in (6.3.13), were $h' = 1$ and $\dot{Y}(t) = 1$.

Conclusion and future work

7.1 Summary and conclusion

When a body starts penetrating into the water's surface, it can be affected by another body inside the water or floating on the water's surface. We expect a change in the water impact process whether in the pressure or motion of these bodies. This thesis investigated such problems for several physical scenarios. There is a various variety of motivations for the work, securing the use of lifeboats, escape crew capsule and aircraft emergency landing, see section 1.2.

By modelling the impact of a rigid body as a blunt body penetrating the free surface, where the free surface is at rest in the initial stage and the body starts to penetrate water surface with time. The fluid is supposed to be in two-dimensional coordinate system. We neglected gravity and surface tension effects, where the entering body is large and the acceleration of the fluid particles are much greater than the gravitational acceleration. In the former case, we studied the formulation of the Wagner problem for a submerged circular cylinder. In the latter case, we studied the water entry problem in the presence of another floating body.

The general problem of water entry problem has been formulated in chapter 2. The fluid is assumed to be in a two-dimensional coordinate system where the effects of gravity and surface tension are neglected and the velocity potential of the flow satisfies the Laplace's equation. There were two main boundary conditions for the problem: the wetted part of the body surface and the elevated free surface. The Wagner model of water impact is presented.

In chapter 3, the formulation of the Wagner problem for a submerged circular cylinder is discussed. We formulated the problem physically and determined the Wagner model of water impact from the physical plane to the Wagner plane. The transformation for the complex flow region φ into a ring in ζ -plane by using the conformal mapping method is provided at

the end of this chapter. The numerical solution of this problem is presented in chapter 4. We found the potential on the cylinder moving under the free surface and the flow caused by impact on the water surface in the presence of a stationary circular cylinder. The pressure acting on the cylinder is calculated for both the fixed cylinder and free to move. The chapter ended with a testing problem to test our work by choosing a parabolic body as a particular case for entering a body without a submerged cylinder.

Chapter 5 covers the water entry problem in the presence of floating body, including the formulation of the problem and the transformation from the physical plane to the Wagner plane. The numerical solution of this problem is presented in chapter 6. The velocity potential is founded, where there is a floating body nearby. The motion of the floating plate is calculated. We ended the chapter with a testing problem to test the work by choosing a parabolic body as a particular case for entering a body without a floating body.

In conclusion, the effects of other floating or submerged bodies on impacts on water were investigated. It was shown that the presence of other bodies can be well neglected if the distances of the bodies from the impact place exceed two diameters of the impacting surface. Motions of other bodies caused by the impact were calculated. It was discovered that floating and/or submerged bodies may move towards the impacting body and come in contact potentially. These results justify that presence of other bodies near impact region may be damaging for the impacting body.

7.2 Future work

There are several cases that can be studied by using the same technique used in the two cases in this thesis. For example, we may investigate a water entry problem in the presence of several submerged bodies. The

submerged bodies can be circular cylinders or other different shapes. Also, these submerged bodies can be a mixture of different shapes, which can be more challenging. Regarding floating bodies on the water's surface, we can investigate a water entry problem in the presence of several floating bodies, where these bodies can be floating plates or other different shapes. For more challenges, we can study a mixture of different shapes as floating objects.

Other cases, investigating a water entry problem in the presence of submerged and floating bodies at the same time. We studied in this thesis, the water entry problem in the presence of a submerged circular cylinder as one case in chapter 3 and a floating flat plate as another case in chapter 5. Now we can combine these two problems and study the solution deeply. For more effortful, we may investigate a water entry problem in the presence of submerged and floating bodies at the same time, where these bodies are a mixture of different shapes

Bibliography

- [1] Abrate, S., 2011. *Hull Slamming*. Applied Mechanics Reviews, 64(6).
- [2] Abramowitz, M. and Stegun, I.A. eds., 1964. *Handbook of mathematical functions with formulas, graphs, and mathematical tables (Vol. 55)*. US Government printing office.
- [3] Aristoff, J.M. and Bush, J.W., 2009. *Water entry of small hydrophobic spheres*. Journal of Fluid Mechanics, 619, pp.45-78.
- [4] Bao, C.M., Wu, G.X. and Xu, G., 2019. *Water entry of a finite width wedge near a floating body*. Applied Ocean Research, 84, pp.12-31.
- [5] Campana, E.F., Carcaterra, A., Ciappi, E. and Iafrati, A., 2000. *Some insights into slamming forces: compressible and incompressible phases*. Proceedings of the Institution of Mechanical Engineers, Part C: Journal of Mechanical Engineering Science, 214(6), pp.881-888.
- [6] Chen, Y, Chen, Y., Khabakhpasheva, T., Maki, K.J. and Korobkin, A., 2019. *Wedge impact with the influence of ice*. Applied Ocean Research, 89, pp.12-22.
- [7] Chang, B., Croson, M., Straker, L., Gart, S., Dove, C., Gerwin, J. and Jung, S., 2016. *How seabirds plunge-dive without injuries*. Proceedings of the National Academy of Sciences, 113(43), pp.12006-12011.
- [8] Duffy, D.G., 2015. *Green's functions with applications*. cRc press.

- [9] Facci, A.L. and Ubertini, S., 2015. *Numerical assessment of similitude parameters and dimensional analysis for water entry problems*. Mathematical Problems in Engineering, 2015.
- [10] Faltinsen, O., 1993. *Sea loads on ships and offshore structures (Vol. 1)*. Cambridge university press.
- [11] Gakhov, F.D., *Boundary Value Problems*. (International Series of Monographs in Pure and Applied Mathematics, Volume 85) Oxford/London/Edinburgh/New York/Paris/Frankfurt 1966.
- [12] Glasheen, J.W. and McMahon, T.A., 1996. *A hydrodynamic model of locomotion in the basilisk lizard*. Nature, 380(6572), pp.340-342.
- [13] Gradshteyn I. S, Ryzhik, I. M. and Jeffrey, A. *Table of integrals, series, and products*. 4th edn. New York: Academic Press, 1965.
- [14] Iafrati, A. and Korobkin, A.A., 2004. *Initial stage of flat plate impact onto liquid free surface*. Physics of fluids, 16(7), pp.2214-2227.
- [15] Jalalisendi, M., Benbelkacem, G. and Porfiri, M., 2018. *Solid obstacles can reduce hydrodynamic loading during water entry*. Physical Review Fluids, 3(7), p.074801.
- [16] Korobkin, A., 2004. *Analytical models of water impact*. European Journal of Applied Mathematics, 15(6), pp.821-838.
- [17] Korobkin, A., 2019. *Water entry problem*. Lecture notes, University of East Anglia.
- [18] Kantorovich, L.V., 1964. *Approximate methods of higher analysis*. Translated by CD Benster, Interscience Publishers Inc., New York, USA, Printed by: P. Noordhoff Ltd., Groningen, The Netherlands.
- [19] Kreyszig, E., Kreyszig, H. and Norminton, E.J., 2011 *Advanced engineering mathematics*. 10th ed., International student version. Wiley.
- [20] Khabakhpasheva, T.I., Chen, Y., Korobkin, A.A. and Maki, K., 2018. *Water impact near the edge of a floating ice sheet*. In Proc. 33rd

International Workshop Water Waves Floating Bodies, Guidel-Plages, France (pp. 4-7).

- [21] Khabakhpasheva, T., Chen, Y., Korobkin, A. and Maki, K., 2018. *Impact onto an ice floe*. Journal of Advanced Research in Ocean Engineering, 4(4), pp.146-162.
- [22] Lubbad, R. and Løset, S., 2011. *A numerical model for real-time simulation of ship-ice interaction*. Cold Regions Science and Technology, 65(2), pp.111-127.
- [23] Maki, K.J., Ye, H., Khabakhpasheva, T.I. and Korobkin, A.A., 2017. *Impact of a wedge-shaped body with influence of broken ice*. In Proceedings of 32nd International Workshop on Water Waves and Floating Bodies.
- [24] Monaghan, R.J., 1947. *A review of the essentials of impact force theories for seaplanes and suggestions for approximate design formulae*.
- [25] Monaghan, R.J., 1952. *A theoretical examination of the effect of deadrise on wetted area and associated mass in seaplane impacts..*
- [26] Oliver, J.M., 2007 *Second-order Wagner theory for two-dimensional water-entry problems at small deadrise angles*. Journal of fluid mechanics, 572, pp.59-85.
- [27] Prudnikov, A.P., Brychkov, I.A., Bryčkov, J.A. and Marichev, O.I., 1986. *Integrals and Series*. Gordan and Breach, New York, vols. I (1986), II (1986), III (1990).
- [28] Russo, S., Jalalisendi, M., Falcucci, G. and Porfiri, M., 2018. *Experimental characterization of oblique and asymmetric water entry*. Experimental Thermal and Fluid Science, 92, pp.141-161.
- [29] Seddon, C.M. and Moatamedi, M., 2006. *Review of water entry with applications to aerospace structures*. International Journal of Impact Engineering, 32(7), pp.1045-1067.

-
- [30] Strang, G. and Herman, E., 2016. *Calculus - Volume 1*. Houston, Texas: OpenStax.
- [31] Vincent, L., Xiao, T., Yohann, D., Jung, S. and Kanso, E., 2018. *Dynamics of water entry*. Journal of Fluid Mechanics, 846, pp.508-535.
- [32] Von Karman, T., 1929. *The impact on seaplane floats during landing*.
- [33] Wagner, H., 1932. *Über stoß-und gleitvorgänge an der oberfläche von flüssigkeiten*. ZAMM-Journal of Applied Mathematics and Mechanics/Zeitschrift für Angewandte Mathematik und Mechanik, 12(4), pp.193-215.
- [34] Zhao, R. and Faltinsen, O., 1996. *Water entry of two-dimensional bodies*. Journal of fluid mechanics, 246, pp.593-612.

A

Appendix

A.1

To derive another formulae for $A_{nm}^{(cc)}$ and $A_{nm}^{(ss)}$ which are suitable for calculations when $A \rightarrow 0$ or $A \rightarrow 1$. By using (4.3.61), (4.3.63) and (4.3.67), we got

$$A_{nm}^{(ss)} = \frac{4nm}{\pi A^4} \frac{(-1)^{n+m}}{m^2 - n^2} \left\{ S\left(x, \frac{m}{A}\right) - S\left(x, \frac{n}{A}\right) \right\}. \quad (\text{A.1.1})$$

and

$$A_{nn}^{(ss)} = \frac{4n^2}{\pi A^2} \left\{ S_2\left(x, \frac{n}{A}\right) \right\}. \quad (\text{A.1.2})$$

To find $S(x, a)$ and $S_2(x, a)$ defined by (4.3.61) and (4.3.67), where $x = \pi A$ and $a = m/A$, for small value of A , we will present these functions in another form.

Asymptotic behavior of $S(x, a)$ as $A \rightarrow 0$ and $A \rightarrow 1$.

In (4.3.61), where the function $S(x, a)$ is defined, we use the series

$$W_k = \frac{1 - R_1^{2k}}{1 + R_1^{2k}} = \sum_{n=0}^{\infty} \varepsilon_n R_1^{2kn}. \quad (\text{A.1.3})$$

where $\varepsilon_0 = 1$ and $\varepsilon_n = 2(-1)^n$ for $n \geq 1$. Then

$$S(x, a) = \sum_{n=0}^{\infty} \varepsilon_n \sum_{k=1}^{\infty} \frac{\sin^2(kx)}{k(k^2 - a^2)} R_1^{2kn}. \quad (\text{A.1.4})$$

By using

$$\begin{aligned} \left[\frac{d^2}{dx^2} + 4a^2 \right] \sin^2(kx) &= 2k^2 \cos(2kx) + 4a^2 \sin^2(kx) \\ &= 2k^2 \cos(2kx) + 4a^2 \frac{(1 - \cos(2kx))}{2} = 2(k^2 - a^2) \cos(2kx) + 2a^2, \end{aligned} \quad (\text{A.1.5})$$

and (A.1.4), we find

$$\begin{aligned} \left[\frac{d^2}{dx^2} + 4a^2 \right] S(x, a) &= 2 \sum_{n=0}^{\infty} \varepsilon_n \sum_{k=1}^{\infty} \frac{\cos(2kx)}{k} (R_1^{2n})^k \\ &\quad + 2a^2 \sum_{n=0}^{\infty} \varepsilon_n \sum_{k=1}^{\infty} \frac{(R_1^{2n})^k}{k(k^2 - a^2)}. \end{aligned} \quad (\text{A.1.6})$$

Let present the right hand side of (A.1.6) as

$$2 \sum_{n=0}^{\infty} \varepsilon_n F(2x, p) + C, \quad (\text{A.1.7})$$

where C is the constant term in (A.1.6) and $F(2x, p)$ is obtained by using table of integrals [13],

$$F(z, p) = \sum_{k=1}^{\infty} \frac{\cos(kz)p^k}{k} = -\frac{1}{2} \log[1 - 2p \cos(z) + p^2], \quad (\text{A.1.8})$$

where $0 < z < 2\pi$ and $p^2 \leq 1$.

Thus the function $S(x, a)$ satisfies the equation,

$$\frac{d^2 S}{dx^2} + 4a^2 S = - \sum_{n=0}^{\infty} \varepsilon_n \log[1 + R_1^{4n} - 2R_1^{2n} \cos(2x)] + C, \quad (\text{A.1.9})$$

where (A.1.4) at $x = 0$ gives

$$S(0, a) = S_x(0, a) = 0. \quad (\text{A.1.10})$$

The solution of differential equation (A.1.9) which satisfies the initial

conditions (A.1.10) reads

$$S(x, a) = \frac{1}{2a} \int_0^x \left(- \sum_{n=0}^{\infty} \varepsilon_n \log[1 + R_1^{4n} - 2R_1^{2n} \cos(2\tau)] + C \right) \cdot \sin[2a(x - \tau)] d\tau, \quad (\text{A.1.11})$$

which can be confirmed by direct substitution of (A.1.11) into (A.1.9). The formulae (A.1.11) provides

$$S\left(\pi A, \frac{m}{A}\right) = \frac{A}{2m} \int_0^{\pi A} \left(- \sum_{n=0}^{\infty} \varepsilon_n \log[1 + R_1^{4n} - 2R_1^{2n} \cos(2\tau)] + C \right) \cdot \sin\left[2\frac{m}{A}\pi A - 2\frac{m}{A}\tau\right] d\tau, \quad (\text{A.1.12})$$

where

$$\sin\left[2\frac{m}{A}\pi A - 2\frac{m}{A}\tau\right] = -\sin\left(2m\frac{\tau}{A}\right), \quad (\text{A.1.13})$$

Introducing new variable of integration $\tau = A\xi$, we find

$$S\left(\pi A, \frac{m}{A}\right) = \frac{A^2}{2m} \sum_{n=0}^{\infty} \varepsilon_n \cdot \int_0^{\pi} (\log[1 + R_1^{4n} - 2R_1^{2n} \cos(2A\xi)]) \sin(2m\xi) d\xi, \quad (\text{A.1.14})$$

where we used that

$$\int_0^{\pi} C \sin(2m\xi) d\xi = 0, \quad (\text{A.1.15})$$

for any integer m .

By using the formula

$$\begin{aligned} 1 + R_1^{4n} - 2R_1^{2n} \cos(2A\xi) &= 1 - 2R_1^{2n} + R_1^{4n} + 2R_1^{2n}(1 - \cos(2A\xi)) \\ &= (1 - R_1^{2n})^2 + 4R_1^{2n} \sin^2(A\xi) = (1 - R_1^{2n})^2 \left[1 + \left(\frac{2R_1^{2n} \sin(A\xi)}{1 - R_1^{2n}} \right)^2 \right], \end{aligned} \quad (\text{A.1.16})$$

and (A.1.15), we find

$$\begin{aligned}
S\left(\pi A, \frac{m}{A}\right) &= \frac{A^2}{2m} \int_0^\pi \sum_{n=0}^{\infty} \varepsilon_n \log[1 + R_1^{4n} - 2R_1^{2n} \cos(2A\xi)] \sin(2m\xi) d\xi, \\
&= \frac{A^2}{2m} \left\{ \int_0^\pi \log[2 - 2\cos(2A\xi)] \sin(2m\xi) d\xi \right. \\
&\quad \left. + 2 \int_0^\pi \sum_{n=1}^{\infty} (-1)^n \log \left[1 + \frac{4R_1^{2n} \sin^2(A\xi)}{(1 - R_1^{2n})^2} \right] \sin(2m\xi) d\xi \right\}. \quad (\text{A.1.17})
\end{aligned}$$

For small A , we have $(4R_1^{2n} \sin^2(A\xi))/(1 - R_1^{2n})^2$ is small for any n and $0 < \xi < \pi$. The expansion of log-function gives

$$\begin{aligned}
\log \left[1 + \left(\frac{2R_1^n \sin(A\xi)}{1 - R_1^{2n}} \right)^2 \right] &= \left(\frac{2R_1^n}{1 - R_1^{2n}} \right)^2 \sin^2(A\xi) \\
&\quad - \frac{1}{2} \left(\frac{2R_1^n}{1 - R_1^{2n}} \right)^4 \sin^4(A\xi) + O(A^6), \quad (\text{A.1.18})
\end{aligned}$$

and then

$$\begin{aligned}
S\left(\pi A, \frac{m}{A}\right) &= \frac{A^2}{2m} \int_0^\pi \log [4 \sin^2(A\xi)] \sin(2m\xi) d\xi \\
&\quad + \frac{A^2}{m} \int_0^\pi \sum_{n=1}^{\infty} (-1)^n \left\{ \left[\frac{2R_1^n}{1 - R_1^{2n}} \right]^2 \sin^2(A\xi) \right. \\
&\quad \left. - \frac{1}{2} \left[\frac{2R_1^n}{1 - R_1^{2n}} \right]^4 \sin^4(A\xi) + O(A^6) \right\} \sin(2m\xi) d\xi \\
&= \frac{A^2}{m} \int_0^\pi \log |\sin(A\xi)| \sin(2m\xi) d\xi \\
&\quad + \frac{A^2}{m} \left\{ 4 \sum_{n=1}^{\infty} \frac{(-1)^n R_1^{2n}}{(1 - R_1^{2n})^2} \int_0^\pi \sin^2(A\xi) \sin(2m\xi) d\xi \right. \\
&\quad \left. - \frac{16}{2} \sum_{n=1}^{\infty} \frac{(-1)^n R_1^{4n}}{(1 - R_1^{2n})^4} \int_0^\pi \sin^4(A\xi) \sin(2m\xi) d\xi + O(A^6) \right\}. \quad (\text{A.1.19})
\end{aligned}$$

Using the asymptotic formulae,

$$\sin(A\xi) = A\xi - A^3 \frac{\xi^3}{3!} + A^5 \frac{\xi^5}{5!} + O(A^7), \quad (\text{A.1.20})$$

and

$$\begin{aligned}
\log[\sin(A\xi)] &= \log[A] + \log[\xi] + \log\left[1 - A^2\frac{\xi^2}{3!} + A^4\frac{\xi^4}{5!} + O(A^6)\right] \\
&= \log[A] + \log[\xi] - A^2\frac{\xi^2}{3!} + A^4\frac{\xi^4}{5!} - \frac{1}{2}\left(-A^2\frac{\xi^2}{3!} + A^4\frac{\xi^4}{5!}\right)^2 + O(A^6) \\
&= \log[A] + \log[\xi] - A^2\frac{\xi^2}{3!} + A^4\frac{\xi^4}{5!} - \frac{1}{2}\left(A^4\frac{\xi^4}{(3!)^2}\right) + O(A^6), \quad (\text{A.1.21})
\end{aligned}$$

where $A \rightarrow 0$, and introducing the constants

$$\int_0^\pi \log[\xi] \sin(2m\xi) d\xi = Q_m, \quad (\text{A.1.22})$$

$$\int_0^\pi \xi^{2k} \sin(2m\xi) d\xi = q_m^k, \quad (\text{A.1.23})$$

$$4 \sum_{n=1}^{\infty} \frac{(-1)^n R_1^{2n}}{(1 - R_1^{2n})^2} = \tilde{R}_1, \quad (\text{A.1.24})$$

$$8 \sum_{n=1}^{\infty} \frac{(-1)^n R_1^{4n}}{(1 - R_1^{2n})^4} = \tilde{R}_2, \quad (\text{A.1.25})$$

we obtain

$$\begin{aligned}
S\left(\pi A, \frac{m}{A}\right) &= \frac{A^2}{m} \left\{ Q_m - \frac{1}{3!} A^2 q_m^1 + A^4 \left[\frac{1}{5!} - \frac{1}{2(3!)^2} \right] q_m^2 + O(A^6) \right. \\
&\quad \left. + \tilde{R}_1 \int_0^\pi \sin^2(A\xi) \sin(2m\xi) d\xi - \tilde{R}_2 \int_0^\pi \sin^4(A\xi) \sin(2m\xi) d\xi \right\}. \quad (\text{A.1.26})
\end{aligned}$$

Here

$$[\sin(A\xi)]^2 = (A\xi)^2 - \frac{2}{3!} A^4 \xi^4 + O(A^6), \quad (\text{A.1.27})$$

$$[\sin(A\xi)]^4 = (A\xi)^4 - \frac{4}{3!} A^6 \xi^6 + \dots = (A\xi)^4 + O(A^6), \quad (\text{A.1.28})$$

which provide the following asymptotic expansion as $A \rightarrow 0$,

$$\begin{aligned}
S\left(\pi A, \frac{m}{A}\right) &= \frac{A^2}{m} \left\{ Q_m + A^2 \left[\tilde{R}_1 q_m^1 - \frac{1}{3!} q_m^1 \right] \right. \\
&\quad \left. + A^4 \left[\left(\frac{1}{5!} - \frac{1}{2(3!)^2} \right) q_m^2 - \frac{2}{3!} \tilde{R}_1 q_m^2 - \tilde{R}_2 q_m^2 \right] + O(A^6) \right\} \\
&= A^2 \frac{Q_m}{m} + A^4 \left(\tilde{R}_1 - \frac{1}{6} \right) \frac{q_m^1}{m} + A^6 \left(\frac{1}{120} - \frac{1}{64} - \frac{1}{3} \tilde{R}_1 - \tilde{R}_2 \right) \frac{q_m^2}{m} + \dots
\end{aligned} \tag{A.1.29}$$

The coefficients in (A.1.29) are evaluated as it is shown below. The coefficients Q_m gives by (A.1.22) are calculated by

$$\begin{aligned}
Q_m &= \int_0^\pi \log[\xi] d\left(\frac{1 - \cos(2m\xi)}{2m}\right) = - \int_0^\pi \frac{1 - \cos(2m\xi)}{2m} \frac{d\xi}{\xi} \\
&= - \frac{1}{2m} \int_0^\pi \frac{1 - \cos(2m\xi)}{\xi} d\xi = - \frac{1}{2m} \int_0^{2m\pi} \frac{1 - \cos(v)}{v} dv. \tag{A.1.30}
\end{aligned}$$

For small m we integrate (A.1.30) numerically. For large m we have, see [2],

$$Q_m = - \frac{1}{2m} \{ C_i(2m\pi) - \gamma - \log(2m\pi) \}, \tag{A.1.31}$$

where $C_i(2m\pi)$ is given in [2] as

$$C_i(b) = - \int_b^\infty \frac{\cos(t)}{t} dt. \tag{A.1.32}$$

Integrating (A.1.32) by parts for large b gives

$$\begin{aligned}
\int_b^\infty \frac{\cos(t)}{t} dt &= \int_b^\infty t^{-1} d[\sin(t)] = - \frac{\sin(b)}{b} + \int_b^\infty \sin(t) t^{-2} dt \\
&= - \frac{\sin(b)}{b} + \int_b^\infty t^{-2} d[-\cos(t)] = - \frac{\sin(b)}{b} + \frac{\cos(b)}{b^2} - 2 \int_b^\infty \cos(t) t^{-3} dt \\
&= - \frac{\sin(b)}{b} + \frac{\cos(b)}{b^2} - 2 \int_b^\infty t^{-3} d[-\sin(t)] = \dots \tag{A.1.33}
\end{aligned}$$

we obtain

$$Q_m = \frac{1}{2m} (\gamma + \log[2\pi m]) - \frac{1}{2m} C_i(2\pi m), \tag{A.1.34}$$

where $\gamma = 0.5772156649$ is Euler's constant and from [2] we have

$$\begin{aligned} C_i(2\pi m) &= f(2\pi m) \sin(2\pi m) - g(2\pi m) \cos(2\pi m) = -g(2\pi m) \\ &= \frac{-1}{(2\pi m)^2} \left(1 - \frac{3!}{(2\pi m)^2} + \frac{5!}{(2\pi m)^4} - \frac{7!}{(2\pi m)^6} + \dots \right), \quad 2\pi m \geq 1, \end{aligned} \quad (\text{A.1.35})$$

where $f(2\pi m)$ and $g(2\pi m)$ are auxiliary functions.

$$Q_m = \frac{1}{2m} (\gamma + \log[2\pi m]) + \frac{1}{(2m)^3 \pi^2} \left(\sum_{k=1}^N (-1)^{k-1} \frac{(2k-1)!}{(2\pi m)^{2k-2}} + \varepsilon_N \right), \quad (\text{A.1.36})$$

where (A.1.36) can be used for large m only. The coefficients q_m^k are calculated by (A.1.23) for $k = 1, 2$ and $m \geq 1$ by introducing new variable integration $2m\xi = \lambda$. Then

$$q_m^k = \int_0^{2m\pi} \left(\frac{\lambda}{2m} \right)^{2k} \sin(\lambda) \frac{d\lambda}{2m} = \frac{1}{(2m)^{2k+1}} \int_0^{2m\pi} \lambda^{2k} \sin(\lambda) d\lambda. \quad (\text{A.1.37})$$

$$\begin{aligned} q_m^1 &= \frac{1}{(2m)^3} \int_0^{2\pi m} \lambda^2 \sin(\lambda) d\lambda = (2m)^{-3} [2\lambda \sin(\lambda) - (\lambda^2 - 2) \cos]_0^{2m\pi} \\ &= \frac{1}{(2m)^3} (2 - (2m\pi)^2 - 2) = -\frac{\pi^2}{2m}. \end{aligned} \quad (\text{A.1.38})$$

$$\begin{aligned} q_m^2 &= \frac{1}{(2m)^5} \int_0^{2\pi m} \lambda^4 \sin(\lambda) d\lambda \\ &= \frac{1}{(2m)^5} (-24 + 12(2m\pi)^2 - (2m\pi)^4 + 24) = \frac{(2m\pi)^2 [12 - (2m\pi)^2]}{(2m)^5} \\ &= -\frac{\pi^4}{2m} + \frac{12\pi^2}{(2m)^3} = -\frac{\pi^4}{2m} + \frac{3\pi^2}{2m^3}. \end{aligned} \quad (\text{A.1.39})$$

Substitution (A.1.29) into (4.3.63) gives for $n \neq m$

$$\begin{aligned}
A_{nm}^{(cc)} = & \frac{4(-1)^{n+m}}{\pi m^2 - n^2} \left\{ mQ_m + A^2 \left(\tilde{R}_1 - \frac{1}{6} \right) \left(-\frac{\pi^2}{2} \right) \right. \\
& + A^4 \left(\frac{1}{120} - \frac{1}{64} - \frac{1}{3}\tilde{R}_1 - \tilde{R}_2 \right) \left(-\frac{\pi^4}{2} + \frac{3\pi^2}{2m^2} \right) + \dots \\
& \quad \left. - nQ_n - A^2 \left(\tilde{R}_1 - \frac{1}{6} \right) \left(-\frac{\pi^2}{2} \right) \right. \\
& \left. - A^4 \left(\frac{1}{120} - \frac{1}{64} - \frac{1}{3}\tilde{R}_1 - \tilde{R}_2 \right) \left(-\frac{\pi^4}{2} + \frac{3\pi^2}{2n^2} \right) + \dots \right\}, \quad (\text{A.1.40})
\end{aligned}$$

and similarly for $A_{nm}^{(ss)}$ we have

$$\begin{aligned}
A_{nm}^{(ss)} = & \frac{4nm(-1)^{n+m}}{\pi m^2 - n^2} \left\{ \frac{Q_m}{m} + A^2 \left(\tilde{R}_1 - \frac{1}{6} \right) \left(-\frac{\pi^2}{2m^2} \right) \right. \\
& + A^4 \left(\frac{1}{120} - \frac{1}{64} - \frac{1}{3}\tilde{R}_1 - \tilde{R}_2 \right) \left(-\frac{\pi^4}{2m^2} + \frac{3\pi^2}{2m^4} \right) + \dots \\
& \quad \left. - \frac{Q_n}{n} - A^2 \left(\tilde{R}_1 - \frac{1}{6} \right) \left(-\frac{\pi^2}{2n^2} \right) \right. \\
& \left. - A^4 \left(\frac{1}{120} - \frac{1}{64} - \frac{1}{3}\tilde{R}_1 - \tilde{R}_2 \right) \left(-\frac{\pi^4}{2n^2} + \frac{3\pi^2}{2n^4} \right) + \dots \right\}. \quad (\text{A.1.41})
\end{aligned}$$

To determine the asymptotic behavior of $S(\pi A, m/A)$ as $A \rightarrow 1$, we notice that at $A = 1$

$$\lim_{A \rightarrow 1} S \left(\pi A, \frac{m}{A} \right) = \sum_{k=1}^{\infty} \frac{1}{k} \frac{\sin^2(k\pi)}{k^2 - m^2} W_k = 0. \quad (\text{A.1.42})$$

Calculating the derivative dS/dA and taking the limit as $A \rightarrow 1$, we find

$$\begin{aligned}
\lim_{A \rightarrow 1} \frac{d}{dA} S \left(\pi A, \frac{m}{A} \right) &= \lim_{A \rightarrow 1} \sum_{k=1}^{\infty} \frac{W_k}{k} \left\{ \frac{2 \sin(\pi Ak) \cos(\pi Ak) \pi k}{(Ak)^2 - m^2} A^2 \right. \\
& \quad \left. + \frac{\sin^2(\pi Ak)}{(k^2 - (m^2/A^2))^2} (-1)(-m^2)(-2)A^{-3} \right\} \\
&= \sum_{k=1}^{\infty} \frac{W_k}{k} \left(\frac{2\pi k \cos(\pi k)}{k+m} \lim_{A \rightarrow 1} \left\{ \frac{\sin(\pi k A)}{Ak - m} \right\} \right. \\
& \quad \left. - \frac{2m^2}{(k+m)^2} \lim_{A \rightarrow 1} \left\{ \frac{\sin(\pi k A)}{Ak - m} \right\}^2 \right), \quad (\text{A.1.43})
\end{aligned}$$

where

$$\lim_{A \rightarrow 1} \frac{\sin(\pi k A)}{A k - m} = \begin{cases} 0 & k \neq m, \\ \lim_{A \rightarrow 1} \frac{\cos(\pi k A) \pi k}{k} = \pi \cos(\pi k) & k = m, \end{cases} \quad (\text{A.1.44})$$

then

$$\begin{aligned} \frac{dS}{dA}(\pi, m) &= \frac{W_m}{m} \left(\frac{2\pi m \cos(\pi m)}{2m} \pi \cos(\pi k m) - \frac{2m^2}{(2m)^2} \pi^2 \cos^2(\pi k) \right) \\ &= \frac{W_m}{m} \left(\pi^2 - \frac{\pi^2}{2} \right) = \frac{\pi^2 W_m}{2m}. \end{aligned} \quad (\text{A.1.45})$$

Therefore, we have asymptotic behavior for S when $A \rightarrow 1$ as Taylor series given by

$$S\left(\pi A, \frac{m}{A}\right) \approx S(\pi, m) + \frac{d}{dA} S(\pi, m) (A - 1). \quad (\text{A.1.46})$$

Substitution (A.1.46) into (4.3.63) gives

$$A_{nm}^{(cc)} \approx \frac{4}{\pi} A^{-2} \frac{\cos(m\pi) \cos(n\pi)}{m^2 - n^2} \left\{ \frac{m\pi W_m}{2} (A - 1) - \frac{n\pi W_n}{2} (A - 1) \right\}, \quad (\text{A.1.47})$$

and similarly for A_{nm}^{ss} we have

$$A_{nm}^{(ss)} \approx \frac{4nm \cos(m\pi) \cos(n\pi)}{\pi A^2 (m^2 - n^2)} \left\{ \frac{\pi^2 W_m}{2m} (A - 1) - \frac{\pi^2 W_n}{2n} (A - 1) \right\}, \quad (\text{A.1.48})$$

as $A \rightarrow 1$.

A.2

$$B_{nm}^{(cs)} = \frac{4m}{\pi A_p A} \cos(m\pi) \cos(n\pi) \sum_{k=1}^{\infty} \left\{ \frac{\sin(kx_p) \sin(kx)}{k^2 - d^2} \frac{\sin(kx)}{k^2 - a^2} \sin[k(B_p - B)] \right\}, \quad (\text{A.2.1})$$

$$B_{nm}^{(cs)} = \frac{4m}{\pi A_p A} \cos(m\pi) \cos(n\pi) \left[\sum_{k=1, k \neq N}^{\infty} \left\{ \frac{\sin(kx_p)}{k^2 - d^2} \frac{\sin(kx)}{k^2 - a^2} \sin[k(B_p - B)] \right\} + \frac{\pi}{2} \cos(\pi n) \frac{n}{N^2} \frac{\sin(Nx)}{N^2 - a^2} \sin[N(B_p - B)] \right], \quad (\text{A.2.2})$$

$$B_{nm}^{(cs)} = \frac{4m}{\pi A_p A} \cos(m\pi) \cos(n\pi) \left[\sum_{k=1, k \neq M}^{\infty} \left\{ \frac{\sin(kx_p)}{k^2 - d^2} \frac{\sin(kx)}{k^2 - a^2} \sin[k(B_p - B)] \right\} + \frac{\sin(Mx_p)}{M^2 - d^2} \frac{\pi}{2} \cos(\pi n) \frac{n}{M^2} \sin[M(B_p - B)] \right], \quad (\text{A.2.3})$$

$$B_{nm}^{(cs)} = \frac{4m}{\pi A_p A} \cos(m\pi) \cos(n\pi) \left[\sum_{k=1, k \neq M, N}^{\infty} \left\{ \frac{\sin(kx_p)}{k^2 - d^2} \frac{\sin(kx)}{k^2 - a^2} \sin[k(B_p - B)] \right\} + \frac{\sin(Mx_p)}{M^2 - N^2} \frac{\pi}{2} \cos(\pi n) \frac{n}{M^2} \sin[M(B_p - B)] + \frac{\pi}{2} \cos(\pi n) \frac{n}{N^2} \frac{\sin(Nx)}{N^2 - M^2} \sin[N(B_p - B)] \right], \quad (\text{A.2.4})$$

$$B_{nm}^{(cs)} = \frac{4m}{\pi A_p A} \cos(m\pi) \cos(n\pi) \left[\sum_{k=1, k \neq N}^{\infty} \left\{ \frac{\sin(kx_p)}{k^2 - d^2} \frac{\sin(kx)}{k^2 - a^2} \sin[k(B_p - B)] \right\} + \frac{\pi^2}{4} \frac{n^2}{N^4} \sin[N(B_p - B)] \right]. \quad (\text{A.2.5})$$

From (6.0.67) we have

$$A_{p, nm}^{(cc)} = \frac{4A}{\pi A_p} \cos(\pi n) \cos(\pi m) \sum_{k=1}^{\infty} \left\{ k \frac{\sin(kx_p)}{k^2 - d^2} \frac{\sin(kx)}{k^2 - a^2} \cos[k(B - B_p)] \right\}, \quad (\text{A.2.6})$$

using the similar calculations for $A_{p, nm}^{(cs)}$ (6.0.78- 6.0.84) gives

$$A_{p, nm}^{(cc)} = \frac{4A}{\pi A_p} \cos(\pi n) \cos(\pi m) \left[\sum_{k=1, k \neq N}^{\infty} \left\{ k \frac{\sin(kx_p)}{k^2 - d^2} \frac{\sin(kx)}{k^2 - a^2} \cos[k(B - B_p)] \right\} + \frac{\pi}{2} \cos(\pi n) \frac{n}{N^2} N \frac{\cos(Nx)}{N^2 - a^2} \cos[N(B - B_p)] \right], \quad (\text{A.2.7})$$

$$A_{p,nm}^{(cc)} = \frac{4A}{\pi A_p} \cos(\pi n) \cos(\pi m) \left[\sum_{k=1, k \neq M}^{\infty} \left\{ k \frac{\sin(kx_p)}{k^2 - d^2} \frac{\sin(kx)}{k^2 - a^2} \cos[k(B - B_p)] \right\} \right. \\ \left. + M \frac{\sin(Mx_p)}{M^2 - d^2} \frac{\pi}{2} \cos(\pi n) \frac{n}{M^2} \cos[M(B - B_p)] \right], \quad (\text{A.2.8})$$

$$A_{p,nm}^{(cc)} = \frac{4A}{\pi A_p} \cos(\pi n) \cos(\pi m) \left[\sum_{k=1, k \neq M, N}^{\infty} \left\{ k \frac{\sin(kx_p)}{k^2 - d^2} \frac{\sin(kx)}{k^2 - a^2} \cos[k(B - B_p)] \right\} \right. \\ \left. + M \frac{\sin(Mx_p)}{M^2 - N^2} \frac{\pi}{2} \cos(\pi n) \frac{n}{M^2} \cos[M(B - B_p)] \right. \\ \left. + N \frac{\pi}{2} \cos(\pi n) \frac{n}{N^2} \frac{\sin(Nx)}{N^2 - M^2} \cos[N(B - B_p)] \right], \quad (\text{A.2.9})$$

$$A_{p,nm}^{(cc)} = \frac{4A}{\pi A_p} \cos(\pi n) \cos(\pi m) \left[\sum_{k=1, k \neq N}^{\infty} \left\{ k \frac{\sin(kx_p)}{k^2 - d^2} \frac{\sin(kx)}{k^2 - a^2} \cos[k(B - B_p)] \right\} \right. \\ \left. + \frac{\pi^2}{4} \frac{n^2}{N^4} N^2 \cos[N(B - B_p)] \right]. \quad (\text{A.2.10})$$

As to $B_{nm}^{(cc)}$ we have

$$B_{nm}^{(cc)} = \left(\frac{A_p}{A} \right)^2 A_{p,nm}^{(cc)}. \quad (\text{A.2.11})$$

From (6.0.70) we have

$$A_{p,nm}^{(sc)} = \frac{4nA}{\pi A_p} \cos(\pi n) \cos(\pi m) \sum_{k=1}^{\infty} \left\{ \frac{\sin(kx_p)}{k^2 - d^2} \frac{\sin(kx)}{k^2 - a^2} \cos[k(B - B_p)] \right\}, \quad (\text{A.2.12})$$

using the similar calculations for $A_{p,nm}^{(cs)}$ (6.0.78- 6.0.84) gives

$$A_{p,nm}^{(sc)} = \frac{4nA}{\pi A_p} \cos(\pi n) \cos(\pi m) \left[\sum_{k=1, k \neq N}^{\infty} \left\{ \frac{\sin(kx_p)}{k^2 - d^2} \frac{\sin(kx)}{k^2 - a^2} \cos[k(B - B_p)] \right\} \right. \\ \left. + \frac{\pi}{2} \cos(\pi n) \frac{n}{N^2} \frac{\cos(Nx)}{N^2 - a^2} \cos[N(B - B_p)] \right], \quad (\text{A.2.13})$$

$$A_{p,nm}^{(sc)} = \frac{4nA}{\pi A_p} \cos(\pi n) \cos(\pi m) \left[\sum_{k=1, k \neq M}^{\infty} \left\{ \frac{\sin(kx_p)}{k^2 - d^2} \frac{\sin(kx)}{k^2 - a^2} \cos[k(B - B_p)] \right\} + \frac{\sin(Mx_p)}{M^2 - d^2} \frac{\pi}{2} \cos(\pi n) \frac{n}{M^2} \cos[M(B - B_p)] \right], \quad (\text{A.2.14})$$

$$A_{p,nm}^{(sc)} = \frac{4nA}{\pi A_p} \cos(\pi n) \cos(\pi m) \left[\sum_{k=1, k \neq M, N}^{\infty} \left\{ \frac{\sin(kx_p)}{k^2 - d^2} \frac{\sin(kx)}{k^2 - a^2} \cos[k(B - B_p)] \right\} + \frac{\sin(Mx_p)}{M^2 - N^2} \frac{\pi}{2} \cos(\pi n) \frac{n}{M^2} \cos[M(B - B_p)] + \frac{\pi}{2} \cos(\pi n) \frac{n}{N^2} \frac{\sin(Nx)}{N^2 - M^2} \cos[N(B - B_p)] \right], \quad (\text{A.2.15})$$

$$A_{p,nm}^{(sc)} = \frac{4nA}{\pi A_p} \cos(\pi n) \cos(\pi m) \left[\sum_{k=1, k \neq N}^{\infty} \left\{ \frac{\sin(kx_p)}{k^2 - d^2} \frac{\sin(kx)}{k^2 - a^2} \cos[k(B - B_p)] \right\} + \frac{\pi^2}{4} \frac{n^2}{N^4} \cos[N(B - B_p)] \right], \quad (\text{A.2.16})$$

and for $B_{nm}^{(sc)}$ we have

$$B_{nm}^{(sc)} = \left(\frac{A_p}{A} \right)^2 A_{p,nm}^{(sc)}. \quad (\text{A.2.17})$$

From (6.0.75) we have

$$A_{p,nm}^{(ss)} = \frac{4nm}{\pi A_p A} \cos(n\pi) \cos(m\pi) \sum_{k=1}^{\infty} \frac{1}{k} \left\{ \frac{\sin(kx_p)}{k^2 - d^2} \frac{\sin(kx)}{k^2 - a^2} \cos(kB - kB_p) \right\}, \quad (\text{A.2.18})$$

using the similar calculations for $A_{p,nm}^{(cs)}$ (6.0.78 - 6.0.84) gives

$$A_{p,nm}^{(ss)} = \frac{4nm}{\pi A_p A} \cos(n\pi) \cos(m\pi) \left[\sum_{k=1, k \neq N}^{\infty} \left\{ \frac{1}{k} \frac{\sin(kx_p)}{k^2 - d^2} \frac{\sin(kx)}{k^2 - a^2} \cos[k(B - B_p)] \right\} + \frac{\pi}{2} \cos(\pi n) \frac{n}{N^2} \frac{1}{N} \frac{\cos(Nx)}{N^2 - a^2} \cos[N(B - B_p)] \right], \quad (\text{A.2.19})$$

$$A_{p,nm}^{(ss)} = \frac{4nm}{\pi A_p A} \cos(n\pi) \cos(m\pi) \left[\sum_{k=1, k \neq M}^{\infty} \left\{ \frac{1}{k} \frac{\sin(kx_p)}{k^2 - d^2} \frac{\sin(kx)}{k^2 - a^2} \cos[k(B - B_p)] \right\} \right. \\ \left. + \frac{1}{M} \frac{\sin(Mx_p)}{M^2 - d^2} \frac{\pi}{2} \cos(\pi n) \frac{n}{M^2} \cos[M(B - B_p)] \right], \quad (\text{A.2.20})$$

$$A_{p,nm}^{(ss)} = \frac{4nm}{\pi A_p A} \cos(n\pi) \cos(m\pi) \left[\sum_{k=1, k \neq M, N}^{\infty} \left\{ \frac{1}{k} \frac{\sin(kx_p)}{k^2 - d^2} \frac{\sin(kx)}{k^2 - a^2} \cos[k(B - B_p)] \right\} \right. \\ \left. + \frac{1}{M} \frac{\sin(Mx_p)}{M^2 - N^2} \frac{\pi}{2} \cos(\pi n) \frac{n}{M^2} \cos[M(B - B_p)] \right. \\ \left. + \frac{1}{N} \frac{\pi}{2} \cos(\pi n) \frac{n}{N^2} \frac{\sin(Nx)}{N^2 - M^2} \cos[N(B - B_p)] \right], \quad (\text{A.2.21})$$

$$A_{p,nm}^{(ss)} = \frac{4nm}{\pi A_p A} \cos(n\pi) \cos(m\pi) \left[\sum_{k=1, k \neq N}^{\infty} \left\{ \frac{1}{k} \frac{\sin(kx_p)}{k^2 - d^2} \frac{\sin(kx)}{k^2 - a^2} \cos[k(B - B_p)] \right\} \right. \\ \left. + \frac{\pi^2}{4} \frac{n^2}{N^4} \frac{1}{N^2} \cos[N(B - B_p)] \right], \quad (\text{A.2.22})$$

and same for $B_{nm}^{(ss)}$ (6.0.76).